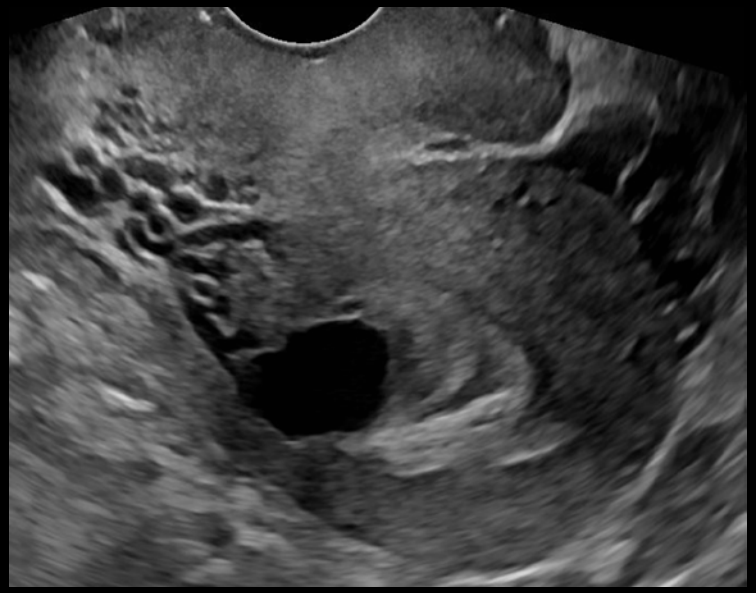
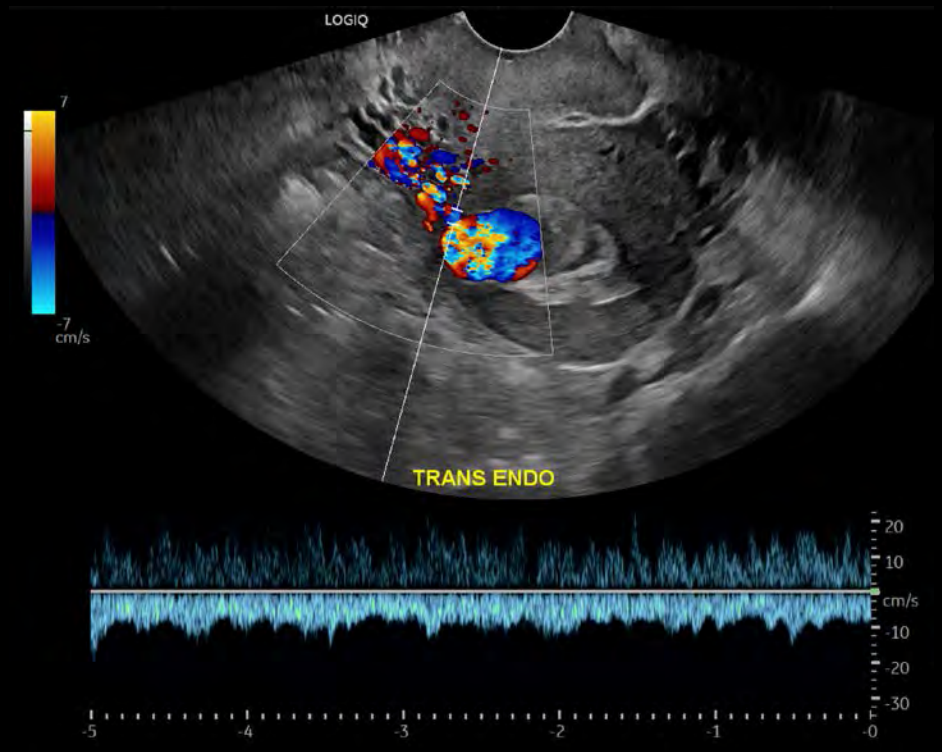
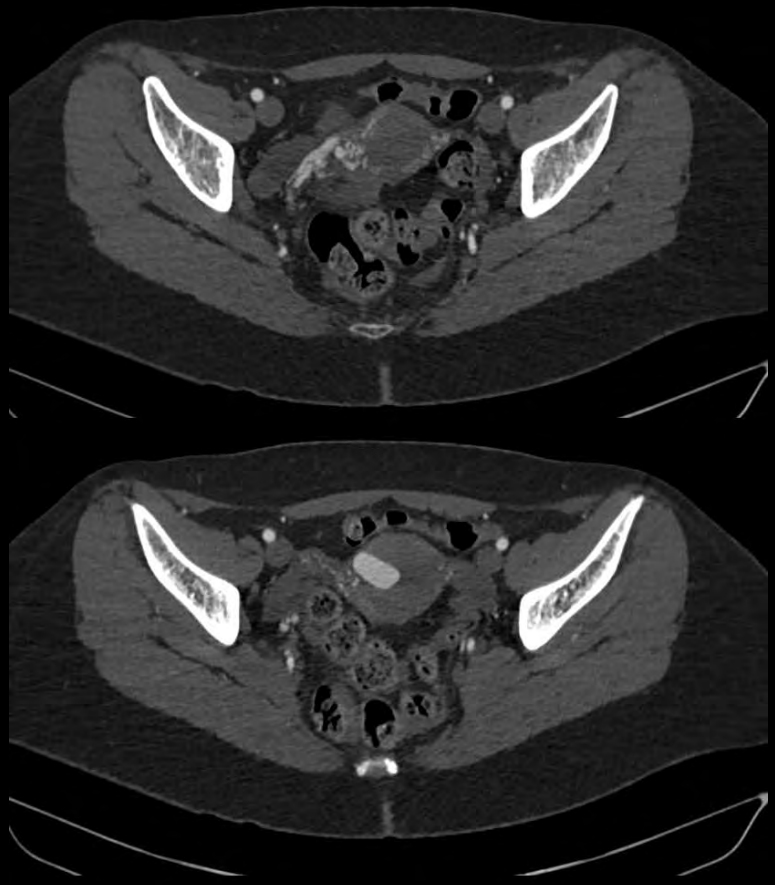
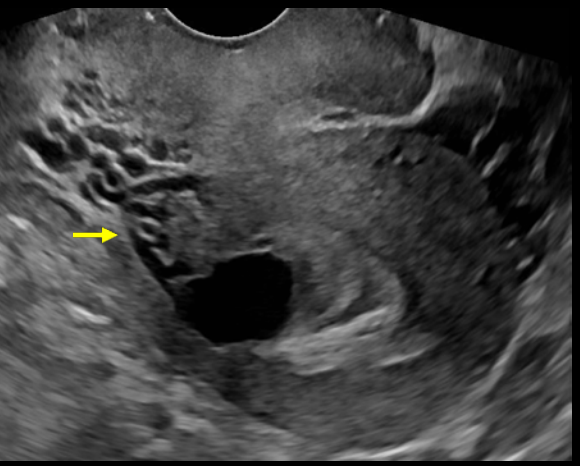
30 y/o female presents to the ED with heavy vaginal bleeding. She is status post laparoscopic right salpingectomy for recurrent right sided ectopic pregnancies 2 weeks prior.

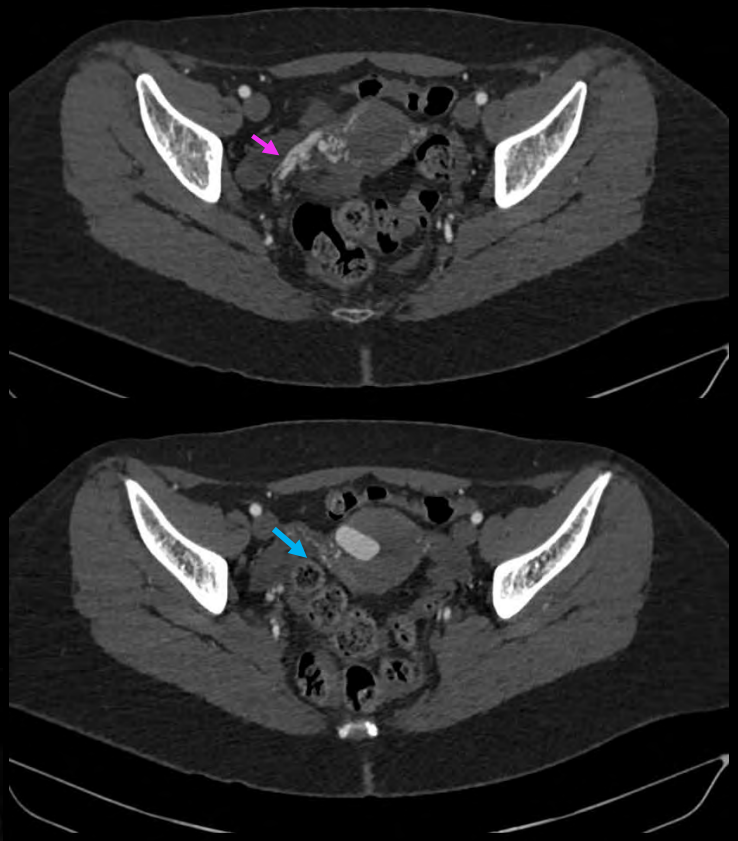


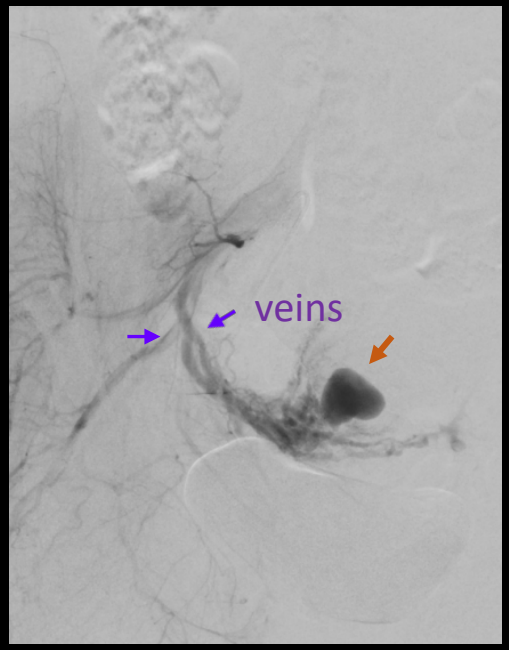

LOGIQ
7
-7
cm/s
TRANS ENDO
20
10
cm/s
-10
-20
-30
-5
-4
-3
-2
-1
-0

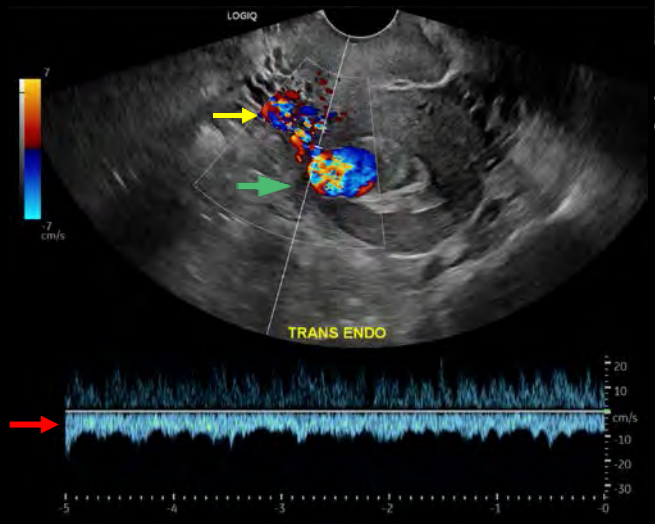


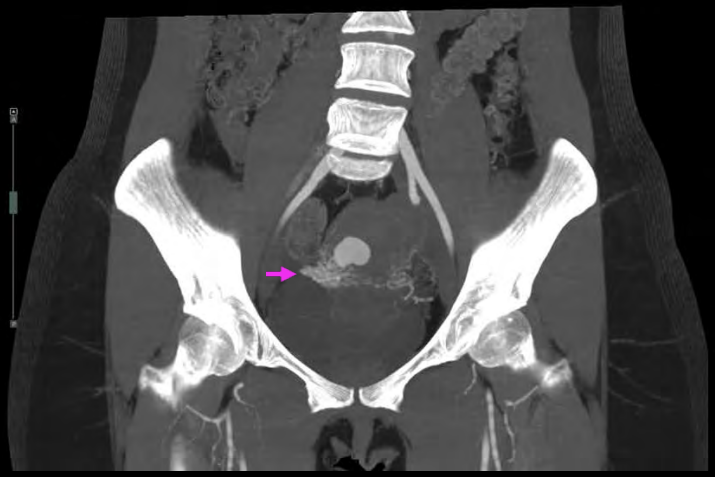







veins


LOGIQ
TRANS ENDO
cm/s





Uterine AV fistula with associated pseudoaneurysm

Imaging Findings: Pelvic ultrasound demonstrates an abnormal uterine vessels (→) extending into the endometrium with prominent pulsatile venous flow and yin-yang appearance(→). At the neck of a saclike structure, spectral Doppler demonstrates a "to-and-fro" waveform, reflecting bidirectional blood flow (→). Subsequent CTA demonstrates a cluster of tortuous and enlarged vessels arising from the right uterine artery with early venous filling (→) and an associated saclike structure (→). There was no evidence of active extravasation or hemoperitoneum. Arteriogram demonstrates a large pseudoaneurysm (→) with arteriovenous communication (→) which was subsequently satisfactorily embolized (→).

Differential Diagnosis: Uterine arteriovenous fistula (AVF); Uterine artery pseudoaneurysm; Acquired uterine arteriovenous malformation (AVM); Retained products of conception (RPOC) with marked vascularity.

Diagnosis: Acquired uterine arteriovenous fistula with associated uterine artery pseudoaneurysm following right salpingectomy.

Discussion: The patient had a recent right ectopic pregnancy treated with right salpingectomy. Acquired uterine vascular abnormalities, including uterine artery pseudoaneurysm and arteriovenous fistula (AVF), are uncommon but recognized complications of gynecologic surgery. A pseudoaneurysm results from arterial wall injury, while an AVF represents a direct communication between an artery and vein, producing high-flow vascularity and early venous filling. This case demonstrates a pseudoaneurysm and early venous opacification consistent with an acquired postprocedural uterine vascular injury. These lesions are clinically important because they can cause delayed or significant uterine bleeding and potentially life-threatening hemorrhage if the pseudoaneurysm ruptures. Transcatheter arterial embolization is typically the preferred treatment, allowing selective embolization of the feeding uterine artery and pseudoaneurysm/AVF while preserving the uterus. Surgical intervention is generally reserved for uncontrolled bleeding or unsuccessful embolization. This case highlights the importance of correlating the patient's recent surgical history with characteristic Doppler and angiographic findings when evaluating marked uterine vascularity after treatment of an ectopic pregnancy. Thick Gelfoam slurry, two detachable coils, and thick EmboCube were deployed in the right uterine artery to achieve flow reduction. Post-embolization angiography demonstrated satisfactory results.

@UpstateRad
@AOCRNews
@upstaterads
@aocrnews

Case courtesy of Antonio Santana Veliz, MD & Katherine Willer, DO
SUNY Upstate Medical University

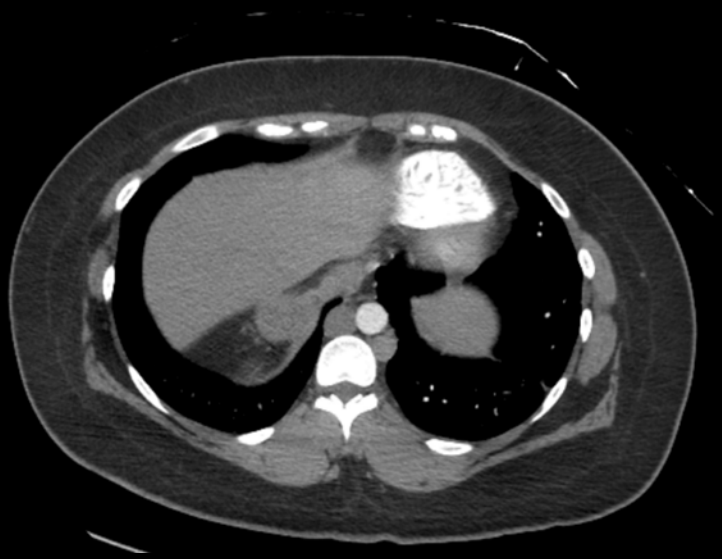
AOCR American Osteopathic College of Radiology

References

- Jung, H. H., & Kim, G. S. (2002). Obstetric iatrogenic arterial injuries of the uterus: Diagnosis with US and treatment with transcatheter arterial embolization. *RadioGraphics, 22*(1). https://doi.org/10.1148/radiographics.22.1.g02ja0735
- Le, N. D., & Nguyen, P. N. (2025). Uterine arteriovenous malformation or uterine artery pseudoaneurysm secondary to uterine aspiration in cesarean scar ectopic pregnancy: A case report and review of the literature. *Journal of Medical Case Reports, 19*(1), 248. https://doi.org/10.1186/s13256-025-05312-0
- Melcer, Y., Pekar-Zlotin, M., Cherniavsky, A., Levinsohn-Tavor, O., Copel, L., & Maymon, R. (2024). Acquired uterine artery pseudoaneurysm: A rare iatrogenic complication following cesarean delivery at complete cervical dilatation. *Archives of Gynecology and Obstetrics, 310*, 2267–2268.

Posted 11/6/2026

27 y/o female with a history of prior PEs and childhood VSD repair presenting with acute pleuritic chest pain and bilateral lower extremity edema.



Axial Contrast-Enhanced CT



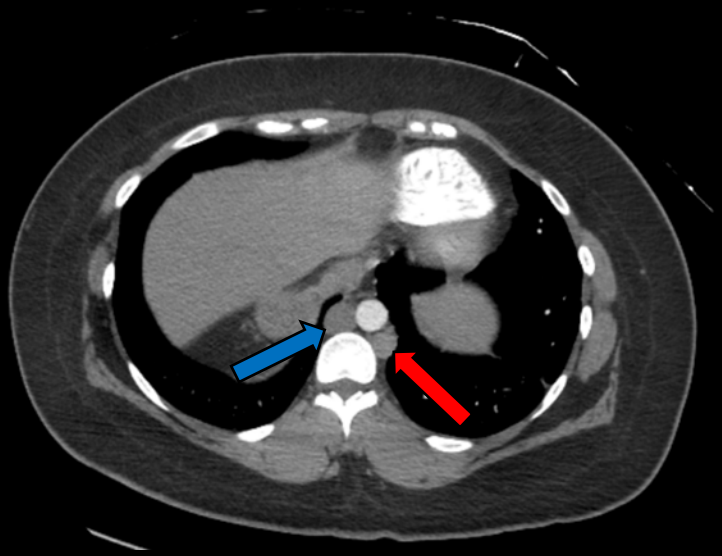
Axial Contrast-Enhanced CT



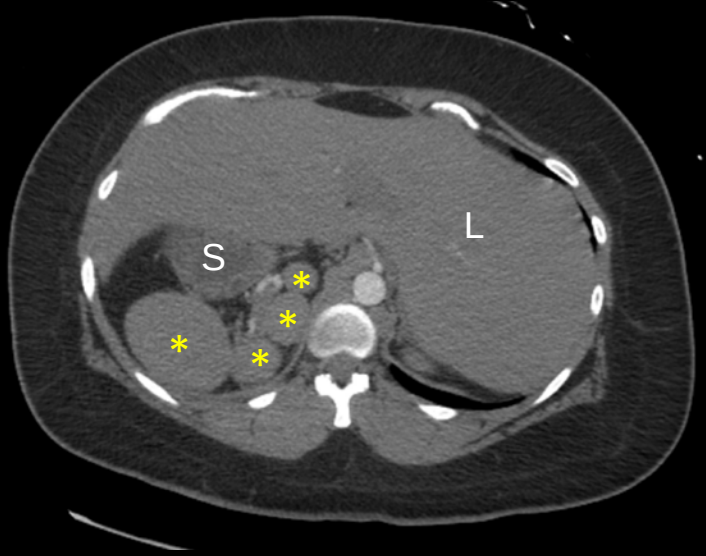
Coronal Contrast-Enhanced CT



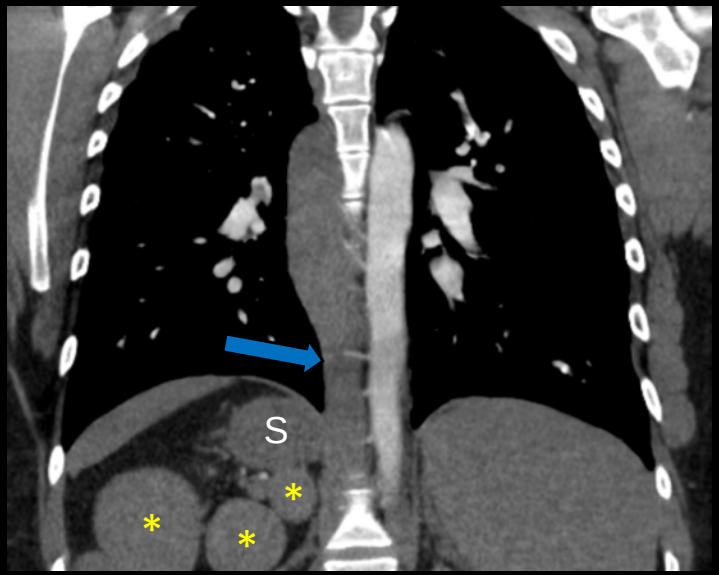
Sagittal Contrast-Enhanced CT



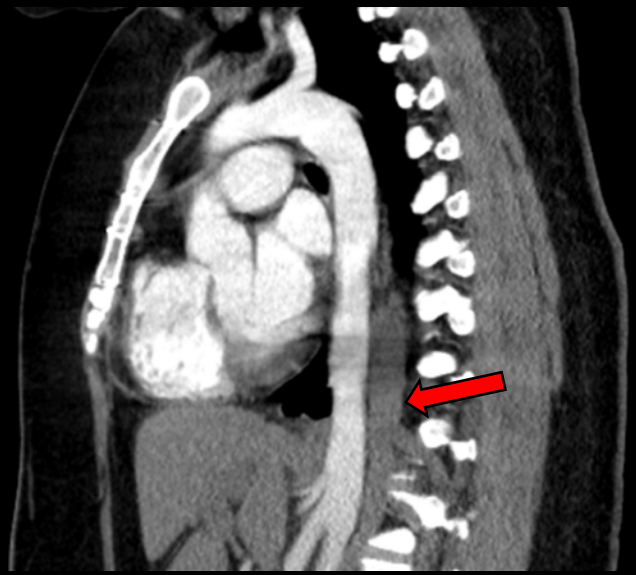
Axial Contrast-Enhanced CT



Axial Contrast-Enhanced CT



Coronal Contrast-Enhanced CT



Sagittal Contrast-Enhanced CT

Polysplenia Syndrome

Imaging findings: Contrast-enhanced CT of the chest reveals dilated azygos (blue arrow) hemiazygos veins (red arrow) with azygos continuation of the inferior vena cava. Multiple splenules (yellow asterisk) are present in the right upper quadrant of the abdomen. The liver (L) and stomach (S) demonstrate reversed positioning within the upper abdomen.

Differential Diagnosis: Polysplenia (left isomerism), Asplenia (right isomerism), Primary Ciliary Dyskinesia

Discussion: Polysplenia syndrome, also known as left isomerism, is a rare form of heterotaxy resulting from abnormal embryologic development of organ asymmetry. Imaging features include multiple splenules, situs ambiguus, bilateral bilobed lungs, bilateral hyparterial bronchi, and abnormal hepatic positioning. A characteristic vascular finding is interruption of the intrahepatic inferior vena cava with azygos or hemiazygos continuation. Intestinal malrotation and congenital heart disease are also observed. Identification of one anomaly should prompt evaluation for additional associated abnormalities. Clinical morbidity is primarily due to congenital heart disease and cardiovascular anomalies, which can significantly impact prognosis. The interrupted inferior vena cava with azygos continuation can predispose patients to deep vein thrombosis and pulmonary embolism. Despite the presence of splenic tissue, its function may be impaired, increasing susceptibility to infections caused by encapsulated organisms. Gastrointestinal complications may arise from intestinal malrotation or biliary atresia, potentially leading to obstruction. Management is multidisciplinary and tailored to the associated abnormalities. Cardiac defects can be corrected with surgical intervention, while significant conduction abnormalities are managed with pacemaker placement. Patients with functional asplenia need appropriate vaccination, antibiotic prophylaxis, and prompt evaluation during illness. Due to the risk of thromboembolism, these patients may require lifelong anticoagulation.

Case courtesy of Mohammad Aljazi, DO PhD[1], Steve Min, DO, MPH, MBA, FAOCR[2]
[1]Michigan State University College of Osteopathic Medicine, [2]Henry Ford Health

References

- Gu X, Xu S, Chen J, et al. Analysis of associated malformations by computed tomography in adults with polysplenia syndrome: A pilot study. *PLoS One*. 2024;19(12):e0312548. Published 2024 Dec 20. doi:10.1371/journal.pone.0312548

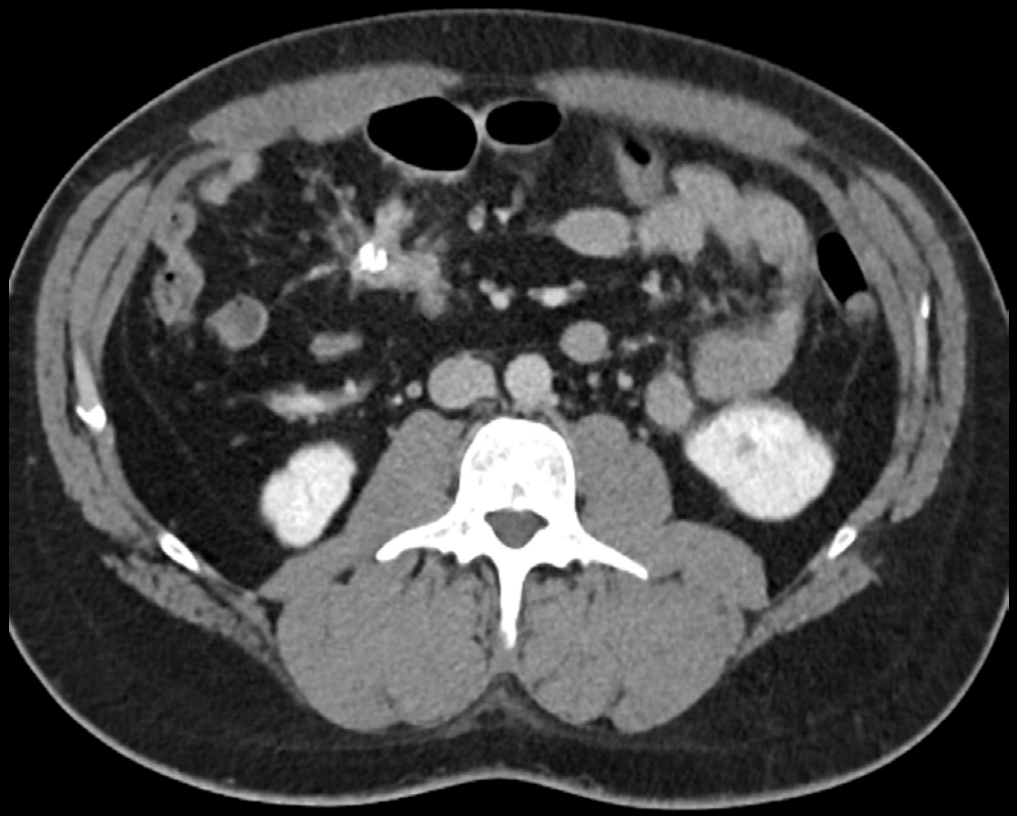
- Adams R, Ramos C, McDaniel M. Pulmonary Embolism in a Patient With Interrupted Inferior Vena Cava With Azygos Continuation and Polysplenia: A Case Report and Literature Review. *Catheter Cardiovasc Interv*. 2026;107(1):383-386. doi:10.1002/ccd.70364

- Nakada K, Kawaguchi F, Wakisaka M, Nakada M, Enami T, Yamate N. Digestive tract disorders associated with asplenia/polysplenia syndrome. *J Pediatr Surg*. 1997;32(1):91-94. doi:10.1016/s0022-3468(97)90103-2

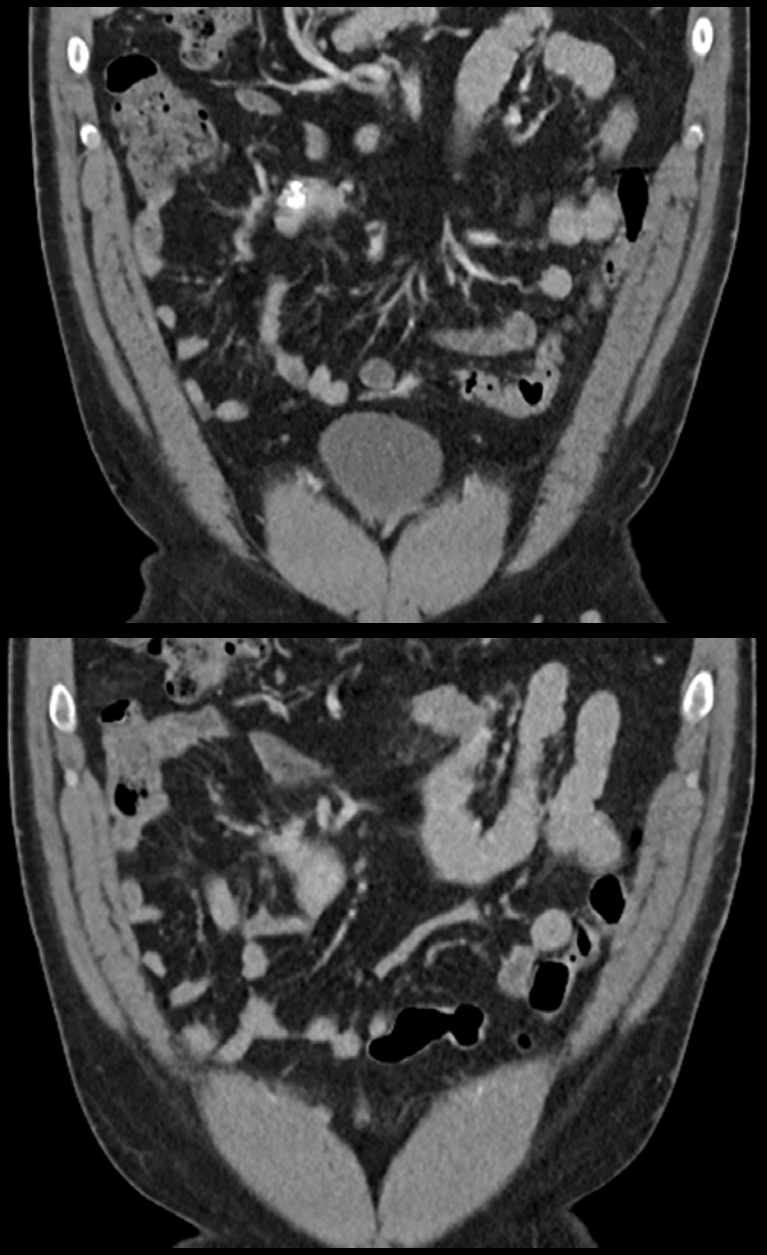
- Saba TG, Geddes GC, Ware SM, et al. A multi-disciplinary, comprehensive approach to management of children with heterotaxy. *Orphanet J Rare Dis*. 2022;17(1):351. Published 2022 Sep 9. doi:10.1186/s13023-022-02515-2

Posted 10/30/2026

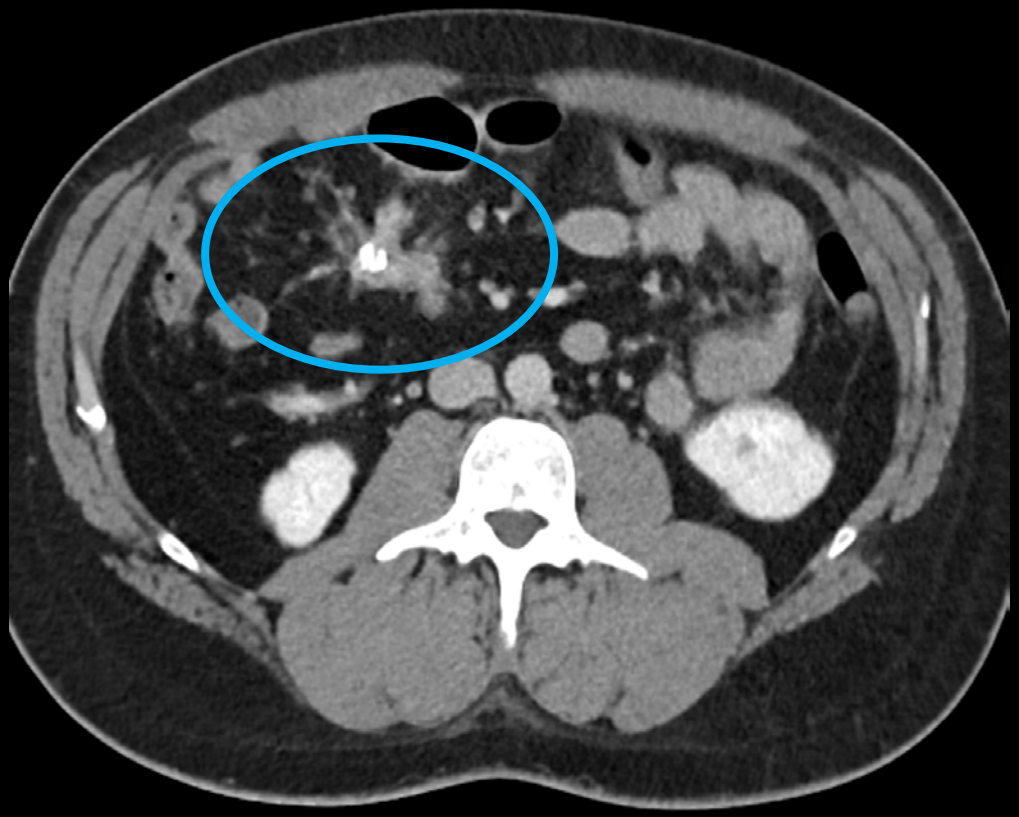
36 y/o male with no pertinent past medical history presenting to the ED with abdominal pain. Patient reported episodic abdominal pain with vomiting and constipation.



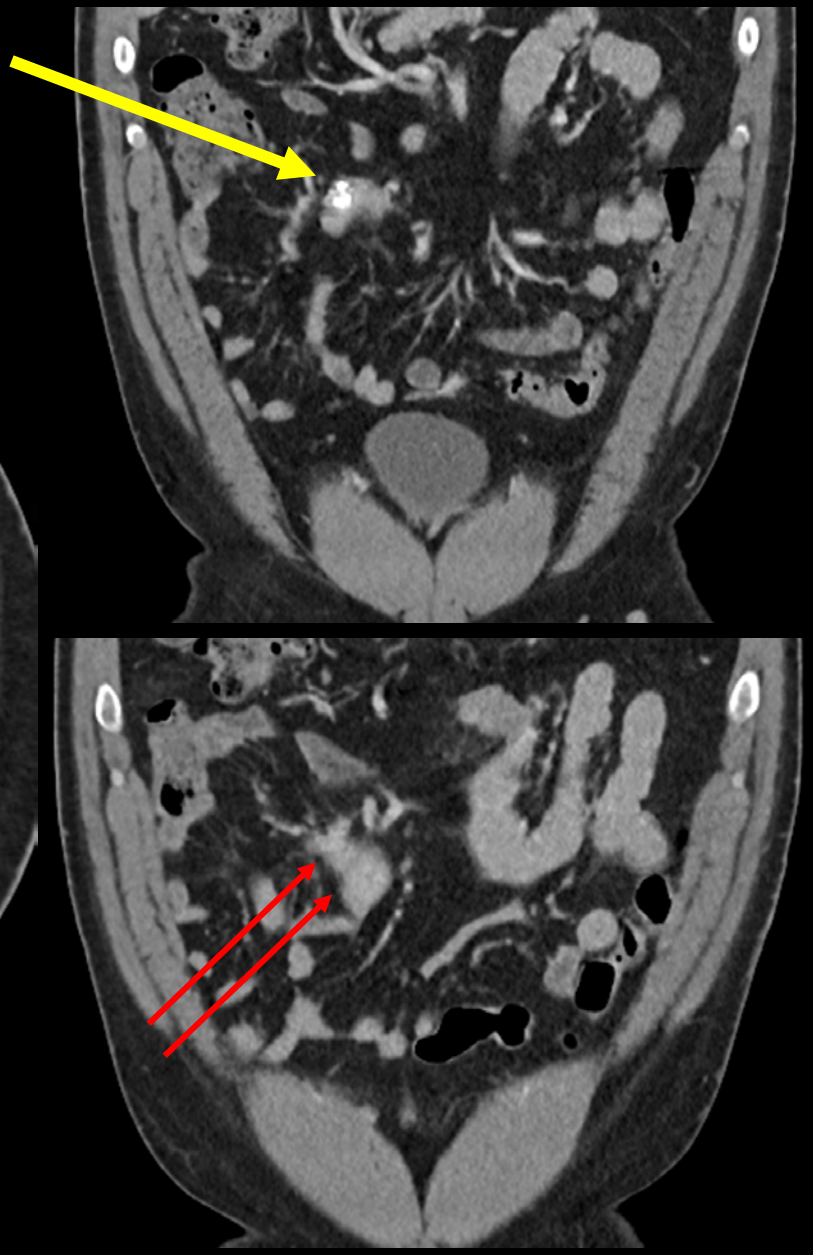
Axial contrast-enhanced CT



Coronal contrast-enhanced CT



Axial contrast-enhanced CT



Coronal contrast-enhanced CT

Small Bowel Neuroendocrine Tumor

Imaging findings: Axial and coronal CT Abdomen and Pelvis images reveal a partially calcified soft tissue lesion (Blue Circle and Yellow Arrow) in the right lower quadrant abutting the small bowel medially (Red Arrows), with a stellate surrounding appearance (Blue Circle).

Differential Diagnosis: Small Bowel Neuroendocrine Tumor, Sclerosing Mesenteritis, Mesenteric Fibromatosis, Lymphoma

Discussion: Neuroendocrine tumors (NET) arise from neuroendocrine cells found at various sites throughout the body, including the gastrointestinal tract, pancreas, and lungs. Small bowel NETs, particularly those originating in the ileum, are associated with a mesenteric desmoplastic reaction, reported in up to roughly half of cases. This reaction is characterized by dense, scar-like fibrous tissue developing around nodal and mesenteric metastases. Although the mechanism is not completely understood, this fibrotic response is thought to result from tumor-derived serotonin and other profibrotic mediators. These mediators activate cancer-associated fibroblasts, promoting collagen deposition. Clinically, patients often present with nonspecific findings such as abdominal pain, diarrhea, weight loss, or fatigue. More advanced disease may cause bowel obstruction, mesenteric ischemia, or carcinoid syndrome, usually in the setting of hepatic metastases. On CT, the desmoplastic reaction typically appears as a spiculated calcified mesenteric soft tissue mass. Imaging may demonstrate radiating strands and mesenteric retraction, producing a characteristic spoke-wheel appearance. Associated bowel wall thickening and tethering may be present. These findings are an important indicator of underlying small bowel neoplasm and should prompt evaluation for nodal and hepatic metastases. Despite frequent metastatic presentation, small bowel NETs generally have a favorable prognosis due to their indolent, well-differentiated biology. For localized disease, management typically requires surgical resection with regional lymphadenectomy. In patients with unresectable or metastatic disease, somatostatin analogs and peptide receptor radionuclide therapy may be used. For this patient, resection was performed, with subsequent tissue pathology demonstrating small bowel well-differentiated neuroendocrine tumor, grade 1.

Case courtesy of Mohammad Aljazi, DO, PhD[1], John Rogers, DO[2], Elias Antypas, MD, PhD[2]
[1]Michigan State University College of Osteopathic Medicine, [2]Corewell Health East

References

- Vijayvergia N, Lee LS, Katona BW. Gastroenteropancreatic Neuroendocrine Tumors. *Gastroenterology*. 2026;170(1):34-49. doi:10.1053/j.gastro.2025.07.004

- Ratnayake GM, Laskaratos FM, Mandair D, Caplin ME, Rombouts K, Toumpanakis C. What Causes Desmoplastic Reaction in Small Intestinal Neuroendocrine Neoplasms?. *Curr Oncol Rep*. 2022;24(10):1281-1286. doi:10.1007/s11912-022-01211-5

- Giambelluca D, Cannella R, Midiri M, Salvaggio G. The "spoke wheel" sign in mesenteric carcinoid. *Abdom Radiol (NY)*. 2019;44(5):1949-1950. doi:10.1007/s00261-019-01913-8

- Gupta A, Lubner MG, Liu JB, Richards ES, Pickhardt PJ. Small bowel neuroendocrine neoplasm: what surgeons want to know. *Abdom Radiol (NY)*. 2022;47(12):4005-4015. doi:10.1007/s00261-022-03485-6

- Del Rivero J, Perez K, Kennedy EB, et al. Systemic Therapy for Tumor Control in Metastatic Well-Differentiated Gastroenteropancreatic Neuroendocrine Tumors: ASCO Guideline. *J Clin Oncol*. 2023;41(32):5049-5067. doi:10.1200/JCO.23.01529

Posted 10/23/2026

50 y/o m underwent bone marrow aspirate concentrate (BMAC) procedure of the calcaneus for stem cell harvesting, with subsequent injection into the Achilles tendon due to chronic pain. MRI was obtained 1 month and 4 months after the procedure due to persistent tenderness.

A



Sagittal T1 Ankle

B



Sagittal STIR Ankle

C



Coronal T1 Ankle

D



Sagittal T1 Ankle
3 months later

E



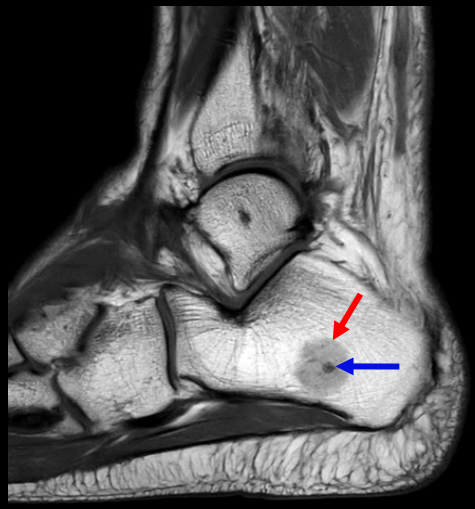
Sagittal STIR Ankle
3 months later

F



Sagittal T1 Ankle
3 months later

A



Sagittal T1 Ankle

B



Sagittal STIR Ankle

C



Coronal T1 Ankle

D



Sagittal T1 Ankle
3 months later

E



Sagittal STIR Ankle
3 months later

F



Sagittal T1 Ankle
3 months later

Expected Post-BMAC Changes

Imaging Findings: Focal area of hypointense T1 signal measuring 1.7 x 1.7 x 1.7 cm (A, red arrow), with a central region of increased hypointensity within the calcaneus (A, C, F, blue arrow). Focal area of hyperintensity on STIR (B, green arrow). Resolution of focal hypointensity (D, E).

Differential Diagnosis: Bone marrow edema, osteomyelitis, osteonecrosis, hematoma

Discussion: Bone marrow aspirate concentrate (BMAC) is an orthobiologic therapy containing stem cells and growth factors, designed to accelerate healing in chronic tendinopathies. Peripheral anatomical harvest sites, such as the calcaneus, may be chosen due to surgical convenience and proximity during foot and ankle interventions. Radiologists must recognize expected postprocedural intraosseous changes to avoid misdiagnosing benign iatrogenic findings as aggressive pathology.

MRI remains essential in the evaluation of postprocedural bone changes. STIR sequence enables fat suppression, with hyperintensity on STIR suggesting the presence of fluid, edema, or inflammation. This pattern effectively rules out intraosseous lipoma, which demonstrates T1 hyperintensity and suppression on STIR sequences. The key feature of post-procedural marrow edema is its transient, self-limiting nature. In this case, follow-up imaging post-BMAC demonstrates near-complete resolution of the T1 hypointensity and STIR hyperintensity with continuous visualization of the cortical needle track, reflecting normal bone remodeling and healing. This rapid interval resolution allows for exclusion of pathologies with more persistent imaging findings, such as infectious osteomyelitis or osteonecrosis.

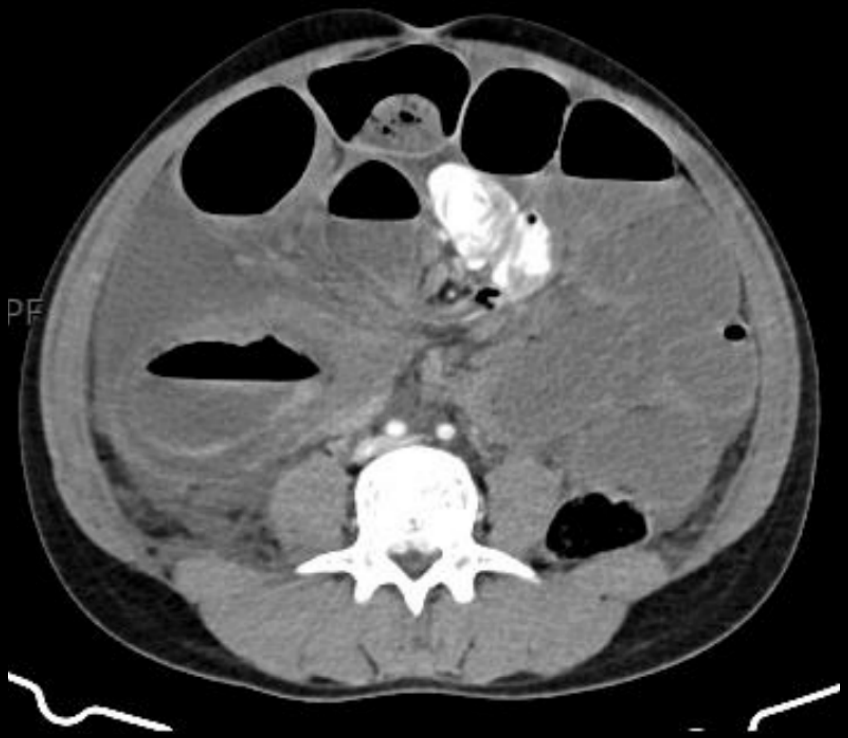
Case courtesy of Maya Shah, OMS IV[1]; Samantha Guerra, DO[2]; Kevin Carter, DO[1,2]
[1]Michigan State University College of Osteopathic Medicine, [2]McLaren Oakland Hospital

References

1. Lana JF, da Fonseca LF, Azzini G, et al. Bone marrow aspirate matrix: A convenient ally in regenerative medicine. *Int J Mol Sci*. 2021;22(5):2762. doi:10.3390/ijms22052762
2. Szaro P, Geijer M, Solidakis N. Traumatic and non-traumatic bone marrow edema in ankle MRI: a pictorial essay. *Insights Imaging*. 2020;11(1):90. doi:10.1186/s13244-020-00900-8
3. Bell D, Jones J. Short tau inversion recovery. Radiopaedia.org. Published November 28, 2011. Accessed July 25, 2026. doi:10.53347/rID-15330

Posted 10/16/2026

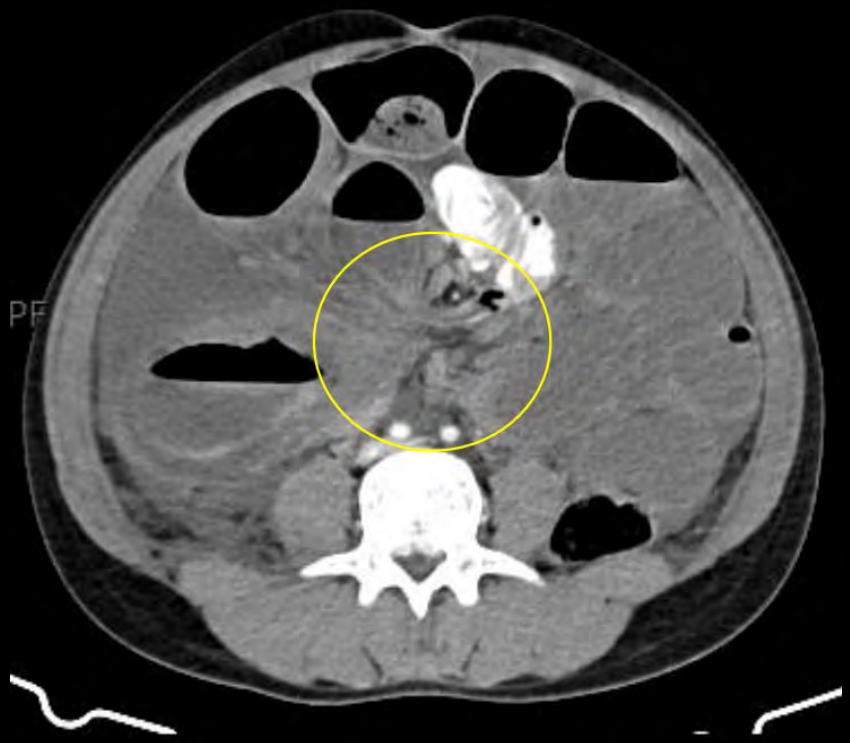
55F presented to the ED with sharp, diffuse abdominal pain and multiple episodes of vomiting over the previous 24h. No previous abdominal surgical hx.



1. Axial CT Abdomen w/ Contrast



2. Coronal CT Abdomen w/ Contrast



1. Axial CT Abdomen w/ Contrast



2. Coronal CT Abdomen w/ Contrast

Transmesenteric Internal Hernia

Imaging findings:

- Fig. 1: Axial contrast-enhanced CT abdomen demonstrates clustered, dilated, fluid-filled small bowl loops with central crowding of mesenteric vessels (yellow circle).
- Fig. 2: Coronal contrast-enhanced CT abdomen shows centralized twisting and stretching of the mesenteric vessels with clustering of small bowel loops (yellow circle).

Differential diagnosis: paraduodenal internal hernia, closed-loop small bowel obstruction, transmesenteric internal hernia

Discussion: Internal hernia, which affects 0.2-0.9% of people annually, is the protrusion of a viscus, usually the small intestine, through a weakness within the peritoneal cavity. Transmesenteric hernias constitute about 8% of all internal hernias and occur when bowel protrudes through the full thickness of a mesenteric opening, typically without a hernial sac. In children, they are the most common subtype and are typically congenital, whereas in adults, prior abdominal surgery (particularly Roux-en-Y gastric bypass) is responsible for over 90% of cases.

Patients often present with acute crampy, periumbilical abdominal pain, nausea, and vomiting. Less frequently, fever and rebound tenderness may occur. Other presenting features may include abdominal distention, peritonitis, and signs of small bowel obstruction (SBO) such as constipation or obstipation. These nonspecific symptoms are insufficient for diagnosis, particularly in cases of bowel ischemia, a surgical emergency. Imaging is necessary to identify the location of the hernia and potential complications. The lack of a hernial sac makes the location of transmesenteric hernia less predictable and more prone to complications.

Contrast-enhanced CT is the first-line modality for diagnosing transmesenteric hernia, with reported sensitivity and specificity values of 63% and 76%, respectively. Key findings include peripherally clustered small bowel loops typically in the right mid-abdomen adjacent to the anterior abdominal wall; lack of omental fat between the loops and the abdominal wall; crowding, stretching, and engorgement of mesenteric vessels; and displacement of the transverse colon caudally or dorsally. Signs of SBO, such as the closed-loop appearance when two ends of a small intestine segment co-herniate, and volvulus within the herniated segment, may be present. The whirlpool sign, formed by the twisting of mesenteric vessels and seen in this set of imaging, is an important diagnostic clue.

Transmesenteric hernias carry a high risk of potentially life-threatening complications, constituting 5.8% of SBOs. The absence of a hernial sac increases bowel loop mobility, making transmesenteric hernias particularly prone to developing volvulus, strangulation, and ischemia. Reported rates of small bowel volvulus in transmesenteric hernias have been reported to exceed 35%, while bowel ischemia occurs in 42.9-66.7% of cases.

In summary, transmesenteric hernia is a rare subtype of internal hernia that may pose diagnostic challenges. Recognizing key diagnostic clues are useful for guiding prompt surgical evaluation and preventing ischemic complications.

@cameronlaurie65
@AOCRNews

@cameron_l_10
@aocrnews

Case courtesy of Cameron C. Laurie, MS2[1], John Halphen Jr, MS2[1], April L. Cox, DO[2]
[1]Baylor College of Medicine, [2]Indiana University School of Medicine

References

- Blachar A, Federle MP, Brancatelli G, Peterson MS, Oliver JH 3rd, Li W (2001) Radiologist performance in the diagnosis of internal hernia by using specific CT findings with emphasis on transmesenteric hernia. Radiology 221(2):422-8 (PMID: 11687686)
- Blachar A, Federle MP, Dodson SF (2001) Internal hernia: clinical and imaging findings in 17 patients with emphasis on CT criteria. Radiology 218(1):68-74 (PMID: 11152781)
- Fan HP, Yang AD, Chang YJ, Juan CW, Wu HP (2008) Clinical spectrum of internal hernia: a surgical emergency. Surg Today 38(10):899-904 (PMID: 18820864)
- Ghiassi S, Nguyen SQ, Divino CM, Byrn JC, Schlager A (2007) Internal hernias: clinical findings, management, and outcomes in 49 nonbariatric cases. J Gastrointest Surg 11(3):291-5 (PMID: 17458600)
- Martin LC, Merkle EM, Thompson WM (2006) Review of internal hernias: radiographic and clinical findings. AJR Am J Roentgenol 186(3):703-17 (PMID: 16498098)
- Mathieu D, Luciani A; GERMAD Group (2004) Internal abdominal herniations. AJR Am J Roentgenol 183(2):397-404 (PMID: 15269032)
- Murali Appavoo Reddy UD, Dev B, Santosham R (2014) Internal hernias: surgeons dilemma-unravelled by imaging. Indian J Surg 76(4):323-8 (PMID: 25278660)

Posted 10/9/2026

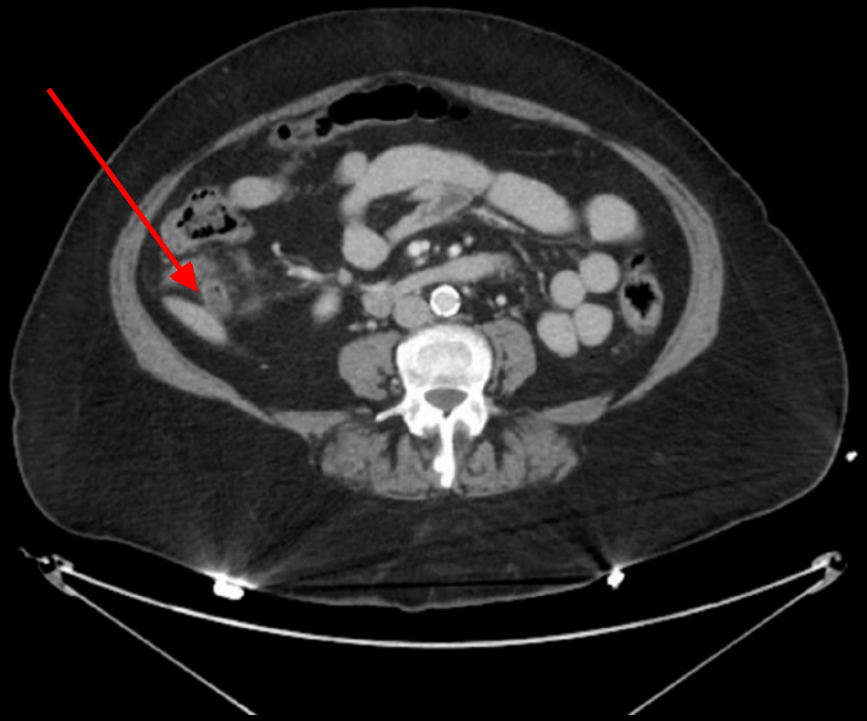
68F presented with acute RUQ abdominal pain, nausea, and vomiting. Subsequent examination demonstrated RLQ and periumbilical tenderness. CT abdomen/pelvis with contrast was performed for further evaluation.



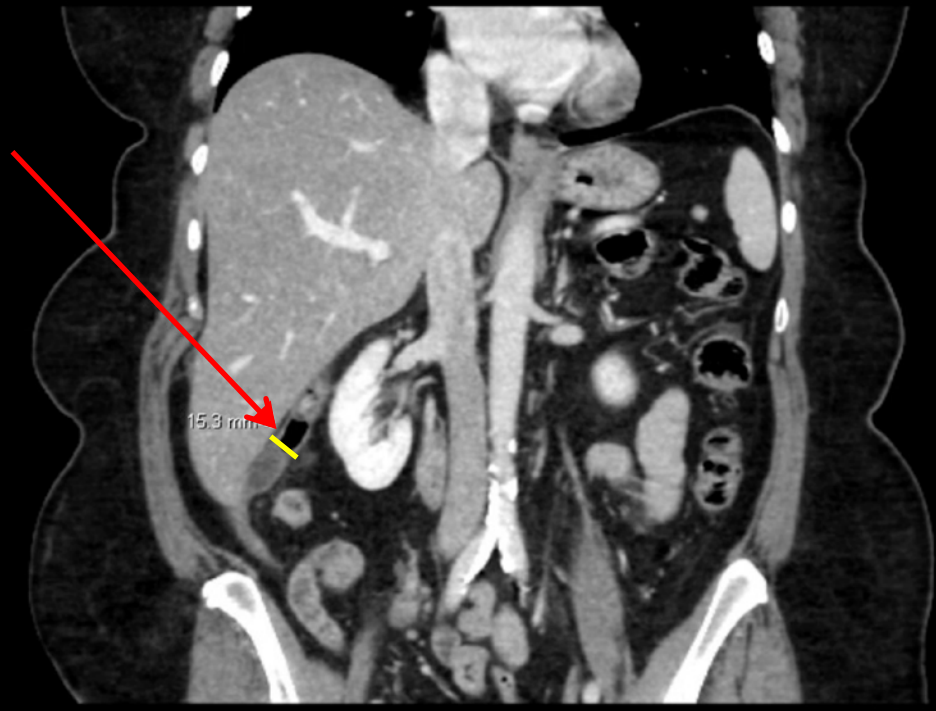
Axial Contrast Enhanced CT



Coronal Contrast Enhanced CT



Axial Contrast Enhanced CT



Coronal Contrast Enhanced CT

Acute Retrocecal Appendicitis

Imaging Findings:

- **Fig. A**: Axial CT abdomen-pelvis with contrast demonstrates a dilated, inflamed retrocecal appendix with surrounding inflammatory fat stranding (red arrow).
- **Fig. B**: Coronal CT demonstrates the retrocecal appendix extending superiorly toward the inferior margin of the liver (red arrow), measuring approximately 15.3 mm in diameter (yellow line).

Differential Diagnosis:

Acute appendicitis, right-sided diverticulitis, terminal ileitis, infectious colitis, epiploic appendagitis, pyelonephritis, and ureterolithiasis

Discussion:

Acute appendicitis is a common cause of acute abdominal pain requiring surgical intervention. Patients classically develop periumbilical pain that migrates to the RLQ; however, variation in appendiceal position may result in atypical symptoms. The retrocecal position is a common anatomical variant in which the appendix lies posterior to the cecum.

When a retrocecal appendix extends superiorly toward the liver, inflammation may produce RUQ or flank pain and mimic hepatobiliary or urinary pathology. In this case, the patient initially presented with RUQ pain, later reporting RLQ pain radiating to the RUQ and back. Intraoperatively, the appendix was found retrocecal and extending superiorly toward the liver without evidence of perforation.

CT plays a central role in diagnosing atypical appendicitis. Common findings include appendiceal dilation, wall thickening and enhancement, periappendiceal fat stranding, and appendicoliths. For atypical presentations, multiplanar reformations and diagnostic laparoscopy can further delineate the course and position of the appendix. In this case, axial and coronal CT demonstrated marked appendiceal dilation, appendicoliths, and surrounding inflammatory changes.

This case highlights the importance of considering a superiorly ascending retrocecal appendix in patients presenting with otherwise unexplained RUQ or right-sided abdominal pain. Careful evaluation of multiplanar CT images can identify the underlying anatomy and help prevent diagnostic delay.

@yash_khiraya
@AOCRNews

@yash.khiraya
@aocrnews

Case courtesy of Yash Khiraya, OMS II[1]; Steve Min, DO, MPH, MBA, FAOCR[2]
[1]Michigan State University College of Osteopathic Medicine, [2]Henry Ford Hospital

References

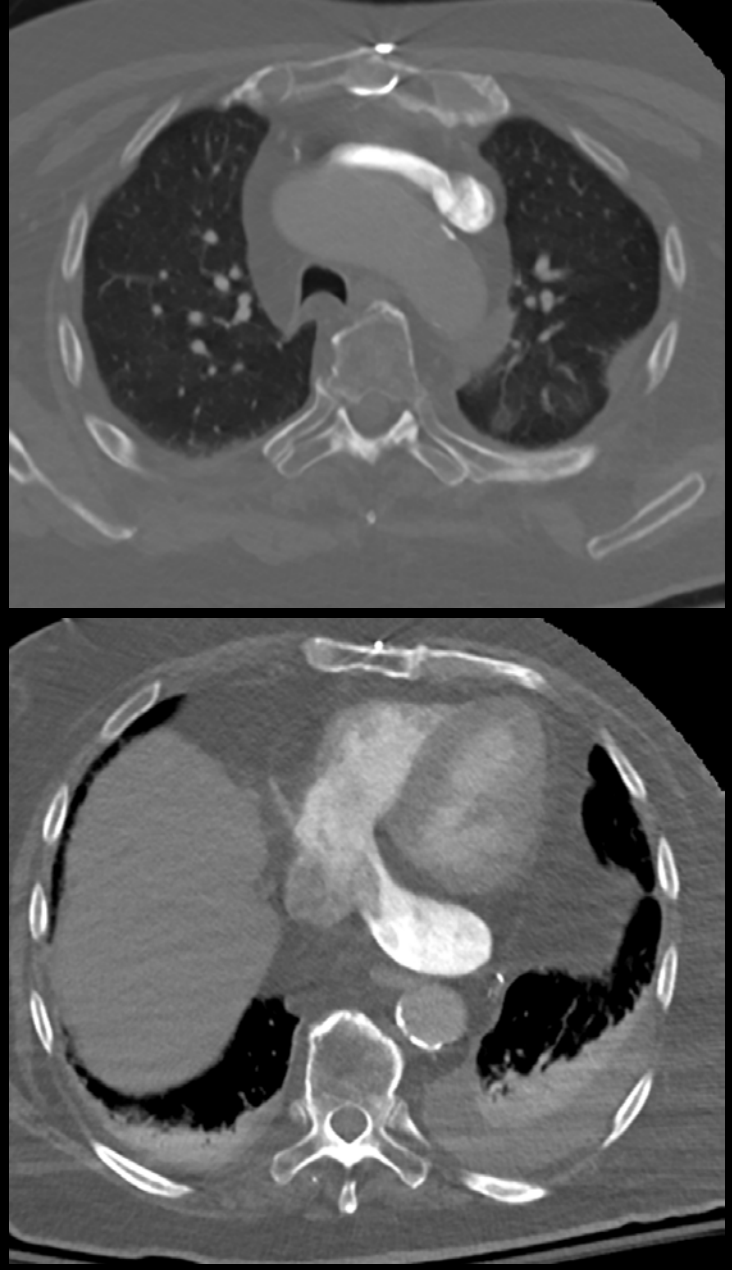
1. Ong EM, Venkatesh SK. Ascending retrocecal appendicitis presenting with right upper abdominal pain: utility of computed tomography. World J Gastroenterol. 2009;15(28):3576-3579. doi:10.3748/wjg.15.3576
2. Meyers MA, Oliphant M. Ascending retrocecal appendicitis. Radiology. 1974;110(2):295-299. doi:10.1148/110.2.295
3. Kim, H. C., Yang, D. M., Jin, W., & Park, S. J. (2008). Added diagnostic value of multiplanar reformation of multidetector CT data in patients with suspected appendicitis. Radiographics : a review publication of the Radiological Society of North America, Inc, 28(2), 393–406. https://doi.org/10.1148/rg.282075039
4. Lee JH, Jeong YK, Park KB, Park JK, Jeong AK, Hwang JC. Operator-dependent techniques for graded compression sonography to detect the appendix and diagnose acute appendicitis. AJR Am J Roentgenol. 2005;184(1):91-97. doi:10.2214/ajr.184.1.01840091
5. Moris, D., Paulson, E. K., & Pappas, T. N. (2021). Diagnosis and Management of Acute Appendicitis in Adults: A Review. JAMA, 326(22), 2299–2311. https://doi.org/10.1001/jama.2021.20502
6. Oruc M, Muminagic S, Denjalic A, Tandir S, Hodzic H. Retrocaecal appendix position--findings during the clasic appendectomy. Med Arch. 2012;66(3):190-193. doi:10.5455/medarh.2012.66.190-193
7. See TC, Watson CJ, Arends MJ, Ng CS. Atypical appendicitis: the impact of CT and its management. J Med Imaging Radiat Oncol. 2008;52(2):140-147. doi:10.1111/j.1440-1673.2008.01932.x
8. Echevarria S, Rauf F, Hussain N, et al. Typical and Atypical Presentations of Appendicitis and Their Implications for Diagnosis and Treatment: A Literature Review. Cureus. 2023;15(4):e37024. Published 2023 Apr 2. doi:10.7759/cureus.37024
9. Bahrami M, Mirgaloyebayat H, Mohajeri Z, et al. The diagnostic value of the computed tomography scan and ultrasonography in acute appendicitis. Am J Nucl Med Mol Imaging. 2023;13(1):11-17. Published 2023 Feb 15.
10. Quadri R, Vasan V, Hester C, Porembka M, Fielding J. Comprehensive review of typical and atypical pathology of the appendix on CT: cases with clinical implications. Clin Imaging. 2019;53:65-77. doi:10.1016/j.clinimag.2018.08.016

Posted 10/2/2026

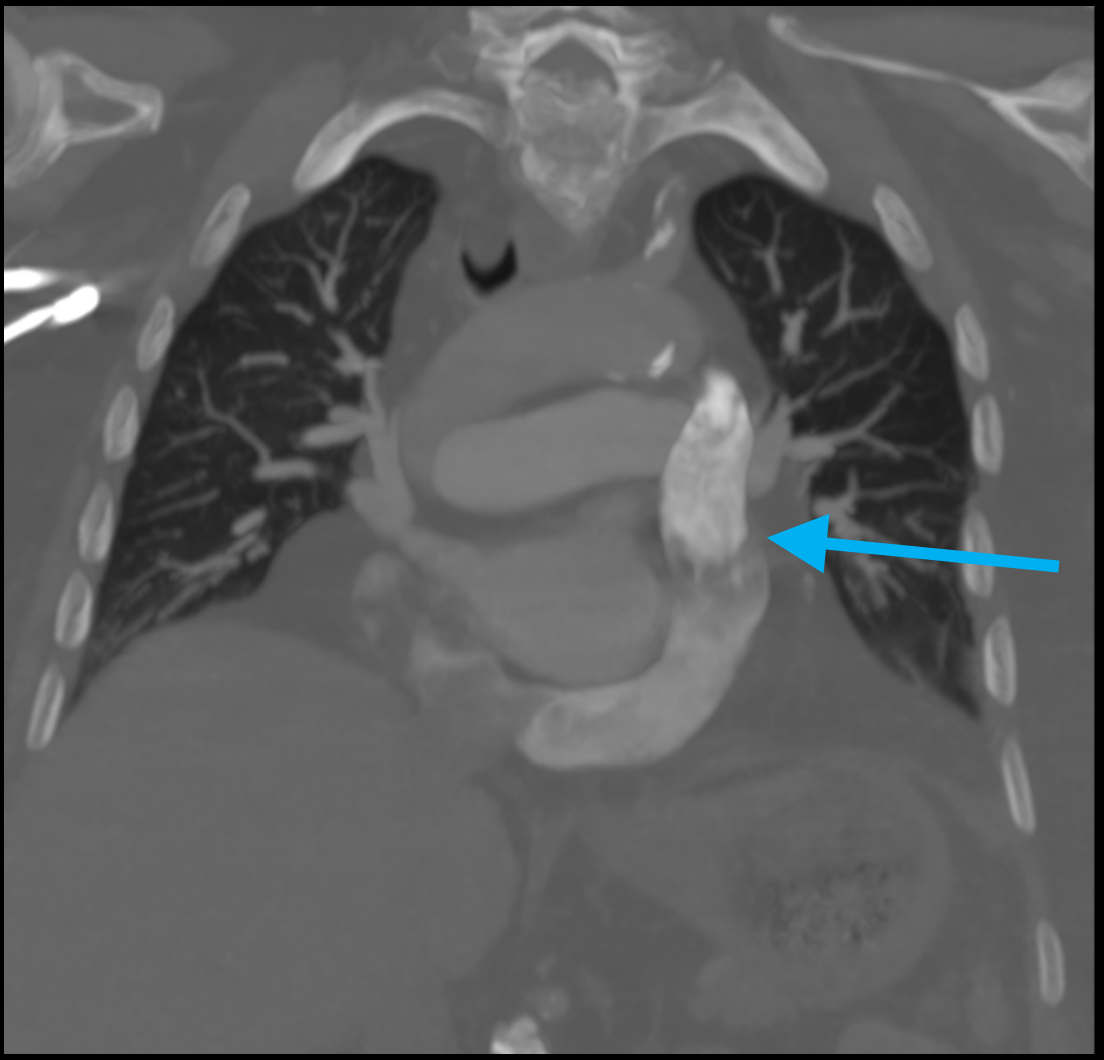
78 y/o m with a hx of congestive heart failure, paroxysmal atrial fibrillation, and prior CABG develops shortness of breath, tachycardia, and increased oxygen requirements while in in-patient rehabilitation following a hospital stay for congestive heart failure exacerbation.



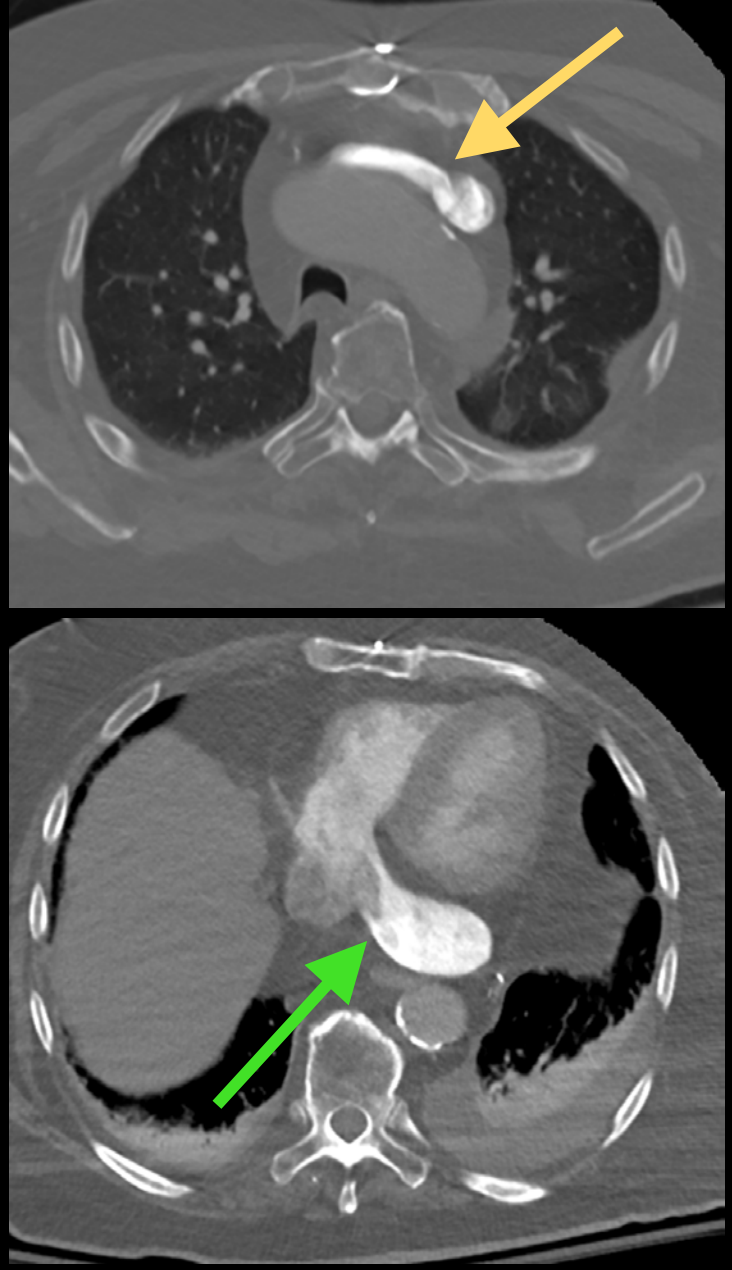
Coronal contrast-enhanced CT



Axial contrast-enhanced CT



Coronal contrast-enhanced CT



Axial contrast-enhanced CT

Isolated Persistent Left-Sided Superior Vena Cava

Imaging Findings: Axial and coronal CTA PE Thorax demonstrate the right and left brachiocephalic veins joining on the left side of the heart (yellow arrow), with aberrant continuation of a common vessel inferiorly (blue arrow) before crossing midline and entering the heart at the dilated coronary sinus (green arrow).

Differential Diagnosis: Other congenital abnormalities and variants that may cause similar imaging findings include: Superior vena cava duplication, partial anomalous pulmonary venous return, anomalous (retro-aortic) left brachiocephalic vein, and levoatrialcardinal vein.

Discussion: Persistent left superior vena cava (PLSVC) is the most common congenital thoracic venous malformation, with a prevalence of 0.3-0.9% and up to 10% among individuals with congenital heart disease. In most cases, PLSVC drains into the coronary sinus and subsequently the right atrium. Less commonly, it may drain into the left atrium directly. Although usually clinically silent, recognition is important due to its implications for invasive cardiovascular procedures. It is frequently discovered incidentally during central line placement, cardiac device implantation, or cardiothoracic surgery. When unrecognized, PLSVC increases the risk of catheter/device malposition and creates surgical complications. In addition, PLSVC-associated coronary sinus dilation has been linked to conduction abnormalities and arrhythmias.

For this case, CTA demonstrated abnormal venous anatomy consistent with an isolated-PLSVC. Review of prior medical records revealed an aborted invasive cardiac procedure, with operative notes describing difficulty accessing central venous structures due to distorted anatomy. Although CTA was recommended, no further imaging was obtained at that time. This case highlights the importance of recognizing PLSVC, particularly in patients with a history of challenges during invasive cardiac procedures. Early identification can facilitate procedural planning and reduce the risk of complications.

Case courtesy of Dr. John Rogers, DO, Dr. Mohammed Aljazi, DO/PhD, and Dr. Andrew Mizzi, DO, FAOCR, Corewell Health East – Farmington Hills

References

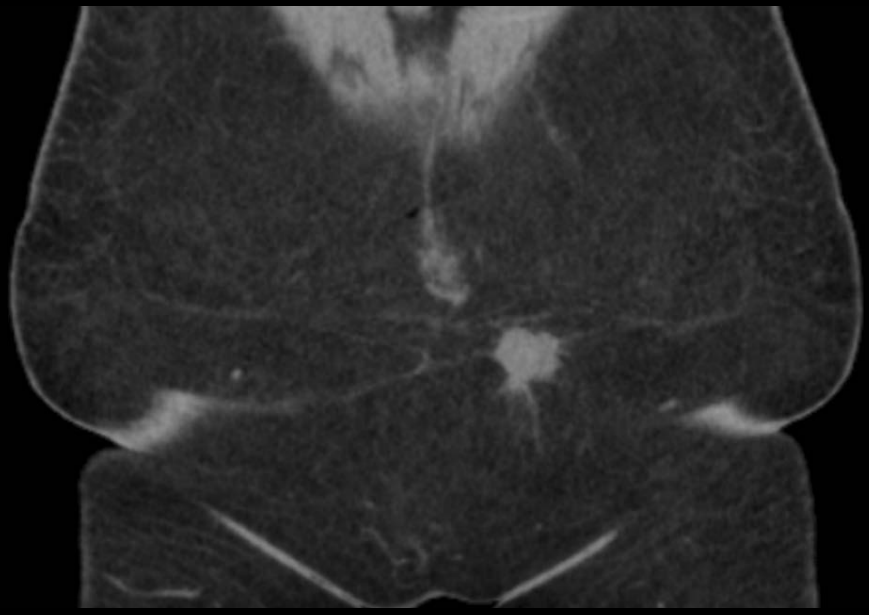
- Gondorf D, Triantafyllou G, Paschopoulos I, et al. Prevalence of persistent left superior vena cava in the general population: a systematic review with meta-analysis. *Anat Sci Int*.
- Jeong ER, Kang EJ, Jeun JH. Pictorial Essay: Understanding of Persistent Left Superior Vena Cava and Its Differential Diagnosis. *J Korean Soc Radiol*. 2022;83(4):846-860. doi:10.3348/jksr.2021.0192
- Azizova A, Onder O, Arslan S, Ardali S, Hazirolan T. Persistent left superior vena cava: clinical importance and differential diagnoses. *Insights Imaging*. 2020;11(1):110.
- Louviere CD, Serrano-Berrios A, Gopireddy DR, Harmon TS, Adler GA, Abu Hana R. Persistent Left Superior Vena Cava: Implications for Long-Term Arteriovenous Fistula Patency and Potential Cardiac Complications. Cureus. 2025;17(8):e90296. Published 2025 Aug 17.
- Sardar U, Bukhari HA, Khan AJ, et al. Incidental Identification of a Persistent Left Superior Vena Cava During Central Venous Catheterization: A Case Report. *Cureus*. 2025;17(7):e88847.

Posted 9/25/2026

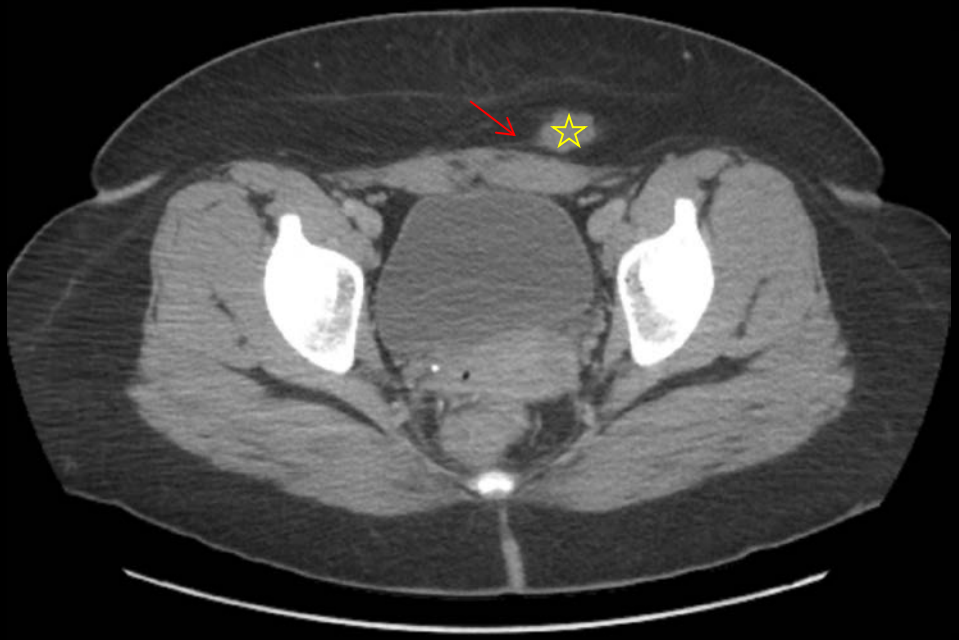
29-year-old G4P4 female, all delivered by C-section, presenting with pelvic pain and a lump to the left side of the C-section incision.



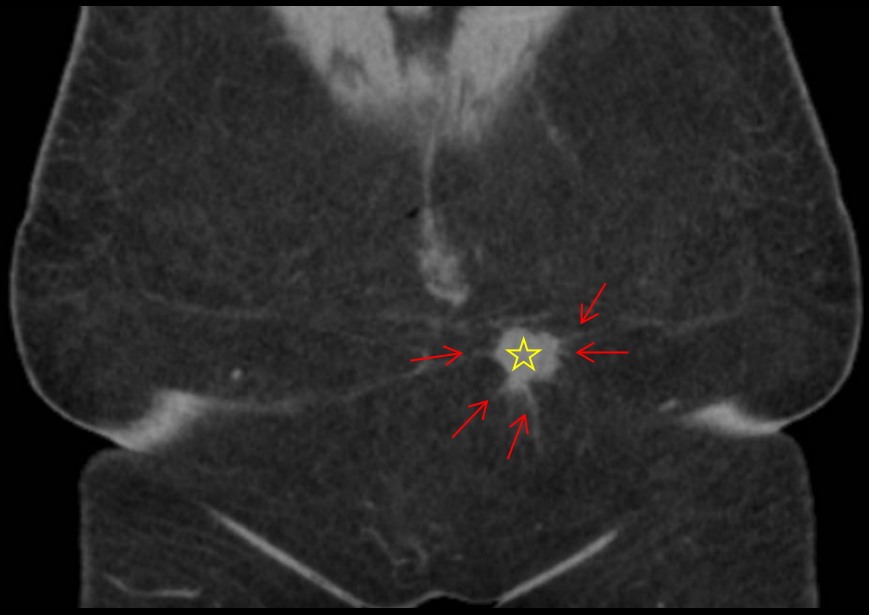
Axial Contrast-Enhanced CT



Coronal Contrast-Enhanced CT



Axial Contrast-Enhanced CT



Coronal Contrast-Enhanced CT

Cesarean Scar Endometriosis

Imaging findings: Axial and coronal contrast-enhanced CT of the abdomen showing a left subcutaneous anterior pelvic wall soft tissue mass (yellow star) measuring 2.6 x 2.0 cm. Multiple linear infiltrations (red arrows) radiating from the mass into the surrounding subcutaneous fat.

Differential Diagnosis: Cesarean scar endometriosis, abdominal wall hernia, desmoid tumor, suture granuloma, soft tissue sarcoma

Discussion: Cesarean scar endometriosis is a rare complication of cesarean delivery that arises when endometrial tissue is implanted within or near the prior surgical incision. The ectopic tissue may involve the skin, subcutaneous tissue, fascia, muscle, or uterine scar. Patients typically present with a painful mass at the cesarean scar, classically accompanied by cyclical pain and swelling that worsen during menstruation. Because symptoms may not present until years after surgery, the diagnosis is frequently delayed. Ultrasound is usually the initial imaging modality, whereas MRI is the most sensitive, demonstrating hemorrhagic foci that suggest endometriosis. On CT, cesarean scar endometriosis typically appears as an ill-defined or spiculated soft tissue mass along the prior surgical incision with mild to moderate enhancement. These lesions may also show linear soft tissue extensions radiating from a central nodule, referred to as the “gorgon sign”, which has been reported to be 97% specific for abdominal wall endometriosis. Definitive diagnosis is established by biopsy with histopathology demonstrating endometrial glands and stroma. Wide surgical excision with clear margins is the treatment of choice, and hormonal therapy may be used to provide symptomatic relief.

Case courtesy of Mohammad Aljazi, DO PhD[1], Saifuddin Vohra, DO[2]
[1]Michigan State University College of Osteopathic Medicine, [2]Henry Ford Health

AOCR American Osteopathic College of Radiology

References

- Arkoudis NA, Moschovaki-Zeiger O, Prountzos S, Spiliopoulos S, Kelekis N. Caesarean-section scar endometriosis (CSSE): clinical and imaging fundamentals of an underestimated entity. *Clin Radiol*. 2023;78(9):644-654. doi:10.1016/j.crad.2023.05.020

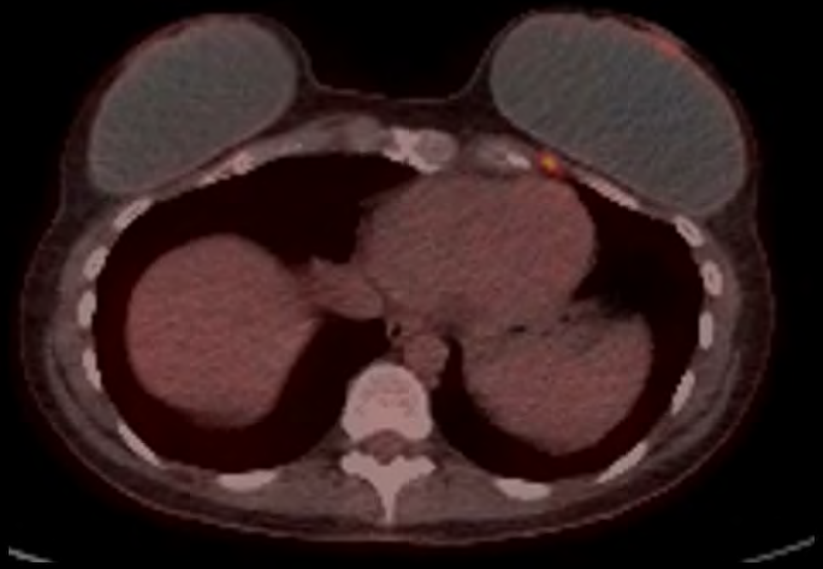
- Gidwaney R, Badler RL, Yam BL, et al. Endometriosis of abdominal and pelvic wall scars: multimodality imaging findings, pathologic correlation, and radiologic mimics. *Radiographics*. 2012;32(7):2031-2043. doi:10.1148/rg.327125024

- Salmeri N, Ragusi A, Buffo C, Viganò P, Somigliana E, Vercellini P. Abdominal Wall Endometriosis After Cesarean Section: A Systematic Review of Clinical Presentation, Timing, and Outcomes. *J Minim Invasive Gynecol*. 2026;33(6):694-702. doi:10.1016/j.jmig.2026.01.015

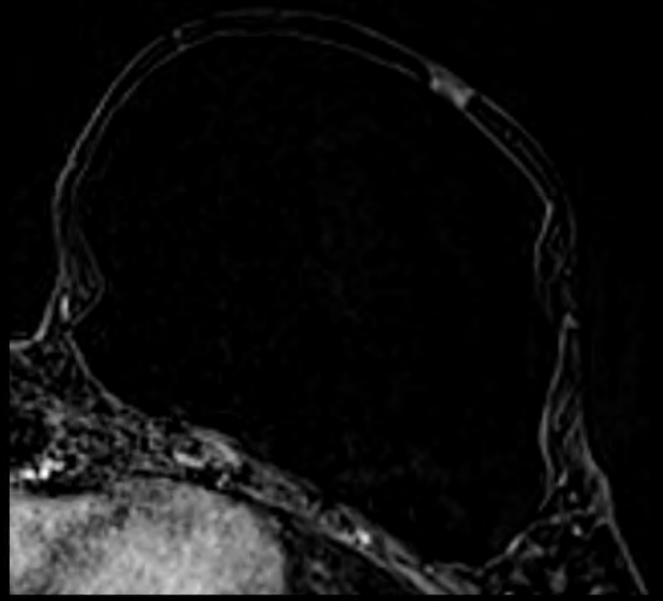
- Yarmish G, Sala E, Goldman DA, et al. Abdominal wall endometriosis: differentiation from other masses using CT features. *Abdom Radiol (NY)*. 2017;42(5):1517-1523. doi:10.1007/s00261-016-0998-y

Posted 9/18/2026

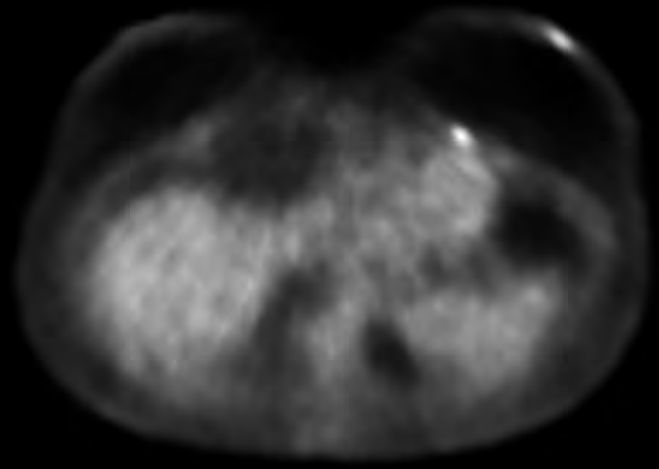
Premenopausal female status post left mastectomy several years prior for breast cancer. Presents with new metastatic disease to left axillary lymph node.



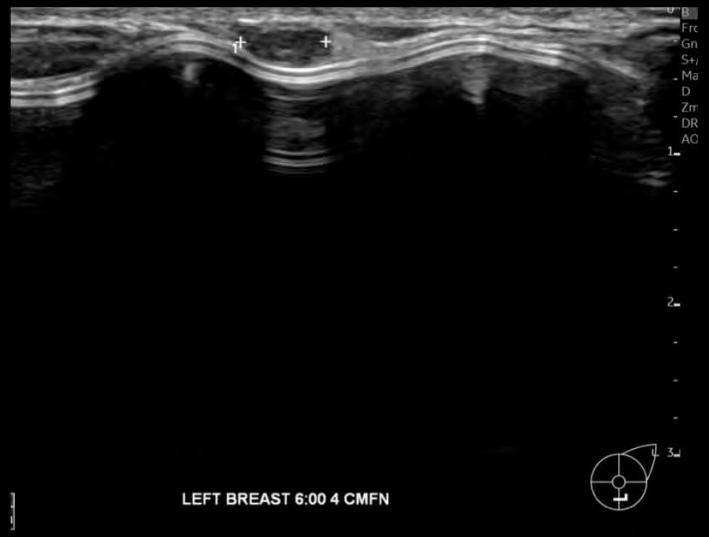
PET/CT Fused Axials



Breast MRI SUB Peak Axial



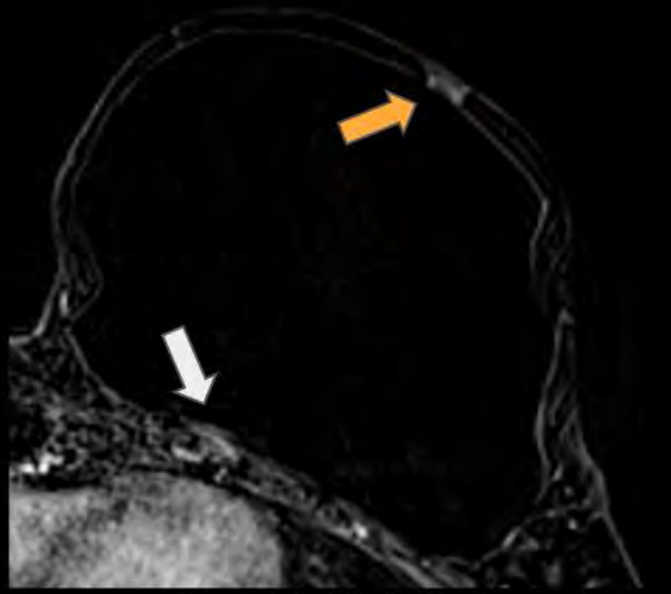
PET/CT axial AC



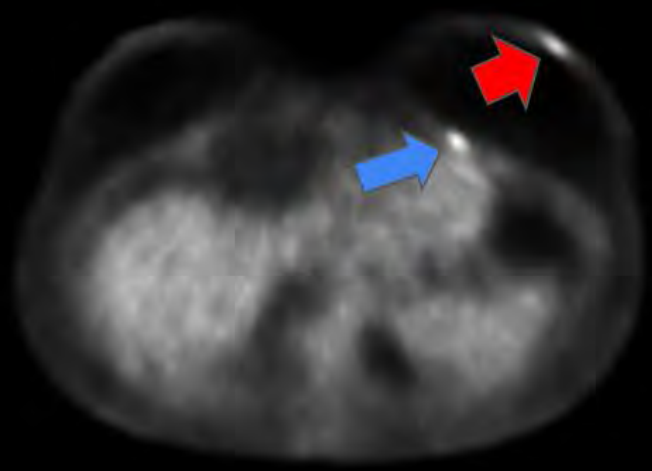
Breast US Antiradial



PET/CT Fused Axials



Breast MRI SUB Peak Axial



PET/CT axial AC



Breast US Antiradial

Recurrent Invasive ductal carcinoma

Findings: PET/CT axial images demonstrate increased FDG uptake in the inferior aspect of the left breast with SUV max of 5.7 ( ) and increased FDG uptake in a small soft tissue nodule in the left anterior chest wall, deep to the left breast prosthesis with SUV max of 8.0 ( ). Breast MRI SUB peak images demonstrate a superficial focus of heterogeneous enhancement, which does reach the minimum threshold percentage within the region of FDG uptake identified within the inferior aspect of the left breast ( ) and a 1.3 cm oval and enhancing mass demonstrating type III kinetics which appears to be located within the chest wall ( ) in the region of FDG uptake demonstrated within the left anterior chest wall. Breast US image demonstrates one of the two palpable masses within the left breast, ( ) both of which were subsequently biopsied.

Differential Diagnosis: Axillary node: Benign reactive, non-breast tumor malignancy, lymphoma. Breast lesion: Inflammation, capsulitis, fat necrosis, recurrent breast cancer. Chest wall: Scar tissue healing, local recurrence, infection.

Diagnosis: Recurrent invasive ductal carcinoma (IDC) involving axillary lymph nodes, residual breast tissue and chest wall.

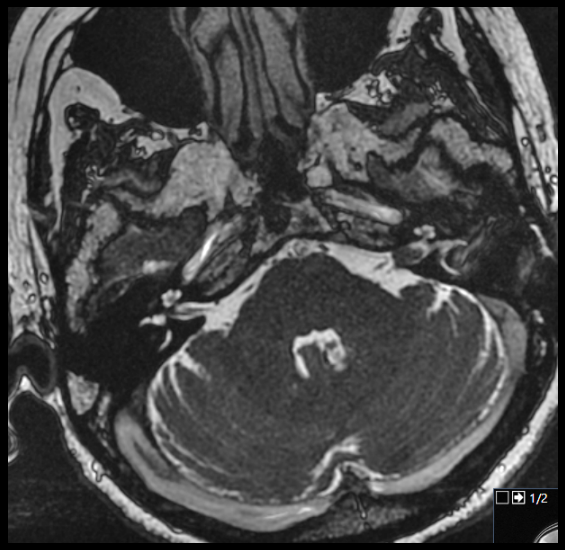
Discussion: IDC is the most common type of breast cancer. It is an infiltrating and malignant proliferation of neoplastic cells in the breast. IDC recurrence rates vary widely. Recurrence can be local (recurring near the original site), regional (involving the lymph nodes), or distant (appearing in other area of the body). This case demonstrates regional recurrence with the biopsied axillary lymph node and local recurrence within the left breast. Treatment options include breast surgery,m chemotherapy, radiation therapy, hormonal therapy and immunotherapy. In this case, the patient underwent surgical excision of the locally recurrent breast disease, chest wall disease and axillary dissection.

Case courtesy of Savanah Atwal, DO & Katherine Willer, DO
SUNY Upstate Medical University

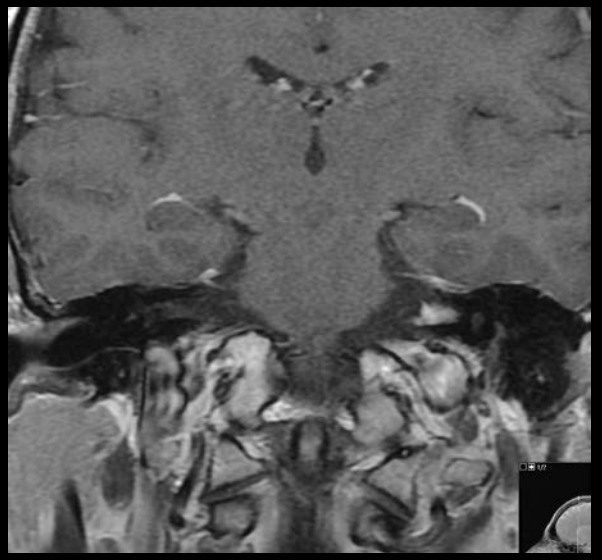
References

- “Invasive Ductal Cancer | Radiology Case.” *Radiopaedia*, radiopaedia.org/cases/invasive-ductal-cancer-1?lang=us. Accessed 28 July 2026.
- Shockney, Lillie. “Invasive Ductal Carcinoma (IDC): Overview, Treatment & Prognosis.” *National Breast Cancer Foundation*, 11 June 2026, www.nationalbreastcancer.org/invasive-ductal-carcinoma/.

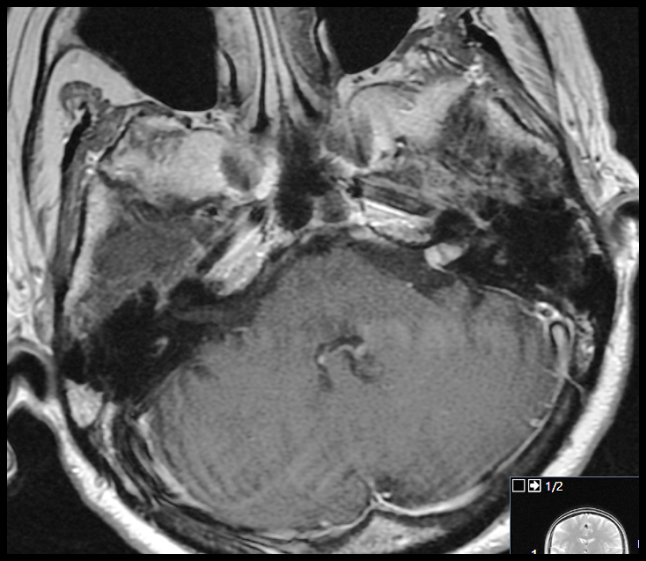
56 y/o F with hx of Crohn’s disease, discoid lupus, & depression presents with left facial weakness, severe vertigo, & hearing loss. These symptoms were preceded by vertigo, nausea, & gait instability. No vesicular rash was noted. She improved with valacyclovir & prednisone, though vertigo & hearing loss persisted. She had presented to the ED one week prior for left-sided facial droop and was treated for Bell’s palsy. She has a history of chicken pox as a child.



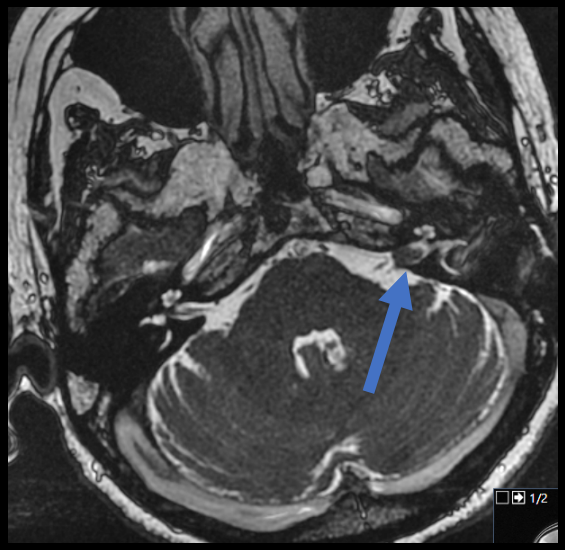
Axial T2-weighted MRI



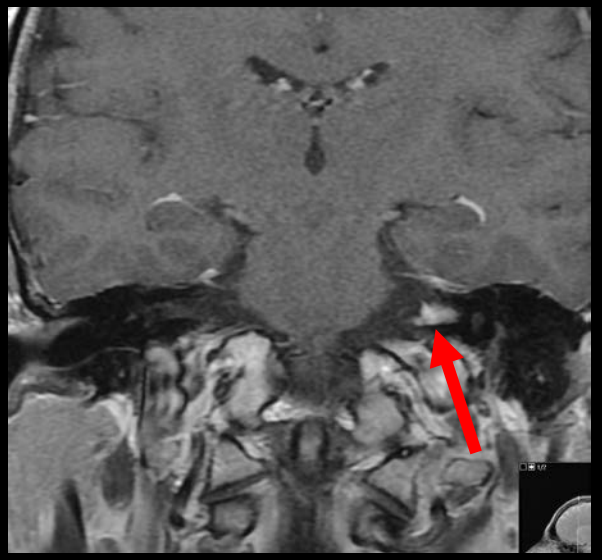
Coronal T1-weighted post-contrast MRI



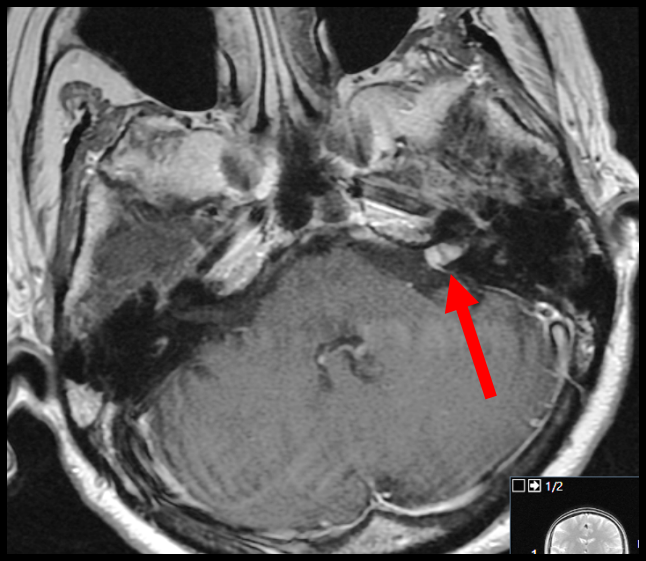
Axial T1-weighted post-contrast MRI



Axial T2-weighted MRI



Coronal T1-weighted post-contrast MRI



Axial T1-weighted post-contrast MRI

Ramsay Hunt Syndrome

Image Findings: Imaging shows asymmetric thickening of the left VII/VIII nerve complex (blue arrow) and enhancement of the left VII/VIII nerve complex (red arrows) at the CP angle extending into the internal auditory canal.

Differential Diagnosis: Ramsay Hunt Syndrome, vestibular schwannoma, neurosarcoidosis

Discussion: Ramsay Hunt syndrome is caused by a reactivation of the varicella zoster virus in the geniculate ganglion of the facial nerve. It is characterized by a clinical triad of ipsilateral facial weakness, otalgia, and vesicular eruption on the ear, typically in individuals older than 60 years. Up to one-third of patients have no vesicular eruption at all, making Ramsay Hunt syndrome clinically indistinguishable from Bell's palsy. Suspect Ramsay Hunt syndrome over Bell's palsy in patients with vestibulocochlear symptoms, severe otalgia, and involvement of multiple cranial nerves. Ramsay Hunt syndrome is self-limiting, although antivirals and corticosteroids can help reduce long-term complications. Prognosis is generally worse than with Bell's palsy.

@AOCRNews

@aocrnews

Case courtesy of Gabriel Raytsis, MS2; Sraavya Pinjala, MS3; Robert Koenigsberg, DO, FAOCR
Lewis Katz School Of Medicine / Temple University
Case reprinted with permission from American College of Radiology Case In Point

References

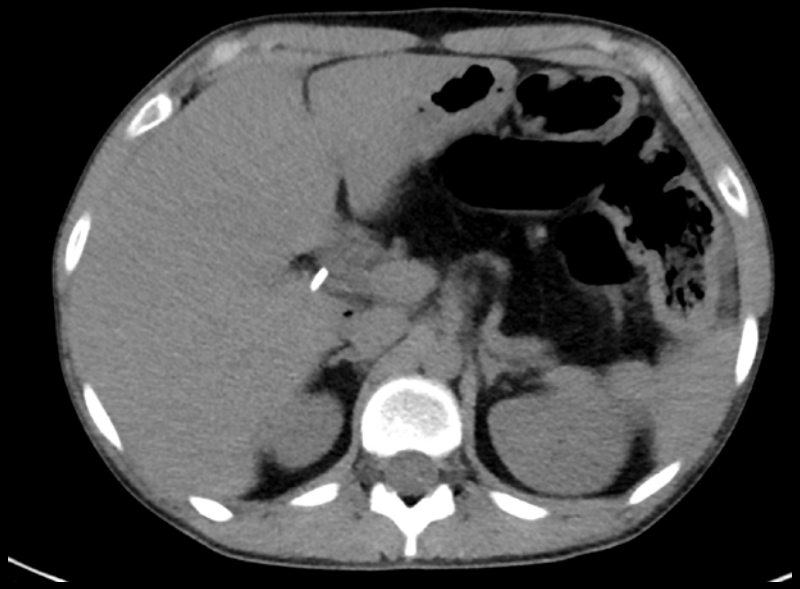
- Crouch AE, Hohman MH, Moody MP, et al. Ramsay Hunt Syndrome. [Updated 2023 Aug 28]. In: StatPearls [Internet]. Treasure Island (FL): StatPearls Publishing; 2026 Jan-. Available from: https://www.ncbi.nlm.nih.gov/books/NBK557409/
- Uscategui A, Doree C, Chamberlain IJ, Burton MJ. Antiviral therapy for Ramsay Hunt syndrome (herpes zoster oticus with facial palsy) in adults. Cochrane Database of Systematic Reviews. 2008;(4):CD006851. DOI: 10.1002/14651858.CD006851.pub2. Accessed 15 Jun 2026.
- Sweeney CJ, Gilden DH. Ramsay Hunt syndrome. J Neurol Neurosurg Psychiatry. 2001 Aug;71(2):149-54. doi: 10.1136/jnnp.71.2.149. PMID: 11459884; PMCID: PMC1737523.
- Stornaiuolo A, Iodice R, De Simone R, Russo C, Rubino M, Braca S, Miele A, Tozza S, Nolano M, Manganelli F. Multiple cranial neuropathy due to varicella zoster virus reactivation without vesicular rash: a challenging diagnosis. Neurol Sci. 2023 Oct;44(10):3687-3689. doi: 10.1007/s10072-023-06833-6. Epub 2023 May 9. PMID: 37156980; PMCID: PMC10495477.

Posted 9/4/2026

32F with hx of cystic fibrosis presented to ED with complaints of abdominal pain with nausea and vomiting.



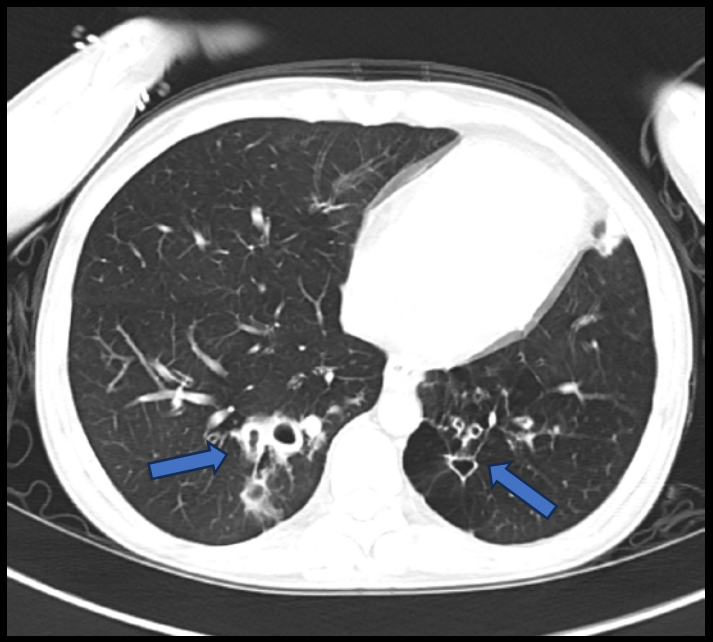
A) Axial CT Chest, Lung Window



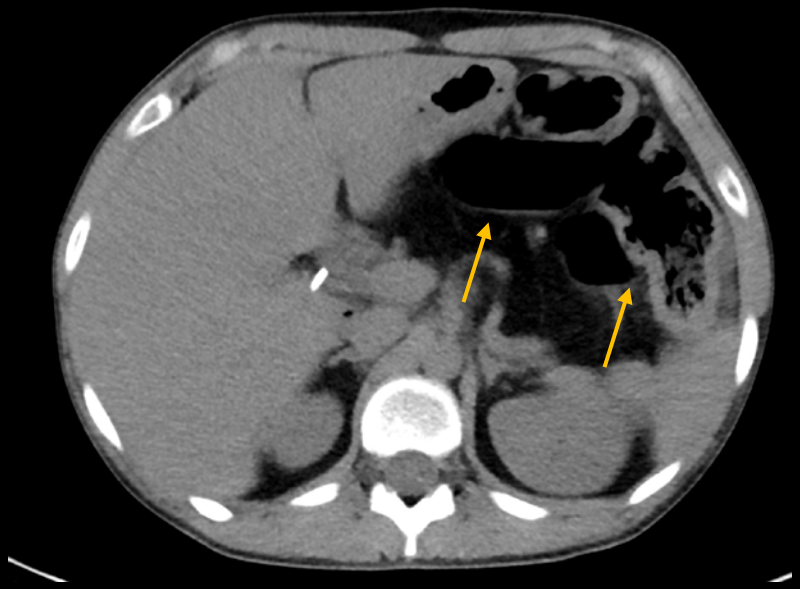
B) Axial noncontrast CT abdomen



C) Coronal noncontrast CT abdomen/pelvis



A) Axial CT Chest, Lung Window



B) Axial noncontrast CT abdomen



C) Coronal noncontrast CT abdomen/pelvis

Distal Intestinal Obstruction Syndrome

Imaging Findings: (A) Axial chest CT image displayed in lung windows demonstrates bilateral lower-lobe cylindrical bronchiectasis and bronchial-wall thickening. Several dilated bronchi are larger than their accompanying pulmonary arterial branches, producing a signet-ring appearance (blue arrows), consistent with cystic fibrosis–related lung disease. (B) Axial noncontrast CT of the abdomen demonstrates dilated gas- and fluid-filled small-bowel loops consistent with small-bowel obstruction (yellow arrows). (C) Coronal noncontrast CT of the abdomen and pelvis demonstrates multiple dilated distal small-bowel loops containing mottled gas and fecal-like material, with inspissated contents in the distal ileal/ileocecal region and upstream bowel dilation (green arrows). In the setting of cystic fibrosis, these findings support distal intestinal obstruction syndrome.

Differential Diagnosis: Distal Intestinal Obstruction Syndrome (DIOS), Constipation, Ileus, Adhesive small-bowel obstruction, Intussusception, Intestinal Volvulus

Discussion: Distal intestinal obstruction syndrome is a gastrointestinal complication unique to cystic fibrosis, characterized by partial or complete obstruction from thick fecal and mucoid material within the terminal ileum and proximal colon. Abnormal CFTR-mediated intestinal secretion, pancreatic insufficiency, dysmotility, and dehydration contribute to the formation of inspissated intestinal contents. Patients typically present with acute or subacute abdominal pain, distention, nausea, and vomiting. CT findings include fecalized material within the distal small bowel or ileocecal region with upstream bowel dilation and air-fluid levels. DIOS can be distinguished from constipation by its acute obstructive presentation and focal ileocecal impaction, whereas constipation generally produces chronic symptoms and fecal loading throughout the colon. Initial treatment includes rehydration and osmotic laxatives or polyethylene glycol lavage. Surgery is reserved for complications or obstruction that fails medical treatment. Because recurrence is common, adequate hydration and a maintenance bowel regimen are important.

@AOCRNews

@mckayberges
@aocrnews

Case courtesy of Mckay Berges OMS IV[1]; Ryan Flynn, DO[2]; Eric Chevrette, DO[2]
[1]Rocky Vista University College of Osteopathic Medicine; [2]Kettering Health Hospital

AOCR American Osteopathic College of Radiology

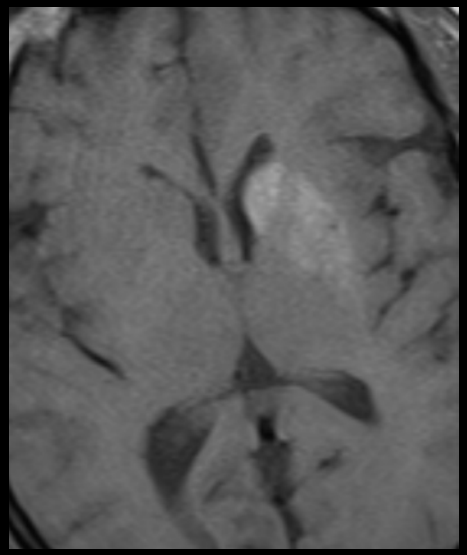
References

1. Munck, A., Alberti, C., Colombo, C., Kashirskaya, N., Ellemunter, H., Fotoulaki, M., Houwen, R., Robberecht, E., Boizeau, P., & Wilschanski, M. (2016). International prospective study of distal intestinal obstruction syndrome in cystic fibrosis: Associated factors and outcome. *Journal of Cystic Fibrosis*, *15*(4), 531–539. https://doi.org/10.1016/j.jcf.2016.02.002
2. Hort, A., Hameed, A., Middleton, P. G., & Pleass, H. C. (2019). Distal intestinal obstruction syndrome: An important differential diagnosis for abdominal pain in patients with cystic fibrosis. *ANZ Journal of Surgery*, *90*(5), 681–686. https://doi.org/10.1111/ans.15357
3. Colombo, C., Ellemunter, H., Houwen, R., Munck, A., Taylor, C., & Wilschanski, M. (2011). Guidelines for the diagnosis and management of distal intestinal obstruction syndrome in cystic fibrosis patients. *Journal of Cystic Fibrosis*, *10*. https://doi.org/10.1016/s1569-1993(11)60005-2
4. Dray, X., Bienvenu, T., Desmazes—dufeu, N., Dusser, D., Marteau, P., & Hubert, D. (2004). Distal intestinal obstruction syndrome in adults with cystic fibrosis. *Clinical Gastroenterology and Hepatology*, *2*(6), 498–503. https://doi.org/10.1016/s1542-3565(04)00169-7

Posted 8/28/2026

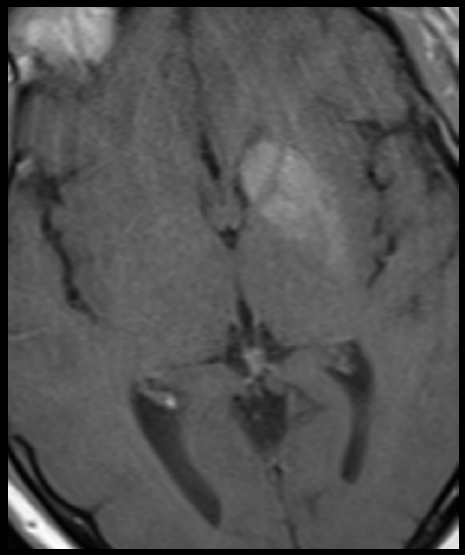
46 y/o F with hx of T2DM and blood glucose 435 mg/dL presenting with hemichoreoathetotic movements, dizziness, uncontrollable right foot movements, right facial twitching, and right-sided upper and lower extremity weakness.

A



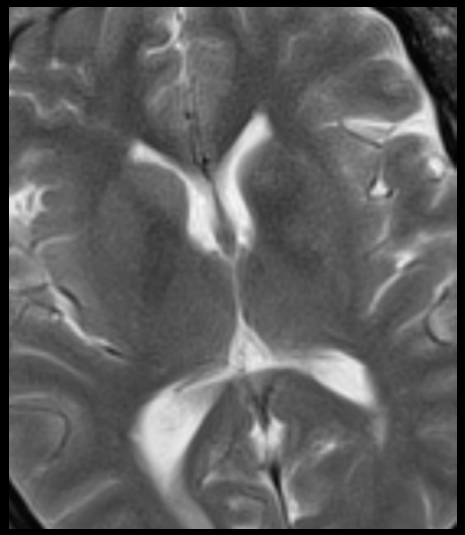
Axial T1 Precontrast

B



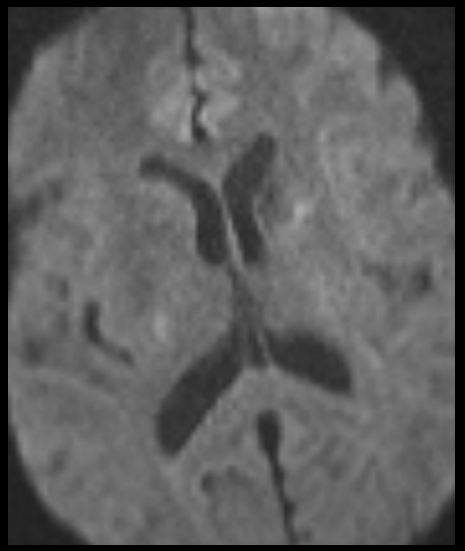
Axial T1 Postcontrast

C



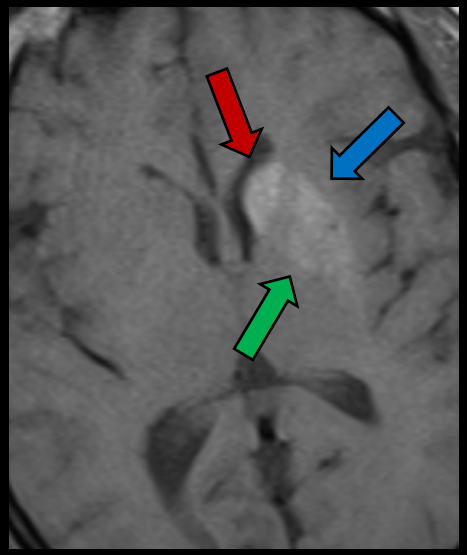
Axial T2

D



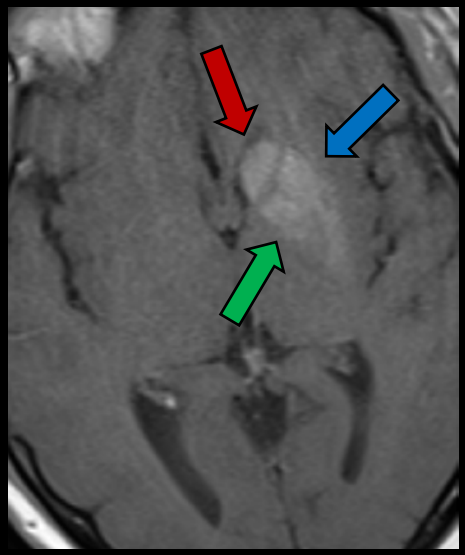
DWI

A



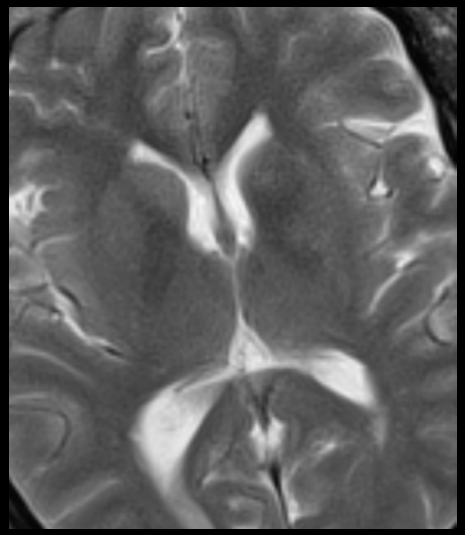
Axial T1 Precontrast

B



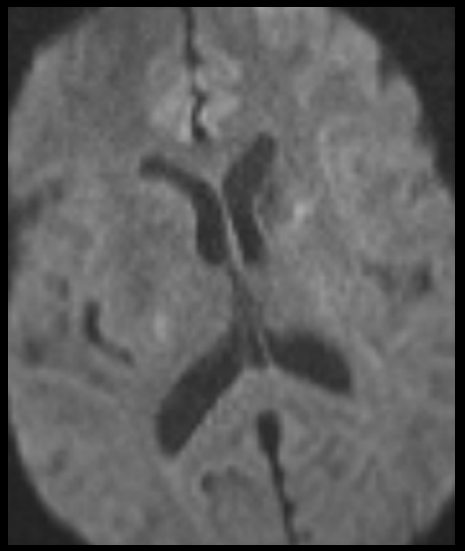
Axial T1 Postcontrast

C



Axial T2

D



DWI

Diabetic Striatopathy

Imaging findings: A) Axial T1-weighted MRI demonstrates marked unilateral hyperintensity involving the left caudate nucleus (red arrow), putamen (blue arrow), and globus pallidus (green arrow). B) Axial T1-weighted MRI following intravenous contrast administration shows no appreciable enhancement within these structures. C) Corresponding axial T2-weighted imaging demonstrates no significant signal abnormality. D) Diffusion-weighted imaging (DWI) shows no restricted diffusion.

Differential Diagnosis: Diabetic Striatopathy, Striatocapsular Infarct, Wilson's Disease, Basal Ganglia Calcification, Basal Ganglia Hemorrhage, Hepatic Encephalopathy

Discussion: Diabetic striatopathy (DS), also referred to as non-ketotic hyperglycemic hemichorea (NHH), is a rare metabolic complication of poorly controlled diabetes mellitus, with a reported prevalence of approximately 1 per 100,000 individuals. Approximately 90% of reported cases occur in patients of Asian ethnicity. Proposed diagnostic criteria include hyperglycemia associated with chorea/ballism and/or striatal hyperdensity on CT or T1 hyperintensity on MRI.

Patients typically present with involuntary hyperkinetic movements accompanied by T1 hyperintensity of the striatum, most often affecting the putamen, with less frequent involvement of the caudate nucleus and globus pallidus. T1 hyperintensity is the most consistent MRI finding, whereas T2/FLAIR, SWI, and DWI findings are variable. Striatal hyperdensity on CT may mimic intracerebral hemorrhage, potentially leading to misdiagnosis. In contrast, MRI typically demonstrates no significant enhancement, mass effect, or surrounding edema, helping distinguish DS from hemorrhagic or ischemic stroke. Unlike other metabolic disorders affecting the basal ganglia, which typically produce bilateral changes, DS most often presents with unilateral striatal involvement. Clinical and imaging findings may be discordant, with some patients remaining asymptomatic despite characteristic imaging abnormalities, while others present with movement disorders despite unremarkable neuroimaging.

The pathophysiology underlying the neuroimaging findings remains unclear and is likely multifactorial. Although not fully understood, other proposed mechanisms for the imaging findings include: (1) protein desiccation during Wallerian degeneration and (2) reactive astrocytosis with an abundance of gemistocytes.

Management consists of prompt correction of hyperglycemia, optimization of long-term glycemic control, and symptomatic treatment with antidopaminergic agents when indicated. The imaging findings and symptoms typically improve and can completely resolve with adequate blood glucose control.

Case courtesy of Mohammad Aljazi, DO PhD[1], Macksood Aftab, DO[2]
[1]Michigan State University College of Osteopathic Medicine, [2]MSU-CHM, CMU-CM

References

- Arecco A, Ottaviani S, Boschetti M, Renzetti P, Marinelli L. Diabetic striatopathy: an updated overview of current knowledge and future perspectives. J Endocrinol Invest. 2024;47(1):1-15. doi:10.1007/s40618-023-02166-5

- Dubey S, Biswas P, Ghosh R, Chatterjee S, Kanti Ray B, Benito-León J. Neuroimaging of Diabetic Striatopathy: More Questions than Answers. Eur Neurol. 2022;85(5):371-376. doi:10.1159/000524936

- Wilson TJ, Than KD, Stetler WR Jr, Heth JA. Non-ketotic hyperglycemic chorea-hemiballismus mimicking basal ganglia hemorrhage. J Clin Neurosci. 2011;18(11):1560-1561. doi:10.1016/j.jocn.2011.03.010

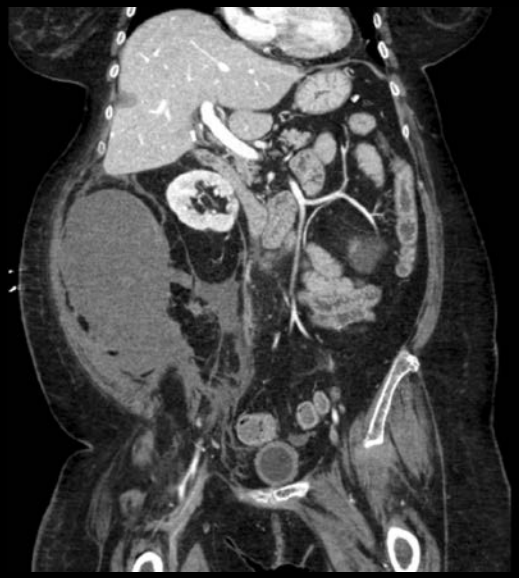
- Tsalta-Mladenov ME, Georgieva DK, Andonova SP. Hyperglycemic hemichorea due to diabetic striatopathy: case-based review. Curr Med Res Opin. 2022;38(3):365-369. doi:10.1080/03007995.2021.2015159

- Huang X, Qi J, Li Y, Li J, Yang MG. Diabetic Striatopathy Complicated With Acute Ischemic Stroke: A Case Report. Front Neurosci. 2022;16:877479. Published 2022 Jul 12. doi:10.3389/fnins.2022.877479

Posted 8/21/2026

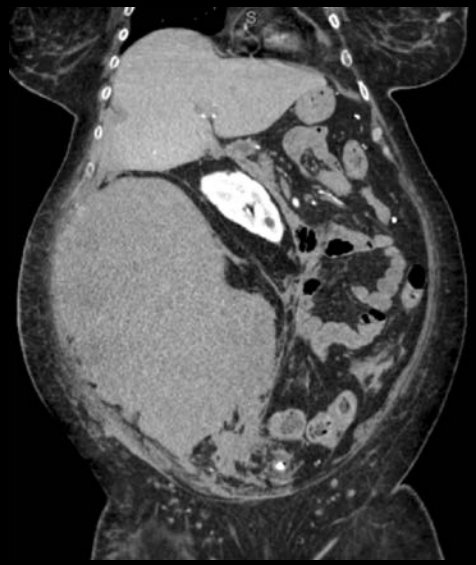
56 y/o F with hx of DVT/PE on therapeutic anticoagulation, SLE, HTN, and T2DM presented to the ED with generalized weakness, abdominal discomfort, hypotension, and tachycardia.

A



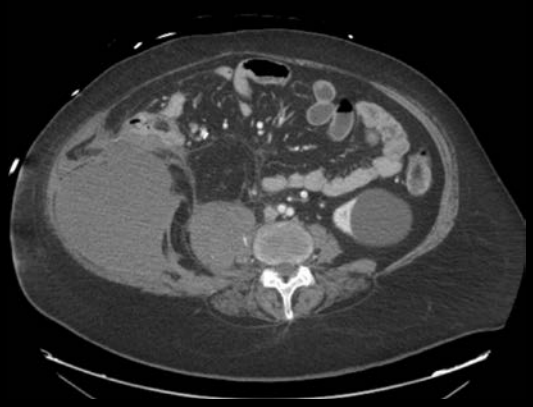
Coronal Contrast-Enhanced CT

C



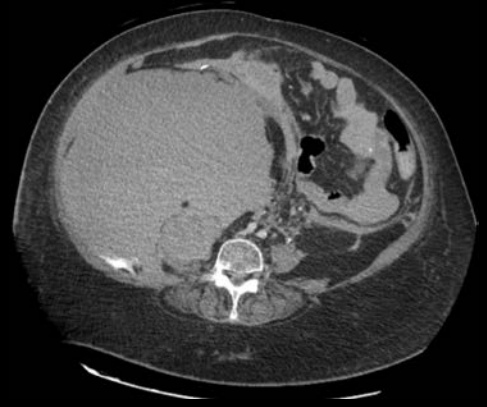
Coronal Contrast-Enhanced CT

B



Axial Contrast-Enhanced CT

D



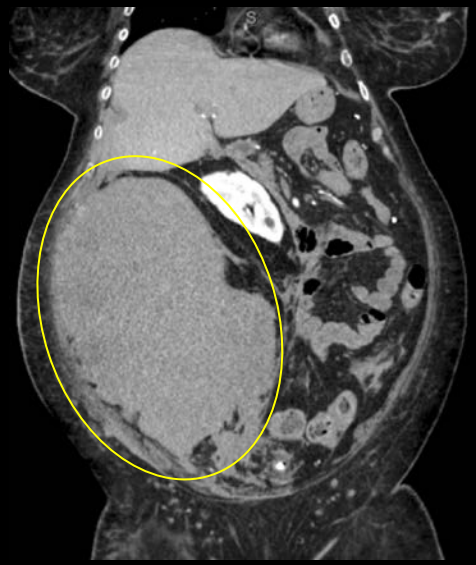
Axial Contrast-Enhanced CT

A



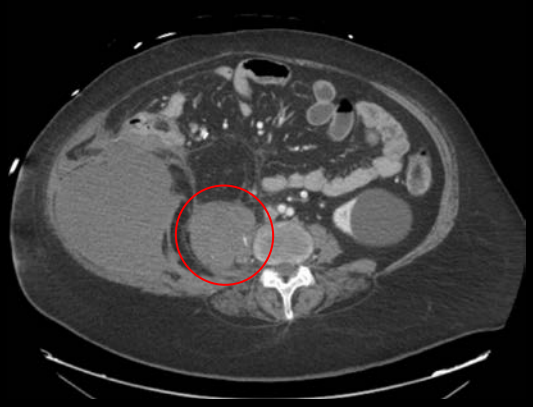
Coronal Contrast-Enhanced CT

C



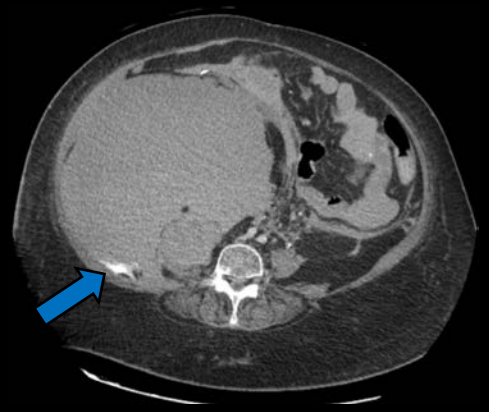
Coronal Contrast-Enhanced CT

B



Axial Contrast-Enhanced CT

D



Axial Contrast-Enhanced CT

Spontaneous retroperitoneal hematoma

Imaging findings: Coronal and axial contrast-enhanced CT of the abdomen and pelvis (Figures A and B) demonstrate a large right retroperitoneal hematoma (yellow circle) with significant mass effect, displacing the right kidney anteromedially and the right colon anteriorly measuring at11.3 x 9.3 x 17.4 cm. An associated right psoas hematoma (red circle) which measures at 6.3 x 5.8 cm with multifocal foci of active contrast extravasation. Post-embolization contrast-enhanced CT (Figures C and D) demonstrates interval enlargement of the retroperitoneal hematoma measuring at 25 x 5 x 24 cm, with new foci of active contrast extravasation (blue arrow) in the inferior hematoma.

Differential Diagnosis: Spontaneous retroperitoneal hematoma, vasculitis-related vascular rupture, retroperitoneal vascular malformation, hemorrhagic retroperitoneal neoplasm

Discussion: Spontaneous retroperitoneal hematoma (SRH) is a rare but potentially life-threatening cause of internal hemorrhage occurring without preceding trauma or invasive intervention. Although most frequently associated with anticoagulation therapy, SRH may also occur in the setting of coagulopathy and vascular disorders. Clinical presentation is often nonspecific, ranging from abdominal, flank, or back pain to generalized weakness and signs of hypovolemia. Due to the large capacity of the retroperitoneal space, substantial blood loss may occur before clinical deterioration, contributing to delayed diagnosis.

Contrast-enhanced CT is the imaging modality of choice for SRH, allowing evaluation of hematoma extent and detection of active hemorrhage. Management is guided by hemodynamic status and may include supportive care, reversal of anticoagulation, transcatheter arterial embolization, or surgical intervention.

In the presented case, CT obtained during evaluation for suspected pulmonary embolism incidentally revealed a large right retroperitoneal hematoma. Imaging demonstrated multifocal active hemorrhage requiring two embolization procedures with a total of 60 coils targeting multiple arterial territories, including iliac, intercostal, and lumbar branches. Despite endovascular intervention, the patient developed progressive hematoma expansion, abdominal compartment syndrome, and multisystem organ failure, ultimately resulting in death. While the likely diagnosis is SRH, given the patient's past medical history, an underlying vasculitis-associated vascular injury may have synergistically contributed to the clinical presentation. This case highlights the complexity of managing extensive SRH and underscores the importance of early diagnosis, prompt intervention, and close clinical monitoring.

Case courtesy of Mohammad Aljazi, DO[1], Steve Min, DO, MPH, MBA, FAOCR[2]
[1]Michigan State University College of Osteopathic Medicine, [2]Henry Ford Hospital

References

- Mondie C, Maguire NJ, Rentea RM. Retroperitoneal Hematoma. In: *StatPearls*. Treasure Island (FL): StatPearls Publishing; June 7, 2024.

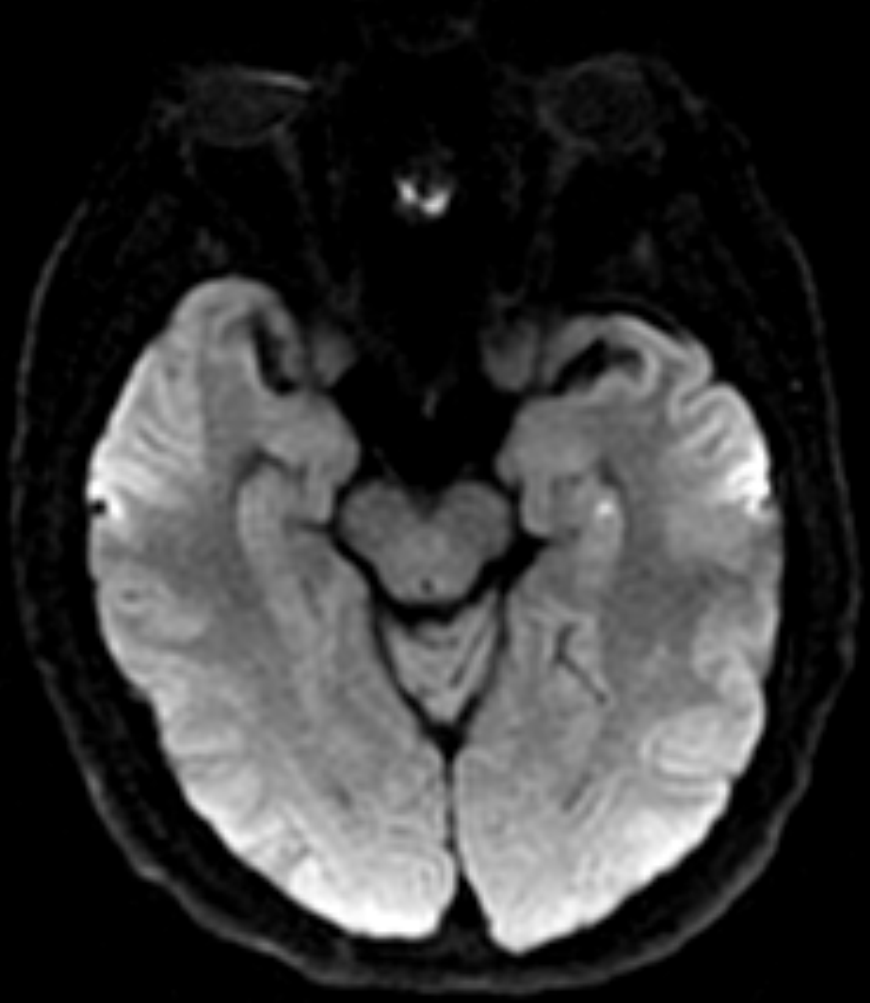
- Kurotaki T, Okada N, Sakurai Y, et al. Spontaneous retroperitoneal hematoma: a case report. *J Med Case Rep*. 2023;17(1):70. Published 2023 Feb 28. doi:10.1186/s13256-023-03794-4

- Oh CH, Cho SB, Kwon H. Clinical Outcomes and Safety of Transcatheter Arterial Embolization in Patients with Traumatic or Spontaneous Psoas and Retroperitoneal Hemorrhage. *J Clin Med*. 2024;13(11):3317. Published 2024 Jun 4. doi:10.3390/jcm13113317

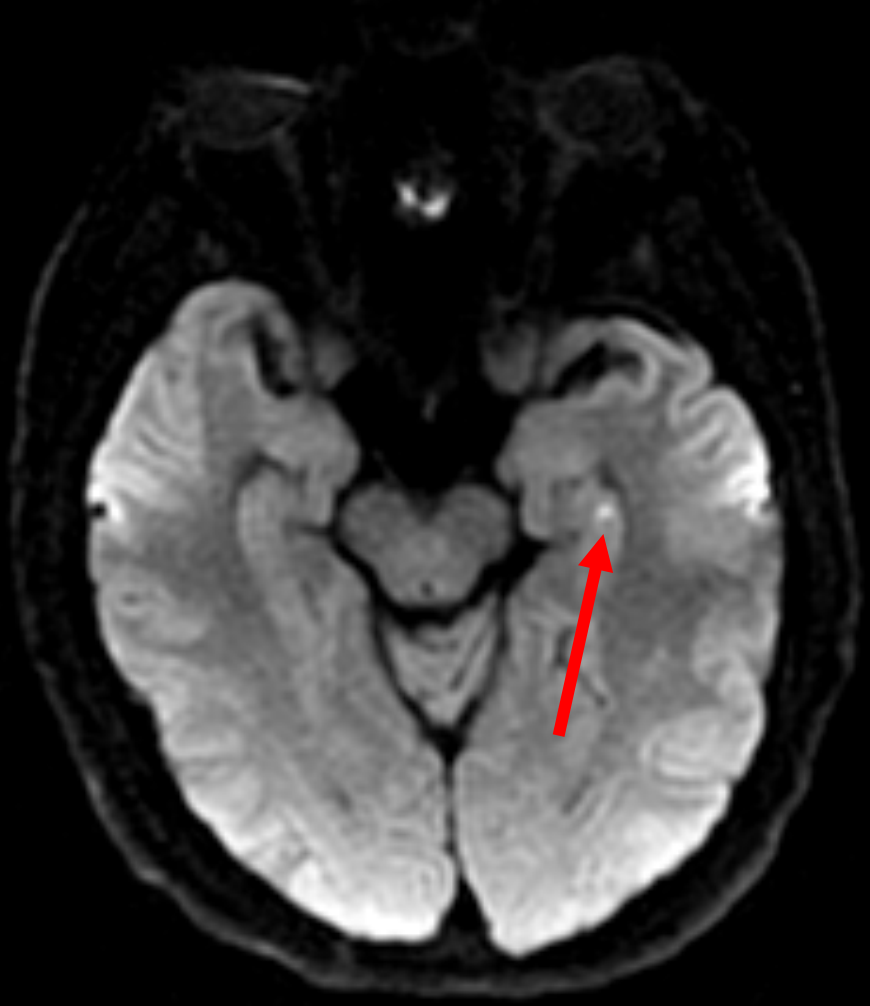
- Chan YC, Morales JP, Reidy JF, Taylor PR. Management of spontaneous and iatrogenic retroperitoneal haemorrhage: conservative management, endovascular intervention or open surgery?. *Int J Clin Pract*. 2008;62(10):1604-1613. doi:10.1111/j.1742-1241.2007.01494.x

Posted 8/14/2026

59 y/o male presented with memory loss/altered mental status with concern for embolic infarcts on CT head.



Axial



Axial

Transient Global Amnesia

Imaging Findings: Punctate hippocampal lesion on DWI

Differential Diagnosis: Transient global amnesia, ischemic amnesia, transient epileptic amnesia, dissociative amnesia

Discussion: Transient global amnesia (TGA) is an acute, self-limited syndrome characterized by sudden-onset anterograde amnesia, mild retrograde amnesia, and repetitive questioning. TGA usually resolves within 6 hours, and always resolves within 24 hours. It most commonly affects individuals older than 50 years, with an incidence of 3-8 per 100,000 person-years. Common triggers include emotional stress, physical exertion, and sexual intercourse. TGA classically lacks focal neurologic deficits. However, ischemic amnesia, a common mimic, may also lack focal neurologic deficits. DWI may distinguish between the two, with TGA featuring isolated hippocampal lesions, and ischemic amnesia typically featuring extrahippocampal lesions.

@AOCRNews

@aocrnews

Case courtesy of Gabriel Raytsis, MS2; Robert Martin, DO; Robert Koenigsberg, DO, FAOCR
Lewis Katz School of Medicine / Temple University

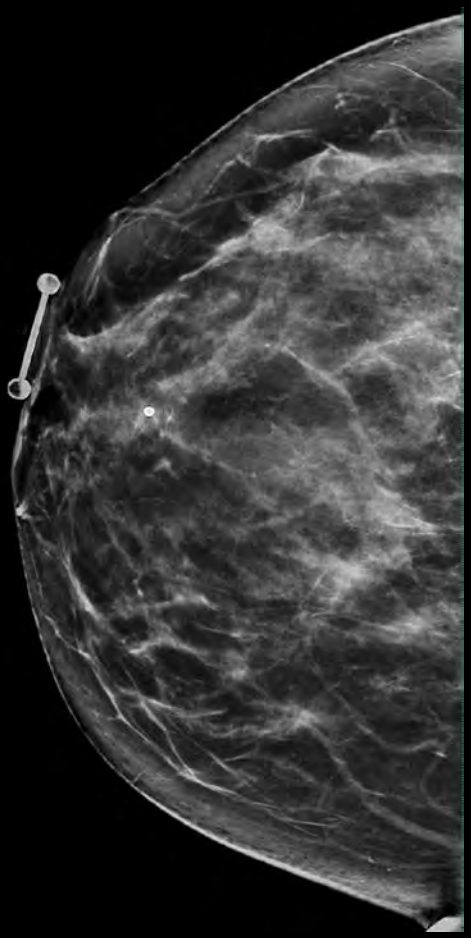
AOCR American Osteopathic College of Radiology

References

- Ropper AH. Transient Global Amnesia. N Engl J Med. 2023 Feb 16;388(7):635-640. doi: 10.1056/NEJMra2213867. PMID: 36791163.
- Sealy D, Tiller RJ, Johnson K. Transient Global Amnesia. Am Fam Physician. 2022 Jan 1;105(1):50-54. PMID: 35029951.
- Michel P, Beaud V, Eskandari A, Maeder P, Demonet JF, Eskioglou E. Ischemic Amnesia: Causes and Outcome. Stroke. 2017 Aug;48(8):2270-2273. doi: 10.1161/STROKEAHA.117.017420. Epub 2017 Jun 5. PMID: 28584000.
- Bartsch T, Deuschl G. Transient global amnesia: functional anatomy and clinical implications. Lancet Neurol. 2010 Feb;9(2):205-14. doi: 10.1016/S1474-4422(09)70344-8. PMID: 20129169.

Posted 8/7/2026

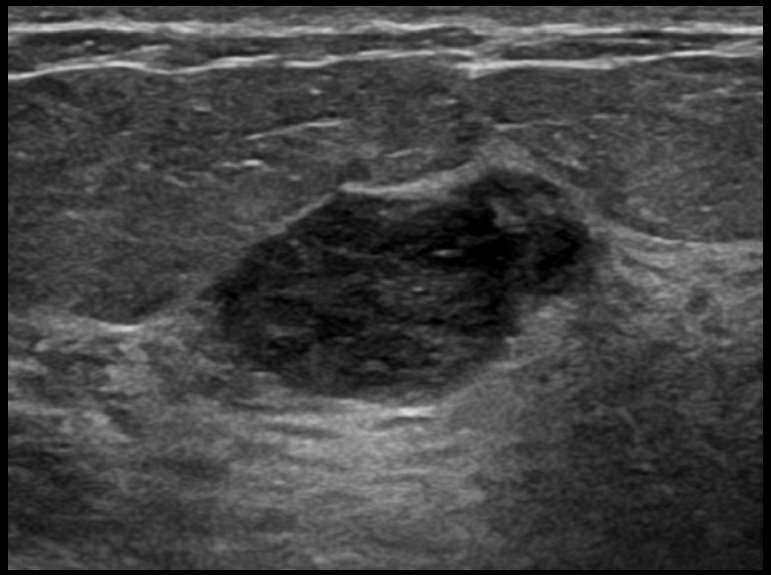
32F with palpable right breast mass in the setting of elevated familial breast cancer risk.



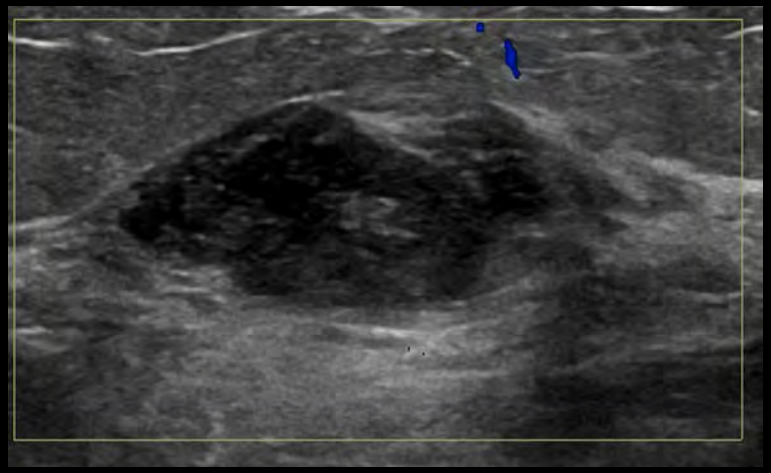
A) Right breast mammogram, RCC 2D synthesized view



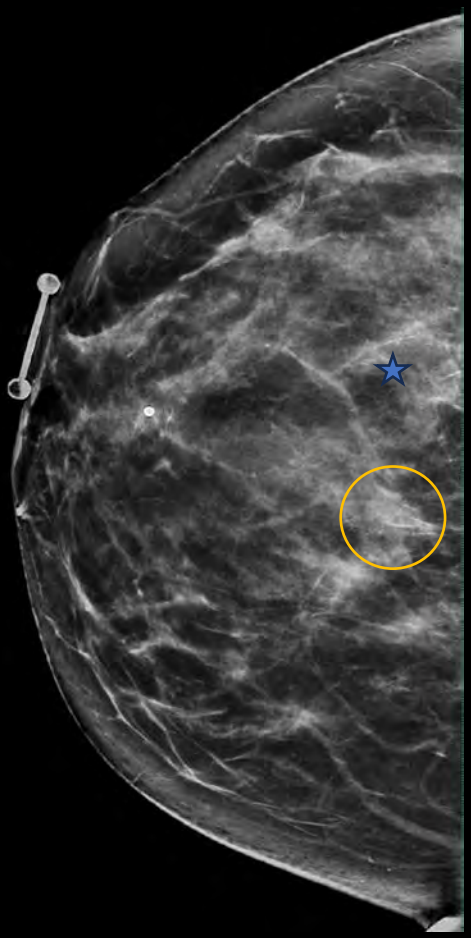
B) Right breast mammogram, RMLO 2D synthesized view



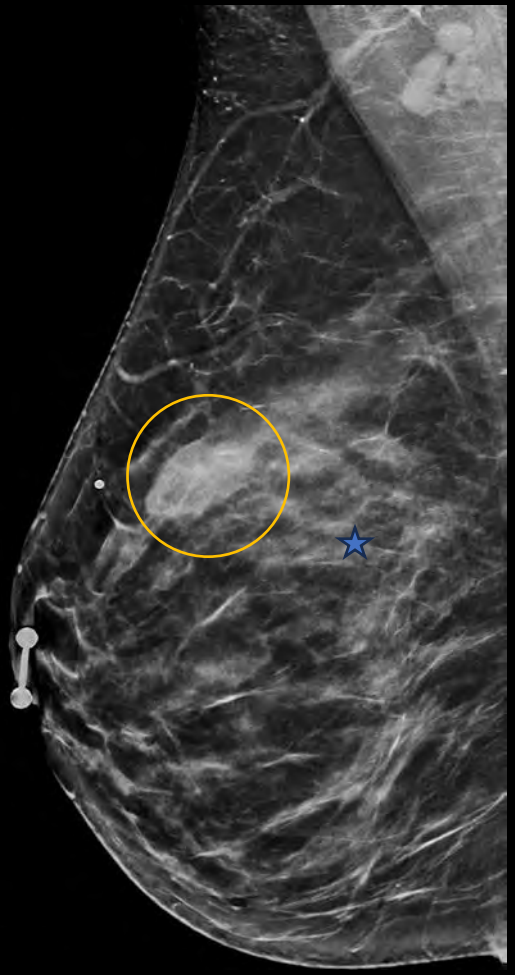
C) Right breast ultrasound, 12:00 position, 3cm from right nipple



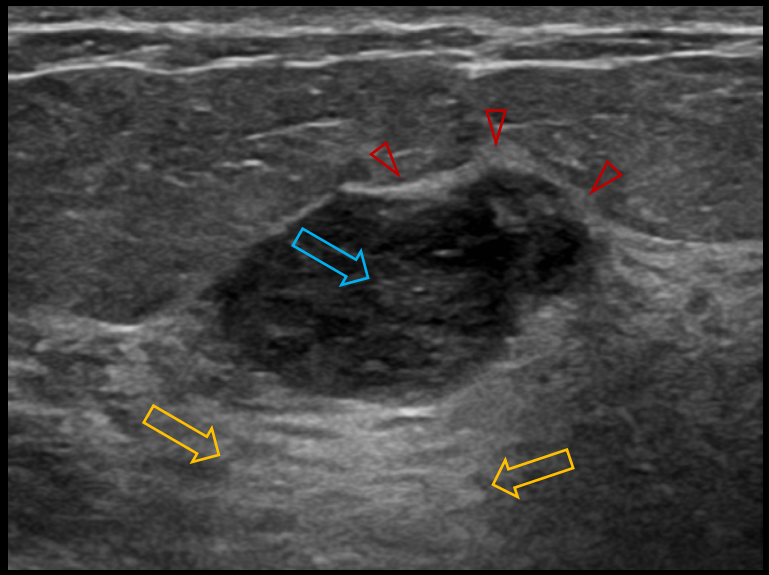
D) Right breast doppler ultrasound, 12:00 position, 3cm from right nipple



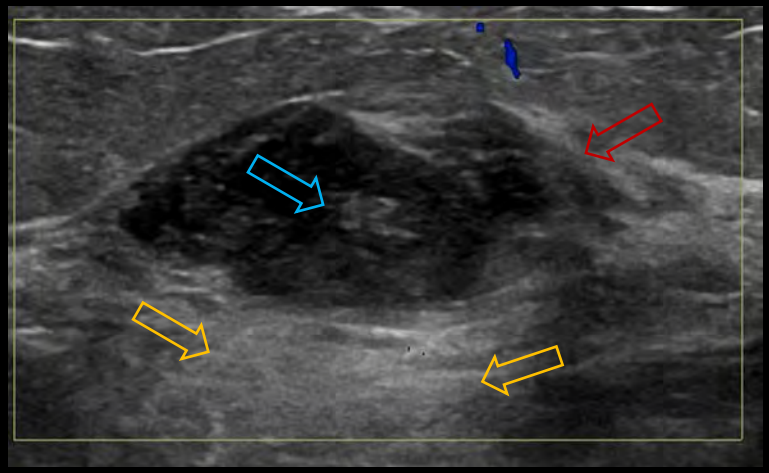
A) Right breast mammogram, RCC 2D synthesized view



B) Right breast mammogram, RMLO 2D synthesized view



C) Right breast ultrasound, 12:00 position, 3cm from right nipple



D) Right breast doppler ultrasound, 12:00 position, 3cm from right nipple

Angiomyxoma of the breast

Imaging Findings: (A, B) Partially circumscribed mass measuring 1.9 x 2.9 cm within the right upper breast (yellow circle), in a background of heterogeneously dense breast tissue (blue star). (C, D) Oval complex cystic mass (blue arrow) with irregular margins (red arrowheads) measuring 2.9 x 2.0 x 1.9 cm. The mass demonstrates increased through transmission (yellow arrow) and lack of vascularity (red arrow). This BI-RADS 4 mass underwent subsequent biopsy.

Differential Diagnosis: Fibroadenoma, phyllodes tumor, complex fibrocystic changes, intraductal papilloma, breast cancer.

Discussion: Angiomyxoma of the breast is a rare benign mesenchymal tumor composed of hypocellular spindle cells embedded in abundant myxoid stroma. Imaging findings are nonspecific. Mammography typically demonstrates a circumscribed or partially circumscribed round, oval, or lobulated mass without calcifications. Ultrasound findings include an oval or lobulated hypoechoic or complex mass with variable margins. Posterior acoustic enhancement, as observed in this case, is common due to the gelatinous myxoid matrix. Internal vascularity on Doppler imaging is variable, and lesions may demonstrate compressibility related to their myxoid composition. Because of overlap with other benign and malignant breast masses, histopathologic evaluation is required for definitive diagnosis. Complete surgical excision with negative margins is the preferred treatment, with imaging follow-up recommended given the risk of local recurrence. Breast angiomyxoma may rarely be associated with Carney complex, an autosomal dominant syndrome characterized by cardiac and cutaneous myxomas, pigmented skin lesions, and endocrine abnormalities; therefore, clinical assessment for syndromic features, including consideration of genetic evaluation and cardiac screening, may be appropriate.

@UpstateRad
@AOCRNews
@upstaterads
@aocrnews

Case courtesy of Fahad Farooq, MD & Katherine Willer, DO
SUNY Upstate Medical University

AOCR American Osteopathic College of Radiology

References

Baranov E, Alston ELJ, Lester SC, Fletcher CDM, Doyle LA. Angiomyxoma of the breast: a clinicopathologic analysis of 40 cases. Am J Surg Pathol. 2023;47(3):296-306. doi:10.1097/PAS.0000000000001989.

Dubin I, Mortazavi S, Yu T, Riahi IR, Baker JL. Superficial angiomyxoma of the breast in a 16-year-old girl without Carney's complex: a case report. Breast J. 2021;27(12):887-889. doi:10.1111/tbj.14301.

Ilagan C, Putra J. Superficial angiomyxoma. In: PathologyOutlines.com [Internet]. PathologyOutlines.com; [cited 2026 Jul 12]. Available from: https://www.pathologyoutlines.com/topic/skintumornonmelanocyticsuperficialangio.html

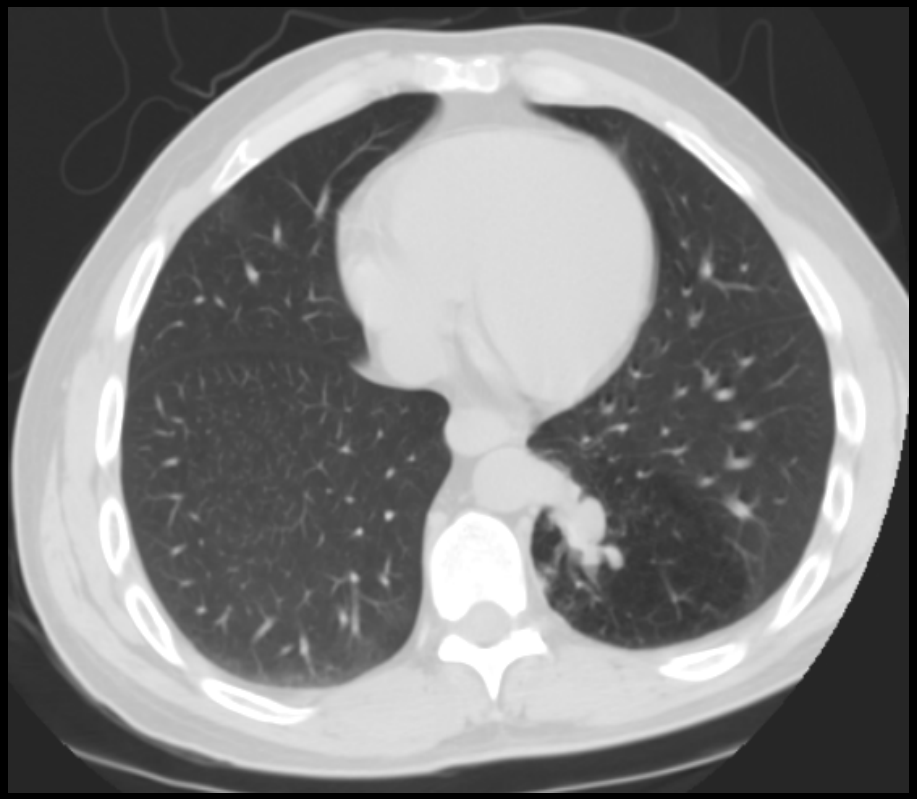
Stratakis CA. Carney complex. In: Adam MP, Bick S, Mirzaa GM, et al., editors. GeneReviews® [Internet]. Seattle (WA): University of Washington, Seattle; 1993–2026 [updated 2023 Sep 21; cited 2026 Jul 12]. Available from: https://www.ncbi.nlm.nih.gov/books/NBK1286/

Meng T, Yin H, Chen L, Zhao Q. Superficial angiomyxoma of the breast in a 25-year-old woman without Carney complex. Asian J Surg. 2023;46(6):2461-2463. doi:10.1016/j.asjsur.2022.12.063.

Posted 7/31/2026

39 M presents to the ER for flank pain (incidental finding in the lung)

Axial CT without IV contrast

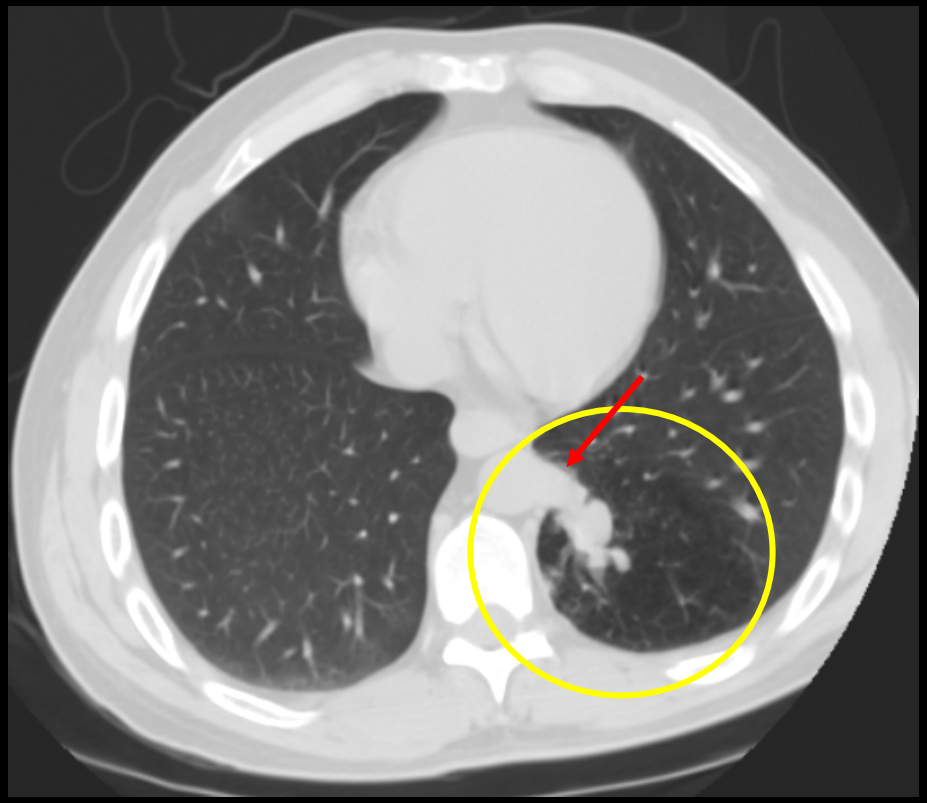


Lung window

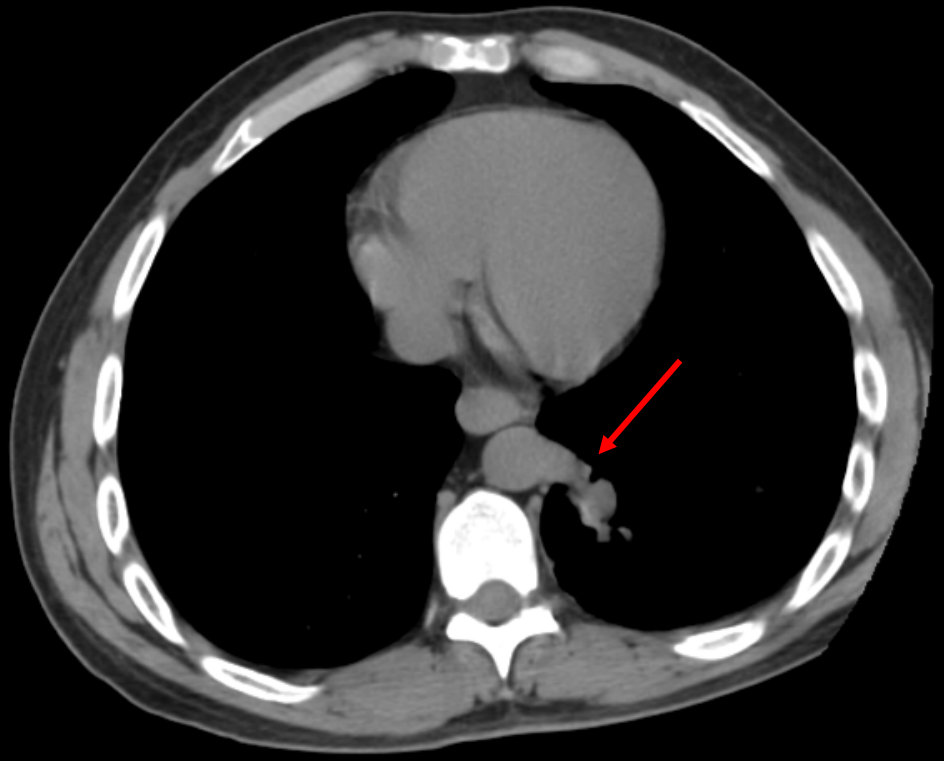


Soft tissue window

Axial CT without IV contrast



Lung window



Soft tissue window

Pulmonary Sequestration

Imaging findings: Within the left lower lobe posterior basal segment, there is a multicystic lesion (yellow circle) with systemic arterial supply (red arrow) arising from the descending thoracic aorta.

Differential diagnosis: congenital pulmonary airway malformation (CPAM), bronchogenic cyst, pleuropulmonary blastoma

Discussion: Pulmonary sequestration is nonfunctioning pulmonary tissue with no connection to the tracheobronchial tree or pulmonary arteries. It receives arterial supply from systemic origin, typically the descending thoracic aorta. There are two types of pulmonary sequestration: intralobar and extralobar. Intralobar sequestration is more common and shares the same pleural covering with adjacent normal lung parenchyma. Intralobar sequestration typically drains to the pulmonary veins, but can also drain into the azygous-hemiazygous sytem, right atrium, portal vein, or IVC. Extralobar sequestration is separated from adjacent normal lung parenchyma by it's own pleural covering and drains through the systemic veins into the right atrium.

Treatment: Conservative. If symptomatic (such as recurrent infections), surgical excision is the treatment of choice.

@DrYoonCho
@AOCRNews
@aocrnews

Case courtesy of Yoon Cho, DO
Oklahoma State University Center for Health and Sciences

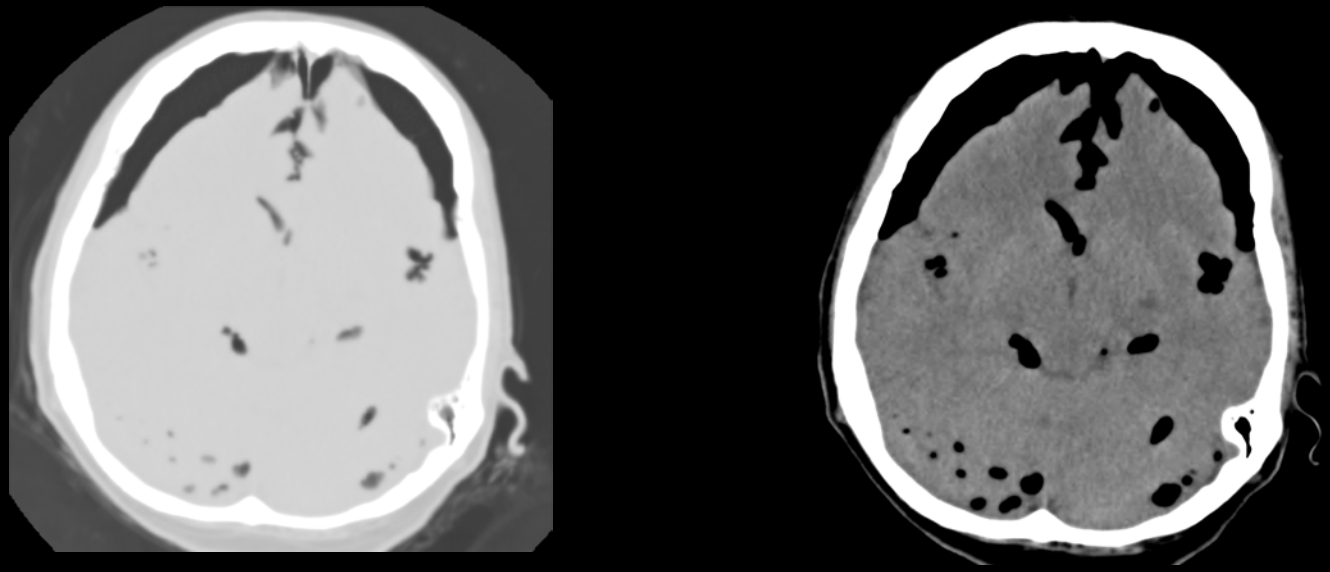
AOCR American Osteopathic College of Radiology

References

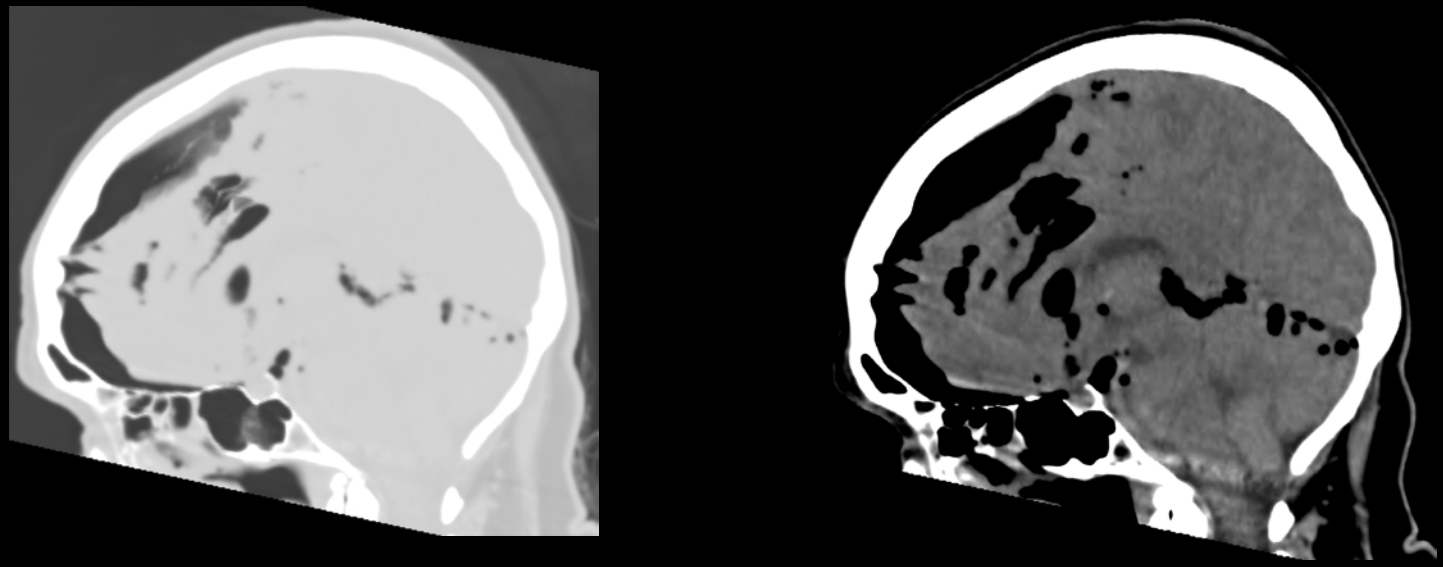
- None

Posted 7/24/2026

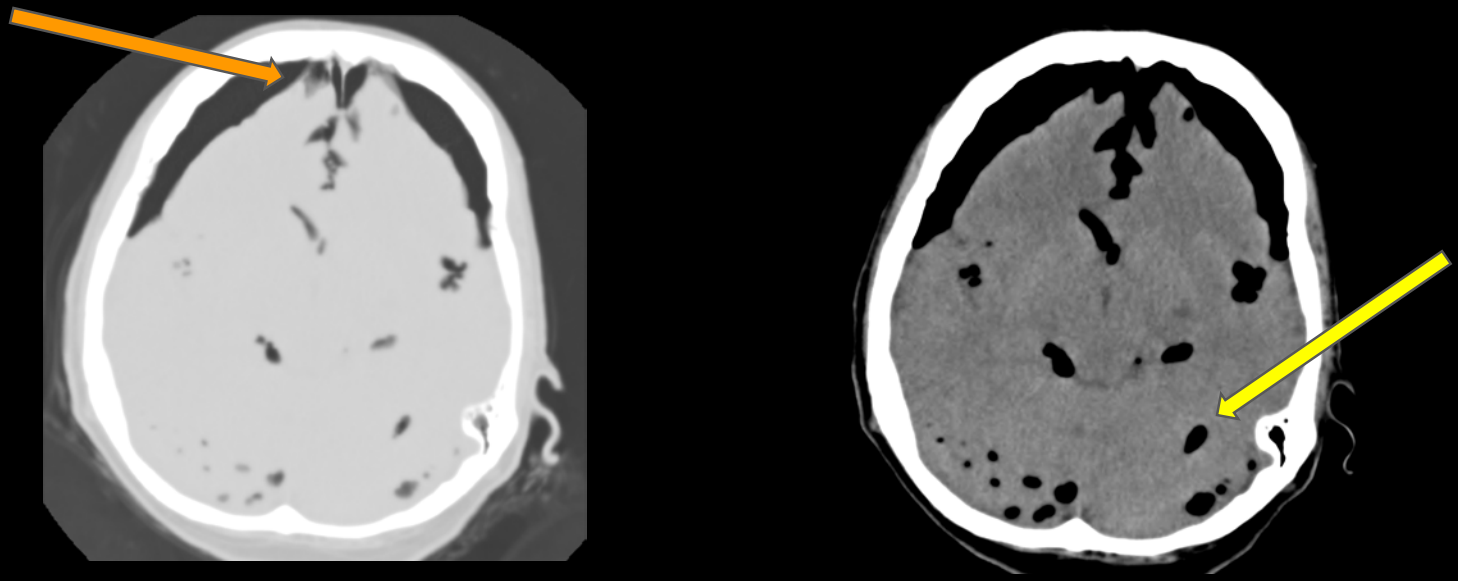
71 y/o F with history of recent sinus surgery who presented to the ED complaining of severe headache for one day associated with vomiting.



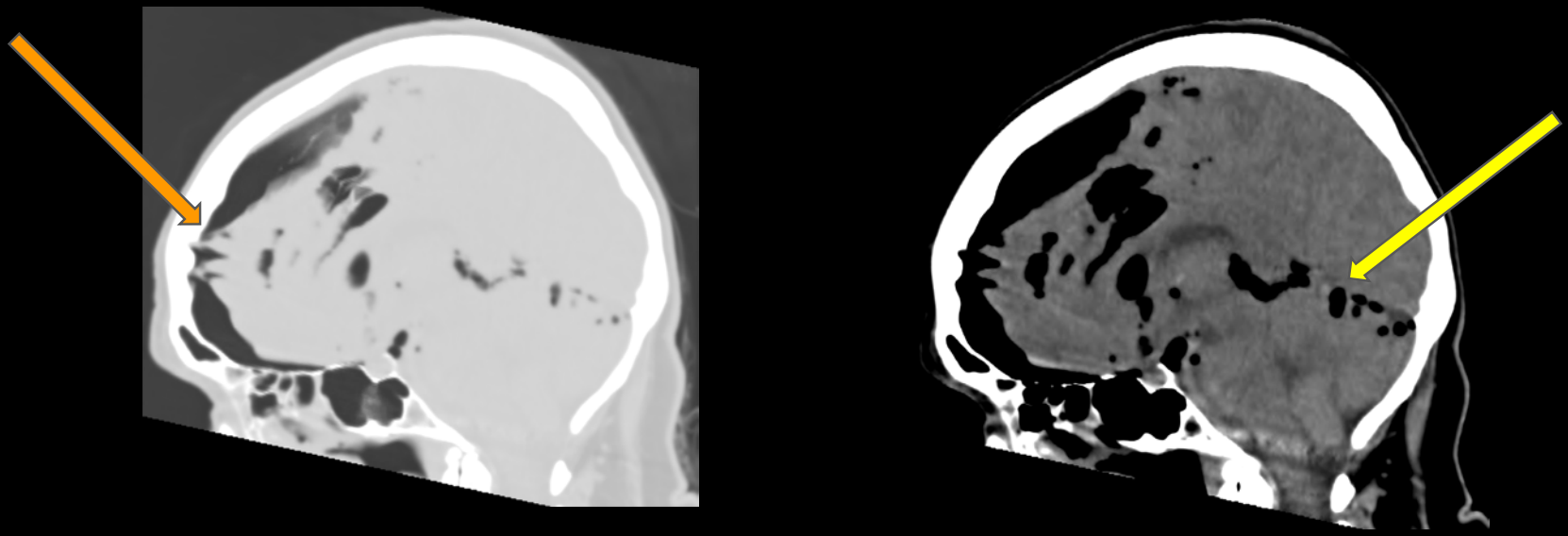
Axial CT Head w/o Contrast



Sagittal CT Head w/o Contrast



Axial CT Head w/o Contrast



Sagittal CT Head w/o Contrast

Tension Pneumocephalus

Imaging Findings: Non-contrast CT head demonstrates a significant amount of subdural air exerting mass effect and compression of the frontal lobes. The frontal lobes demonstrate a peaked appearance with tethering by cortical veins ("Mount Fuji sign", orange arrows). Additionally, there are numerous foci of subarachnoid air throughout the brain ("Air bubble sign", yellow arrows).

Differential Diagnosis: Non-tension pneumocephalus

Discussion: Tension pneumocephalus is a neurosurgical emergency which occurs when a collection of subdural air exerts mass effect on the brain, unable to escape due to a ball-valve mechanism. Commonly this occurs in the setting of recent neuro/sinus surgery, however other etiologies may include trauma, infection, paranasal sinus tumors, and nitrous oxide use. Typical symptoms may include headaches, restlessness, deteriorating mental status, focal neurologic deficits, and cardiac arrest. While the Mount Fuji and air bubble signs are suggestive of tension, they are not pathognomonic and can be seen with pneumocephalus without tension. Thus, clinically deteriorating mental status is an important indicator for neurosurgical decompression.

Case courtesy of Ryan Yamane, DO and Frederick White, DO
Hemet Global Medical Center

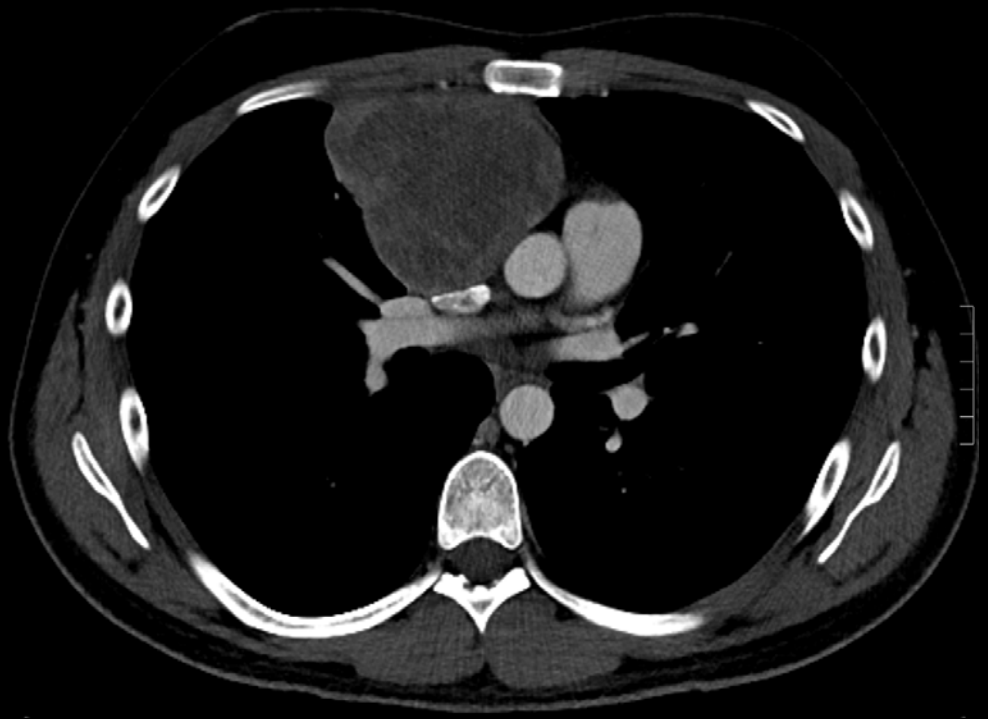
References

- Satapathy GC, Dash HH. Tension pneumocephalus after neurosurgery in the supine position. Br J Anaesth. 2000 Jan;84(1):115-7. doi: 10.1093/oxfordjournals.bja.a013368. PMID: 10740562.
- Pulickal GG, Sitoh YY, Ng WH. Tension pneumocephalus. Singapore Med J. 2014 Mar;55(3):e46-8. doi: 10.11622/smedj.2014041. PMID: 24664394; PMCID: PMC4293999.
- Heckmann JG, Ganslandt O. Images in clinical medicine. The Mount Fuji sign. N Engl J Med. 2004 Apr 29;350(18):1881. doi: 10.1056/NEJMicm020479. PMID: 15115834.
- Michel SJ. The Mount Fuji sign. Radiology. 2004 Aug;232(2):449-50. doi: 10.1148/radiol.2322021556. PMID: 15286317.
- Sinclair AG, Scoffings DJ. Imaging of the post-operative cranium. Radiographics. 2010 Mar;30(2):461-82. doi: 10.1148/rg.302095115. PMID: 20228329.
- Ishiwata Y, Fujitsu K, Sekino T, Fujino H, Kubokura T, Tsubone K, Kuwabara T. Subdural tension pneumocephalus following surgery for chronic subdural hematoma. J Neurosurg. 1988 Jan;68(1):58-61. doi: 10.3171/jns.1988.68.1.0058. PMID: 3335913.
- Sebastian B & Moideen J. Mount Fuji is Not as “Active” as We Think. IJNS. 2018;07(03):278-9. doi:10.1055/s-0038-1667388

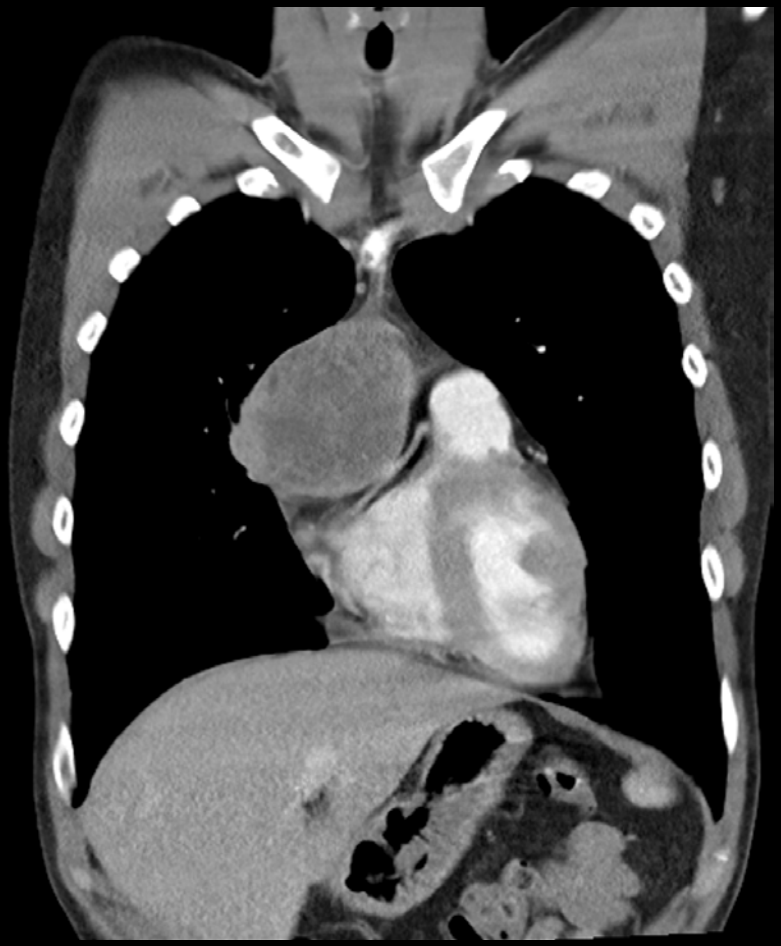
Posted 7/17/2026

25 y/o m with no significant hx presented to PCP with 2-month history of recurrent fever following URI. Additionally, he experienced right-sided chest and shoulder pain as well as shortness of breath.

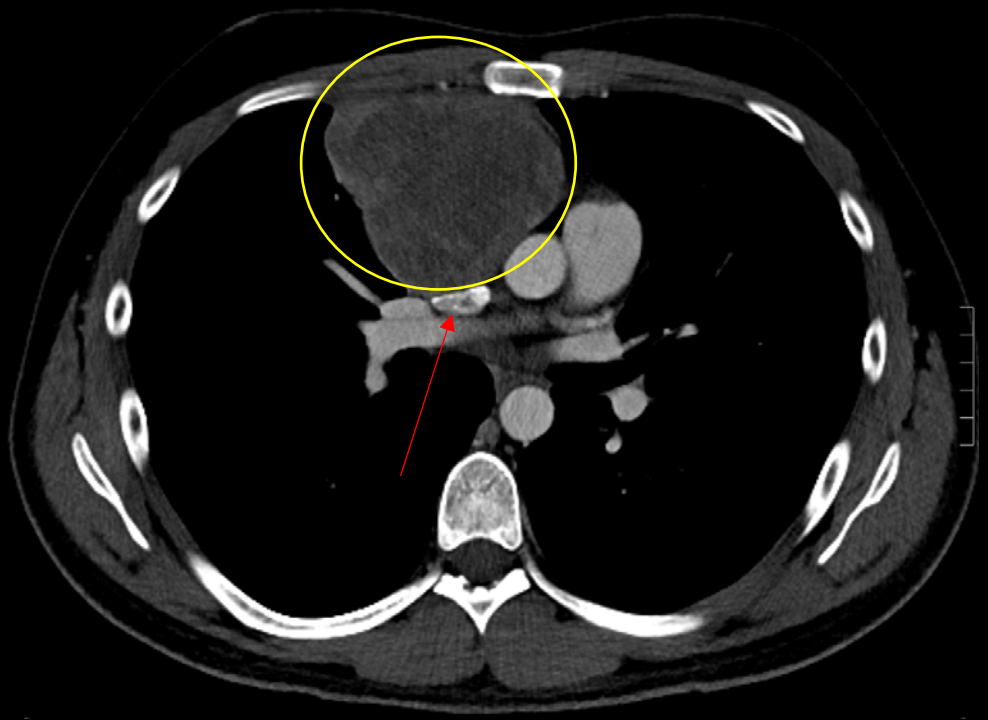
Axial Contrasted CT Chest



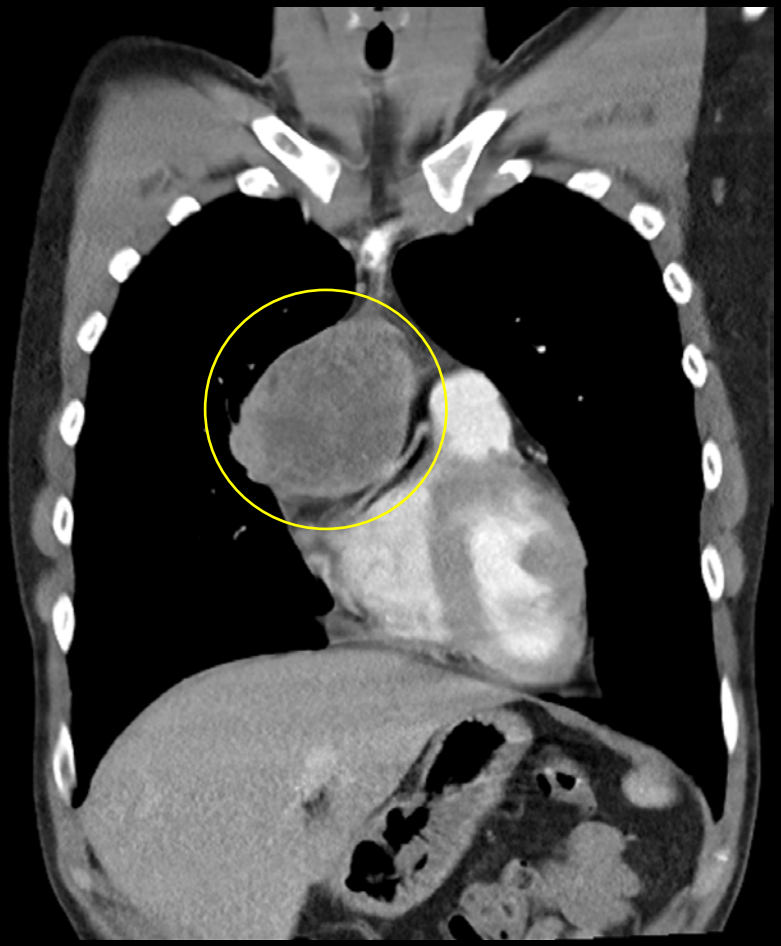
Coronal Contrasted CT Chest



Axial Contrasted CT Chest



Coronal Contrasted CT Chest



Mediastinal Yolk Sac Tumor

Imaging Findings: Right-sided heterogeneous anterior mediastinal mass (yellow circles) superior to the right atrium which measures 8.6 x 7.7 x 7.3 cm and exerts mass effect on the adjacent vascular structures, most notably the superior vena cava (red arrow).

Pathology: Germ cell tumor with morphological and immunohistochemical profile favoring yolk sac tumor.

Serum tumor markers: AFP (+), HCG (-)

Differential Diagnosis: Germ cell tumor, lymphoma, thymus or thyroid neoplasm

Discussion: Germ cell tumors (GST) are one of the causes of anterior mediastinal masses, accounting for approximately 15% of all mediastinal cysts and tumors. Primary mediastinal GCTs represent about 10–15% of mediastinal masses and are the most common location of primary extragonadal GCTs. Extragonadal GCTs represent 1 to 5% of all GCTs. Pediatric GCTs have a bimodal age distribution, with peaks during infancy and after puberty. Histologically, the primary distinction is seminoma vs nonseminomatous germ cell tumor (NSGCT). NSGCT can be further subdivided into teratoma (most common, accounting for approximately 60% of mediastinal germ cell tumors), embryonal carcinoma, choriocarcinoma, yolk sac tumor, and mixed germ cell tumor. Mature teratoma (<50% immature components) is considered benign. All of the other entities are considered malignant. It is difficult to distinguish between the various malignant histologies on imaging, and thus serum markers (AFP, serum HCG) and biopsy are usually required for definitive diagnosis. This case was a biopsy-proven yolk sac tumor, which has an unfavorable prognosis if it is not treated aggressively.

@AOCRNews

@haydenmfox
@aocrnews

Case courtesy of Hayden M. Fox, DO, Joshua Moore, DO, Nicholas Strle, DO | Oklahoma State University Center for Health Sciences

References

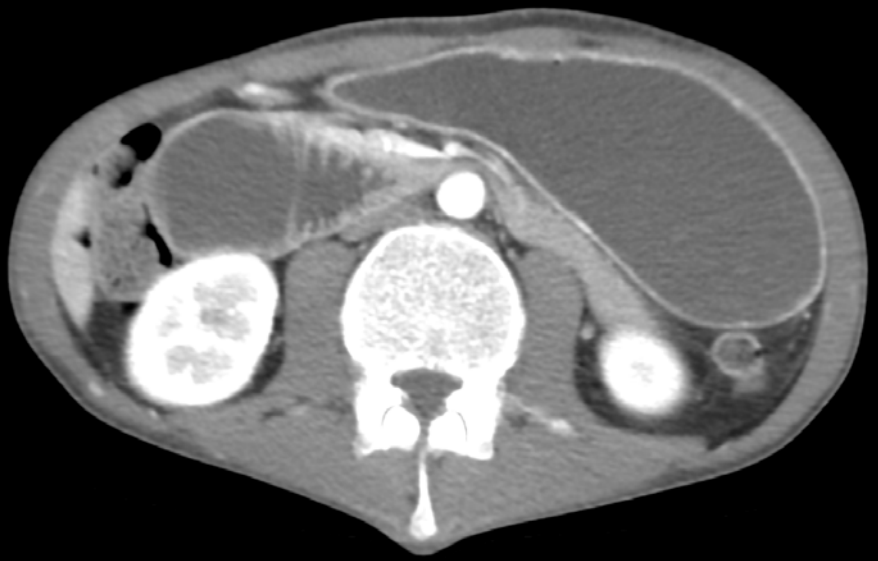
- Gkampeta A, Tziola TS, Tragiannidis A, Papageorgiou T, Spyridakis I, Hatzipantelis E. Primary posterior mediastinal germ cell tumor in a child. *Turk Pediatri Ars*. 2019;54(3):185-188.
- Arumugam D, Thandavarayan P, Chidambaram L, Boj S, Marudasalam S. Primary nasopharngeal yolk sac tumor: A case report. *J Clin Diagn Res*. 2016;10(5):ED06-7.
- Gaillard F. Anterior mediastinal germ cell tumours. In: *Radiopaedia.org*. Radiopaedia.org; 2010. doi:10.53347/rid-9214

Posted 7/10/2026

26M with hx of anorexia nervosa presents to the ED with 4 weeks of progressive failure to thrive and inability to eat or drink.



A) Sagittal CT with IV contrast



B) Axial CT with IV contrast



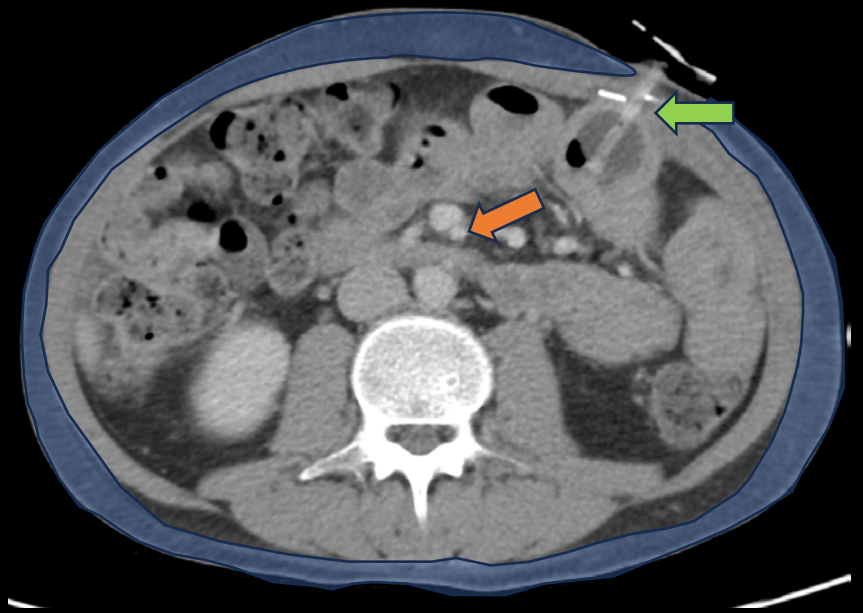
C) Axial CT with IV contrast one month post diagnosis and treatment



A) Sagittal CT with IV contrast



B) Axial CT with IV contrast



C) Axial CT with IV contrast one month post diagnosis and treatment

Superior Mesenteric Artery Syndrome

Imaging findings: A) and B) Initial CT scan with IV contrast shows compression of the third part of the duodenum between the superior mesenteric artery (SMA) and aorta. The stomach and proximal duodenum are markedly distended with fluid. Aortomesenteric angle (AMA) and distance are 31º and 4.6 mm, respectively. C) Axial CT scan one month post diagnosis and treatment shows alleviation of compression of the duodenum by the SMA. The AMA and distance have increased to 51º and 15.3 mm, respectively. A jejunostomy tube is in place. Interval increase in abdominal wall adipose tissue reflects substantial weight restoration.

Differential Diagnosis: SMA syndrome, duodenal stricture, and other cause of duodenal obstruction (e.g. cancer)

Discussion: SMA syndrome is compression of the third part of the duodenum due to narrowing of the AMA, typically secondary to rapid weight loss. Predisposing conditions include psychiatric illness, drug abuse, anatomic anomalies (e.g. low origin SMA, intestinal malrotation), post operative states such as bariatric surgery, and cancer. Common symptoms are anorexia and vague postprandial symptoms including epigastric pain, nausea, and vomiting. Radiographic findings include AMA <22º and distance < 8 mm (normal is 38-65º and 10-28 mm, respectively). Reduced aortomesenteric distance has been shown to be more sensitive and specific for SMA syndrome than AMA alone, as demonstrated in this case. Given the nonspecific symptoms and common history of anorexia nervosa, SMA syndrome is frequently misdiagnosed clinically; therefore, these characteristic radiographic findings are critical for proper diagnosis and treatment. Following jejunostomy tube placement and nutritional rehabilitation, the patient's BMI increased from 12 to 18.9 kg/m² over one month.

@AOCRNews

@zachbkamp
@aocrnews

Case courtesy of Zachary Bohnenkamp, OMS III; Lance Borup, DO
ATSU-KCOM

References

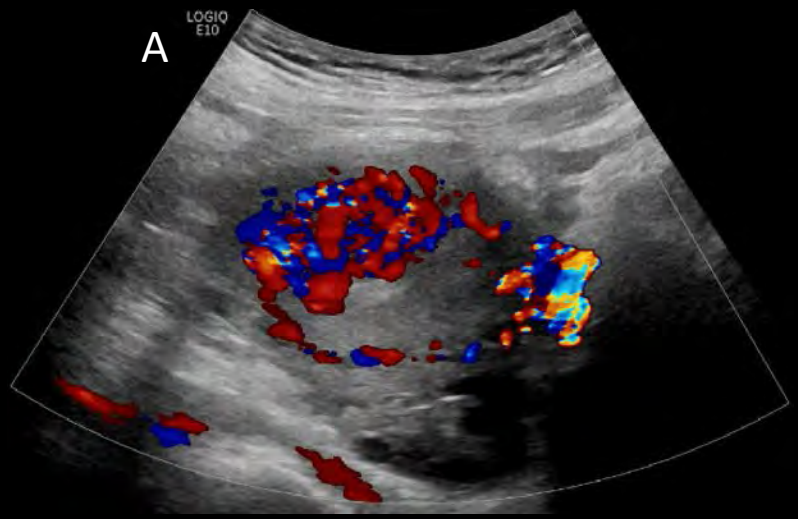
Ganss A, Rampado S, Savarino E, Bardini R. Superior mesenteric artery syndrome: a prospective study in a single institution. J Gastrointest Surg. 2019;23(5):997-1005. doi:10.1007/s11605-018-3984-6

Van Horne N, Jackson JP. Superior mesenteric artery syndrome. In: StatPearls. StatPearls Publishing; 2026. Updated July 17, 2023. Accessed May 18, 2026. https://www.ncbi.nlm.nih.gov/books/NBK482209/

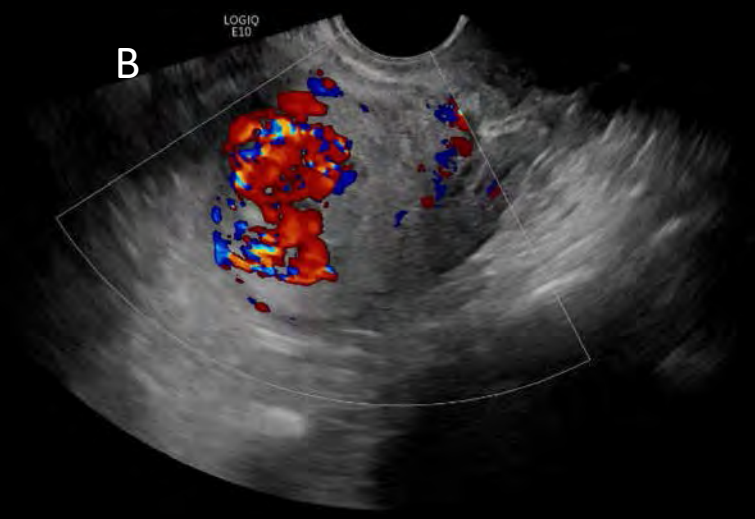
Unal B, Aktaş A, Kemal G, Bilgili Y, Güliter S, Daphan C, Aydinuraz K. Superior mesenteric artery syndrome: CT and ultrasonography findings. Diagn Interv Radiol. 2005 Jun;11(2):90-5. PMID: 15957095.

Posted 7/3/2026

25 y/o G4P2113 presenting with heavy vaginal bleeding two months following surgical termination of pregnancy.



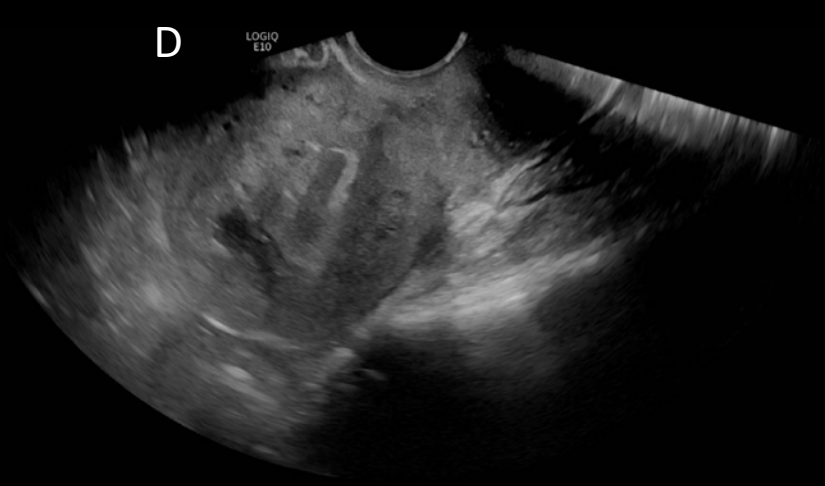
Transvaginal Ultrasound with color Doppler (TVUS)



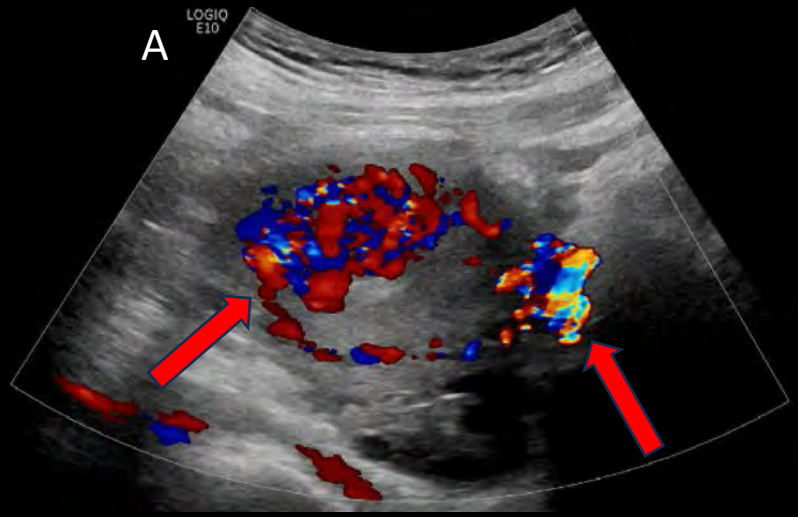
Transvaginal Ultrasound with color Doppler (TVUS)



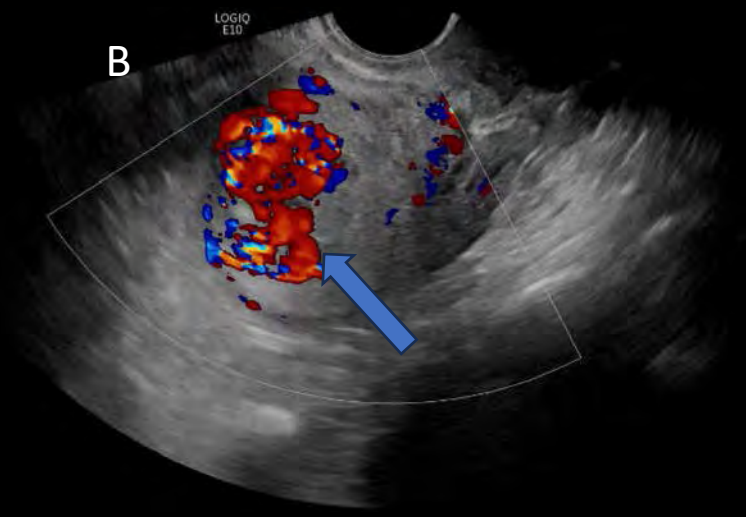
Transvaginal Ultrasound (TVUS) gray scale



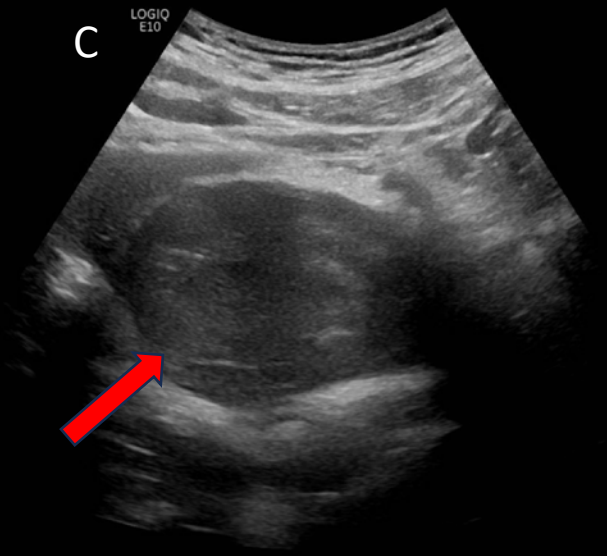
Transvaginal Ultrasound (TVUS) gray scale



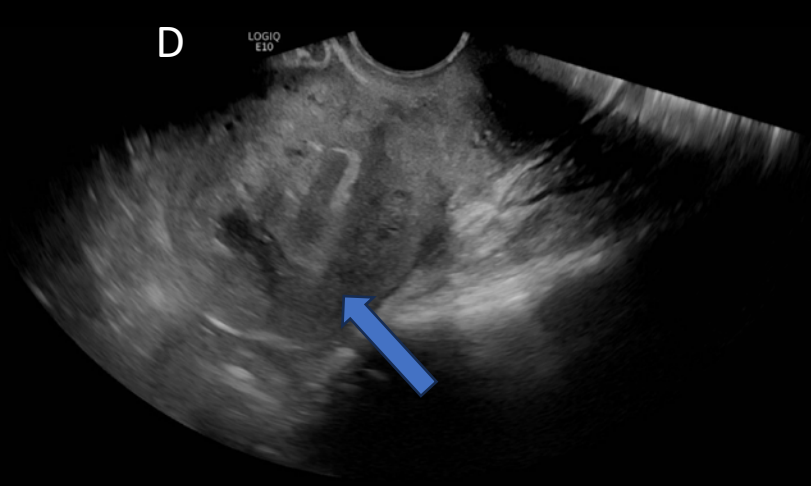
Transvaginal Ultrasound with color Doppler (TVUS)



Transvaginal Ultrasound with color Doppler (TVUS)



Transvaginal Ultrasound (TVUS) gray scale



Transvaginal Ultrasound (TVUS) gray scale

Retained Products of Conception

Image Findings: Transvaginal ultrasound with color Doppler demonstrates diffuse, chaotic high-flow vascularity centered within the endometrial cavity (red arrows), raising concern for uterine arteriovenous malformation. Additional views demonstrate more focal endometrial vascularity without clear involvement of the surrounding myometrium (blue arrow), favoring retained products of conception.

Differential Diagnosis: Enhanced myometrial vascularity (EVM) versus Congenital uterine AVM

Discussion: Enhanced myometrial vascularity (EMV) represents persistent or involuting uteroplacental circulation in the postpregnancy uterus and may persist in the presence of retained products of conception (RPOC). Although EMV and congenital uterine arteriovenous malformations (AVMs) may demonstrate similar high-velocity, low-resistance Doppler flow, they are fundamentally distinct entities. RPOC associated hypervascularity reflects EMV within the spectrum of postpregnancy vascular remodeling, whereas congenital AVMs are rare vascular malformations arising from abnormal embryologic vascular development. Accurate differentiation is critical, as EMV often resolves spontaneously or following treatment of associated RPOC, while congenital AVMs frequently require embolization.

Case courtesy of Drew Warren, OMS III[1]; Steve Min, DO, MPH, MBA, FAOCR[2]
[1]Michigan State University College of Osteopathic Medicine, [2]Henry Ford Hospital

References

1. Huang MW, Muradali D, Thurston WA, Burns PN, Wilson SR. Uterine arteriovenous malformations: gray-scale and Doppler US features with MR imaging correlation. *Radiology*. 1998;206(1):115–123.
2. Kamaya A, Ro K, Benedetti NJ, Chang PL, Desser TS. Retained products of conception: spectrum of color Doppler findings. *J Ultrasound Med*. 2009;28(8):1031–1041.
3. Sellmyer MA, Desser TS, Maturen KE, Jeffrey RB Jr, Kamaya A. Physiologic, histologic, and imaging features of retained products of conception. *Radiographics*. 2013;33(3):781–796.

Posted 6/26/2026

42M presented to the ED with left wrist pain after sustaining a crush injury from a motor earlier that day. Images were obtained to assess for carpal instability or fracture. No other clinical history was available.



1. PA Radiograph Left Wrist



2. Lateral Radiograph Left Wrist



1. PA Radiograph Left Wrist



2. Lateral Radiograph Left Wrist

Lunate Dislocation

Imaging findings:

- Fig. 1: PA radiograph of the left wrist demonstrates volar displacement of the lunate (yellow circle).
- Fig. 2: Lateral radiograph of the left wrist shows volar displacement with lunate rotation and loss of alignment with the radius, ulna, and capitate (yellow circle).

Differential diagnosis: lunate dislocation, perilunate dislocation, trans-scaphoid perilunate fracture-dislocation

Discussion: The lunate is widely known to be the most dislocated carpal bone, yet lunate dislocation is often missed on initial presentation, posing the potential to exacerbate effects long term. Dislocation is mechanistically dependent, with few pertinent risk factors contributing to the likelihood of occurrence, though scaphoid discontinuity may be associated with perilunate pathology in lower-energy trauma cases. Generally, these dislocations result from high-energy trauma–falls, sports or crush injuries, MVAs–and are independent of patient-specific factors like bone density or laxity of ligaments. The commonplace nature of these wrist injuries can be attributed to the space of Poirier, an anatomical weak point lying at the intersection of the capitate and lunate that allows for volar displacement upon high-energy trauma to the area. The exact mechanism of impact to the wrist, such as the conformation of the wrist at the time of trauma and the direction of the force vector, plays a role in determining whether lunate or perilunate dislocation occurs.

Depending on the source of initial trauma, concurrent injuries may or may not be present. Patients generally present with pain, swelling, and decreased range of motion. Gross deformity may not be noted as the lunate is physically small.

Carpal anatomy in combination with the typical force vector that causes lunate dislocation results in a predictable imaging pattern on plain film. Lunate dislocations belong to stage IV of the Mayfield classification system of perilunar instability, in which the lunate is displaced and rotated volarly while the other carpals maintain normal alignment. Typical lateral view shows a volar tilt more than 10^{o} (spilled teacup sign), while appearance of the lunate on PA radiograph is triangular due to rotation (piece of pie sign). Contrarily, perilunate dislocation is significant for normal alignment of the lunate with the distal radius, dorsal displacement of the remaining carpus, and a scapholunate interval >2 mm (Terry Thomas sign).

Open reduction with internal fixation is the gold standard treatment; closed reduction may provide initial stabilization. Failure to treat may lead to consequences such as carpal tunnel syndrome, carpal instability or pain, arthritis, and osteonecrosis.

In summary, prompt imaging recognition, which is generally accomplished through radiography alone, is essential for treatment of lunate dislocations. It is also important to assess for concurrent fractures or dislocations of other bones or ligaments, as these may further diminish wrist stability.

@cameronlaurie65
@AOCRNews
@cameron_l_10
@aocrnews
Case courtesy of Cameron C. Laurie, MS1[1], Maddox Linder, MS1[1], April L. Cox, DO[2]
[1]Baylor College of Medicine, [2]Indiana University School of Medicine

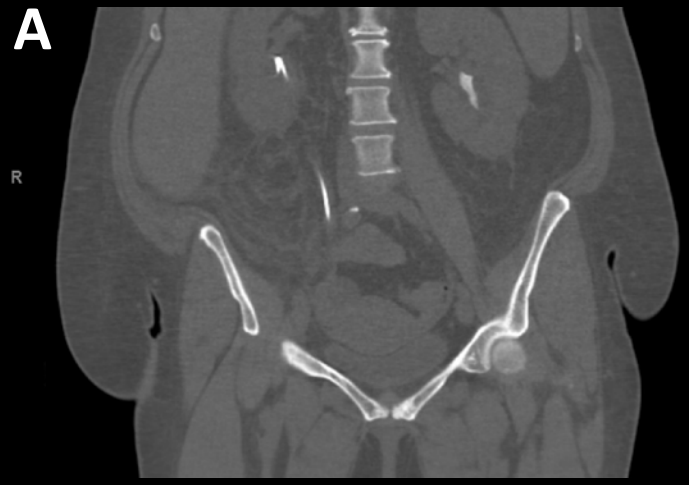
References

- Heineman N, Do DH, Golden A (2023) Carpal dislocations. J Hand Surg Eur Vol 48(2_suppl):11S-17S
- Alt V, Sicre G (2004) Dorsal transscaphoid-transtriquetral perilunate dislocation in pseudarthrosis of the scaphoid. Clin Orthop Relat Res (426):135-7
- Wilke B, Kakar S (2015) Delayed Avascular Necrosis and Fragmentation of the Lunate Following Perilunate Dislocation. Orthopedics 38(6):e539-42
- Takase K (2008) Dorsal transscaphoid transtriquetral perilunate dislocation with pseudoarthrosis of the scaphoidy. Orthopedics 31(10):orthosupersite.com/view.asp?rID=31526
- Scalcione LR, Gimber LH, Ho AM, Johnston SS, Sheppard JE, Taljanovic MS (2014) Spectrum of carpal dislocations and fracture-dislocations: imaging and management. AJR Am J Roentgenol 203(3):541-50
- Naam NH, Smith DK, Gilula LA (1992) Transtriquetral perihamate ulnar axial dislocation and palmar lunate dislocation. J Hand Surg Am 17:762-766
- Perron AD, Brady WJ, Keats TE, Hersh RE (2001) Orthopedic pitfalls in the ED: lunate and perilunate injuries. Am J Emerg Med 19:157-162
- Kapoor G, Heire P, Turmezei T, Chojnowski A, Toms AP (2020) Perilunate injuries: biomechanics, imaging, and classification. Clin Radiol 75(2):81-87
- Stanbury SJ, Elfar JC (2011) Perilunate dislocation and perilunate fracture-dislocation. J Am Acad Orthop Surg 19(9):554-62
- Szabo RM (2008) Scapholunate ligament repair with capsulodesis reinforcement. J Hand Surg Am 33(9):1645-54
- Budoff JE (2008) Treatment of acute lunate and perilunate dislocations. J Hand Surg Am 33(8):1424-1432
- Johnson RP (1980) The acutely injured wrist and its residuals. Clin Orthop Relat Res (149):33-44
- Goodman AD, Harris AP, Gil JA, Park J, Raducha J, Got CJ (2019) Evaluation, Management, and Outcomes of Lunate and Perilunate Dislocations 42(1):e1-e6
- Israel D, Delclaux S, André A, Apredoaei C, Rongières M, Bonnevialle P, Mansat P (2016) Peri-lunate dislocation and fracture-dislocation of the wrist: retrospective evaluation of 65 cases. Orthop Traumatol Surg Res 102(3):351-355

Posted 6/19/2026

50 y/o f with hx of recurrent nephrolithiasis presents with acute right flank pain, dysuria, and gross hematuria 6 days after percutaneous nephrolithotomy (PCNL) with ureteral stent placement.

A



Coronal CT

B



Coronal CT

C



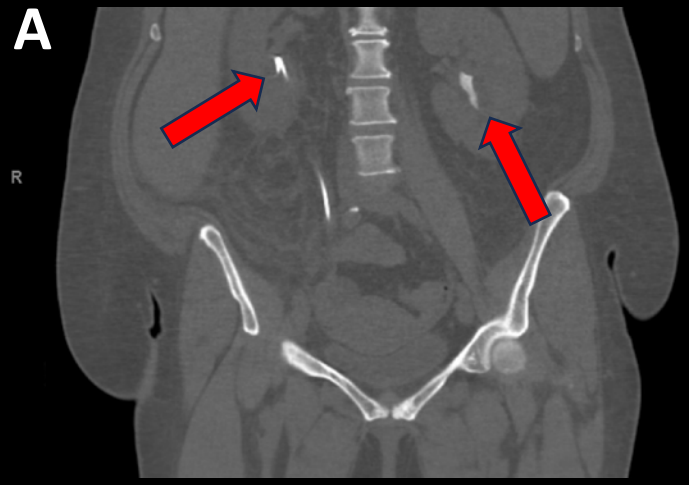
Axial CT

D



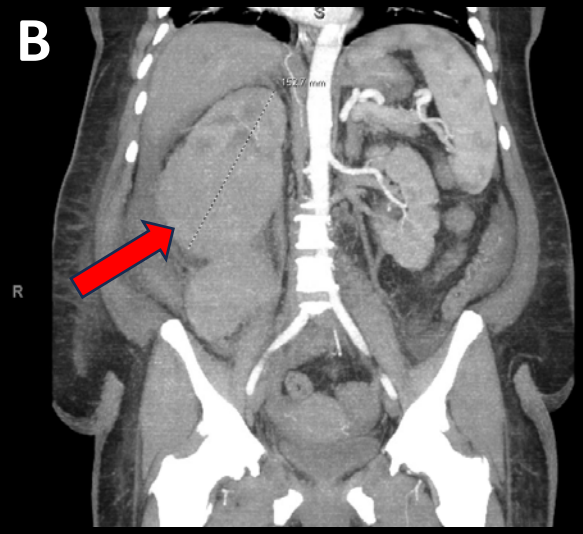
Axial CT

A



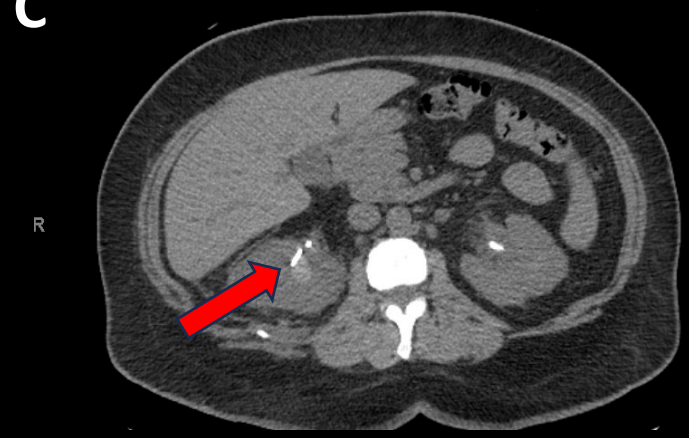
Coronal CT

B



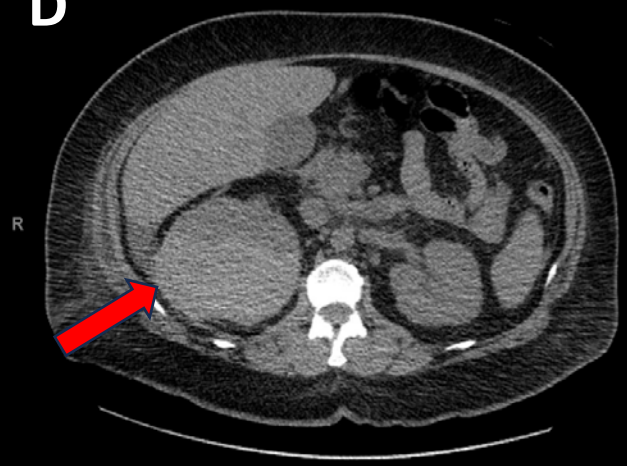
Coronal CT

C



Axial CT

D



Axial CT

Renal Subcapsular Hematoma

Image Findings: Coronal and axial CT scans of the abdomen and pelvis (Figures A and C) depict right-sided ureteral stent placement following percutaneous nephrolithotomy (PCNL). Additional imaging (Figures B and D) demonstrates development of right-sided subcapsular fluid collection causing renal compression and mass effect.

Differential Diagnosis: Renal subcapsular hematoma, retained nephrolithiasis, pyelonephritis, post-procedural urine leak, renal vein thrombosis, primary renal malignancy, systemic autoimmune process (e.g., Lupus nephritis).

Discussion: Delayed post-PCNL hemorrhage may manifest several days after the initial procedure. The clinical presentation often mimics nephrolithiasis, or infection, which can lead to a delay in the proper diagnosis. Because early CT may be subtle or nonspecific, serial imaging comparison is critical to identify an evolving hemorrhage. Sudden onset acute anemia should immediately raise concern for occult retroperitoneal bleeding. A large subcapsular hematoma can lead to significant renal parenchyma compression, a phenomenon known as Page kidney, which may trigger secondary hypertension. It is important to maintain a high index of suspicion for clinically significant hemorrhage in this setting.

@AOCRNews

@aocrnews

Courtesy of Drew Warren, OMS III[1]; Rory Vindischman, OMS III[1]; Steve Min, DO, MPH, MBA, FAOCR[2]
[1]Michigan State University College of Osteopathic Medicine, [2]Henry Ford Hospital

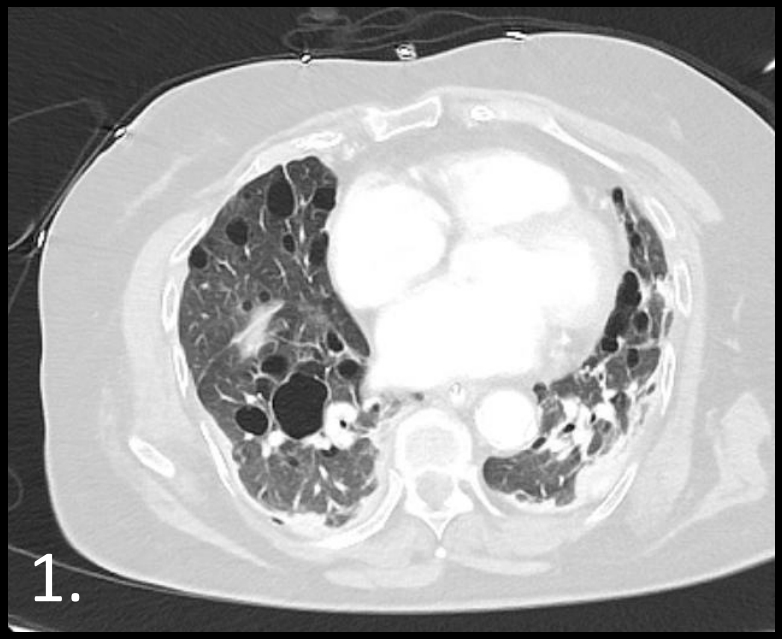
AOCR American Osteopathic College of Radiology

References

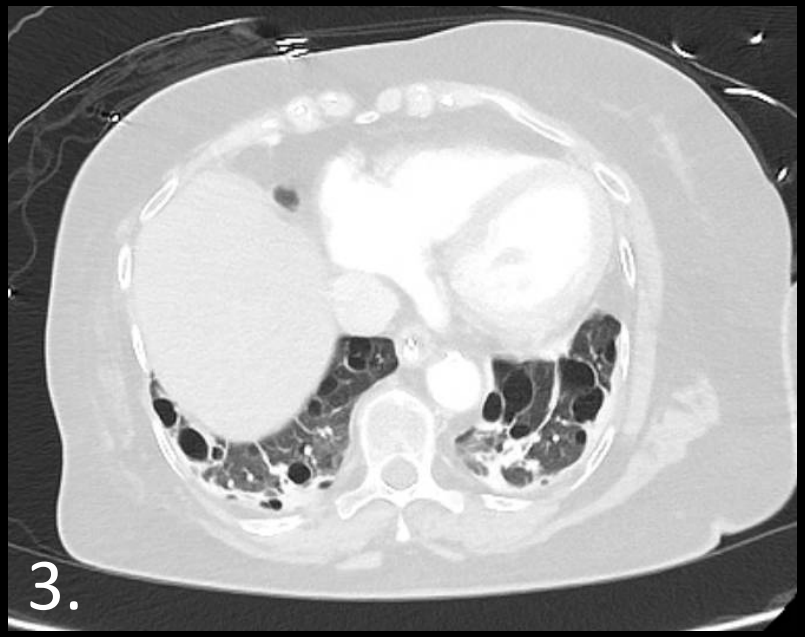
1. Burrel M, Barrufet M, Sebastià MC, et al. Diffuse renal cortical hemorrhage in the setting of subcapsular hematoma: diagnosis and treatment with embolization. *J Vasc Interv Radiol.* 2017;28(11):1557-1562.e1. doi:10.1016/j.jvir.2017.06.017
2. Dopson SJ, Jayakumar S, Velez JC. Page kidney as a rare cause of hypertension: case report and review of the literature. *Am J Kidney Dis.* 2009;54(2):334-339. doi:10.1053/j.ajkd.2008.11.014
3. Feit L, John D, Delgado Torres N, Sinert R. Flank pain and hematuria is not always a kidney stone. *Am J Emerg Med.* 2021;40:225.e1-225.e2. doi:10.1016/j.ajem.2020.07.046
4. Sheth S, Casalino DD, Remer EM, et al.; Expert Panel on Urologic Imaging. American College of Radiology ACR appropriateness criteria: renal trauma. *American College of Radiology website.* http://acsearch.acr.org/docs/69373/Narrative/. Updated 2012. Accessed 15 August 2017
5. Tao W, Cai CJ, Sun CY, Xue BX, Shan YX. Subcapsular renal hematoma after ureteroscopy with holmium:yttrium-aluminum-garnet laser lithotripsy. *Lasers Med Sci.* 2015;30(5):1527-1532. doi:10.1007/s10103-015-1760-3

Posted 6/12/2026

78 y/o female with a history of HTN, HLD, CAD presented to ED after a mechanical fall.

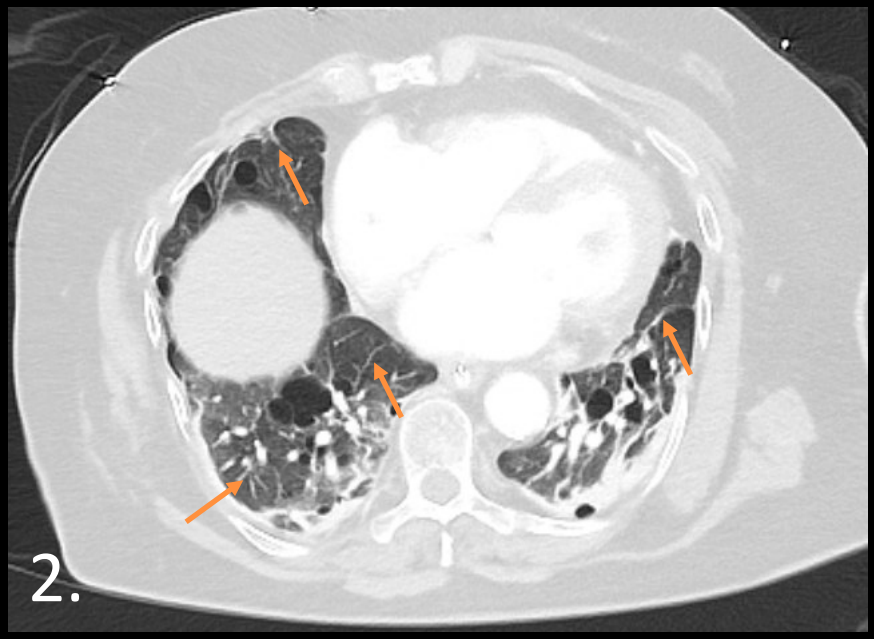

1.


2.

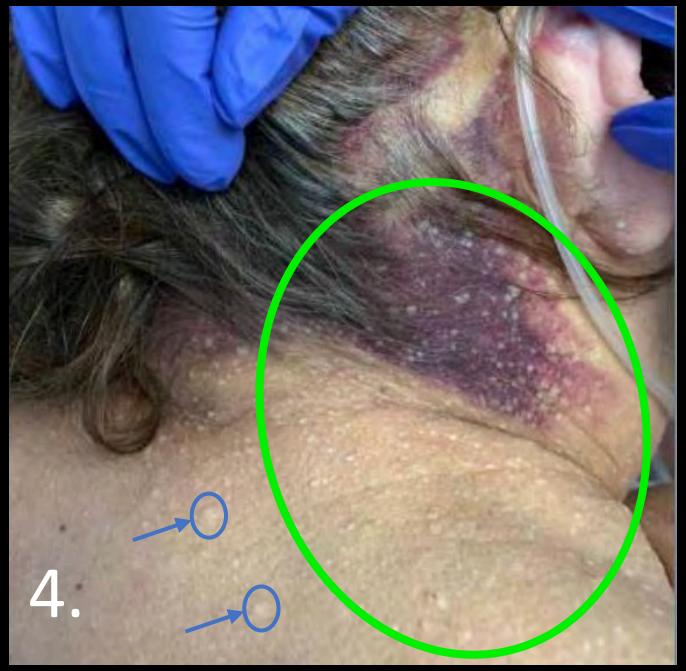

3.


4.


1.


2.


3.


4.

Birt-Hogg-Dubé Syndrome

Image Findings:

Figs 1-3: Axial CT chest with contrast shows multiple thin-walled pulmonary cysts of various size, predominantly in the mid to lower lung zones (red circles), and some reticulations (orange).

Fig 4: Physical exam showing numerous small flesh-colored papules involving the postauricular region and posterior neck. (green circle). Individual lesions can be seen in (blue).

Differential Diagnosis: Birt-Hogg-Dubé syndrome, lymphangioleiomyomatosis (sporadic or TSC-associated), pulmonary Langerhans cell histiocytosis, lymphoid interstitial pneumonia, bullous emphysema, fibrofolliculomas, acrochordons, milia, sebaceous hyperplasia

Discussion: This patient was later discovered to have a history of Birt-Hogg-Dubé syndrome (BHD), though there is no documented genetic testing. BHD is a rare autosomal dominant inherited syndrome caused by mutations in the *FLCN* tumor suppressor gene located on chromosome 17p11.2.[1] The syndrome affects multiple organ systems, most commonly involving the lungs, kidneys, and skin. Although cutaneous manifestations, such as fibrofolliculomas, often develop during the third to fourth decades of life, pulmonary cysts and spontaneous pneumothoraces may represent the earliest manifestations of disease.[1,2] Renal tumors typically present later, most commonly between the fourth and seventh decades of life.[1] Thoracic manifestations are among the most common radiologic findings in BHD and are frequently identified incidentally on imaging. Characteristic CT findings include multiple irregular thin-walled pulmonary cysts predominantly seen in the mid to lower lung fields, as seen in this patient, as well as the fibrofolliculomas seen behind her ear on trauma exam.[1,3] This patient was also found to have a renal lesion of indeterminate etiology on trauma imaging (not pictured here), a finding further suggestive of BHD.

The pathogenesis of pulmonary cyst formation in BHD remains incompletely understood, though folliculin dysfunction is believed to contribute to abnormal cellular signaling pathways involving mTOR regulation, cellular adhesion, and extracellular matrix integrity.[1] Histopathologic studies suggest cyst formation may occur adjacent to interlobular septa and alveolar structures, contributing to the characteristic lower lobe and peri-fissural distribution seen on imaging.[3] Rupture of these cysts predisposes affected patients to recurrent spontaneous pneumothoraces, which may require interventions including pleurodesis or thoracic surgery.

Renal manifestations represent the major source of morbidity and mortality in BHD patients. Approximately 14-34% of affected individuals develop renal tumors, which are frequently bilateral or multifocal.[1,2] The most commonly associated neoplasms include hybrid oncocytic/chromophobe tumors, chromophobe renal cell carcinoma, clear cell renal cell carcinoma, and oncocytomas.[1] Early recognition of these imaging findings is important to facilitate earlier detection and treatment of renal malignancies.

There is currently no curative therapy for BHD. Management is primarily directed toward surveillance and prevention of complications. Recommendations commonly include periodic renal imaging surveillance with MRI or CT, counseling regarding pneumothorax risk, smoking avoidance, and genetic counseling for affected patients and family members. Radiologists play a critical role in recognizing the characteristic imaging manifestations of BHD, particularly when these findings are incidentally identified. This case highlights the importance of careful evaluation of incidental thoracoabdominal findings on trauma imaging, as recognition of syndromic imaging patterns may significantly alter long-term patient management and surveillance strategies. [2]

@aocrnews
@AOCRNews

Case courtesy of Caroline Malkin M3[1], Sarah Staskiewicz DO[2], Mark DiMarcangelo DO[2]
[1]Cooper Medical School of Rowan University, [2]Cooper University Hospital

AOCR American Osteopathic College of Radiology

References

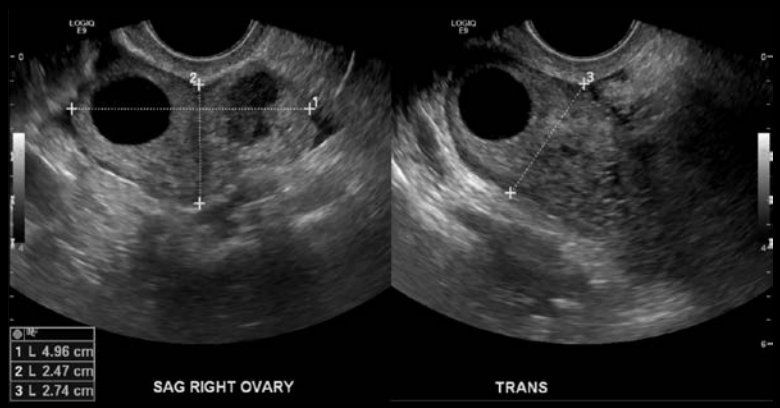
1. Gupta S, Kang HC, Ganeshan D, et al. The ABCs of BHD: An In-Depth Review of Birt-Hogg-Dubé Syndrome. *AJR Am J Roentgenol.* 2017;209(6):1291-1296. doi:10.2214/AJR.17.18071.
2. Menko FH, van Steensel MAM, Giraud S, et al. Birt-Hogg-Dubé syndrome: diagnosis and management. *Lancet Oncol.* 2009;10(12):1199-1206.
3. Tobino K, Gunji Y, Kurihara M, et al. Characteristics of pulmonary cysts in Birt-Hogg-Dubé syndrome: thin-section CT findings of the chest in 12 patients. *Eur J Radiol.* 2011;77(3):403-409.

Posted 6/5/2026

47F presented to the ED with sudden-onset RLQ abdominal pain. CT on Day 1 was performed to evaluate for appendicitis. Day 2 TVUS raised concern with recommendation for f/u. Repeat US was performed on Day 3.

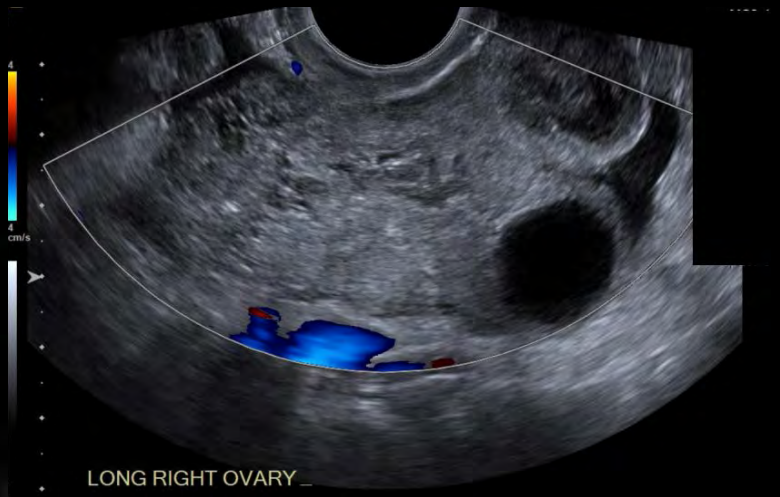


1. Day 1 Axial CT



2. Day 2 Sagittal and Transverse TVUS

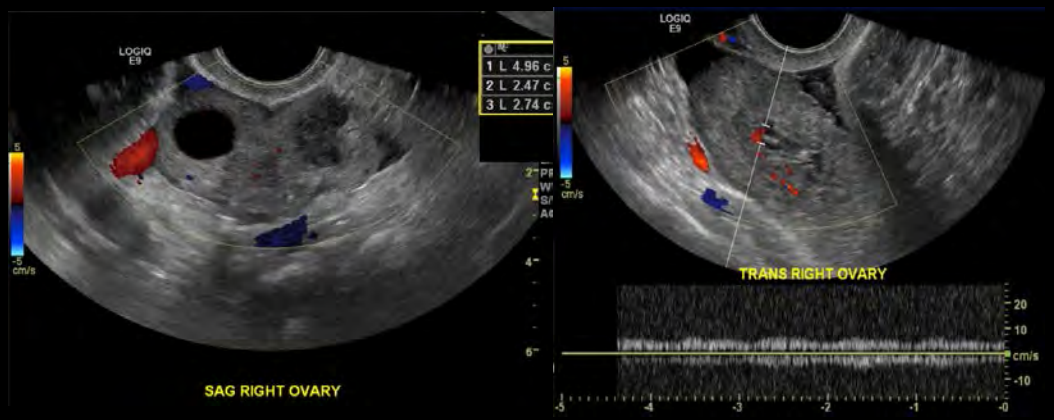




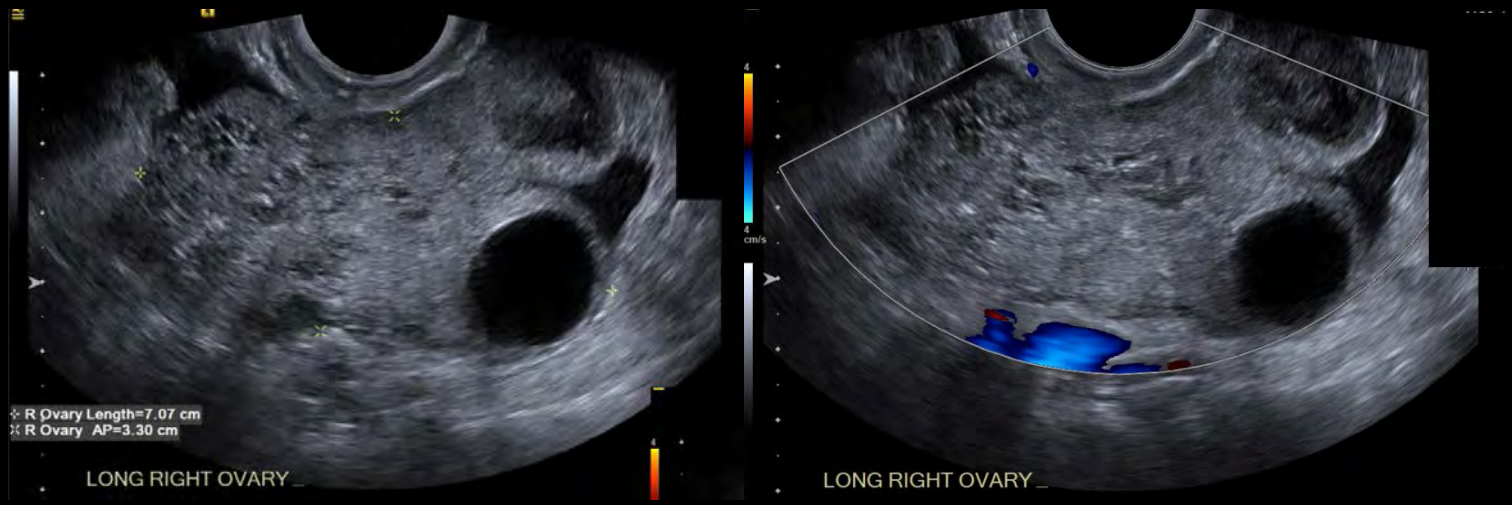
3. Day 3 Longitudinal US



1. Day 1 Axial CT



2. Day 2 Sagittal and Transverse TVUS



3. Day 3 Longitudinal US

Ovarian Torsion

Imaging findings:

- Fig. 1: Day 1 axial CT abdomen and pelvis visualizes an enlarged, heterogenously attenuated right ovary with no clearly visible free fluid or adnexal mass (yellow circle).
- Figs. 2A-B: Day 2 sagittal TVUS demonstrates an enlarged, heterogenous right ovary. Color Doppler is significant for significantly reduced vascular blood flow. Transverse TVUS shows markedly reduced blood flow with visible arterial waveform.
- Figs. 3A-B: Day 3 longitudinal US shows an increased size of the right ovary with persistently heterogeneous echotexture. Color Doppler US demonstrates no central blood flow.

Differential diagnosis: ovarian torsion, hemorrhagic ovarian cyst, ruptured ovarian cyst, acute appendicitis, ovarian mass

Discussion: Ovarian torsion involves a twisting of the ovary and constitutes one of the most common gynecologic emergencies seen in women of reproductive age. Over 90% of cases occurs in premenopausal women, and the median age at which a patient presents is in the late third decade of life. An ovarian diameter exceeding 5 cm elevates torsion risk, alongside several anatomical factors including the presence of an ovarian cyst (especially in adults), long ovarian ligaments, ligamental instability, and a small uterine size. Pathophysiology lies in a partial or complete rotation of the ovary, typically due to ovarian hypermobility or an adnexal mass, and is often accompanied by fallopian torsion. Impaired venous and lymphatic drainage may lead to ischemia and infarction if left untreated. The right ovary is more often implicated, likely due to protection of the left ovary by the descending colon.

Patients often present with pelvic or abdominal pain, typically localized to the RLQ, and may experience nausea and/or vomiting. Diagnosis may be complicated by a lack of sudden onset or severity. The general constellation of symptoms overlapping with other conditions, most notably acute appendicitis, makes imaging key to diagnostic workup and guidance of management.

TVUS plays a central role in initial assessment, with pooled sensitivity and specificity values of 79% and 76%, respectively. Typical features include ovarian enlargement, variable echotexture, cystic degeneration, follicular displacement, and free pelvic fluid. Venous flow reduction is a common, highly suggestive finding and tends to precede arterial flow changes. A whirlpool sign may indicate a twisted pedicle. Findings on Doppler display considerable variability, and preserved blood flow does not exclude ovarian torsion from the differential. Ambiguous findings on US make MRI a useful modality to exclude suspicious ovarian mass or alternative diagnosis. CT may show ovarian enlargement, lead mass, twisted vascular pedicle, uterine displacement to the involved side, or free fluid.

Once diagnosis is confirmed, laparoscopic detorsion is generally preferred over oophorectomy, even in cases of apparent necrosis intraoperatively. Intraoperative accuracy of necrosis may be inaccurate in up to 80% of cases.

As a final take-home message, nonspecific symptoms and imaging features frequently lead to delayed or misdiagnosis of ovarian torsion. Maintaining a high index of suspicion is essential. Doppler findings are highly variable, and normal vascularity does not rule out ovarian torsion.

@cameronlaurie65
@AOCRNews

@cameron_l_10
@aocrnews

Case courtesy of Cameron C. Laurie, MS1[1], April L. Cox, DO[2]
[1]Baylor College of Medicine, [2]Indiana University School of Medicine

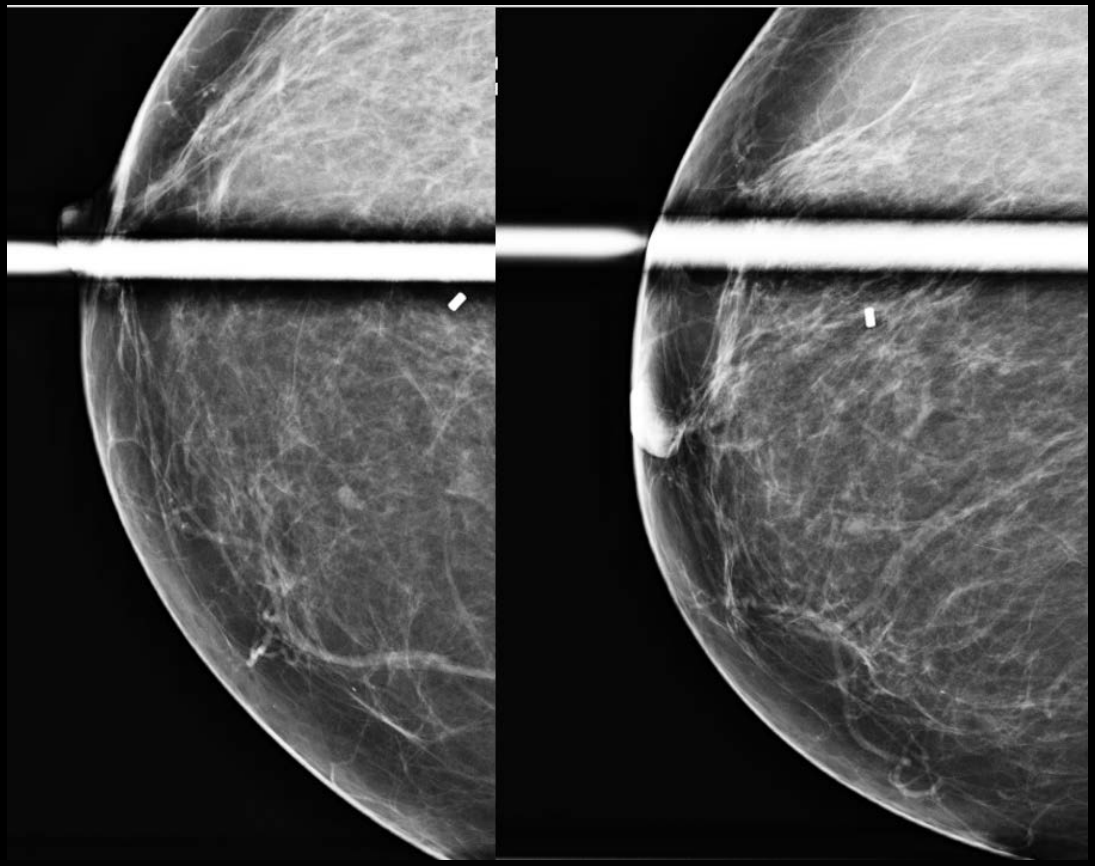
AOCR American Osteopathic College of Radiology

References

- Tabbara F, Hariri M, Hitti E (2024) Ovarian torsion: A retrospective case series at a tertiary care center emergency department. PLoS One 19(3):e0297690
- Moro F, Bolomini G, Sibal M, Vijayaraghavan SB, Venkatesh P, Nardelli F, Pasciuto T, Mascilini F, Pozzati F, Leone FPG, Josefsson H, Epstein E, Guerriero S, Scambia G, Valentin L, Testa AC (2020) Imaging in gynecological disease (20): clinical and ultrasound characteristics of adnexal torsion. Ultrasound Obstet Gynecol 56(6):934-943
- Strachowski LM, Choi HH, Shum DJ, Horrow MM (2021) Pearls and Pitfalls in Imaging of Pelvic Adnexal Torsion: Seven Tips to Tell It's Twisted. Radiographics 41(2):625-640. Erratum in: Radiographics 41(3):E97
- Dawood MT, Naik M, Bharwani N, Sudderuddin SA, Rockall AG, Stewart VR (2021) Adnexal Torsion: Review of Radiologic Appearances. Radiographics 41(2):609-624
- Bridwell RE, Koyfman A, Long B (2022) High risk and low prevalence diseases: Ovarian torsion. Am J Emerg Med 56:145-150(2019) Adnexal Torsion in Adolescents: ACOG Committee Opinion No, 783. Obstet Gynecol 134(2):e56-e63
- Brook OR, Dadour JR, Robbins JB, et al. (2024) ACR Appropriateness Criteria® Acute Pelvic Pain in the Reproductive Age Group: 2023 Update. Journal of the American College of Radiology 21(6):S3-S20
- Albayram F, Hamper UM (2002) Ovarian and adnexal torsion: spectrum of sonographic findings with pathologic correlation. J Ultrasound Med 20(10):1083-94
- Nizar K, Deutsch M, Filmer S et-al. (2009) Doppler studies of the ovarian venous blood flow in the diagnosis of adnexal torsion. Journal of clinical ultrasound 37(8):436-9
- Béranger-Gibert S, Sakly H, Ballester M, Rockall A, Bornes M, Bazot M, Daraï E, Thomassin-Naggara I (2016) Diagnostic Value of MR Imaging in the Diagnosis of Adnexal Torsion. Radiology 279(2):461-70
- Hiller N, Appelbaum L, Simanovsky N, Lev-Sagi A, Aharoni D, Sella T (2007) CT features of adnexal torsion. AJR Am J Roentgenol 189(1):124-9
- Duigenan S, Oliva E, Lee SI (2012) Ovarian torsion: diagnostic features on CT and MRI with pathologic correlation. AJR Am J Roentgenol 198(2):W122-31
- American College of Obstetricians and Gynecologists' Committee on Practice Bulletins—Gynecology (2016) Practice Bulletin No. 174: Evaluation and Management of Adnexal Masses. Obstet Gynecol 128(5):e210-e226
- Chang-Patel EJ, Palacios-Helgeson LK, Gould CH (2022) Adnexal torsion: a review of diagnosis and management strategies. Curr Opin Obstet Gynecol 1;34(4):196-203

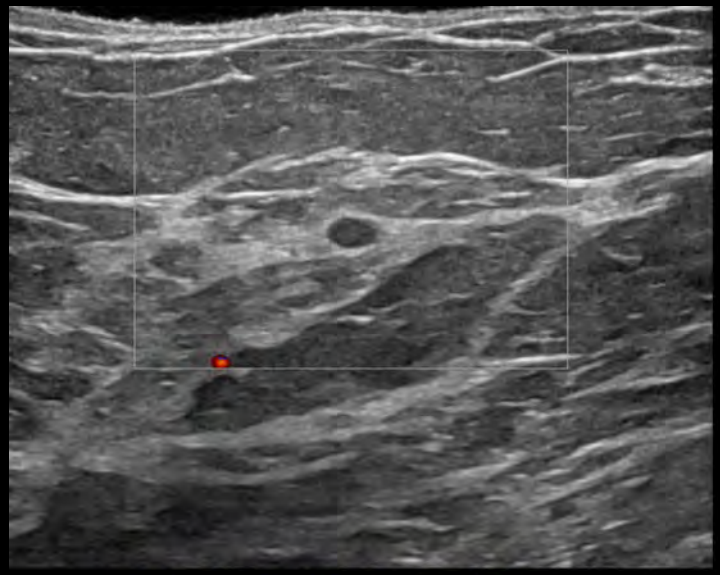
Posted 5/29/2026

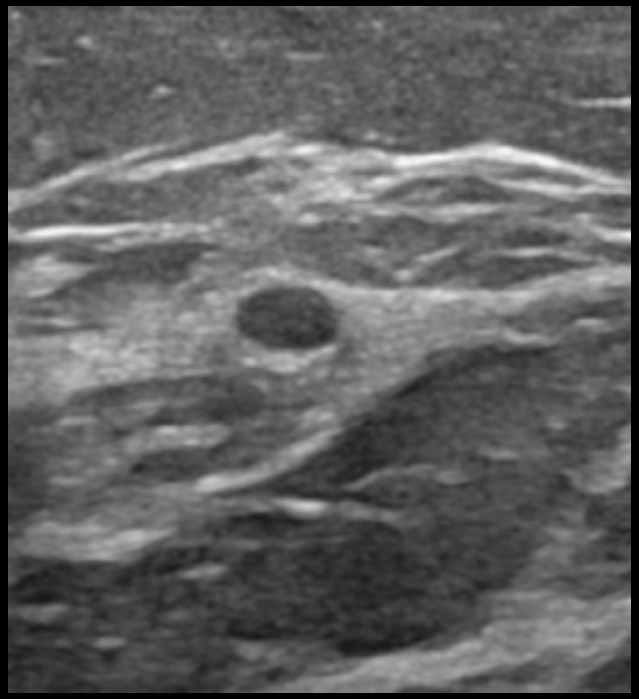
65-year-old woman with new mass seen on screening mammogram

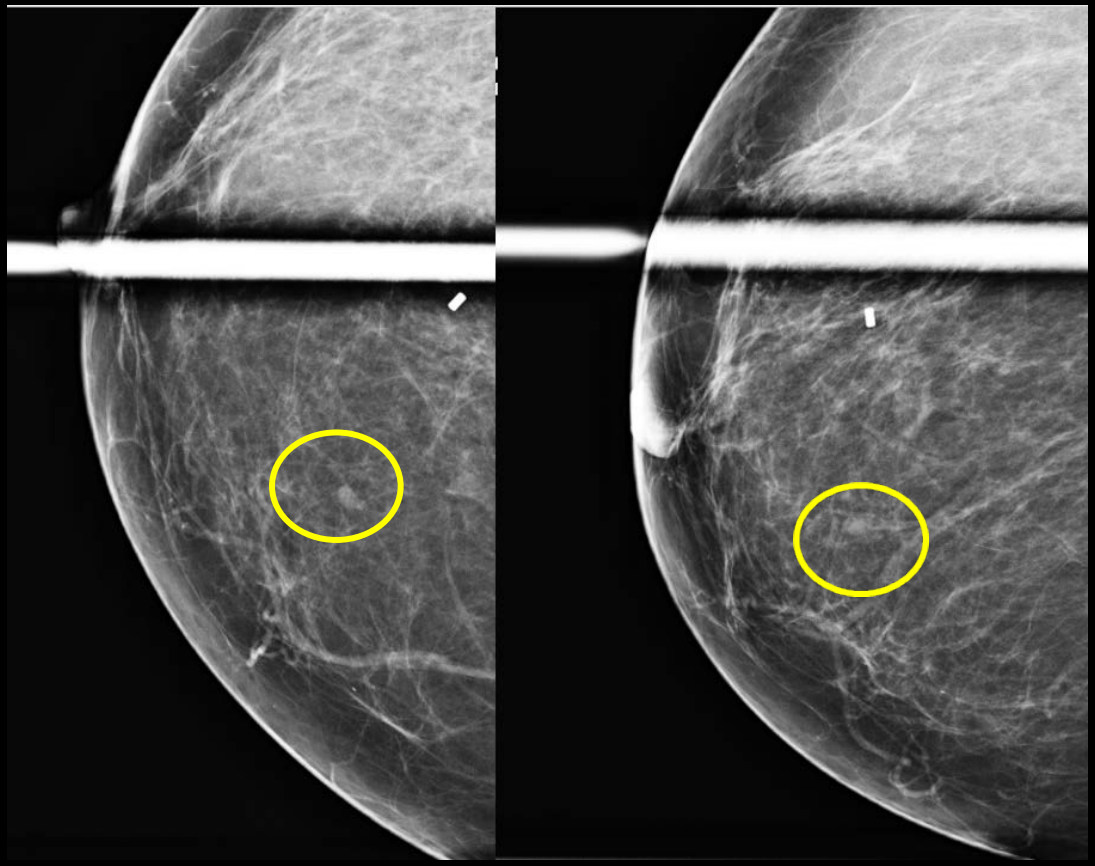


CC spot

MLO spot

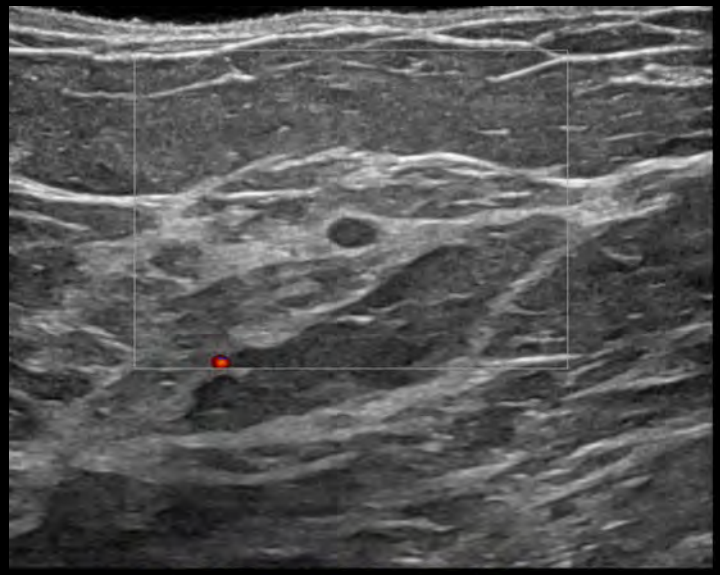


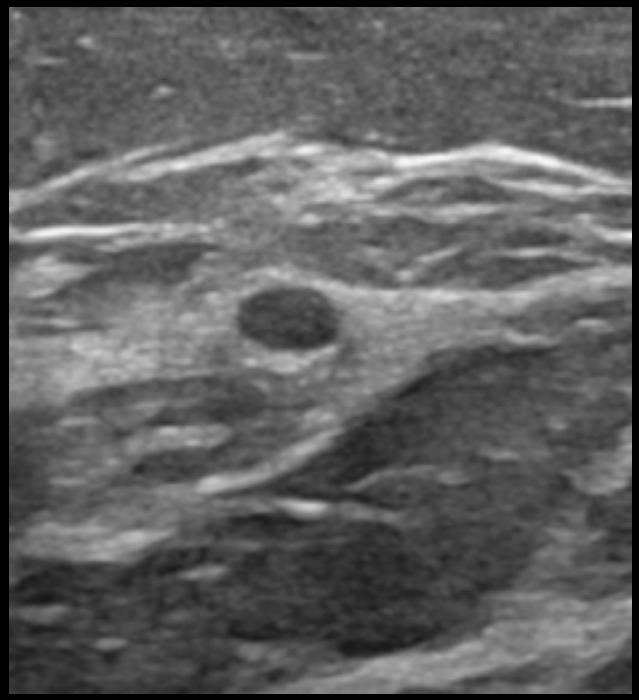




CC spot

MLO spot





Intraductal papilloma with ductal carcinoma in situ

Imaging Findings: Spot compression diagnostic mammography of the right breast in the MLO and CC projections demonstrate a 0.4 cm oval mass in the 3 o'clock position. Subsequent ultrasound shows a circumscribed homogenous hypoechoic mass demonstrating posterior enhancement and no internal vascularity. Aspiration of the mass was performed and demonstrated papillary neoplasm. The mass resolved on aspiration. The mass was excised.

Differential Diagnosis: Complicated cyst, fat necrosis, fibroadenoma, intraductal papilloma, carcinoma.

Surgical Pathology Diagnosis: Intraductal papilloma with ductal carcinoma in situ.

Discussion: Intraductal papillomas are proliferative tumors composed of epithelial/myoepethial cells and a fibrovascular core. Solitary papillomas are typically benign while multiple papillomas are associated with an increased risk of malignancy. It is rare to have ductal carcinoma in situ within a solitary intraductal papilloma. Mammography typically shows a circumscribed mass, dilated ducts, and/or a cluster of calcifications. Ultrasonography typically shows a well-circumscribed mass within a dilated duct and Doppler imaging may show flow through its fibrovascular core. Ultimately, histopathological confirmation is needed to determine if a concurrent malignancy is present. Although the presence of DCIS is rare in solitary papillomas, it is important to maintain a high index of suspicion in individuals with a strong family history of breast cancer.

@UpstateRad
@AOCRNews
@upstaterads
@aocrnews
Mehvish Durrani, DO & Katherine Willer, DO
SUNY Upstate Medical University

References

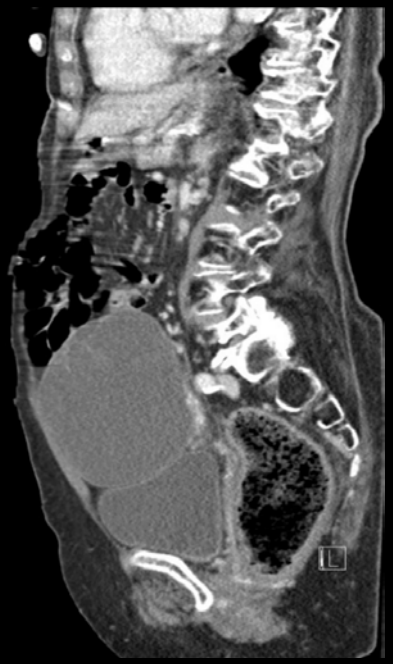
- Badrawi N, AlSayegh AA. Ductal carcinoma in situ of the breast arising in a solitary intraductal papilloma. *Radiol Case Rep*. 2022;18(2):449-451. Published 2022 Nov 23. doi:10.1016/j.radcr.2022.11.014
- Woods E, Helvie M, Ikeda D, Mandell S, Chapel K, Adler D. Solitary Breast Papilloma: Comparison of Mammographic, Galactographic, and Pathologic Findings. *AJR Am J Roentgenol.* 1992;159(3):487-91.

Posted 5/22/2026

52F presented to the ED with non-bloody diarrhea and persistent lower abdominal and pelvic pain x 2 days. She denied nausea, vomiting, and fever. No past surgical or gynecologic history was known at the time of imaging.



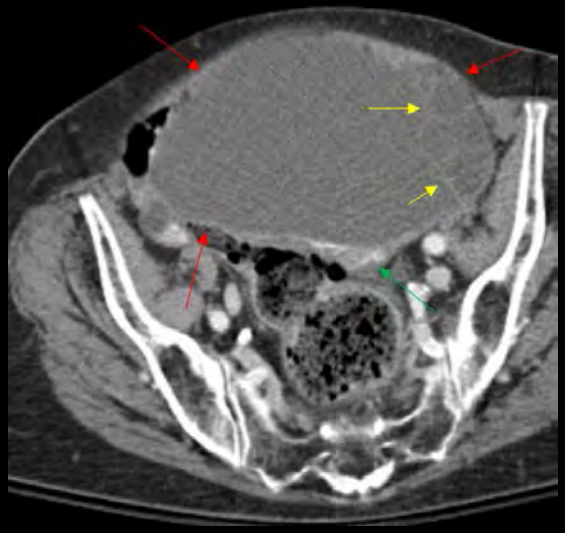
1. Axial Contrast-Enhanced CT



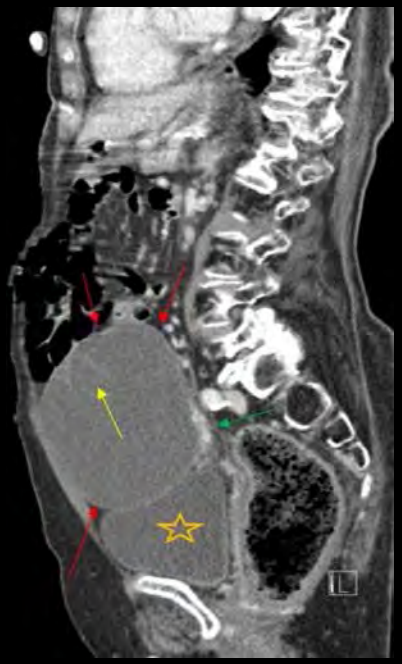
2. Sagittal Contrast-Enhanced CT



3. Coronal Contrast-Enhanced CT



1. Axial Contrast-Enhanced CT



2. Sagittal Contrast-Enhanced CT



3. Coronal Contrast-Enhanced CT

Ovarian Mucinous Cystadenoma

Imaging findings:

- Fig. 1: Axial contrast-enhanced CT pelvis demonstrates a complex, multiloculated, cystic pelvic mass (red arrows) arising from the left ovary (green arrow). Thin septations are visible (yellow arrows).
- Fig. 2: Sagittal view CT with contrast shows the full craniocaudal boundary of a large cystic mass (red arrows) with thin septations (yellow arrow). The left ovary is seen (green arrow). The bladder located inferiorly is normal (star).
- Fig. 3: Coronal contrast-enhanced CT reveals the mediolateral extent of a large, multiloculated, thinly septated (yellow arrows) cystic mass (red arrows). Normal bladder is visualized (star).

Differential diagnosis: mucinous cystadenoma, serous cystadenoma, cystmucinous cystadenocarcinoma, cystic teratoma, paraovarian

Discussion: Ovarian mucinous cystadenomas are common benign neoplasms representing >10% of ovarian tumors and approximately 80% of all mucinous ovarian neoplasms. Females of reproductive age are most often affected, with a median age of 36 years. The major implicated risk factor is smoking: a 20 or greater pack-year smoking history is associated with an odds ratio of 2.7 for benign mucinous neoplasms. Nearly all mucinous cystadenomas exhibit gastrointestinal-type metaplasia, expressing Claudin-18 and CDX2 on immunohistochemistry. Interestingly, benign mucinous neoplasms show overlap in molecular signaling alterations with their more aggressive counterparts. Nearly half of all benign and over two-thirds of all borderline cystadenomas display concurrent p16 loss and RAS/MAPK defects.

Clinical manifestations are highly nonspecific–pelvic pain, weight loss, bloating–though most patients present with profound pelvic masses that are rarely bilateral. Many cases present asymptomatically and are discovered incidentally on imaging. Although most mucinous cystadenomas are benign and have excellent prognoses, malignant transformation potential is non-negligible. Imaging and tumor characterization are thus necessary to minimize the risk of a cystadenoma-to-cystadenocarcinoma sequence.

Characteristic imaging features of ovarian mucinous cystadenomas include large size, multilocularity with numerous thin septations, mural calcification, unilaterality, and variable MRI signal due to variable viscosity of mucinous fluid. Identification depends on differences in imaging manifestations with other lesion types. Serous cystadenomas show smaller size, unilocularity or oligolocularity, no calcifications (generally, though they may be seen on rare occasions), hypointensity on T1 images, hyperintensity on T2 images, and T1+C wall enhancement. CT fat attenuation, high T1 intensity, and Aunt Minnie findings such as calcified teeth are representative of cystic teratomas. Paraovarian cysts can be differentiated by their extraovarian location, unilocular appearance, and small solid nodules. Findings associated with cystadenocarcinoma include septation >3 mm, mural nodules, papillary projections, a soft tissue component, metastatic disease, lymphadenopathy, and ascites. Definitive diagnosis requires correlation of radiologic findings with histopathological examination.

Asymptomatic patients may be managed with observation once a definitive diagnosis is made. Symptomatic or large masses, concern for malignancy, and patient opt-in warrant surgical intervention.

To briefly summarize, incidental ovarian mucinous cystadenomas identified on imaging for non-gynecologic complaints demand systematic evaluation and clinical correlation. Knowledge of characteristic benign imaging patterns ensures accurate interpretation and avoidance of overtreatment secondary to misdiagnosis or concern for malignancy.

@cameronlaurie65
@AOCRNews

@cameron_l_10
@aocrnews

Case courtesy of Cameron C. Laurie, MS1[1], April L. Cox, DO[2]
[1]Baylor College of Medicine, [2]Indiana University School of Medicine

AOCR American Osteopathic College of Radiology

References

- Marko J, Marko KI, Pachigolla SL, Crothers BA, Mattu R, Wolfman DJ (2019) Mucinous Neoplasms of the Ovary: Radiologic-Pathologic Correlation. Radiographics 39(4):982-997
- Silva E, Malpica A, Roma A, Ramalingam P, Kim G, Bakkar R, Loghavi S, Kim S, Shaye-Brown A, Marques-Piubelli ML, Chisholm G, Gershenson DM, Alvarado-Cabrero I (2021) Ovarian mucinous neoplasms, intestinal type, in premenopausal patients, develop in abnormal ovaries. Hum Pathol 108:32-41
- Jordan SJ, Green AC, Whiteman DC, Webb PM; Australian Ovarian Cancer Study Group (2007) Risk factors for benign, borderline and invasive mucinous ovarian tumors: epidemiological evidence of a neoplastic continuum? Gynecol Oncol 107(2):223-30
- Halimi SA, Maeda D, Ushiku-Shinozaki A, Goto A, Oda K, Osuga Y, Fujii T, Ushiku T, Fukayama M (2021) Comprehensive immunohistochemical analysis of the gastrointestinal and Müllerian phenotypes of 139 ovarian mucinous cystadenomas. Hum Pathol 109:21-30
- Hunter SM, Gorringe KL, Christie M, Rowley SM, Bowtell DD; Australian Ovarian Cancer Study Group; Campbell IG (2012) Pre-invasive ovarian mucinous tumors are characterized by CDKN2A and RAS pathway aberrations. Clin Cancer Res 18(19):5267-77
- Sisodia RC, Del Carmen MG (2022) Lesions of the Ovary and Fallopian Tube. N Engl J Med 387(8):727-736
- American College of Obstetricians and Gynecologists' Committee on Practice Bulletins—Gynecology (2016) Practice Bulletin No. 174: Evaluation and Management of Adnexal Masses. Obstet Gynecol 128(5):e210-e226
- Mascilini F, Moro F, Pasciuto T, Sladkevicius P, Froyman W, Jokubkiene L, Van Holsbeke C, Franchi D, Epstein E, Guerriero S, Chiappa V, Buonomo F, Kudla MJ, Alcázar JL, Hochberg L, Ciccarone F, Quagliozzi L, Scambia G, Timmerman D, Valentin L, Testa AC (2025) Imaging in gynecological disease (28): clinical and ultrasound characteristics of serous and mucinous cystadenomas in the adnexa. Ultrasound Obstet Gynecol 66(2):233-241
- Taylor EC, Irshaid L, Mathur M (2021) Multimodality Imaging Approach to Ovarian Neoplasms with Pathologic Correlation. Radiographics 41(1):289-315
- Outwater EK, Siegelman ES, Hunt JL (2001) Ovarian teratomas: tumor types and imaging characteristics. Radiographics 21(2):475-90

Posted 5/15/2026

62 y/o m presents the emergency department with confusion and weakness. Patient history of cirrhosis of the liver with continued alcohol abuse and multiplecomorbidities


A


A

Emphysematous Cholecystitis

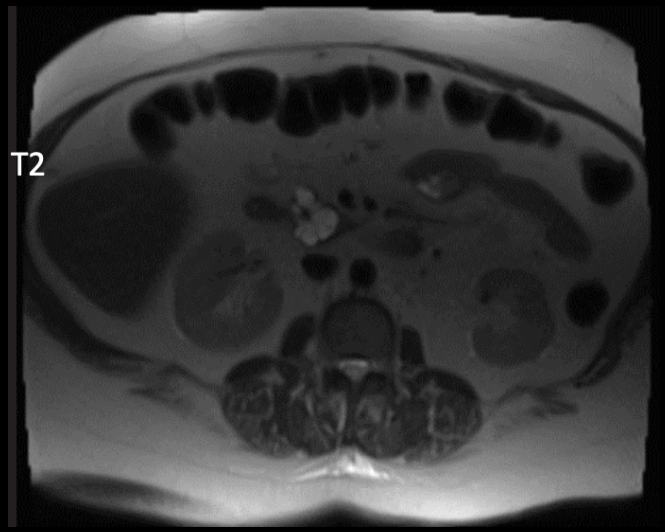
- Image Findings: Gas in the wall of the gallbladder.
- Differential Diagnosis: Recent biliary intervention or incompetent sphincter of Oddi.
- Discussion: Emphysematous cholecystitis is a rare complication in acute cholecystitis due to polymicrobial infection in the walls of the gallbladder most commonly seen in diabetic patients, males greater than females. It is considered a surgical emergency and has a reported mortality rate of approximately 15%. In this case, the patient was too ill to undergo surgery and the patient underwent placement of a percutaneous transhepatic cholecystomy tube.

Posted 5/8/2026

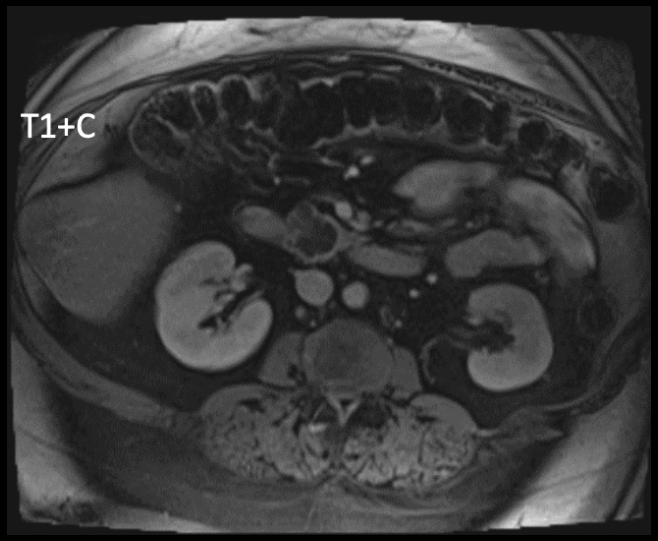
65F underwent CT and MR evaluation for elevated LFTs



1. Axial Non-contrast CT Abdomen



2. Axial T2-weighted MR Abdomen



3. Axial T1-weighted Post-contrast MR Abdomen



1. Axial Non-contrast CT Abdomen



2. Axial T2-weighted MR Abdomen



3. Axial T1-weighted Post-contrast MR Abdomen

Pancreatic Serous Cystadenoma

Imaging findings:

- Fig. 1: Axial CT abdomen without contrast shows a lobulated, hypodense mass in the head of the pancreas with central calcification (yellow circle).
- Fig. 2: Axial T2-weighted MRI demonstrates a multiloculated cystic pancreatic mass with central scarring (red circle).
- Fig. 3: Axial T1-weighted post-contrast MRI illustrates internal septal enhancement (blue circle).

Differential diagnosis: serous cystadenoma, intraductal papillary mucinous neoplasm, mucinous cystic neoplasm, pseudocyst

Discussion: Pancreatic serous cystadenoma (PSC) is a relatively common benign epithelial neoplasm of the pancreas, with malignant transformation to serous cystadenocarcinoma occurring in only ~0.1% of cases. PSC typically presents in women between the fifth to seventh decades of life and constitutes approximately 75% of cases. On histology, PSCs consist of cuboidal epithelium with a pronounced subepithelial capillary network and positive periodic acid-Schiff staining. Alterations to the von Hippel-Lindau (*VHL*) tumor suppressor gene on chromosome 3p25-26 contribute to neoplastic activity.

Most patients are asymptomatic, though symptom frequency correlates with size. Approximately 72% of patients with PSCs >4 cm experience symptoms compared to around 22% with smaller tumors. Reported symptoms include nonlocalized abdominal pain or fullness, jaundice, pancreatitis, and biliary obstruction due to mass effect. Due to the constellation of nonspecific symptoms or the complete absence of symptoms altogether, imaging plays a central role in diagnosis. Once PSC is confidently identified, management is often limited to observation and reassurance given the near-absence of malignant potential. Surgical resection may be indicated for symptomatic, rapidly growing, or diagnostically uncertain lesions with concern for malignancy.

PSCs are increasingly incidental findings due to improvements in advanced imaging technology and reading capabilities. MRI with MRCP or pancreatic protocol CT are first-line, though MRI displays superiority in morphological assessment. EUS is performed secondarily when cross-sectional imaging is inconclusive. There are two distinct imaging patterns that characterize PSCs. The presence of numerous small septations with a “honeycomb” or microcystic appearance is pathognomic for the classical variant; a central stellate calcified scar is specific but present in a minority of cases. The lesser-seen macrocystic variant is rather difficult to diagnose radiologically as it is indistinguishable from mucinous lesions, however these lesions typically demonstrate lobulations, absence of wall enhancement, and location in the pancreatic head on CT.

Prognosis is generally excellent. In fact, once a diagnosis is established, surveillance is not recommended for asymptomatic cases. For those undergoing surveillance, surveillance beyond five years is not recommended when no concerning features develop.

To conclude, PSCs are benign neoplasms of the pancreas with minimal malignant potential. While post-diagnostic management is favorable, recognition of the characteristic imaging patterns and differentiation from more concerning neoplasms, such as intraductal papillary mucinous and mucinous cystic neoplasms, is essential.

@cameronlaurie65
@AOCRNews
@cameron_l_10
@aocrnews

Case courtesy of Cameron C. Laurie, MS1[1], April L. Cox, DO[2]
[1]Baylor College of Medicine, [2]Indiana University School of Medicine

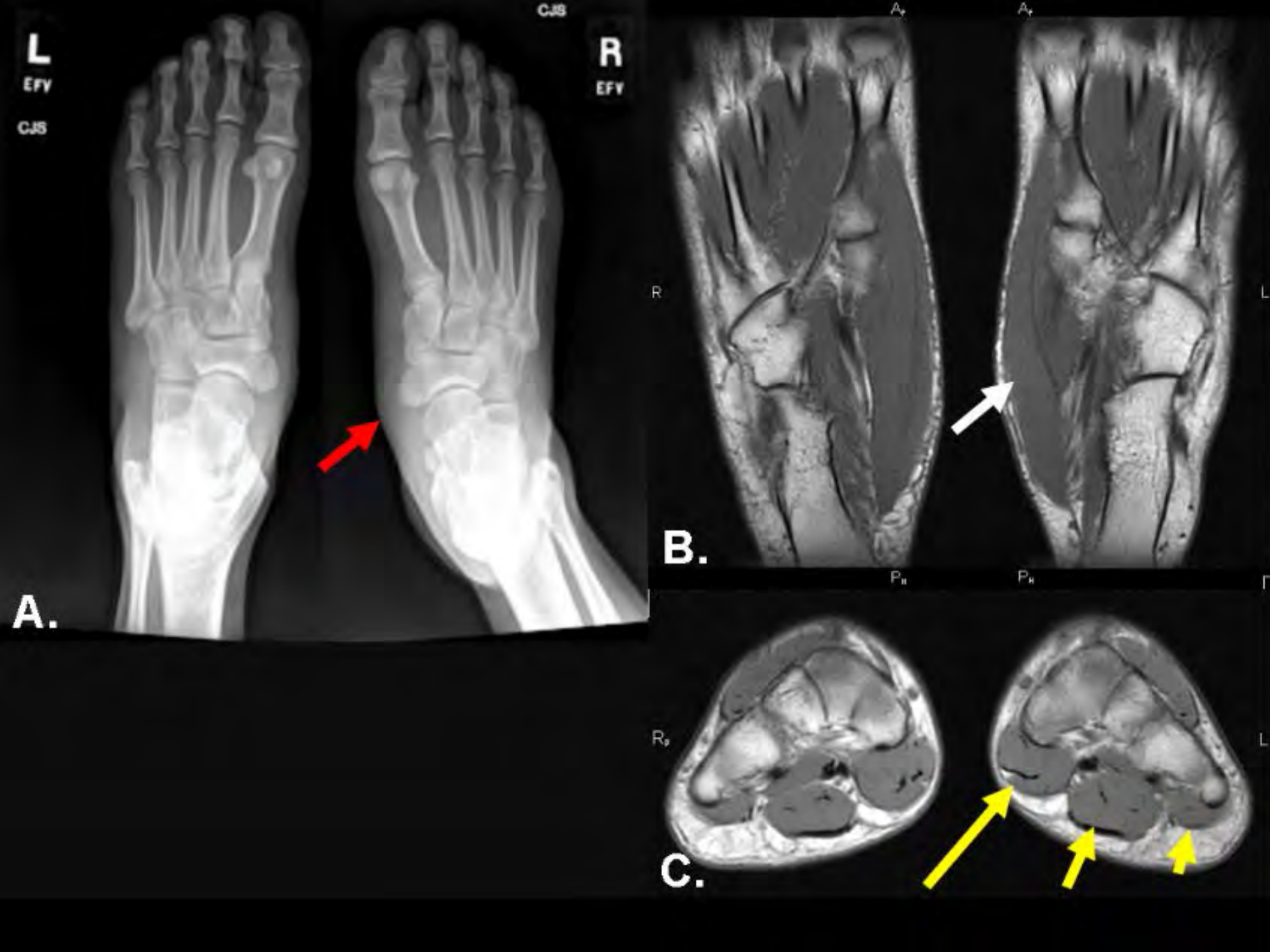
References

- Gonda TA, Cahen DL, Farrell JJ (2024) Pancreatic Cysts. N Engl J Med 391(9):832-843
- Elta GH, Enestvedt BK, Sauer BG, Lennon AM (2018) ACG Clinical Guideline: Diagnosis and Management of Pancreatic Cysts. Am J Gastroenterol 113(4):464-479
- Cuber A, Chopra S (2025) Serous Cystadenoma of the Pancreas: An Easily Missed Cytological Diagnosis and Clues to Diagnosis. Diagn Cytopathol 53(3):139-145
- Vortmeyer AO, Lubensky IA, Fogt F, Linehan WM, Khettry U, Zhuang Z (1997) Allelic deletion and mutation of the von Hippel-Lindau (VHL) tumor suppressor gene in pancreatic microcystic adenomas. Am J Pathol 151(4):951-6
- Tseng JF, Warshaw AL, Sahani DV, Lauwers GY, Rattner DW, Fernandez-del Castillo (2005) Serous cystadenoma of the pancreas: tumor growth rates and recommendations for treatment. Ann Surg 242(3):413-9
- Jais B, Rebours V, Malleo G, Salvia R, Fontana M, Maggino L, Bassi C, Manfredi R, Moran R, Lennon AM, Zaheer A, Wolfgang C, Hruban R, Marchegiani G, Fernández Del Castillo C, Brugge W, Ha Y, Kim MH, Oh D, Hirai I, Kimura W, Jang JY, Kim SW, Jung W, Kang H, Song SY, Kang CM, Lee WJ, Crippa S, Falconi M, Gomatos I, Neoptolemos J, Milanetto AC, Sperti C, Ricci C, Casadei R, Bissolati M, Balzano G, Frigerio I, Girelli R, Delhaye M, Bernier B, Wang H, Jang KT, Song DH, Huggett MT, Oppong KW, Pererva L, Kopchak KV, Del Chiaro M, Segersvard R, Lee LS, Conwell D, Osvaldt A, Campos V, Aguero Garcete G, Napoleon B, Matsumoto I, Shinzeki M, Bolado F, Fernandez JM, Keane MG, Pereira SP, Acuna IA, Vaquero EC, Angiolini MR, Zerbi A, Tang J, Leong RW, Faccinetto A, Morana G, Petrone MC, Arcidiacono PG, Moon JH, Choi HJ, Gill RS, Pavey D, Ouaïssi M, Sastre B, Spandre M, De Angelis CG, Rios-Vives MA, Concepcion-Martin M, Ikeura T, Okazaki K, Frulloni L, Messina O, Lévy P (2016) Serous cystic neoplasm of the pancreas: a multinational study of 2622 patients under the auspices of the International Association of Pancreatology and European Pancreatic Club (European Study Group on Cystic Tumors of the Pancreas). Gut 65(2):305-12
- Lee LS, Gardner TB (2025) Pancreatic Cysts and Pancreatitis in the Older Adult. Am J Gastroenterol 120(Suppl 10):S27-S33
- Stark A, Donahue TR, Reber HA, Hines OJ (2016) Pancreatic Cyst Disease: A Review. JAMA 315(17):1882-93
- Schmitz D, Stenzinger A, Grützmann R, Esposito I, Raatschen HJ, Seufferlein TTW (2025) The Differential Diagnosis and Management of Pancreatic Cystic Neoplasms. Dtsch Arztebl Int 122(22):617-622

29 y/o m with no hx of congenital abnormalities or systemic disease who developed bilateral medial plantar foot pain beginning around age 17 with running & brisk walking. Pain is deep & aching plantar from the navicular & along the longitudinal arch, medially, accompanied by activity-related swelling that resolves with rest; he denies numbness, weakness, or prior trauma.



A. Bilateral weight-bearing AP radiographs of the feet.
B. Bilateral foot MRI coronal gre-T1-weighted
C. Bilateral foot MRI axial gre-T1-weighted


L
EFV
CJS
CJS
R
EFV
A.
B.
R
L
C.

Bilateral Hypertrophy of the Intrinsic Plantar Foot Musculature

Imaging findings: Radiographs' reveal the navicular tubercle regions to be prominent medially, which has been described by some sources as gorilliform navicular morphology. They also reveal increased soft-tissue thickness along the medial midfoot aspect of both feet - without other discrete diagnosis to explain current symptoms (red arrow). Axial T1-weighted MRI of the feet indicate enlarged abductor hallucis muscles (white arrow). Coronal T1 MRI of the feet reveals enlargement of the abductor hallucis, flexor digitorum brevis, and abductor digiti minimi (yellow arrows, respectively left to right).

All MRI images were negative for edema, fatty infiltration, focal mass, or nerve displacement.

Differential Diagnosis: Benign soft-tissue tumor (e.g., lipoma), neurogenic muscle hypertrophy, vascular malformation or hemangioma, congenital or syndromic overgrowth (e.g., hemihyperplasia/overgrowth syndromes).

Discussion: Congenital hypertrophy of intrinsic foot muscles is classically unilateral and localized to one or a few muscles; diffuse bilateral involvement of the entire intrinsic plantar compartment is rare. Cross sectional imaging is critical to confirm hypertrophy of intrinsic plantar foot musculature and guide management, which may be conservative in the absence of deformity or nerve compression.

Case courtesy of Alexander Enabnit, OMS II; Kyran Hines, OMS-I; James Adams, DO | ATSU-KCOM

References

- Hellwinkel, J.E., York, P.J., Leaseburg, J.T. & Hunt, K.J. (2019) Congenital Unilateral Hypertrophy of the Foot Intrinsics: A Rare Case and Review of Literature. *Journal of Orthopaedic Case Reports*, 9, 34–37.
- Abourazzak, F. E., Shimi, M., Azzouzi, H., Mansouri, S., El Mrini, A., & Harzy, T. (2015). An unusual cause of medial foot pain: The cornuate navicular. European Journal of Rheumatology, 2(1), 33–34. https://doi.org/10.5152/eurjrheumatol.2014.14047

Posted 4/24/2026

23M presented to the ER with wrist pain. Radiograph was obtained. F/u imaging was performed 1 year later to assess for morphologic changes to the lunate and surrounding structures.



1. Initial Radiograph



2. 1 Year F/u Radiograph



3. Coronal CT



4. Sagittal CT



1. Initial Radiograph



2. 1 Year F/u Radiograph



3. Coronal CT



4. Sagittal CT

Kienböck's disease

- Imaging findings:
  - Figs. 1-2: Initial PA wrist radiograph demonstrated sclerosis and mild flattening of the lunate (red circle), consistent with osteonecrosis (aka avascular necrosis). Negative ulnar variance was displayed (red arrow). Radiograph at one year follow-up indicated lunate flattening and elevated radiodensity relative to surrounding carpal bones (yellow arrows), supporting an osteonecrotic etiology.
  - Figs. 3-4: Coronal and sagittal CT wrist showed lunate fragmentation collapse of normal trabecular architecture (yellow circles). Secondary degenerative change, including a subchondral cyst in the capitate, was also seen.
- Differential diagnosis: Kienböck's disease, ulnar impaction syndrome, trauma and dorsal intercalated segmental instability (DISI)
- Discussion: Kienböck's disease (KD), otherwise known as osteonecrosis of the lunate, is a disease of progressive wrist pain and dysfunction with a prevalence of around 0.27%. While individuals at any age can be affected, most cases are seen in Caucasians aged 20-40, with men and women affected equally (among the elderly, women are more affected). The etiology may be multifactorial. Risk factors include negative ulnar variance and lunar configuration (shown to be contributory), repeated axial loading, trauma, embolism, and hypercoagulability. For those with earlier stage disease or contraindications to surgery, conservative measures are used (e.g., NSAIDs, splinting, avoidance of risk behaviors). For more advanced disease, there is no definitive treatment. However, commonly performed procedures include radial shortening osteotomy (favorable in this case due to the negative ulnar variance), capitate shortening osteotomy (neutral or positive ulnar variance), vascularized bone grafting, and proximal row carpectomy. In summary, the disrupted blood supply in KD leads to collapse of the lunate, and management is guided by radiographic stage and cartilage condition to maintain wrist function.

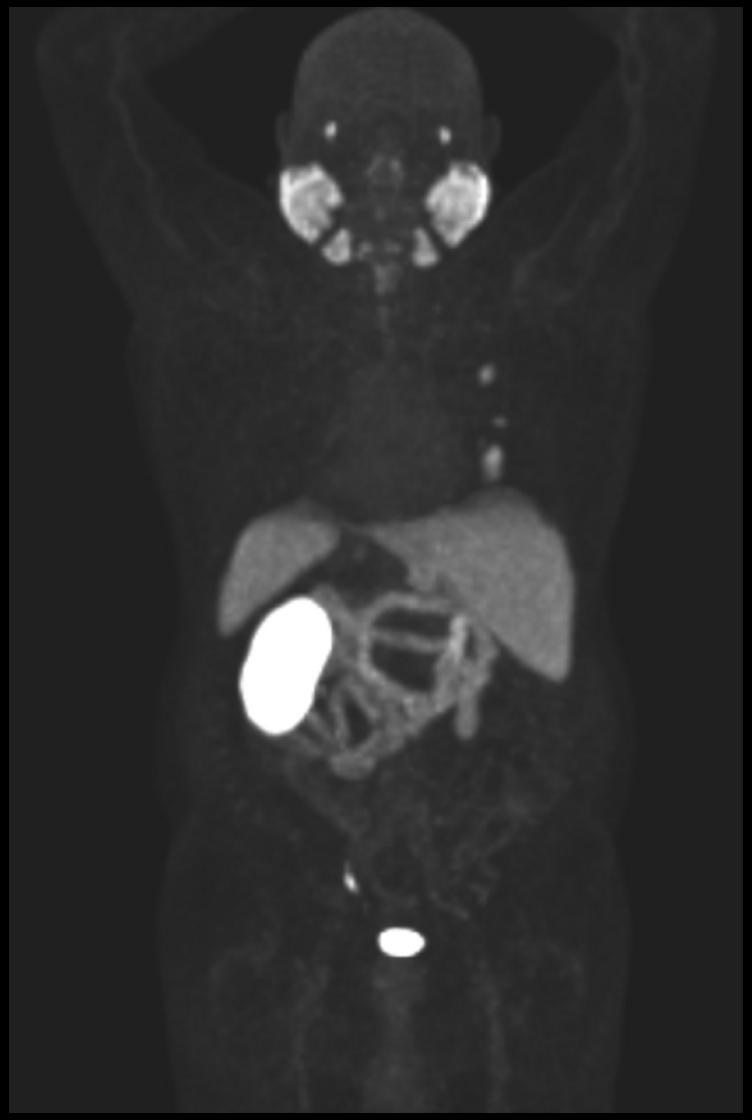
@cameronlaurie65
@AOCRNews
@cameron_l_10
@aocrnews
Case courtesy of Cameron C. Laurie, MS1[1], April L. Cox, DO[2]
[1]Baylor College of Medicine, [2]Indiana University School of Medicine

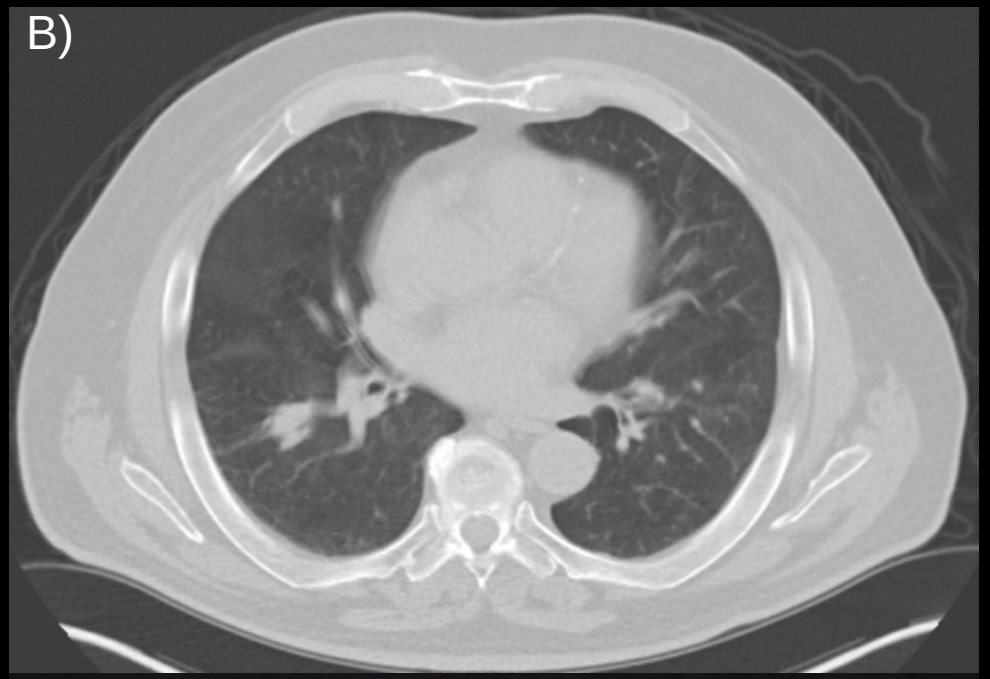
References

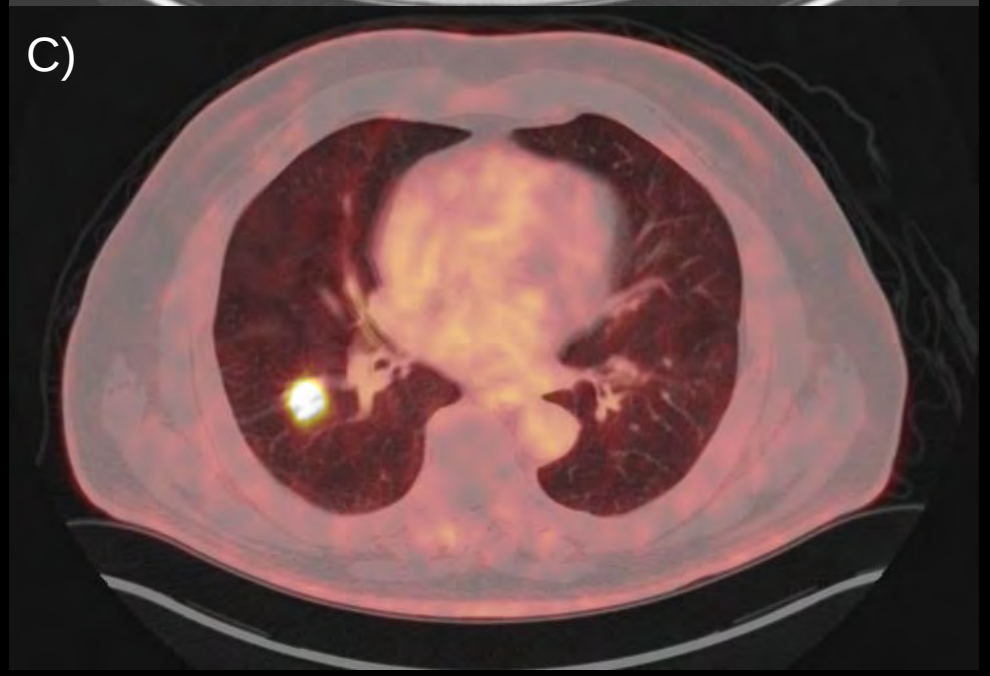
- Allan CH, Joshi A, Lichtman DM. Kienböck's Disease: Diagnosis and Treatment. Journal of the American Academy of Orthopaedic Surgeons. 2001;9(2):128-136. doi: https://doi.org/10.5435/00124635-200103000-00006
- Arnaiz J, Piedra T, Cerezal L, et al. Imaging of Kienböck Disease. American Journal of Roentgenology. 2014;203(1):131-139. doi: https://doi.org/10.2214/ajr.13.11606
- Beredjiklian PK. Kienböck's Disease. The Journal of Hand Surgery. 2009;34(1):167-175. doi: https://doi.org/10.1016/j.jhsa.2008.10.012
- Camus EJ, Van Overstraeten L. Kienböck's disease in 2021. Orthopaedics & Traumatology: Surgery & Research. 2022;108(1, Supplement):103161. doi: https://doi.org/10.1016/j.otsr.2021.103161
- Chojnowski K, Opiełka M, Piotrowicz M, et al. Recent Advances in Assessment and Treatment in Kienböck's Disease. Journal of Clinical Medicine. 2022;11(3):664. doi: https://doi.org/10.3390/jcm11030664
- Cross D, Matullo KS. Kienböck Disease. Orthopedic Clinics of North America. 2014;45(1):141-152. doi: https://doi.org/10.1016/j.ocl.2013.09.004
- Dixon A. Kienböck disease | Radiology Reference Article | Radiopaedia.org. Radiopaedia. https://radiopaedia.org/articles/kienbock-disease-2?lang=us
- Lichtman DM, Pientka WF. Kienböck Disease: Recent Advances in Understanding and Management. Journal of Bone and Joint Surgery. Published online May 8, 2025. doi: https://doi.org/10.2106/jbjs.24.01090
- Lichtman DM, Pientka WF, MacLean S, Bain G. Precision Medicine for Kienböck Disease in the 21st Century. The Journal of Hand Surgery. 2022;47(7):677-684. doi: https://doi.org/10.1016/j.jhsa.2022.03.014
- Stahl S, Hentschel PJH, Held M, et al. Characteristic features and natural evolution of Kienböck's disease: Five years' results of a prospective case series and retrospective case series of 106 patients. Journal of Plastic, Reconstructive & Aesthetic Surgery. 2014;67(10):1415-1426. doi: https://doi.org/10.1016/j.bjps.2014.05.037

Posted 4/17/2026

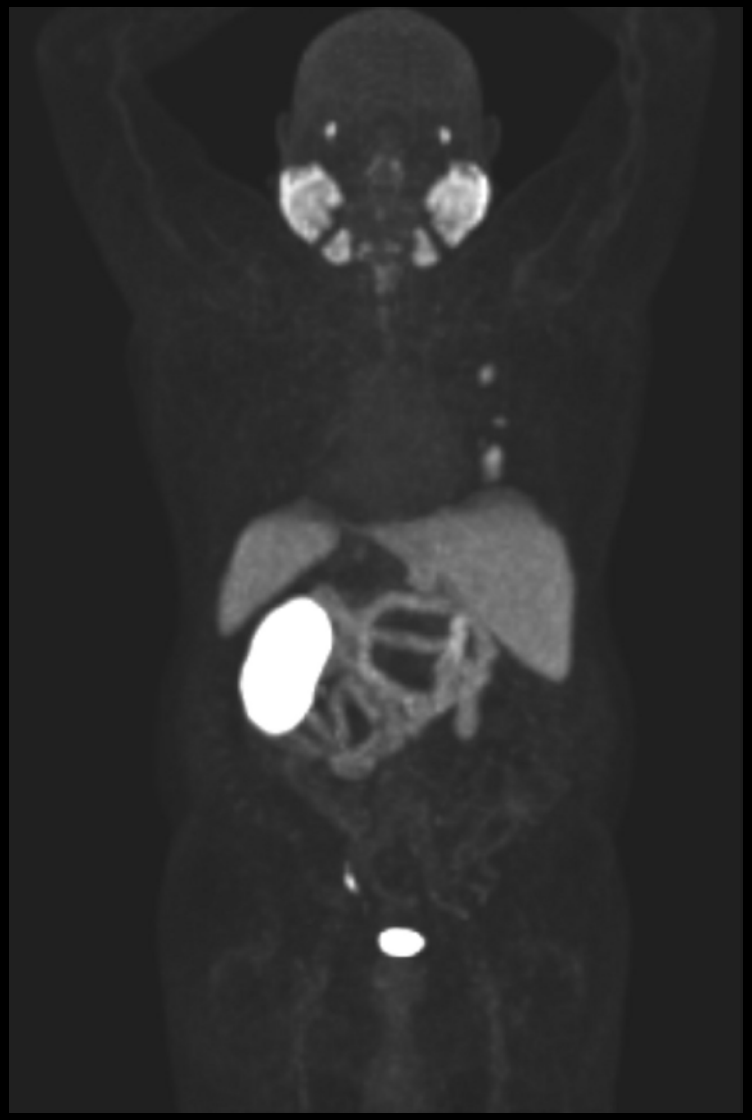
83 y/o m with past Hx of localized prostate cancer previously treated with radiation. He now presents with slowly rising PSA.

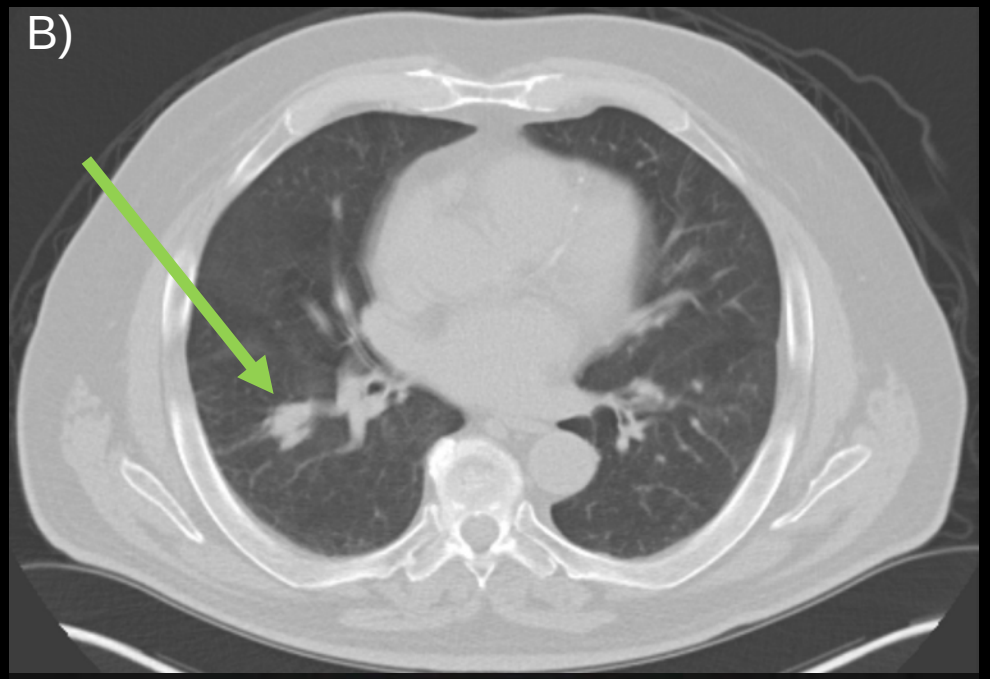






A) 3D-PET, maximum intensity projection (MIP)
B) Axial CT chest without contrast
C) PSMA-PET/CT fused axial image







A) 3D-PET, maximum intensity projection (MIP)
B) Axial CT chest without contrast
C) PSMA-PET/CT fused axial image

Metastatic Prostate Cancer to the Lung

Imaging Findings: The PET MIP shows uptake in the lacrimal glands, salivary glands, small bowel, kidneys/ureters/bladder, liver, and spleen, indicating that this is a PSMA PET scan. Axial CT of the chest demonstrates a mass in the perihilar region of the right lower lobe (green arrow). The PSMA-PET/CT fused axial image shows uptake associated with this lesion (red arrow). Histopathology was consistent with metastasis of prostate origin.

Differential Diagnosis: Primary lung cancer, metastasis of primary malignancy other than prostate, infection (e.g. tuberculosis, histoplasmosis), granulomatous processes (e.g. sarcoidosis).

Discussion: The lung is the 4th most common site of prostate cancer metastasis after the bones, lymph nodes, and liver (1). The majority of prostate cancer lung metastases will be PSMA-positive. However, a significant number of lung metastases can present with a very similar anatomic appearance to primary lung malignancy or benign processes, and can be PSMA-negative (2). It is also possible for primary lung malignancy or metastasis of other primary to overexpress PSMA (3-5). For these reasons, lung lesions in this group of patients may require tissue sampling for definitive diagnosis.

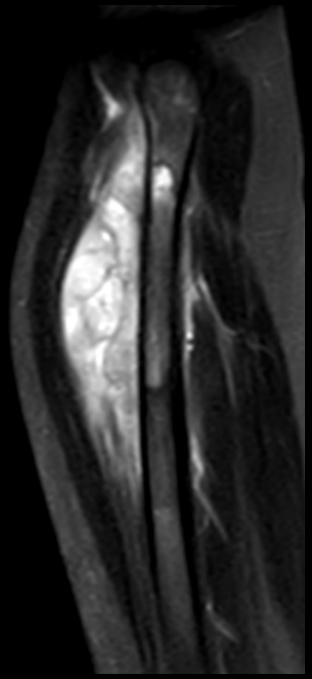
References

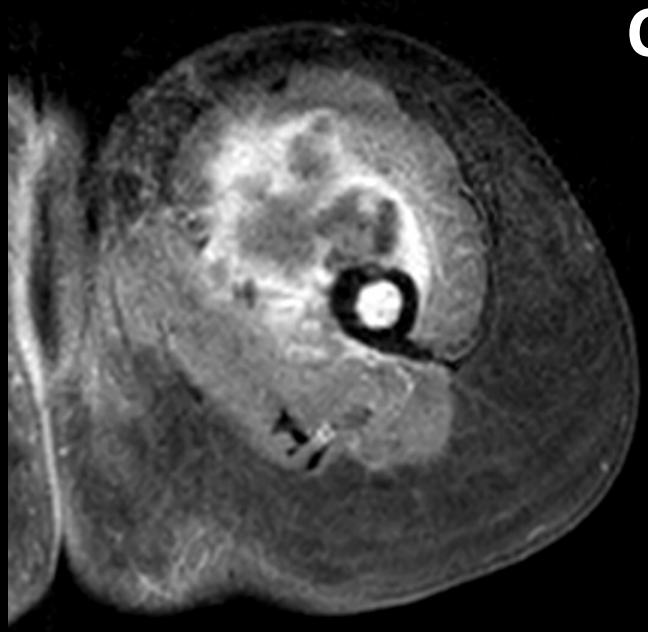
1. Gandaglia G, Abdollah F, Schiffmann J, Trudeau V, Shariat SF, Kim SP, Perrotte P, Montorsi F, Briganti A, Trinh QD, Karakiewicz PI, Sun M. Distribution of metastatic sites in patients with prostate cancer: A population-based analysis. Prostate. 2014 Feb;74(2):210-6. doi: 10.1002/pros.22742. Epub 2013 Oct 16. PMID: 24132735.
2. Damjanovic J, Janssen JC, Furth C, Diederichs G, Walter T, Amthauer H, Makowski MR. ^{68}Ga-PSMA-PET/CT for the evaluation of pulmonary metastases and opacities in patients with prostate cancer. Cancer Imaging. 2018 May 16;18(1):20. doi: 10.1186/s40644-018-0154-8. PMID: 29769114; PMCID: PMC5956855.
3. Shetty D, Loh H, Bui C, Mansberg R, Stevanovic A. Elevated 68Ga Prostate-Specific Membrane Antigen Activity in Metastatic Non-Small Cell Lung Cancer. Clin Nucl Med. 2016 May;41(5):414-6. doi: 10.1097/RLU.0000000000001139. PMID: 26828144.
4. Lütje S, Gomez B, Cohnen J, Umutlu L, Gotthardt M, Poeppel TD, Bockisch A, Rosenbaum-Krumme S. Imaging of Prostate-Specific Membrane Antigen Expression in Metastatic Differentiated Thyroid Cancer Using 68Ga-HBED-CC-PSMA PET/CT. Clin Nucl Med. 2017 Jan;42(1):20-25. doi: 10.1097/RLU.0000000000001454. PMID: 27846003.
5. Haffner MC, Kronberger IE, Ross JS, Sheehan CE, Zitt M, Mühlmann G, Ofner D, Zelger B, Ensinger C, Yang XJ, Geley S, Margreiter R, Bander NH. Prostate-specific membrane antigen expression in the neovasculature of gastric and colorectal cancers. Hum Pathol. 2009 Dec;40(12):1754-61. doi: 10.1016/j.humpath.2009.06.003. Epub 2009 Aug 27. PMID: 19716160.

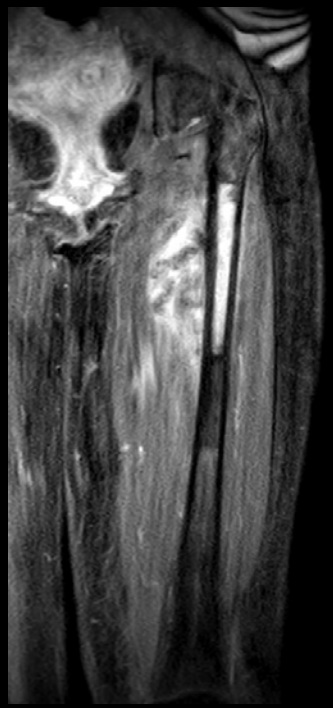
Posted 4/10/2026

14 y/o f presents with 1 month of left thigh pain and acute swelling. Patient has a hx of left upper thigh synovial sarcoma treated with chemotherapy and radiation, in remission for 8 years.







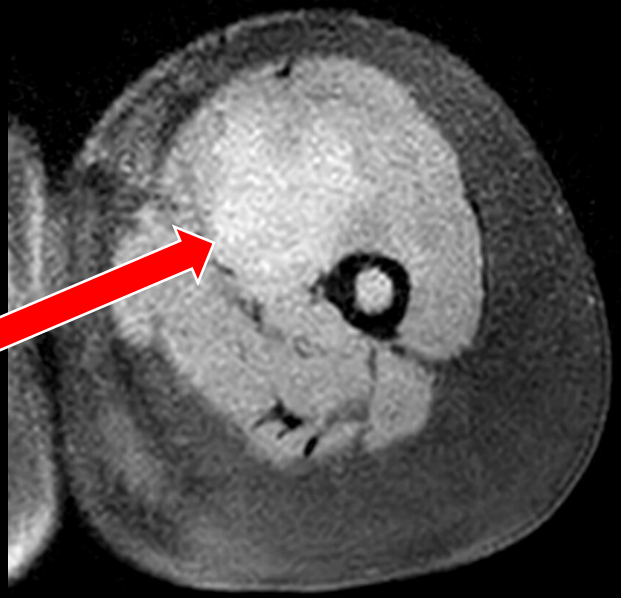


A – Axial T1 fat saturated pre contrast

B – Coronal T2 STIR

C – Axial T1 fat saturated post contrast

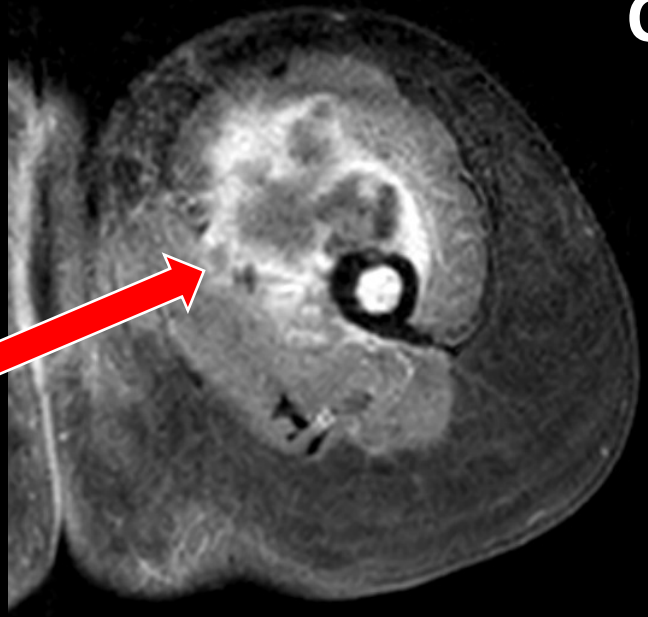
D – Coronal T1 fat saturated post contrast



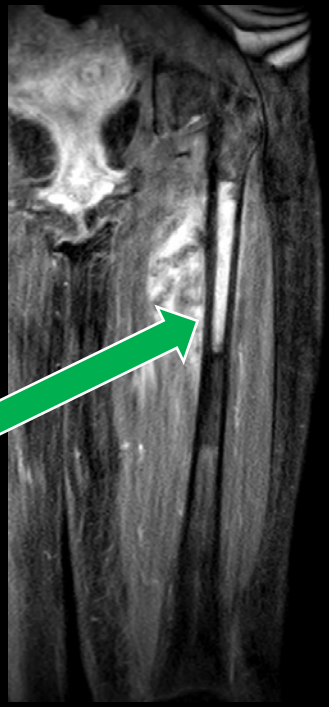
A



B



C



D

A – Axial T1 fat saturated pre contrast

B – Coronal T2 STIR

C – Axial T1 fat saturated post contrast

D – Coronal T1 fat saturated post contrast

Radiation Induced Chondrosarcoma

Imaging Findings: Axial T1 MRI with and without contrast shows a large soft tissue mass in the proximal to mid anterior medial thigh, abutting the femur (red arrows), with periosteal reaction and medullary cavity signal abnormality (green arrow). Large soft tissue mass in a sagittal STIR protocol (blue arrow).

Differential Diagnosis: Radiation induced sarcoma or chondrosarcoma, Recurrent synovial cell sarcoma, Primary malignant bone tumor (ie. Osteosarcoma), Infection (ie. Osteomyelitis and pyomyositis)

Discussion: Radiation induced chondrosarcoma is a rare complication of radiotherapy, often manifesting more than a decade after initial insult. Clinical manifestations of chondrosarcoma are generally nonspecific, commonly presenting as persistent, focal, dull, and progressing pain with swelling at the affected site. The risk is elevated for tumors arising in the prior radiation field, appears to be dose-dependent, and is influenced by younger age at exposure. It may develop de novo or from a radiation-induced benign lesion such as an osteochondroma. Imaging typically reveals a heterogeneous mass with bone and/or soft tissue involvement, and diagnosis is confirmed histologically. These lesions are usually treated with surgical resection with wide margins, as they are generally resistant to conventional chemotherapy. This case involved a pediatric patient who was previously treated for synovial sarcoma. She received surgical resection and radiation therapy to the left thigh and adjuvant chemotherapy eight years prior to this exam. Disarticulation was chosen to treat the radiation induced chondrosarcoma.

@imcolenewton
@AOCRNews
@colenewton
@rvu_ut
@aocrnews

Case courtesy of Cole Newton, OMS 3, Ryan Sanchez, DO, Michael Tall, MD
UTHSC San Antonio, Rocky Vista University COM

References

- Di Muzio B, Murphy A, Yap J, et al. Radiation-induced sarcoma. Reference article, Radiopaedia.org (Accessed on 04 Aug 2025) https://doi.org/10.53347/rID-36661

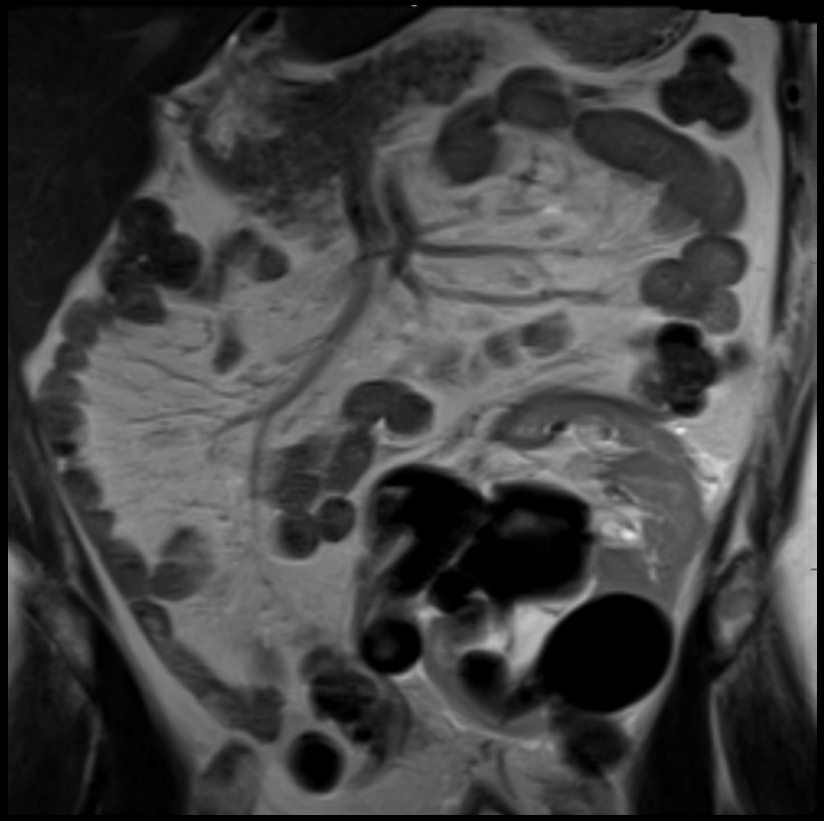
- Kim, J. H., Chu, F. C., Woodard, H. Q., Melamed, M. R., Huvos, A., & Cantin, J. (1978). Radiation-induced soft-tissue and bone sarcoma. *Radiology*, *129*(2), 501–508. https://doi.org/10.1148/129.2.501

- Nagata, S., Shen, R. K., Laack, N. N., Inwards, C. Y., Wenger, D. E., & Amrami, K. K. (2013). Chondrosarcoma arising within a radiation-induced osteochondroma several years following childhood total body irradiation: case report. *Skeletal radiology*, *42*(8), 1173–1177. https://doi.org/10.1007/s00256-013-1608-5

- Weinschenk, R. C., Wang, W. L., & Lewis, V. O. (2021). Chondrosarcoma. *The Journal of the American Academy of Orthopaedic Surgeons*, *29*(13), 553–562. https://doi.org/10.5435/JAAOS-D-20-01188

Posted 4/3/2026

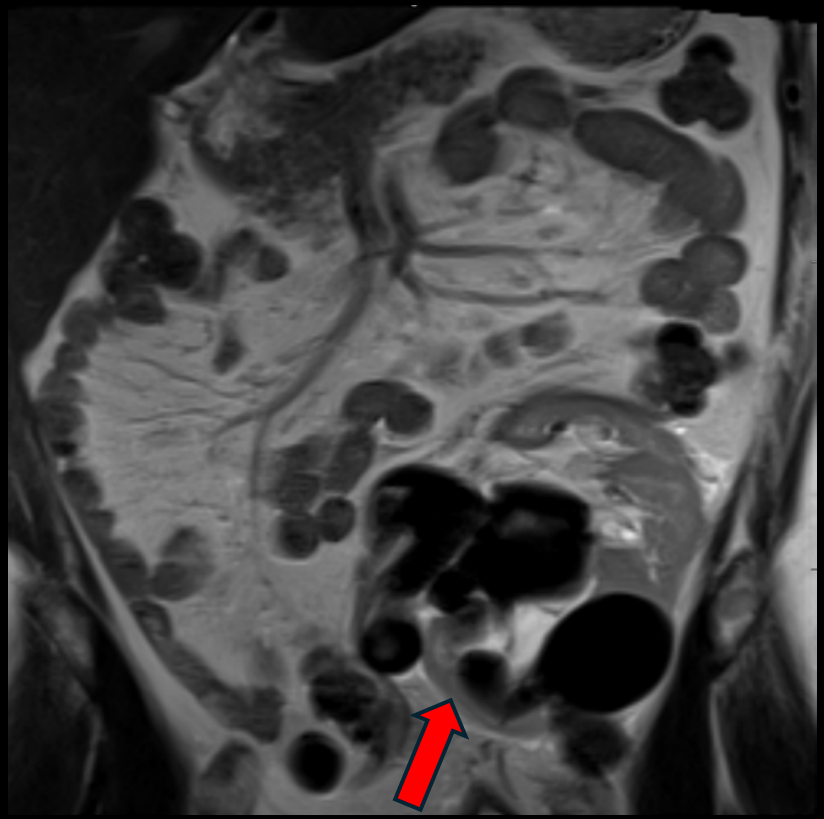
39 y/o F on immunosuppressive therapy with past hx of kidney transplant due to Granulomatosis with polyangiitis presenting with abdominal pain for the past 3 months. She underwent a renal biopsy 20 years ago.



Coronal T2 MRI



Coronal MIP MRI



Coronal T2 MRI



Coronal MIP MRI

Arteriovenous fistula of the transplant kidney

Image Findings: Large arteriovenous fistula (AVF) in the middle and lower third of the transplant kidney in left lower quadrant.

Differential diagnosis: Pseudoaneurysm, Renal vein thrombosis with collateral formation.

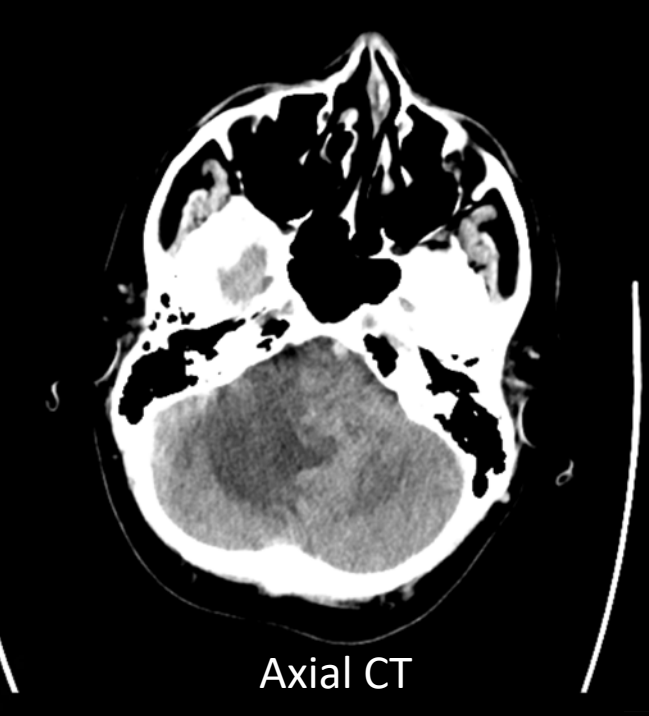
Discussion: AVF is a rare but important complication of renal biopsy. Iatrogenic AVF can complicate up to 16% of transplant renal biopsies. Greater than 95% of patients recover spontaneously within 3 months. The majority of AVFs are diagnosed due to presenting symptoms, such as hematuria, palpable thrill, resistant hypertension, cardiac and renal failure. Patients presenting with hematuria or declining renal function require early intervention. Imaging with color doppler ultrasound can accurately diagnose however the current gold standard is angiography. Treatment options include selective embolization of AVF, and surgical interventions consisting of partial or total nephrectomy.

@Sayed__Aftab
@AOCRNews
@aocrnews
Sayed Aftab OMSIV and Joseph Stein DO
Dartmouth-Hitchcock Medical Center

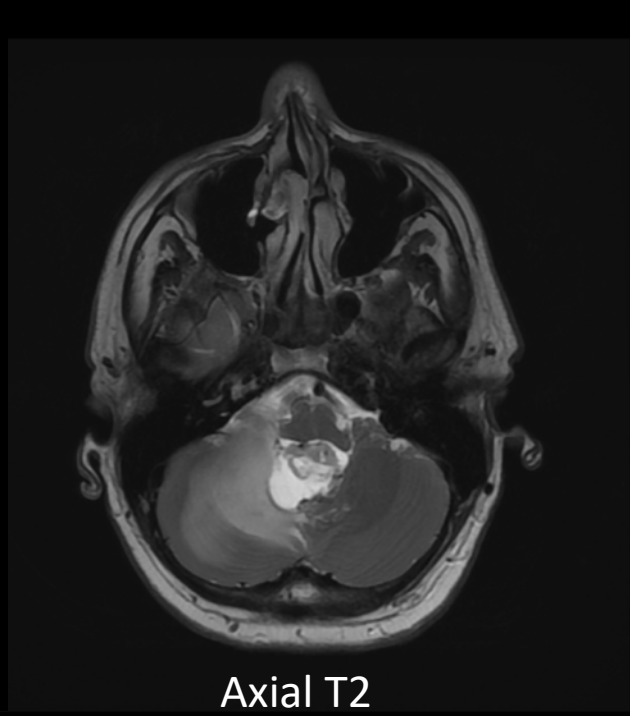
References

1. Jones J, Tawfiq Abukeshek. Post renal biopsy arteriovenous fistula and pseudoaneurysm. *Radiopaediaorg*. Published online September 17, 2021. doi:https://doi.org/10.53347/rid-93100
2. Trivedi SB, Gaba RC. Transplant Renal Biopsy Complicated by Arteriovenous Fistula. *Journal of Vascular and Interventional Radiology*. 2023;34(9):1634-1635. doi:https://doi.org/10.1016/j.jvir.2023.03.032
3. Schwarz A, Hiss M, Gwinner W, Becker T, Haller H, Keberle M. Course and Relevance of Arteriovenous Fistulas After Renal Transplant Biopsies. *American Journal of Transplantation*. 2008;8(4):826-831. doi:https://doi.org/10.1111/j.1600-6143.2008.02160.x
4. Sezer R, Uslu N, Akdur A, Haberal M. Biopsy-Related Renal Allograft Arteriovenous Fistulas. *Transplantation*. 2018;102(Supplement 7):S522. doi:https://doi.org/10.1097/01.tp.0000543359.62730.30

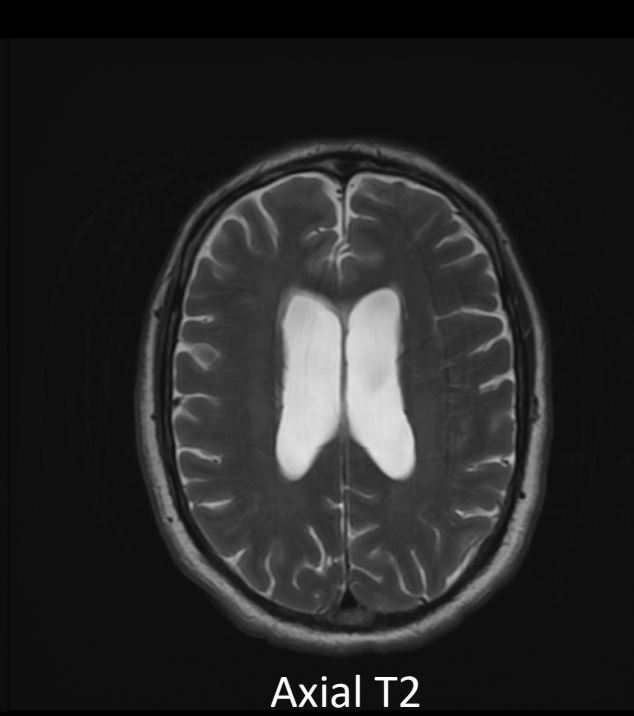
55 y/o m with hx of hypertension, asthma, anxiety, and opioid dependence, who presented to the ED with intractable migraines, nausea, vomiting, and dizziness.



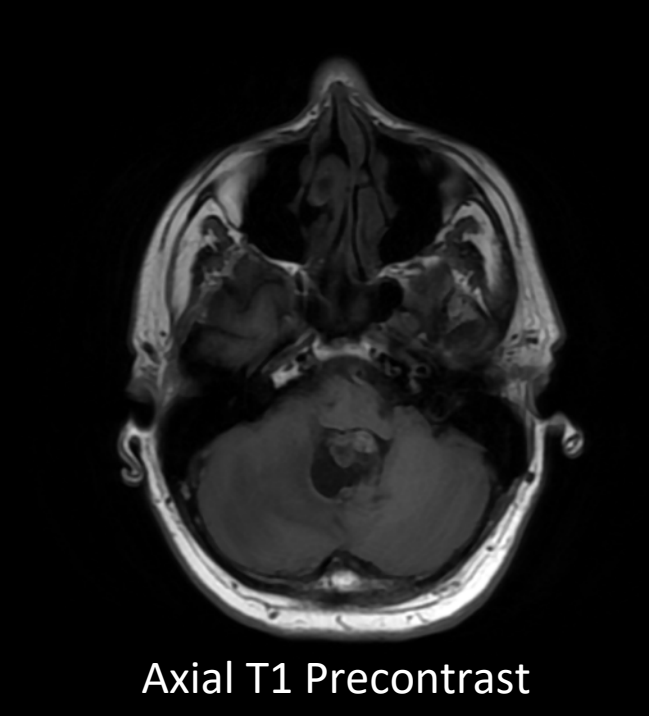
Axial CT



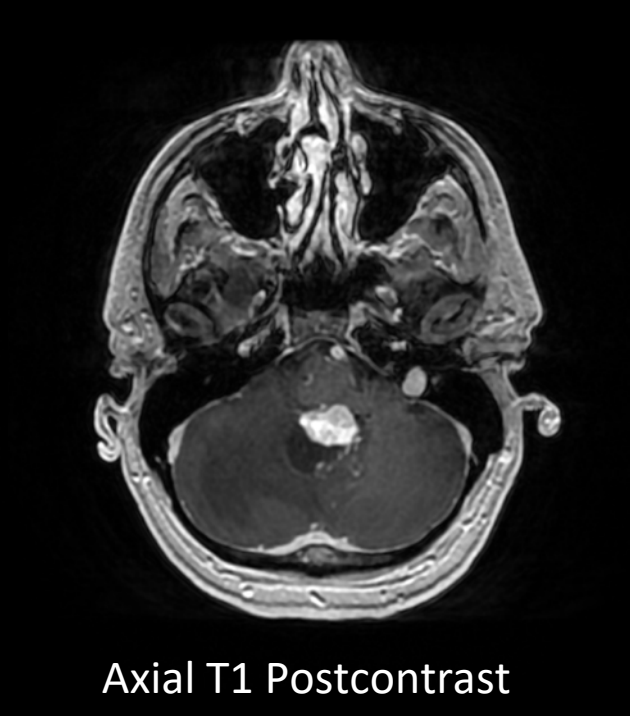
Axial T2



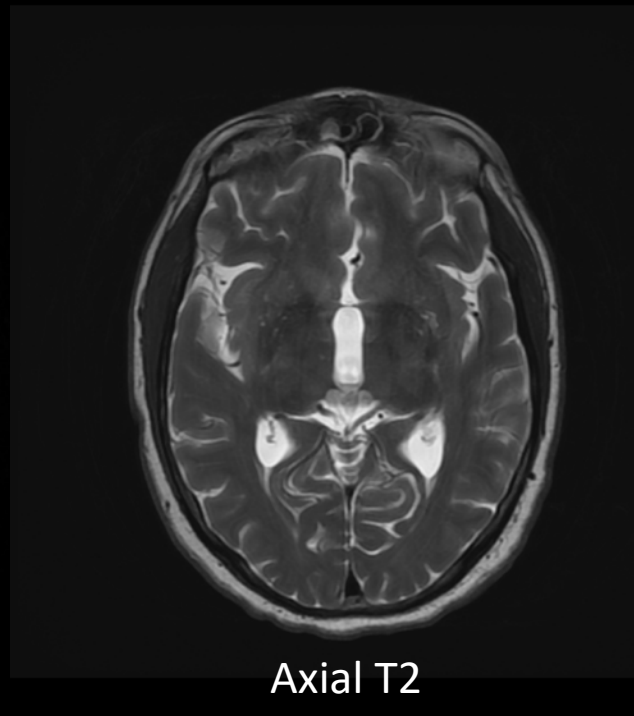
Axial T2



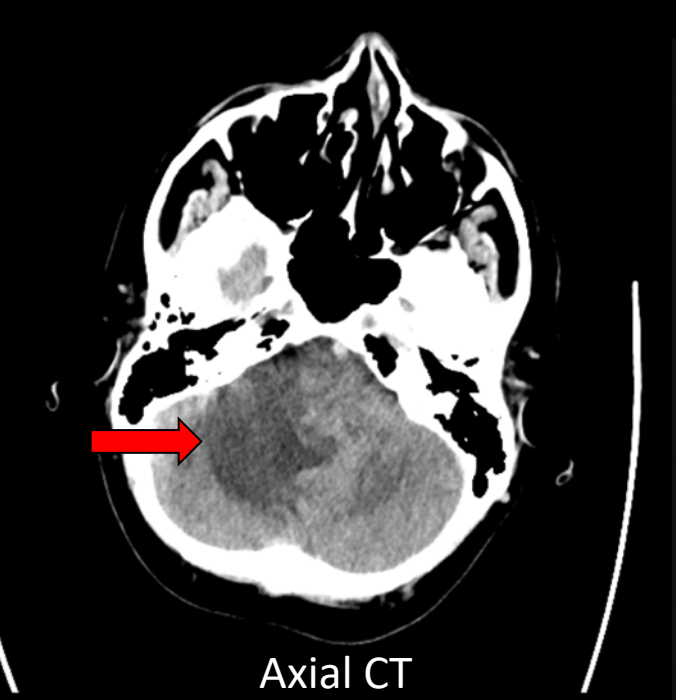
Axial T1 Precontrast



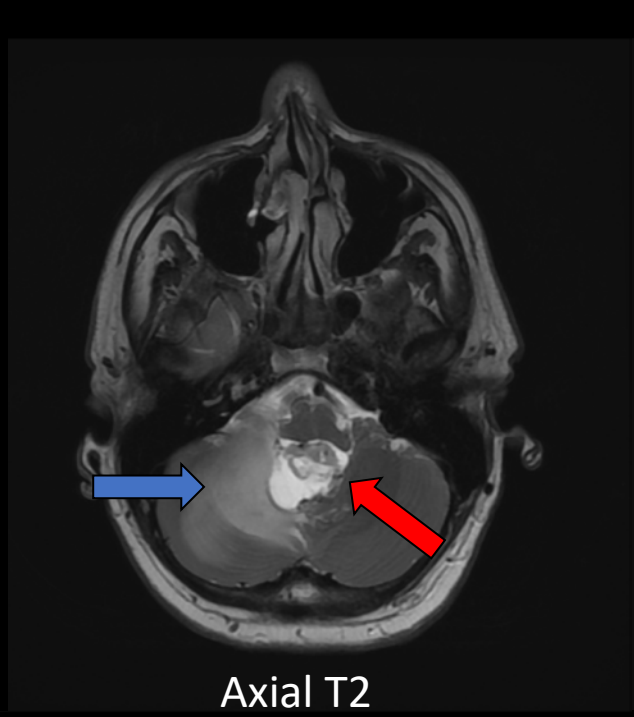
Axial T1 Postcontrast



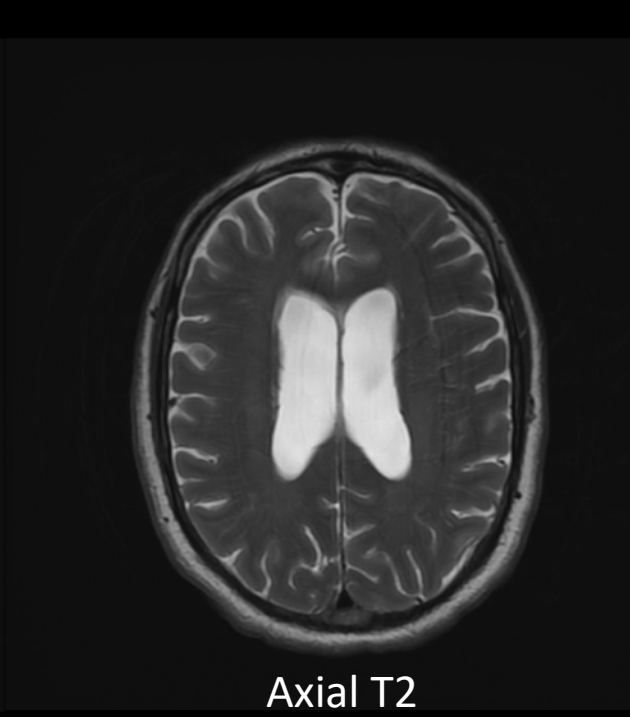
Axial T2



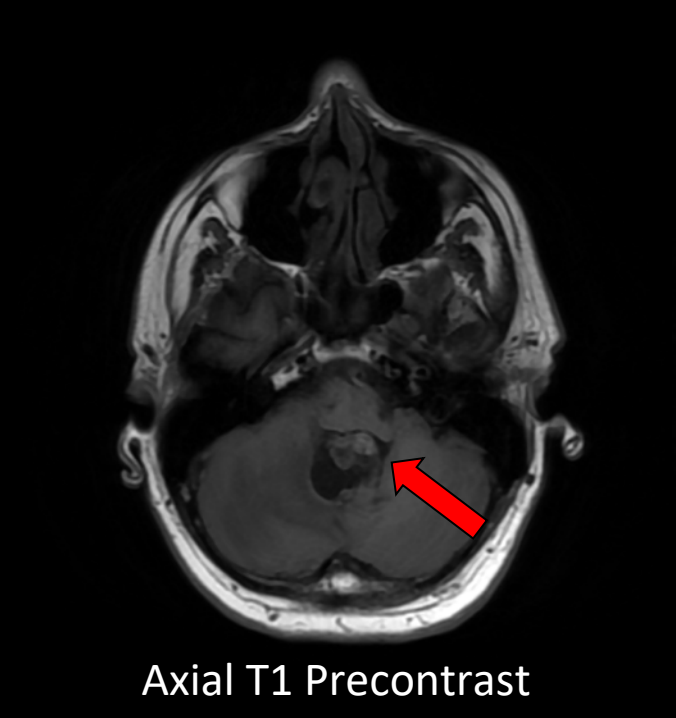
Axial CT



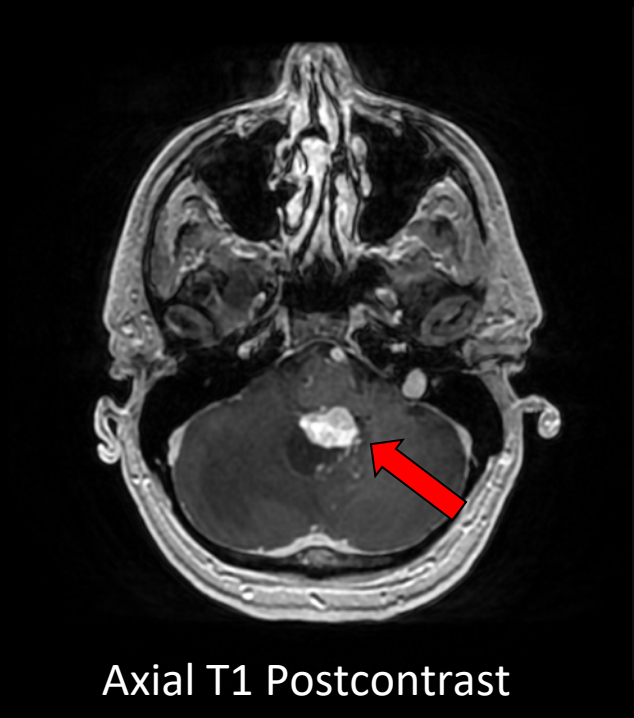
Axial T2



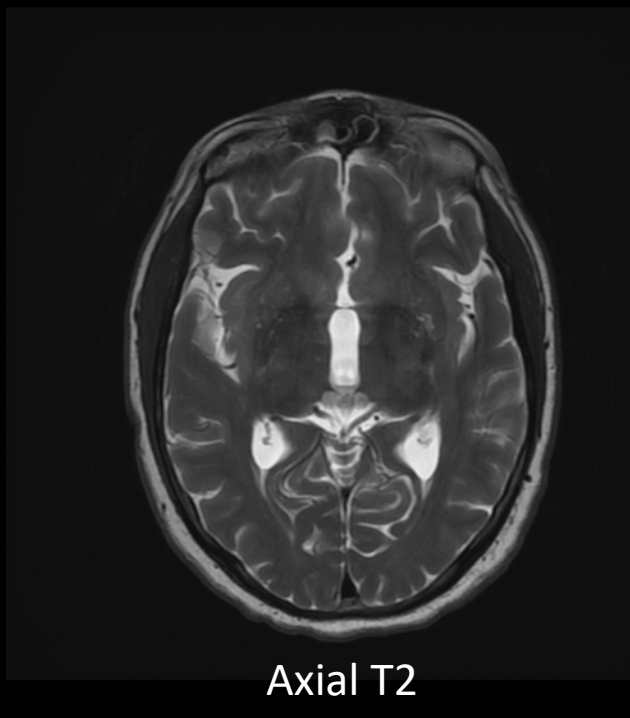
Axial T2



Axial T1 Precontrast



Axial T1 Postcontrast



Axial T2

Hemangioblastoma

Image Findings: MRI demonstrates a cystic mass within the midline posterior fossa along the posterior margin of the 4th ventricle with enhancing solid mural nodule (red arrows). Significant vasogenic edema (blue arrow) within the right cerebellar hemisphere extends into the right middle cerebellar peduncle and posterior lateral margin of the right lower pons. Mild obstructive hydrocephalus is also noted within the lateral and third ventricles.

Differential Diagnosis: Hemangioblastoma, ependymoma, brain metastasis, glioblastoma, medulloblastoma, pilocytic astrocytoma

Discussion: Hemangioblastomas are benign, slow-growing, non-invasive central nervous tumors that occur most frequently in the cerebellum, brainstem, spinal cord, and retina. Hemangioblastomas are rarely found within the supratentorial region. While the majority of these highly vascular tumors are sporadic (as in this case), approximately 20% are associated with von Hippel-Lindau disease. The most common presenting symptoms are headaches, gait ataxia, nausea/vomiting, and vertigo. Symptoms are reliant on tumor location and degree of mass effect. These tumors are important to correctly diagnose as surgery, stereotactic radiosurgery, and VEGF targeting agents can be effective treatments with positive outcomes and recurrence rates of less than 25%.

@AOCRNews

@aocrnews

Case courtesy of Kevin Williams, MS3; Cole Knox, MD, PhD; Faculty: Patrick Pagur, DO | Kettering Health

AOCR American Osteopathic College of Radiology

References

- Lonser, R. R., Butman, J. A., Huntoon, K., Asthagiri, A. R., Wu, T., Bakhtian, K. D., Chew, E. Y., Zhuang, Z., Linehan, W. M., & Oldfield, E. H. (2014). Prospective natural history study of central nervous system Hemangioblastomas in von Hippel-Lindau disease. *Journal of Neurosurgery*, *120*(5), 1055–1062. https://doi.org/10.3171/2014.1.JNS131431

- Khan, M. M. (2025, June 16). *Hemangioblastoma*. StatPearls [Internet]. https://www.ncbi.nlm.nih.gov/books/NBK606126/

- Ortiz de Salazar, A. (n.d.). Cerebellar hemangioblastoma | Radiology Case | radiopaedia.org. https://radiopaedia.org/cases/cerebellar-hemangioblastoma-1?lang=us

Posted 3/20/2026

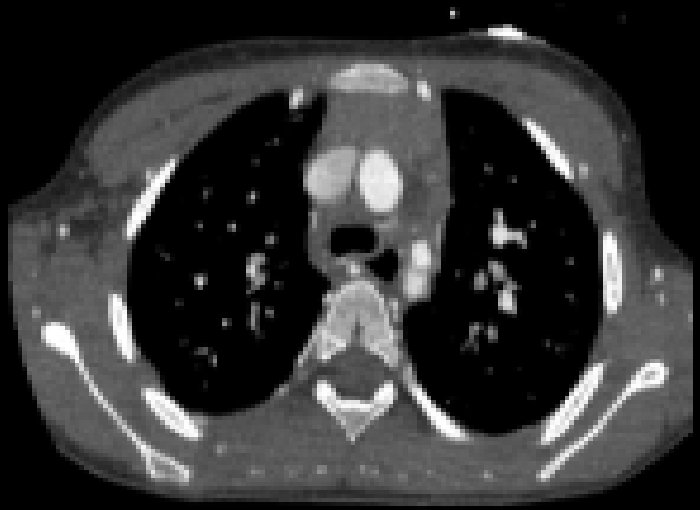
8 y/o male 3 years s/p ev3 Max LD stent placement for aortic coarctation. Presents for interval chest CT angiography.



A. Sagittal CTA of the chest



C. Sagittal CTA of the chest



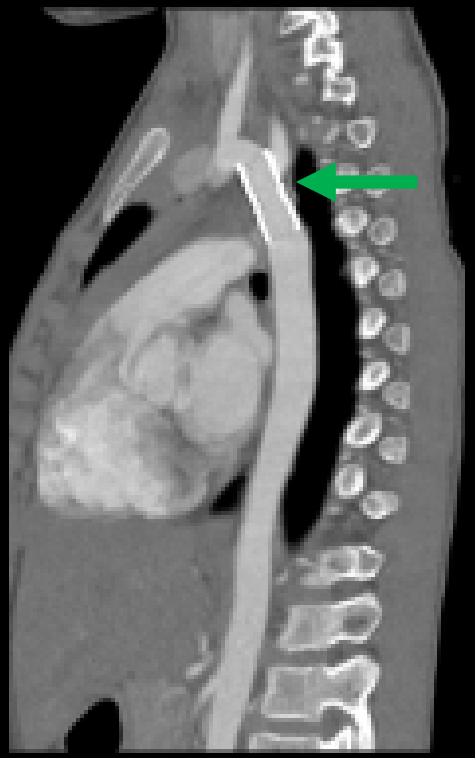
B. Axial CTA of the chest



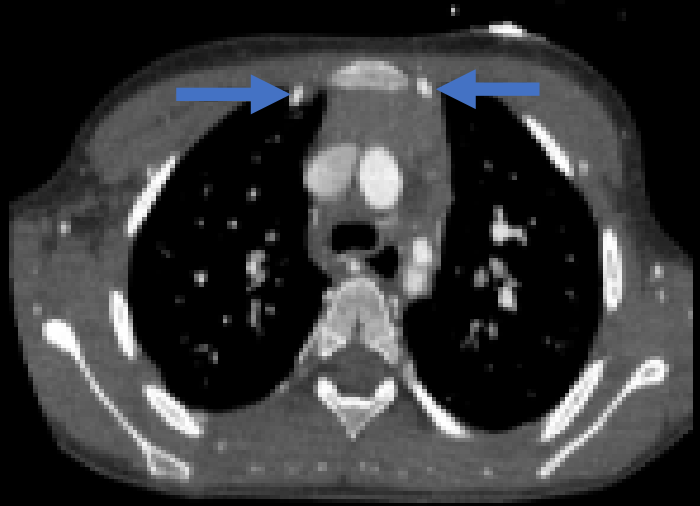
D. Axial CTA of the chest



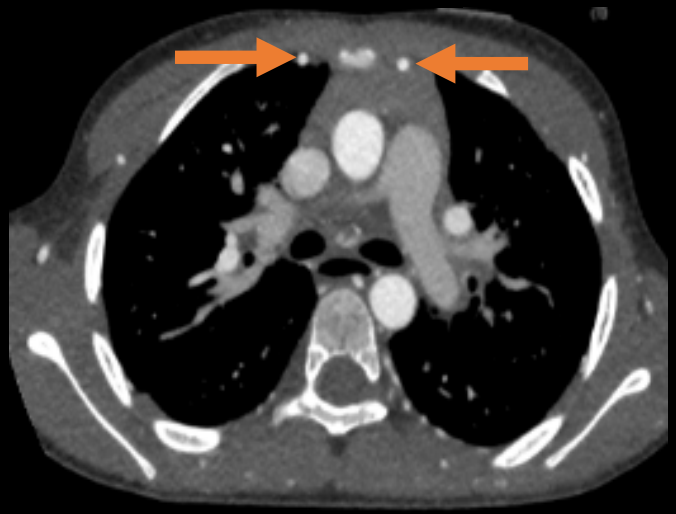
A. Sagittal CTA of the chest



C. Sagittal CTA of the chest



B. Axial CTA of the chest



D. Axial CTA of the chest

Coarctation of the Aorta

Findings: Stenotic proximal descending aorta. The origin of the left subclavian artery arises at the superior margin of the stenotic segment. The aortic diameter proximal to the left subclavian origin measures 9.9mm, narrowing to 2.7mm at the level of stenosis (Red Arrow), and measuring 13.2mm distal to the stenosis consistent with post-stenotic dilatation (Yellow Arrow). The stent extends from the level of the proximal left subclavian arterial wall inferiorly within the descending aorta. The stent unavoidably crosses the ostium of the left subclavian artery with the subclavian artery remaining widely patent. Post-stent measurements demonstrate relief of the previously noted post-stenotic dilatation. Residual soft tissue is noted along the posterior outer margin of the stent at level of coarctation potentially representing a remnant fibrous shelf or web (Green Arrow). Post stent, the collateral blood flow appears decreased as evidenced by the reduction in size of the internal mammary arteries (Blue Arrow pre-stent and Orange Arrow post-stent).

Diagnosis: Coarctation of the Aorta

Discussion: Aortic coarctation is a congenital narrowing of the aortic arch that results in upper-lower extremity blood pressure discrepancies, collateral vessel formation, and long-term risk of aortic aneurysm. Early diagnosis and intervention are important in improving morbidity and mortality. Current endovascular treatment is balloon angioplasty with stent placement which has demonstrated better outcomes when compared to surgical intervention and requires continued surveillance as the child grows. Regular imaging with CT angiography or MRI is required to monitor for stent positioning, re-coarctation, aneurysm formation, and other structural abnormalities and tissue changes. Additionally, stent related complications such as migration and fracture are rare but possible outcomes and reinforce the need for long-term imaging surveillance. Current guidelines recommend a follow up interval of 5 years or less, balancing surveillance needs against radiation exposure when CT is utilized.

@AOCRNews

@aocrnews

Case courtesy of Gregory Mitchell, MS-III, Robert Koenigsberg DO FAOCR
St. Christopher's Hospital for Children
Drexel University College of Medicine, Lewis Katz College of Medicine/Temple University

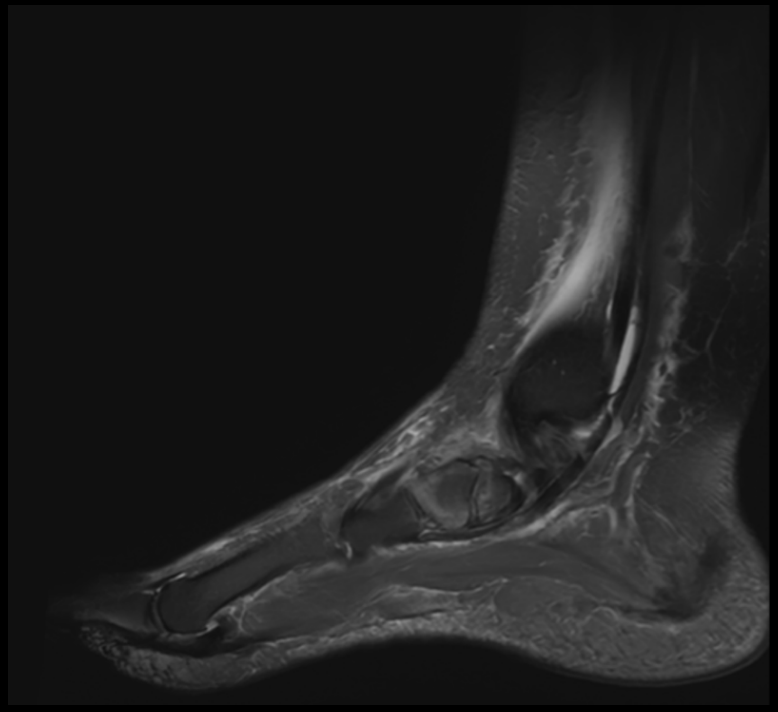
References

1. Law MA, Collier SA, Sharma S, Tivakaran VS. Coarctation of the Aorta. 2024 Dec 11. In: StatPearls [Internet]. Treasure Island (FL): StatPearls Publishing; 2025 Jan–. PMID: 28613663.
2. Suradi H, Hijazi ZM. Current management of coarctation of the aorta. Glob Cardiol Sci Pract. 2015 Nov 18;2015(4):44. doi: 10.5339/gcsp.2015.44. PMID: 26779519; PMCID: PMC4710863.
3. Stout KK, Daniels CJ, Aboulhosn JA, Bozkurt B, Broberg CS, Colman JM, Crumb SR, Dearani JA, Fuller S, Gurvitz M, Khairy P, Landzberg MJ, Saidi A, Valente AM, Van Hare GF. 2018 AHA/ACC Guideline for the Management of Adults With Congenital Heart Disease: A Report of the American College of Cardiology/American Heart Association Task Force on Clinical Practice Guidelines. Circulation. 2019 Apr 2;139(14):e698-e800. doi: 10.1161/CIR.0000000000000603. Erratum in: Circulation. 2019 Apr 2;139(14):e833-e834. doi: 10.1161/CIR.0000000000000683. PMID: 30586767.

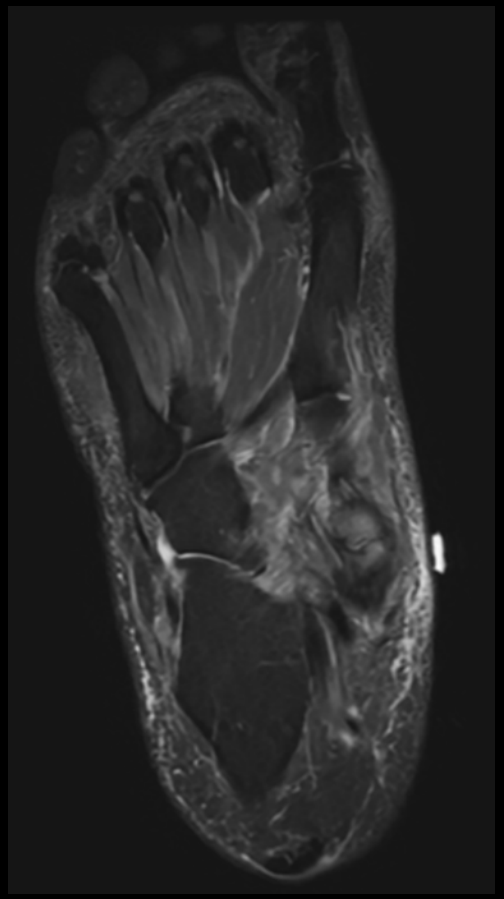
44 y/o f with past hx of T2DM and obesity (BMI 40.4) who presented to the outpatient clinic with chronic foot pain focused at the medial ankle.



AP Radiograph



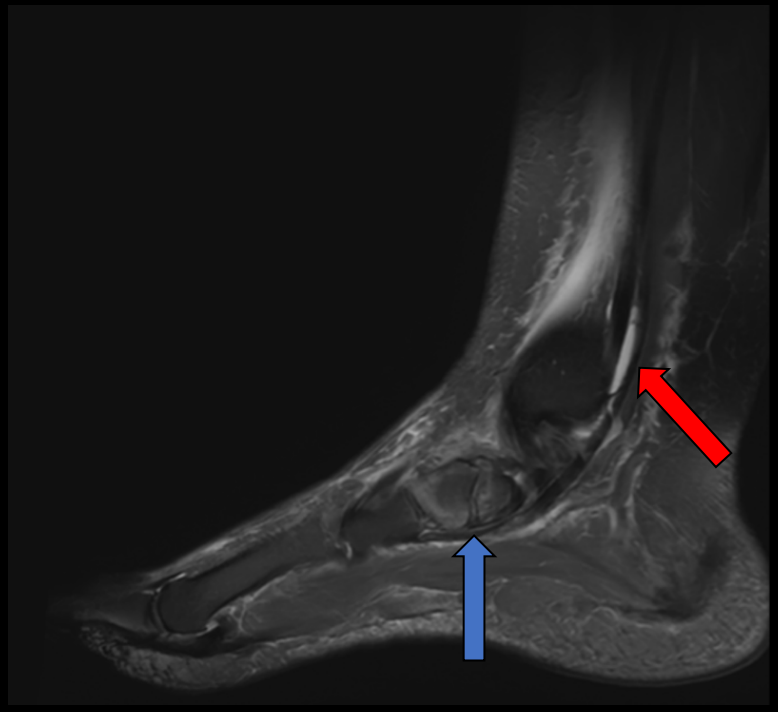
Sagittal T2



Axial T2



AP Radiograph



Sagittal T2



Axial T2

Accessory Navicular Syndrome

Image Findings: Axial radiograph demonstrates soft tissue swelling along the medial aspect of the midfoot with an accessory navicular ossicle. Sagittal and axial T2 fat saturated images demonstrate marrow edema along the margins of a type 2 accessory navicular bone and the posteromedial aspect of the navicular. The posterior tibial tendon (PTT) is intact with a mild amount of fluid in the tendon sheath (red arrow).

Differential Diagnosis: Navicular stress fracture, PTT dysfunction, Mueller-Weiss syndrome, other accessory ossicles

Discussion: Painful accessory navicular bone syndrome is a clinically significant cause of medial midfoot pain. The accessory navicular is a common developmental variant occurring in 17.5% of the population and can be classified into three subtypes. Type 2 is the most common, consisting of an ossicle attached to the navicular tuberosity by a thin fibrocartilaginous or hyaline synchondrosis. Symptoms result from synchondrotic injury either with or without posterior tibialis (PT) dysfunction. Those without PT dysfunction are usually children or young adults who develop medial foot pain from activity. Alternatively, patients with PT dysfunction are generally middle-aged or older, presenting with insidious medial foot pain after minor twisting trauma. Radiographic visualization of the accessory ossicle is diagnostic often with associated bone marrow edema on MRI. Conservative treatment with immobilization and anti-inflammatory medications is often adequate. However, bony excision with an anatomical repair of the posterior tibial tendon might be necessary in cases of recurrent symptoms and failed conservative treatment.

Case courtesy of John Stout, MS3; Cole Knox, MD, PhD; Faculty: Roland Gazaille, DO | Kettering Health

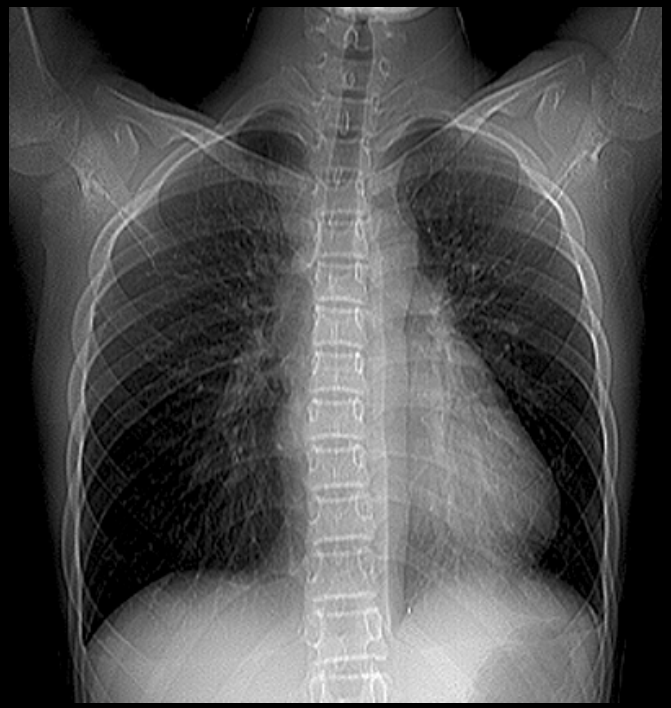
References

- Tuthill HL, Finkelstein ER, Sanchez AM, Clifford PD, Subhawong TK, Jose J. Imaging of tarsal navicular disorders: a pictorial review. *Foot Ankle Spec*. 2014;7(3):211-225. doi:10.1177/1938640014528042.

- Stolarz K, Osiowski A, Preinl M, Osiowski M, Jasiewicz B, Taterra D. The prevalence and anatomy of accessory navicular bone: a meta-analysis. *Surg Radiol Anat*. 2024;46(10):1731-1743. doi:10.1007/s00276-024-03459-x.

- Wariach S, Karim K, Sarraj M, Gaber K, Singh A, Kishta W. Assessing the Outcomes Associated with Accessory Navicular Bone Surgery-a Systematic Review. *Curr Rev Musculoskelet Med*. 2022;15(5):377-384. doi:10.1007/s12178-022-09772-5.

13 y/o m presented to PCP with asymptomatic sternal depression noted. This sternal depression was noted on physical exam. The patient is active and denied any chest pain, difficulty breathing, or exercise intolerance.



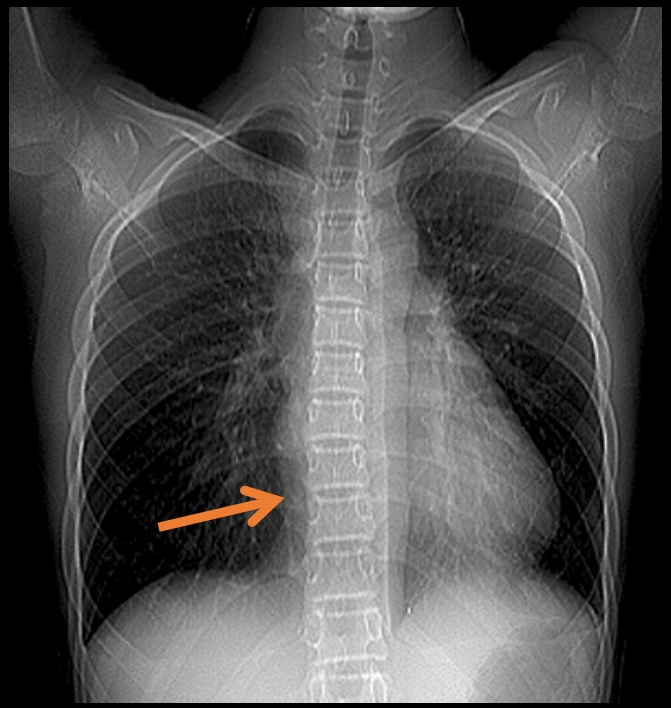
Frontal scout image



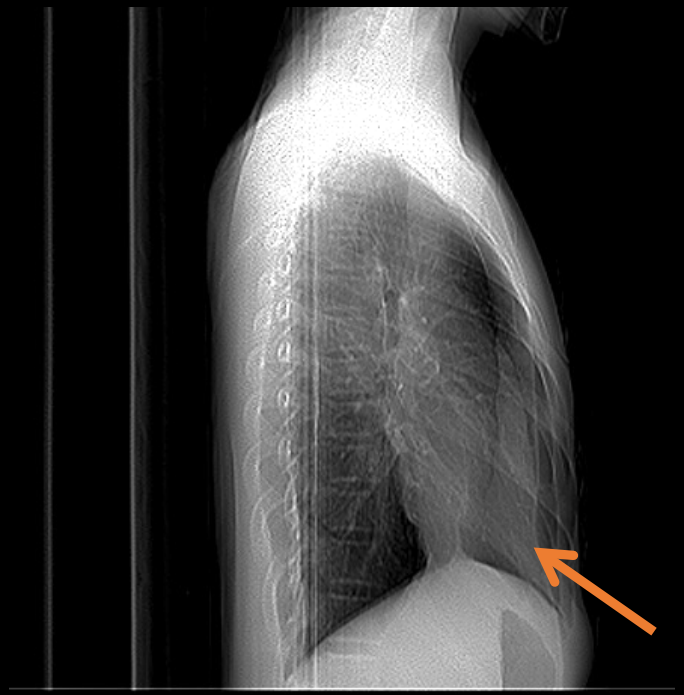
Lateral scout image



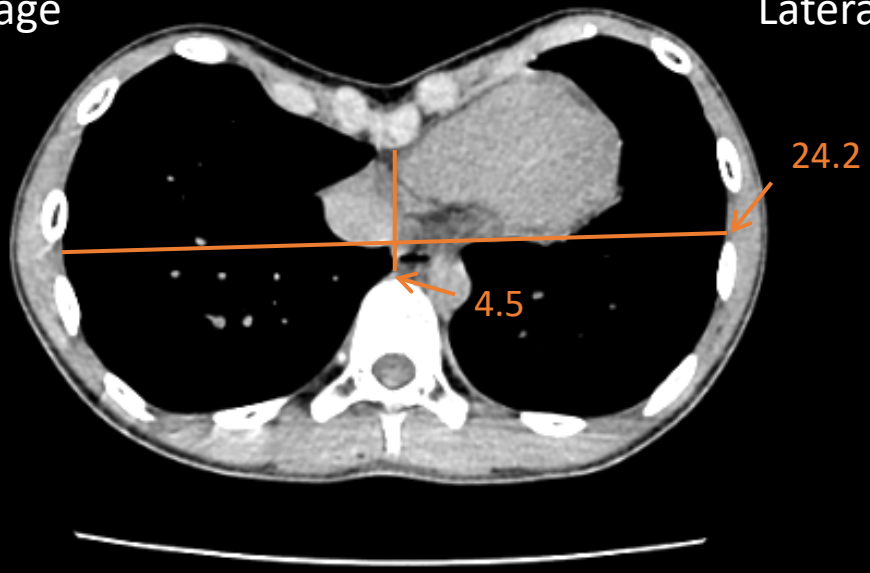
Axial CT without contrast



Frontal scout image



Lateral scout image



Axial CT without contrast

Pectus excavatum

Patient Presentation: Asymptomatic depression of the sternum

Image Findings: Scout imaging shows increased density in the anterior mediastinum, possibly adjacent to the right heart border (Plain films not available). Axial CT shows depression of the sternum and a Haller index of (5.3)

Differential Diagnosis: Right middle lobe consolidation/atelectasis, pectus excavatum, mediastinal mass, pectus arcuatum

Discussion: Pectus excavatum is defined as congenital concave depression of the sternum, and it is responsible for 90% of chest wall deformities. The condition may present as an isolated anomaly or in association with Marfan syndrome, Ehlers Danlos, and NFT1. Patients are often asymptomatic but can present with chest pain, exercise intolerance, cardiopulmonary impairment, or psychological complaints. Diagnosis is often based on physical exam. Most defects are present within the first of year of life, in severe cases, they may be present at birth. Further evaluation, through CT imaging, is often conducted to assess any compression abnormalities. Treatment for asymptomatic patients is often conservative. Patients with severe symptoms may be treated surgically with a Nuss procedure.

Case courtesy of Bryan Gamwo MD (class of 2026),
Robert A. Koenigsberg DO FAOCR | St. Christopher’s Hospital For Children

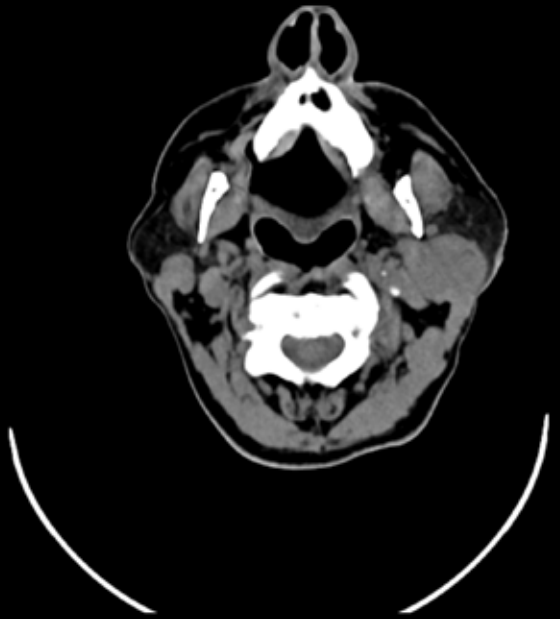
References

Coorens, Nadine A., et al. “Advancements in preoperative imaging of pectus excavatum: A comprehensive review.” *Journal of Thoracic Disease*, vol. 16, no. 1, Jan. 2024, pp. 696–707, https://doi.org/10.21037/jtd-23-662.

Sarwar, Zahir U., et al. “Pectus excavatum: Current imaging techniques and opportunities for dose reduction.” *Seminars in Ultrasound, CT and MRI*, vol. 35, no. 4, Aug. 2014, pp. 374–381, https://doi.org/10.1053/j.sult.2014.05.003.

Posted 2/27/2026

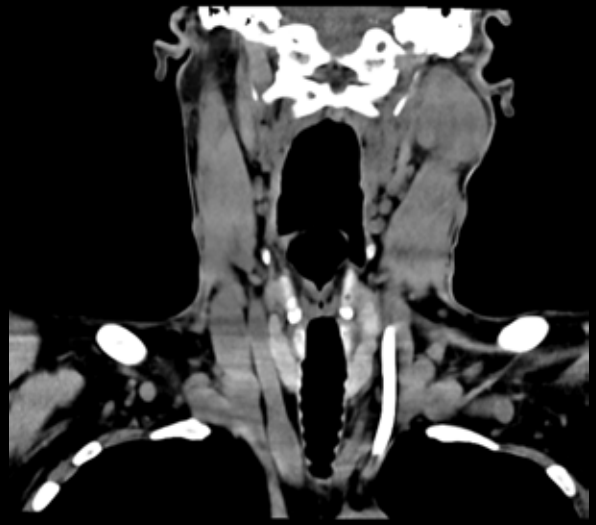
70 y/o m with past hx of tobacco use, ESRD, and renal cell carcinoma status post nephrectomy who presented to his primary care physician with a tender left neck mass.



Axial CT Neck



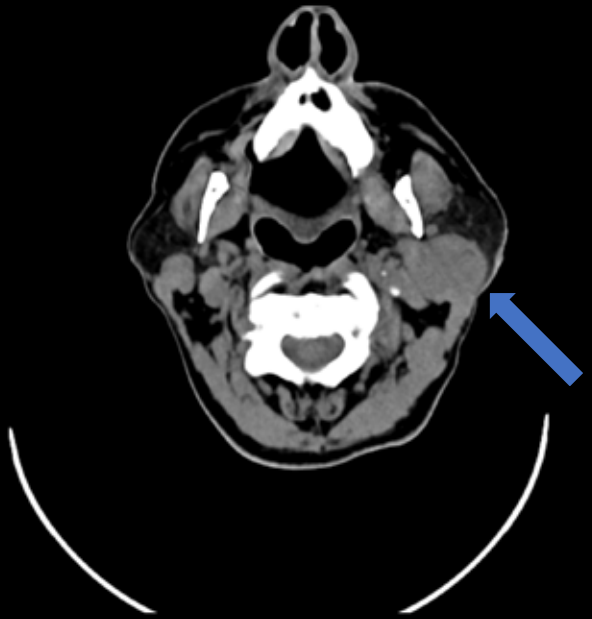
Sagittal CT Neck



Coronal CT Neck



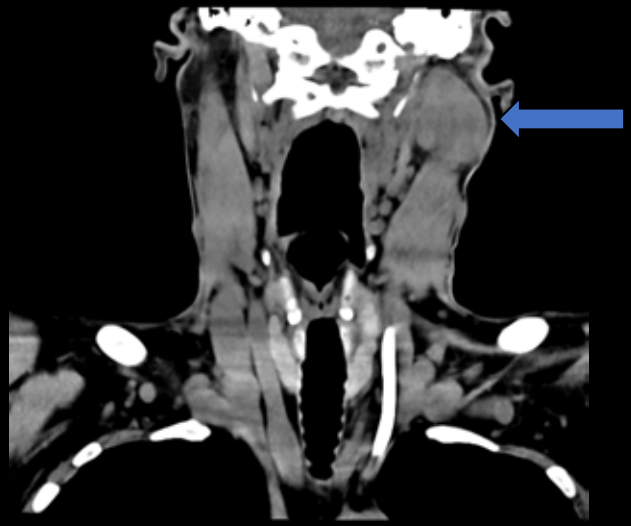
Ultrasound-Guided Biopsy



Axial CT Neck



Sagittal CT Neck



Coronal CT Neck



Ultrasound-Guided Biopsy

Warthin Tumor

Imaging Findings: CT neck demonstrates an isoattenuating 5.2 x 4.1 x 2.6 cm mass (blue arrows) within the left parotid gland, originating in the superficial portion and extending into the deep parotid gland medial to the ramus of the mandible and the stylomastoid process. The mass causes some effacement of the lateral parapharyngeal fat as well as posterior adjacent proximal sternocleidomastoid muscle. There are no inflammatory changes of the left parotid gland. No pathologically enlarged lymph nodes are identified. Ultrasound demonstrates a hypoechoic solid mass in the left parotid gland with internal blood flow.

Differential Diagnosis: Warthin tumor, Pleomorphic adenoma, Metastatic disease, Mucoepidermoid carcinoma, Adenoid cystic carcinoma, Lymphoma

Discussion: Warthin tumors (lymphomatous papillary cystadenomas) are the second most common benign parotid tumor after pleomorphic adenoma, accounting for 2-15% of all parotid tumors. It predominantly affects males over 50 years with a strong smoking association.[1] Warthin tumors typically present as heterogeneous masses with cystic components, commonly located in the superficial lobe or tail of the parotid gland.[2] This patient exhibits the typical size range and anatomical distribution of Warthin tumors. Warthin tumors demonstrate a pathognomonic enhancement pattern on two-phase CT and the presence of cystic components and papillary projections, which correlate to excellent diagnostic accuracy with sensitivity and specificity of 96.1% and 93.5% respectively.[3] The bilateral occurrence potential and multifocal nature of Warthin tumors, particularly in smokers, makes CT imaging crucial for comprehensive evaluation and surgical planning, as these tumors can be managed with less invasive extracapsular dissection rather than superficial parotidectomy when accurately diagnosed preoperatively.

Case courtesy of James Dai, MS3; Cole Knox, MD, PhD;
Faculty: Dhananjay Paranjpe, MD | Kettering Health

References

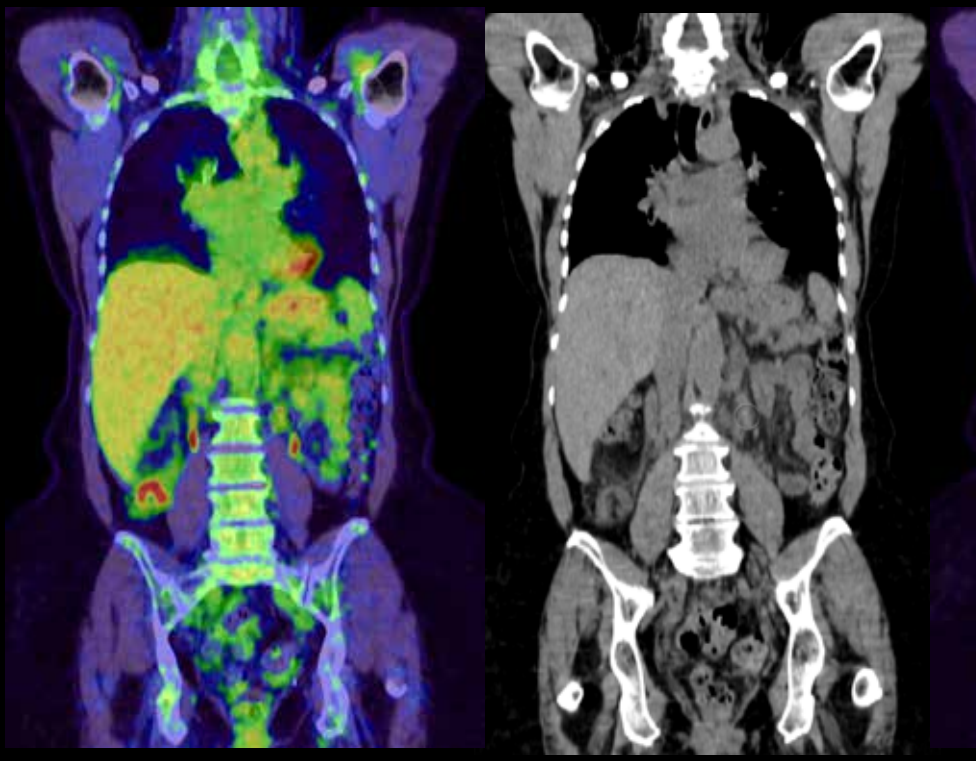
1. Nishikawa H, Kirkham N, Hogbin BM. Synchronous extra-parotid Warthin's tumour. J Laryngol Otol. 1989 Aug;103(8):792-3.

1. Lee YH, Yu IK, Han MH, Lee BH, Kim MS, Song CJ. Warthin's Tumor of the Parotid Gland: CT and MR Features. J Korean Soc Radiol. 2009 Jul;61(1):17-22. https://doi.org/10.3348/jksr.2009.61.1.17.

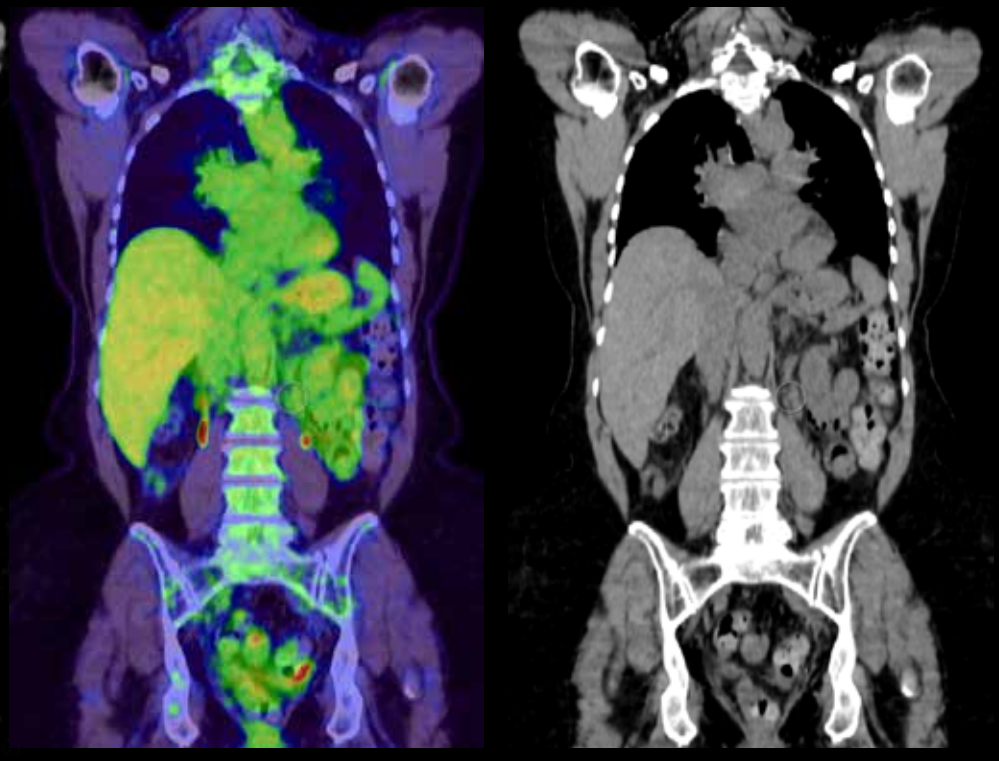
1. Joo YH, Kim JP, Park JJ, Woo SH. Two-phase helical computed tomography study of salivary gland warthin tumors: a radiologic findings and surgical applications. Clin Exp Otorhinolaryngol. 2014 Sep;7(3):216-21. doi: 10.3342/ceo.2014.7.3.216. Epub 2014 Aug 1. PMID: 25177439; PMCID: PMC4135159.

Posted 2/20/2026

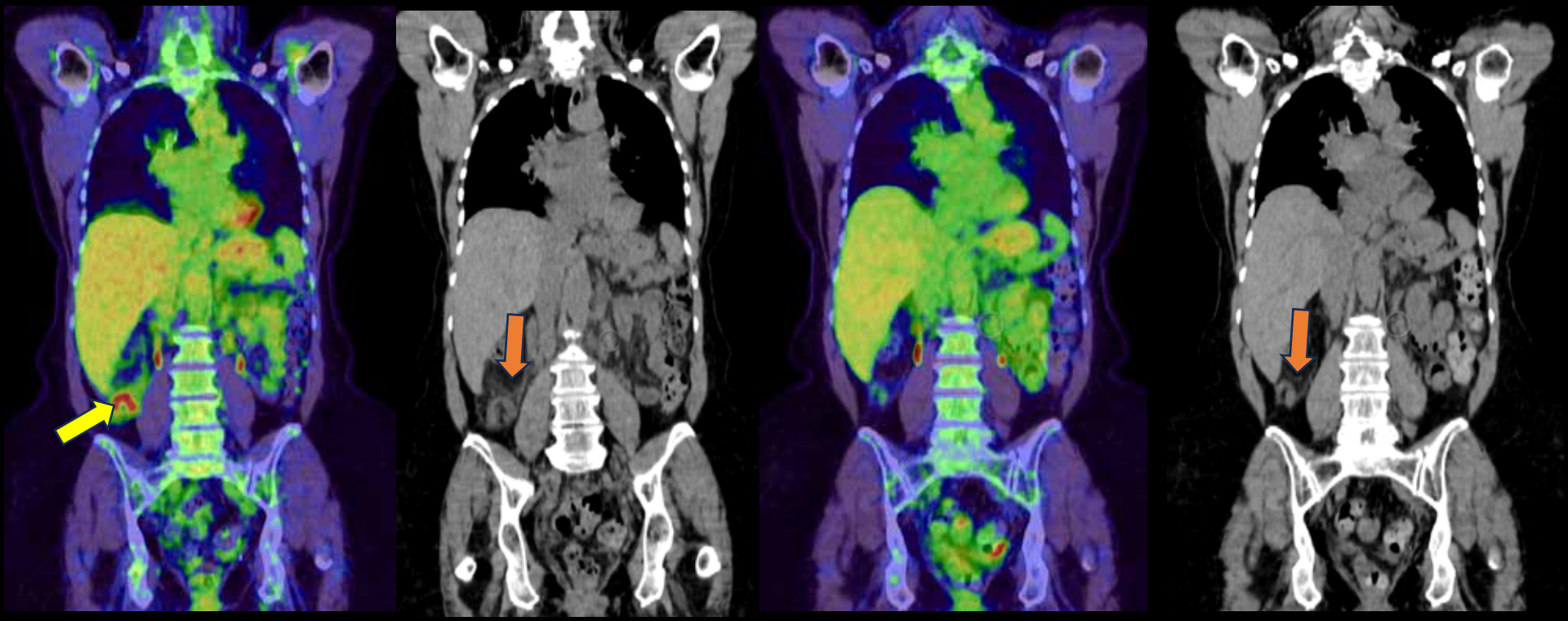
71F with stage II follicular lymphoma underwent routine PET/CT scan. 3 days later she saw her oncologist and reported 2 weeks of intermittent RLQ pain.



A) Current PET/CT



B) PET/CT 6 months prior



A) Current PET/CT

B) PET/CT 6 months prior

Acute on Chronic Appendicitis

Imaging findings: A) The appendix is abnormally thickened measuring 12mm in diameter with moderate surrounding inflammation. The appendix has moderate diffuse hypermetabolic activity measuring 7.3 SUV max. B) Prior PET/CT 6 months earlier shows 9.2mm diameter appendix with small adjacent fat stranding but no hypermetabolic activity. Surrounding inflammation is present on CT in both A and B, with mild interval increase on A and new PET hypermetabolic activity, suggesting acute on chronic appendicitis.

Differential Diagnosis: Normal physiologic radiotracer uptake of bowel, acute versus chronic appendicitis.

Discussion: Acute on chronic appendicitis was confirmed by CT, laparoscopic appendectomy, and pathology. 18F-FDG accumulates in activated neutrophils and macrophages, so acute inflammation can show SUV values that overlap with malignancy. In this patient, a prior PET/CT showed mild periappendiceal stranding and borderline enlargement without FDG uptake, consistent with chronic appendicitis. New focal hypermetabolism (SUV max 7.3) and mural thickening indicated superimposed acute inflammation. Because physiologic radiotracer activity is commonly seen within bowel, distinguishing true intestinal inflammation or malignancy on PET can be challenging. However, focal uptake greater than adjacent bowel, particularly when corresponding CT abnormalities are present, should raise suspicion for inflammation or malignancy.

@AOCRNews

@asa_borup
@aocrnews

Case courtesy of Asa Borup, OMS II; Alexander Enabnit, OMS-II; Lance Borup, DO
ATSU-KCOM

References

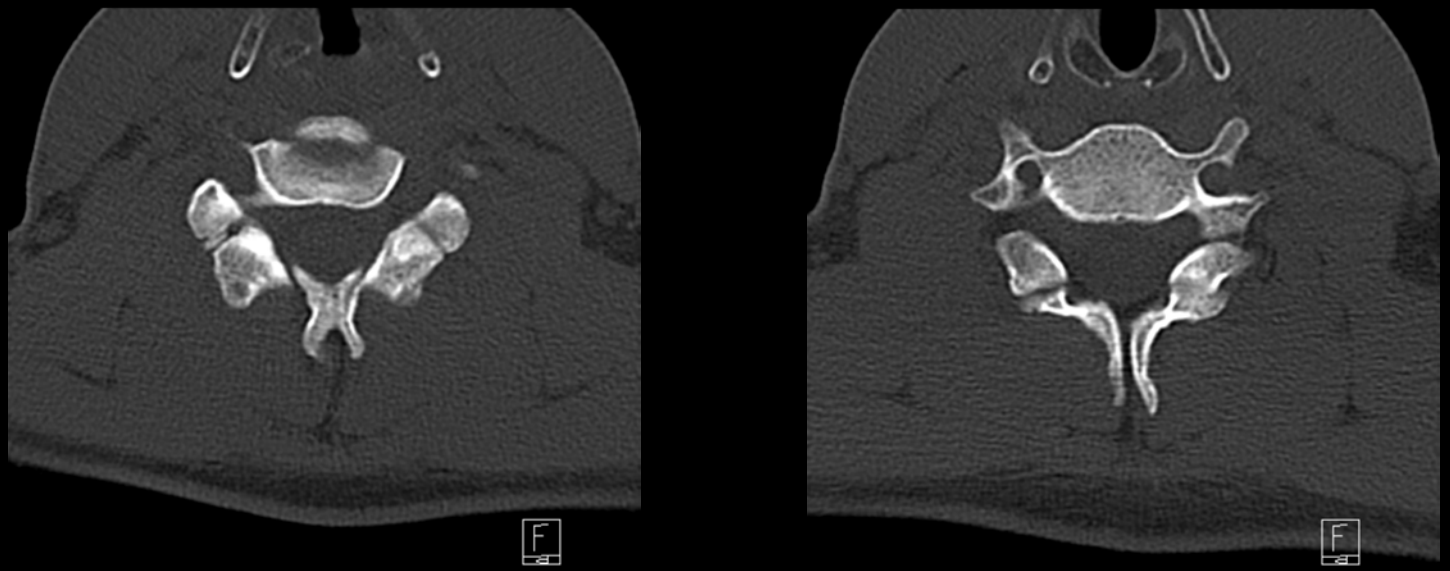
Jain, Bela & Khandelwal, Yogita & Damle, Nishikant & Tripathi, Madhavi & Bal, Chandrasekhar. (2025). Incidental Finding of Acute Appendicitis on FDG PET/CT in Breast Carcinoma. Indian Journal of Nuclear Medicine. 40. 42-43. 10.4103/ijnm.ijnm_68_24.

Koff, Stacey G. MD*; Sterbis, Joseph R. MD*; Davison, Jonathan M. MD†; Montilla-Soler, Jaime L. MD†. A Unique Presentation of Appendicitis: F-18 FDG PET/CT. Clinical Nuclear Medicine 31(11):p 704-706, November 2006. | DOI: 10.1097/01.rlu.0000242723.61455.a8

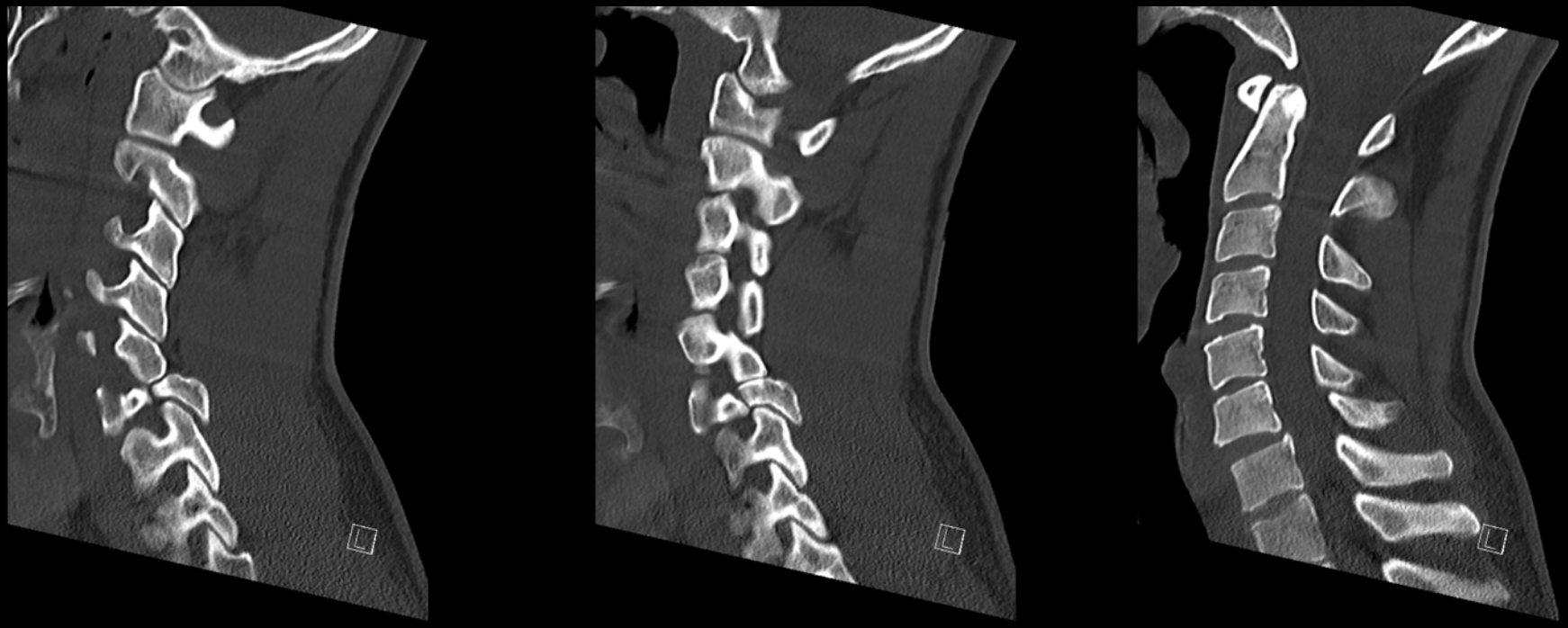
Kubota K, Ogawa M, Ji B, et al. Basic Science of PET Imaging for Inflammatory Diseases. *PET/CT for Inflammatory Diseases*. 2019;1-42. Published 2019 Dec 21. doi:10.1007/978-981-15-0810-3_1

Posted 2/13/2026

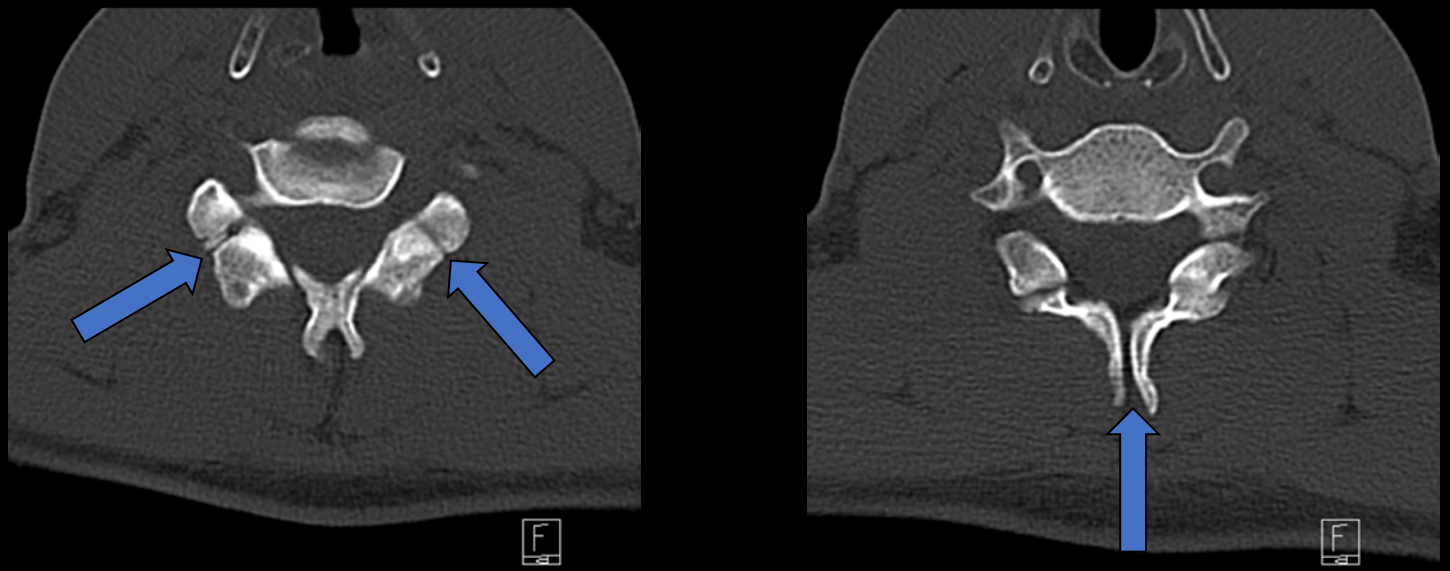
32 y/o M presented to the ER after a ground level fall. Patient hit head on a nightstand on the way down and now has residual occiput and neck pain.



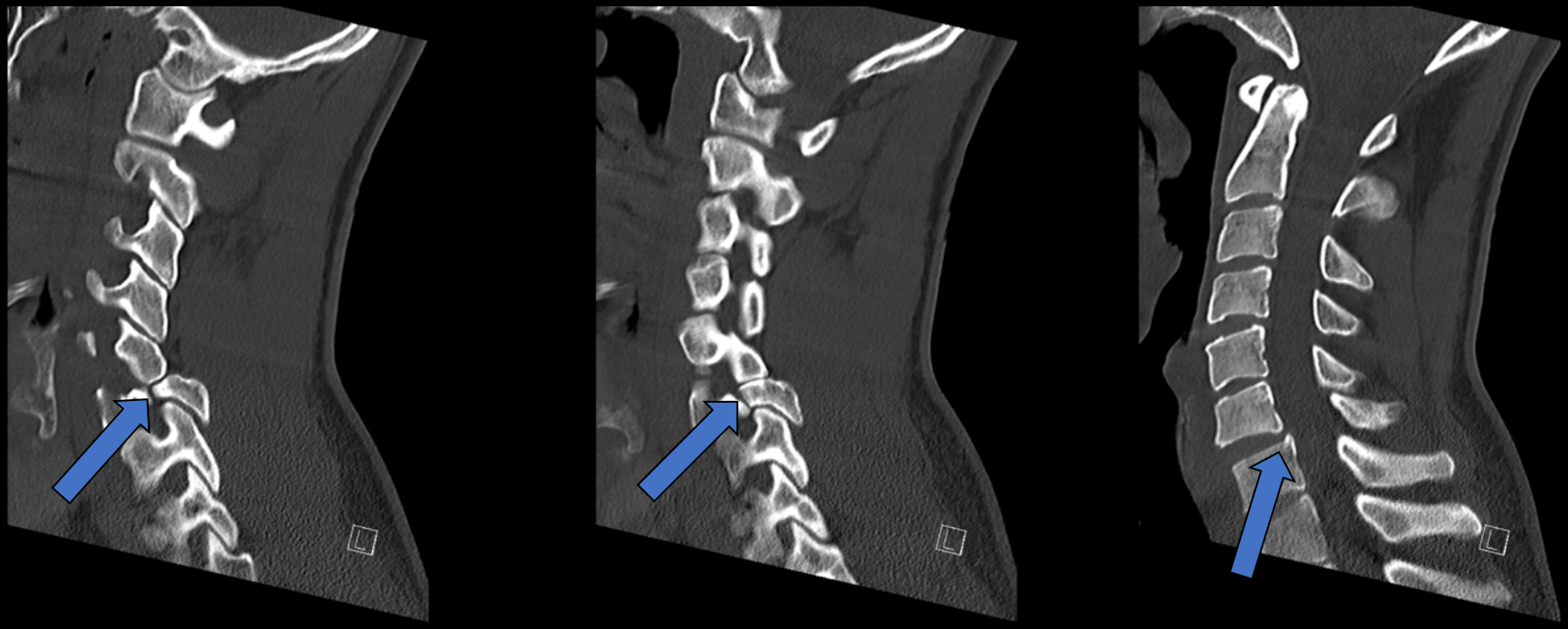
Axial CT Scans of the C6 vertebral body



Sagittal CT scans of the cervical spine



Axial CT Scans of the C6 vertebral body



Sagittal CT scans of the cervical spine

Bilateral C6 Spondylolysis with Spina Bifida

- **Image Findings:** There is bilateral cervical spondylolysis at C6. The cleft seen in the articular pillar bilaterally appears corticated consistent with a chronic condition. There is also evidence for spina bifida posteriorly involving the spinous process at C6. These findings are consistent with congenital bilateral C6 spondylolysis with spina bifida.
- **Differential:** Bilateral C6 spondylolysis with spina bifida, C6 pars interarticularis fracture, Absent pedicle syndrome
- **Discussion:** Congenital cervical spondylolysis is a rare developmental anomaly characterized by a well-corticated bony cleft in the pars interarticularis (articular pillar) of a cervical vertebra, most commonly at C6. This defect often leads to a spondylolisthesis at the affected level, in this case a grade I anterolisthesis of C6 on C7 was present. The coexistence of other bony anomalies, such as a spina bifida occulta of the involved vertebra (failure of the posterior elements to fuse), strongly supports a congenital etiology. Importantly, the margins of a congenital cleft are sclerotic and well-defined, which helps differentiate it from an acute traumatic fracture that would show sharp, irregular edges. Most patients with cervical spondylolysis are asymptomatic, and the condition is often discovered incidentally (frequently after minor trauma prompts imaging). In the absence of instability or neurological impairment, management is conservative and focuses on observation and symptomatic relief. Surgical intervention (spinal fusion) is reserved for cases with significant instability or neurologic compression, which are uncommon in this condition.

@AOCRNews

@aocrnews

Case courtesy of Mohamed Malek Soumakieh, MS4; Cole Knox, MD, PhD; Ryan Borgemenke, DO; Faculty: Kyle Tharp, MD | Kettering Health

AOCR American Osteopathic College of Radiology

References

- Sahri, I. E., Tlemcani, Z. C., Hakkou, E., Mohammed Yassaad, O., & Abdessamad, E. (2022). Congenital spondylolytic spondylolisthesis of the cervical spine: A case report and literature review. Radiology case reports, 17(6), 2092–2096. https://doi.org/10.1016/j.radcr.2022.03.054

- Margetis K, Gillis CC. Spondylolisthesis. [Updated 2025 Mar 28]. In: StatPearls [Internet]. Treasure Island (FL): StatPearls Publishing; 2025 Jan. Available from: https://www.ncbi.nlm.nih.gov/books/NBK430767/

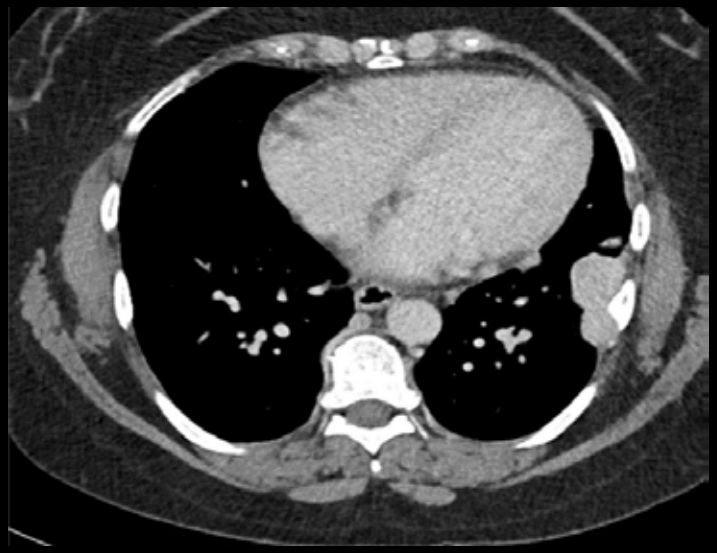
- Nedelea, D. G., Vulpe, D. E., Gherghiceanu, F., Capitanu, B. S., Dragosloveanu, S., & Stoica, I. C. (2025). Surgical and non-surgical management of spondylolisthesis: a comprehensive review. Journal of medicine and life, 18(3), 196–207. https://doi.org/10.25122/jml-2025-0039

Posted 2/6/2026

46F with an incidental pleural-based mass on CT neck was seen for f/u. Further questioning revealed the patient had a hx of remote trauma.



1. Axial contrast-enhanced CT chest



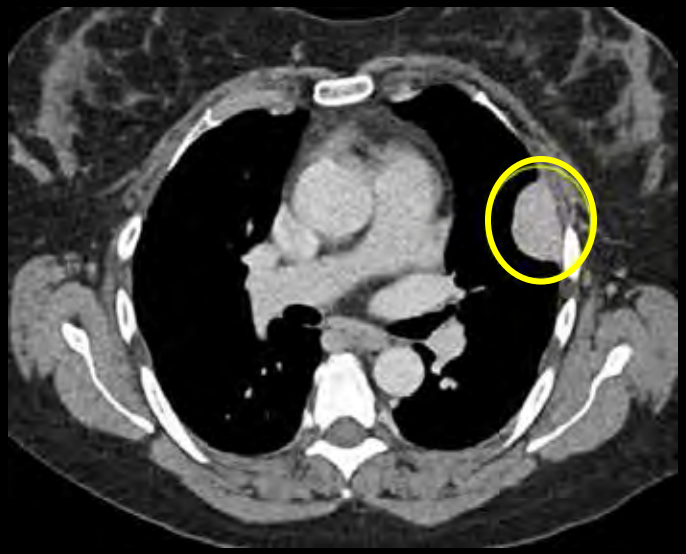
2. Axial contrast-enhanced CT chest



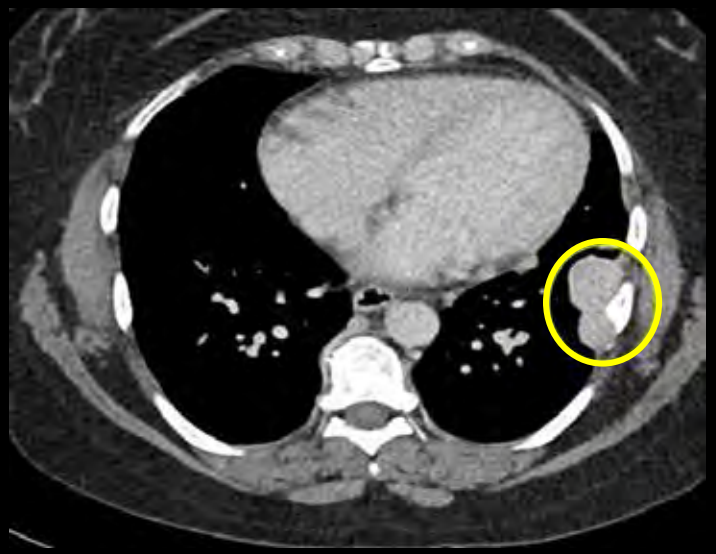
3. Coronal contrast-enhanced CT chest



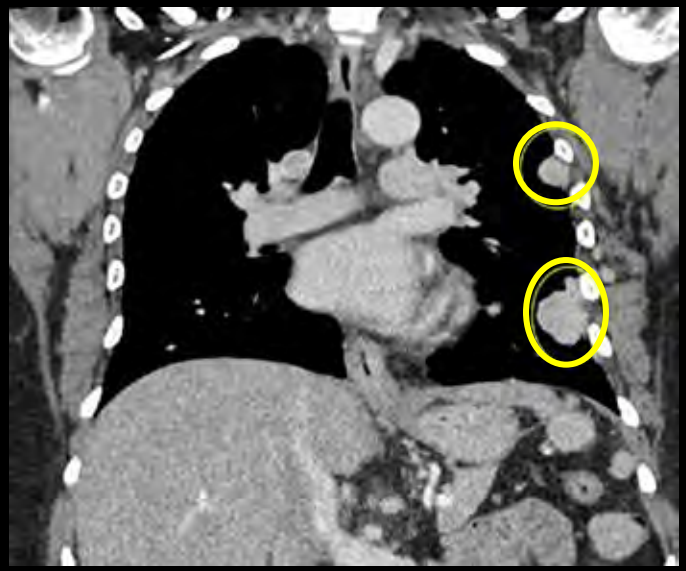
4. ^{99m}Tc-SC liver-spleen scan



1. Axial contrast-enhanced CT chest



2. Axial contrast-enhanced CT chest



3. Coronal contrast-enhanced CT chest



4. ^{99m}Tc-SC liver-spleen scan

Intrathoracic Splenosis

Imaging findings:

- Figs. 1-3: Axial and coronal contrast-enhanced CT chest showed multiple distinct well-circumscribed, soft tissue masses (yellow circles) along the pleural region of the left hemithorax. The masses demonstrated homogenous enhancement with similar attenuation to normal splenic tissue. Asplenia was visible in the left upper quadrant with only bowel loops present.
- Fig. 4: Liver-spleen scan was notable for uptake of ^{99m}Tc-SC (sulfur colloid) in the pleural-based masses (red circles), a finding consistent with intrathoracic splenic tissue. Normal liver uptake was also seen.

Differential diagnosis: intrathoracic splenosis, pleural malignancy (mesothelioma), pleural metastasis, pleural lymphoma, extramedullary hematopoiesis

Discussion: Intrathoracic splenosis describes ectopic seeding of splenic tissue within the thoracic cavity that can be post-traumatically acquired through splenic or diaphragmatic injury. Inherited (congenital) cases have been reported only a handful of times in the literature. In traumatic cases, implantation of splenic tissue along the pleura provokes ectopic growth. Interestingly, many cases are diagnosed incidentally years after initial insult, with the absence of typical features of intrathoracic splenosis and undocumented history of trauma contributing to the difficulty of diagnosis. While most cases of intrathoracic splenosis present as an asymptomatic mass or masses, cases may mimick malignant conditions or infection with symptoms often related to mass effect.

Findings on CT and MRI are typically incidental and present as nonspecific masses with similar enhancement to splenic tissue. These modalities are rarely diagnostic but useful for suggesting splenosis and prompting subsequent evaluation. Radionuclide imaging with ^{99m}Tc-labeled heat-damaged RBCs (DRBC) or SC (used here) is the superior modality for definitive diagnosis, with ^{99m}Tc-DRBC having greater specificity to splenic tissue. Generally, treatment involves conservative management. Surgical removal is not typically recommended unless symptoms arise or diagnostic uncertainty remains. The vitality of lifelong prophylaxis for infections is minimal when splenic tissue is functional.

In this case, follow-up imaging revealed multiple benign pleural-based masses in the left hemithorax. The asymptomatic nature of this patient's presentation, history of remote trauma, and positive SC uptake were diagnostic of intrathoracic splenosis. Conservative management was recommended. This case highlights the importance of including intrathoracic splenosis in the differential diagnosis of pleural-based masses, especially in patients with a previous history of trauma.

@cameronlaurie65
@AOCRNews
@cameron_l_10
@aocrnews

Case courtesy of Cameron C. Laurie, MS1[1], April L. Cox, DO[2]
[1]Baylor College of Medicine, [2]Indiana University School of Medicine

References

- Baldolli A, Coeuret S, Le Pennec V, Agostini D, Verdon R. Thoracic splenosis mimicking a pleuropneumonia. Medicine. 2017;96(29):e7552. doi:10.1097/md.0000000000007552
- Fremont RD, Rice TW. Splenosis: A Review. Southern Medical Journal. 2007;100(6):589-593. doi:10.1097/smj.0b013e318038d1f8
- Gelsomino F, Castellani MR, Marchianò A, et al. Pitfalls in oncology: a unique case of thoracic splenosis mimicking malignancy in a patient with resected breast cancer. J Thorac Dis. 2016;8(6):E403-E407. doi:10.21037/jtd.2016.04.54
- Hagman TF, Winer-Muram HT, Meyer CA, Jennings SG. Intrathoracic Splenosis*. Chest. 2001;120(6):2097-2098. doi:10.1378/chest.120.6.2097
- Kesim S, Inanir S. 99m-technetium-labeled red blood cells' single-photon emission computed tomography/computed tomography in situs ambiguous with polysplenia. Indian J Nucl Med. 2020;35(1):84. doi:10.4103/ijnm.ijnm_157_19
- Khan AM, Manzoor K, Gordon D, Berman A. Thoracic splenosis: A diagnosis by history and imaging. Respirology. 2008;13(3):481-483. doi:10.1111/j.1440-1843.2008.01272.x
- Lopes B, Almeida LR, Vicente AA, et al. Thoracic splenosis as a differential diagnosis of juxtapleural nodules. Respiratory Medicine Case Reports. 2014;11:1-3. doi:10.1016/j.rmcr.2013.10.001
- Naylor MF, Karstaedt N, Finck SJ, Burnett OL. Noninvasive methods of diagnosing thoracic splenosis. The Annals of Thoracic Surgery. 1999;68(1):243-244. doi:10.1016/s0003-4975(99)00492-0
- O'Connor JV, Brown CC, Thomas JK, Williams J, Wallsh E. Thoracic splenosis. The Annals of Thoracic Surgery. 1998;66(2):552-553. doi:10.1016/s0003-4975(98)00506-2
- Sawhney H, Gandhi D, Parmar G, Serhal M, Miller FH, Magnetta M. Post-traumatic intrathoracic splenosis and role of Tc-99m Sulfur colloid scintigraphy in confirmation. Radiology Case Reports. 2021;16(9):2742-2745. doi:10.1016/j.radcr.2021.06.069
- Suraju MO, Peyton N, Mooers B, Jensen C, Shilyansky J. Congenital intrathoracic accessory spleen is a very rare trick of nature: a case report. J Cardiothorac Surg. 2020;15(1). doi:10.1186/s13019-020-01270-4
- Yammine JN, Yatim A, Barbari A. Radionuclide Imaging in Thoracic Splenosis and a Review of the Literature. Clinical Nuclear Medicine. 2003;28(2):121-123. doi:10.1097/01.rlu.0000048681.29894.ba

Posted 1/30/2026

62 y/o f with past hx of gastric bypass & cholecystectomy presented to the ED with acute onset left sided abdominal pain and vomiting. Patient was unable to tolerate oral intake. Denies hematemesis & hematochezia/melena.

A



B



A - Coronal CT

B - Coronal CT

C - Axial CT

D - Axial CT

*All images obtained with IV contrast.

C



D





A - Coronal CT

B - Coronal CT

C - Axial CT

D - Axial CT

*All images obtained with IV contrast.







Closed Loop Small Bowel Obstruction

Imaging Findings: CT abdomen and pelvis with IV contrast demonstrates a closed-loop small bowel obstruction involving a dilated fluid-filled loop (up to 3.8 cm) in the left abdomen (orange arrow), distal to the gastric bypass. Two distinct transition points: the proximal transition point (yellow arrow) and distal transition point (red arrow) with focal wall thickening are noted. The gastric pouch is moderately distended. There is no pneumatosis, portal venous gas, free air, or free fluid.

Differential Diagnosis: Closed loop small bowel obstruction, open loop small bowel obstruction, volvulus, internal or external hernias

Discussion: Closed-loop small bowel obstructions (SBO) differ from open-loop SBOs by involving two points of obstruction within the same bowel segment, creating a closed loop that rapidly increases intraluminal pressure and predisposes to ischemia and necrosis. CT imaging typically demonstrates a U- or C-shaped, fluid-filled dilated loop, the mesenteric whirl sign, and two closely spaced transition points. This case is notable for an internal hernia causing a closed-loop SBO in a patient with a history of Roux-en-Y gastric bypass (RYGB). Internal hernia is a recognized late complication of RYGB, with a reported incidence of approximately 3.1%, and accounts for most closed-loop SBO cases in this population. Early diagnosis and prompt surgical intervention are necessary to decompress the closed-loop prior to ischemia, rupture, or necrosis.

@AOCRNews

@dom_the_creator
@aocrnews

Case courtesy of Domenick Bartoletti, MS3; Cole Knox, MD, PhD;
Faculty: Roland Gazaille, DO | Kettering Health

References

- Higa KD, Ho T, Boone KB. Internal hernias after laparoscopic Roux-en-Y gastric bypass: incidence, treatment and prevention. *Obes Surg*. 2003;13(3):350-354. doi:10.1381/096089203765887642.

- Stenberg E, Szabo E, Ågren G, et al. Closure of mesenteric defects in laparoscopic gastric bypass: a multicentre, randomised, parallel, open-label trial. *Lancet*. 2016;387(10026):1397-1404. doi:10.1016/S0140-6736(15)01126-5.

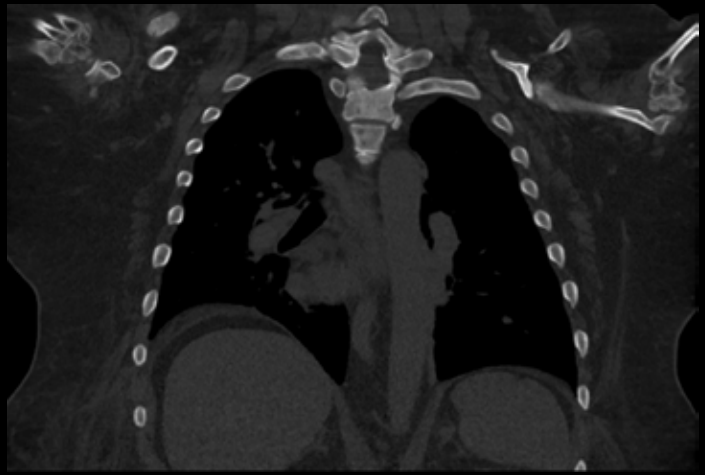
- Balthazar EJ, Birnbaum BA, Megibow AJ, Gordon RB, Whelan CA, Hulnick DH. Closed-loop and strangulating intestinal obstruction: CT signs. *Radiology*. 1992;185(3):769-775. doi:10.1148/radiology.185.3.1438761.

Posted 1/23/2026

48 y/o m who presented with shortness of breath. A CT chest without IV contrast was performed, which incidentally demonstrated bilateral upper extremity phocomelia.



CT Chest w/o contrast



CT Chest w/o contrast



CT Chest w/o contrast

Adams-Oliver phocomelia

Imaging Findings: Coronal CT chest without contrast, bilateral upper-limb reduction defects. Left: Nonvisualized humerus and radius/ulna; clustered carpal-metacarpal ossicles adjacent to the glenoid. Right: Hypoplastic humerus; nonvisualized radius/ulna with rudimentary distal elements.
Differential Diagnosis: Adams–Oliver syndrome, Thalidomide embryopathy, Amniotic band sequence, Roberts (pseudothalidomide) syndrome, Isolated terminal transverse limb defects
Diagnosis: Adams–Oliver syndrome with severe terminal transverse upper-limb defects (“phocomelia” pattern)
Discussion: Adams–Oliver syndrome features patchy absence of scalp skin (aplasia cutis) with terminal transverse limb reductions. Pathogenic variants are described in Notch-pathway and cytoskeletal genes (e.g., NOTCH1, DLL4, RBPJ, DOCK6). Congenital heart disease occurs in about 25% of cases. CNS or other vascular malformations occur in about 25% as well. Cutis marmorata telangiectatica congenita is also reported. Head CT or MRI assesses calvarial defects under the scalp lesion. Echocardiography or chest CT/MR screens the heart and great vessels. Vascular ultrasound or angiography can show hypoplastic or absent distal arteries. Management is multidisciplinary: protect the scalp, support limb function, and address cardiac and vascular disease. Prognosis depends on the severity of scalp, cardiac, and vascular involvement. Early, coordinated care improves outcomes.

@AOCRNews

@aocrnews

Case courtesy of Nathan Sampson OMS-IV, Janet Tam DO, Chase Jeppesen DO | MountainView Hospital

References

Snape KM, Ruddy D, Zenker M, et al. The spectra of clinical phenotypes in Adams–Oliver syndrome. Am J Med Genet A. 2009;149A(6):1231-1237. doi:10.1002/ajmg.a.32859

Meester JAN, Southgate L, Stittrich AB, et al. Haploinsufficiency of NOTCH1 causes Adams–Oliver syndrome. Am J Hum Genet. 2015;97(3):475-482. doi:10.1016/j.ajhg.2015.07.012

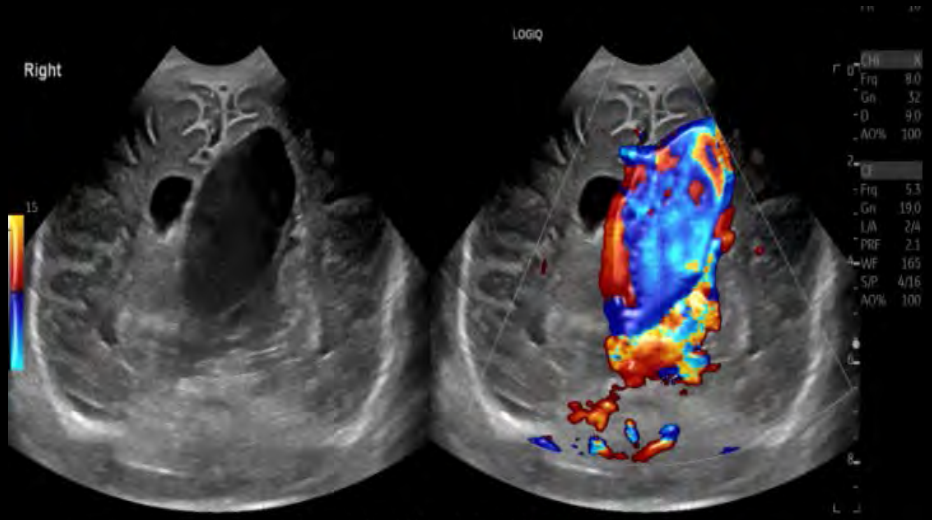
Southgate L, Sukalo M, Karountzos AS, et al. Adams–Oliver syndrome: mutations in RBPJ and NOTCH pathway genes. Am J Med Genet A. 2016;170A(4):1027-1035. doi:10.1002/ajmg.a.37544

Lehman A, Wuyts W, Patel MS, et al. Adams–Oliver syndrome: a multidisciplinary review. J Med Genet. 2016;53(12):801-810. doi:10.1136/jmedgenet-2016-103891

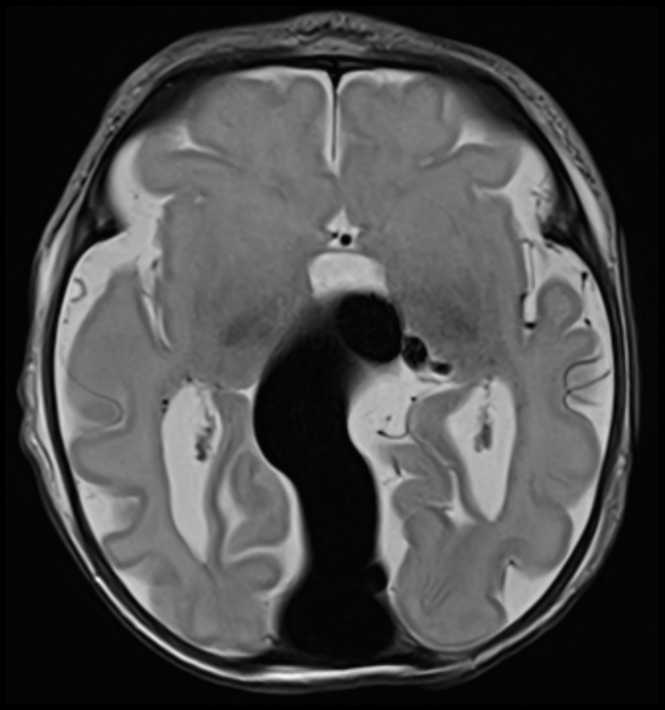
StatPearls [Internet]. Adams–Oliver Syndrome. Treasure Island (FL): StatPearls Publishing; 2025.

Posted 1/16/2026

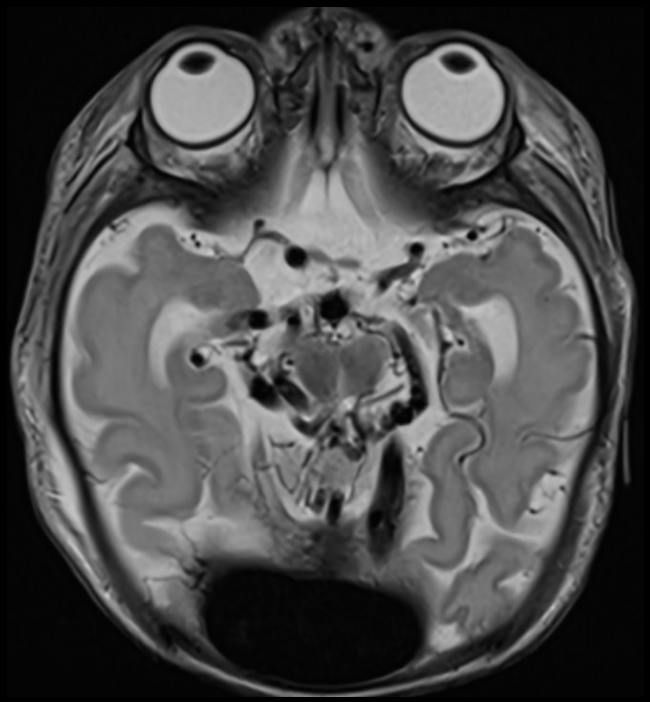
3-day old m presented from an outside hospital with a known vein of Galen malformation (VOGM) discovered on ultrasound late in pregnancy. Maternal history: P1001, 34 months 2 days gestation on ultrasound.



A)



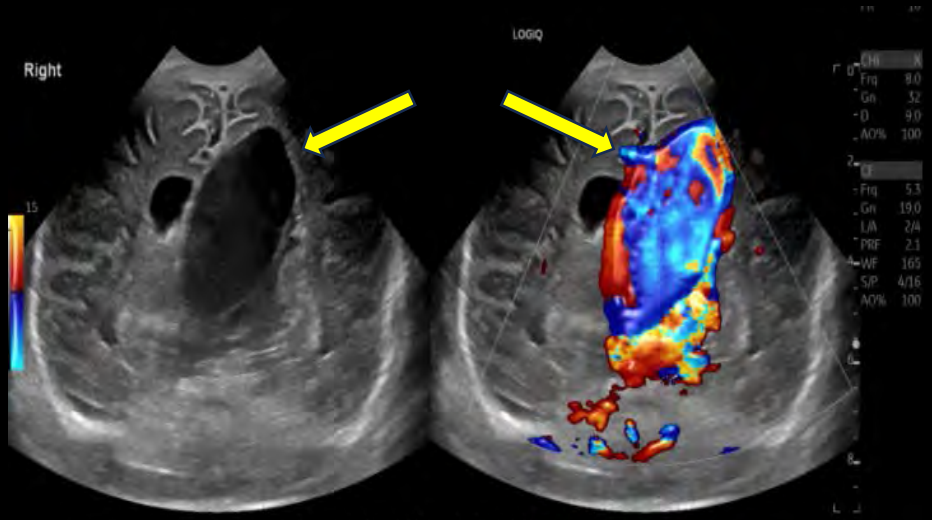
B)



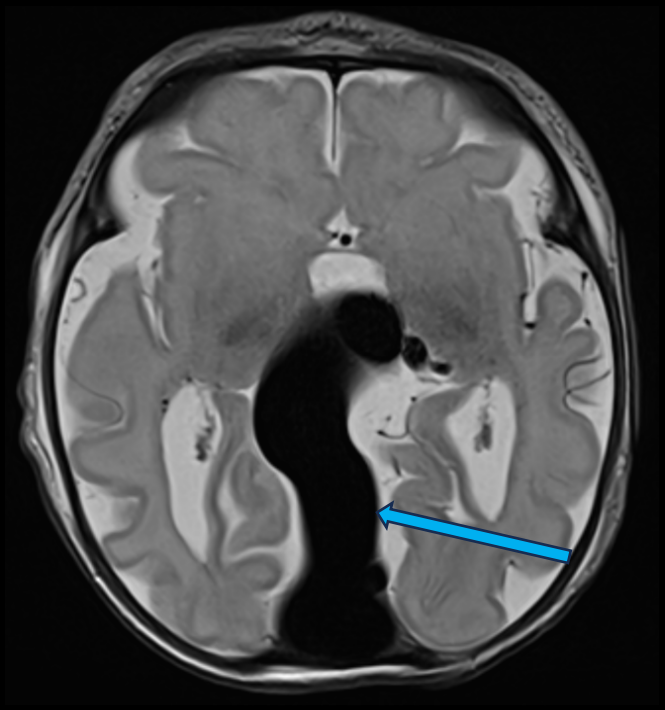
C)

A) Ultrasound encephalogram with doppler

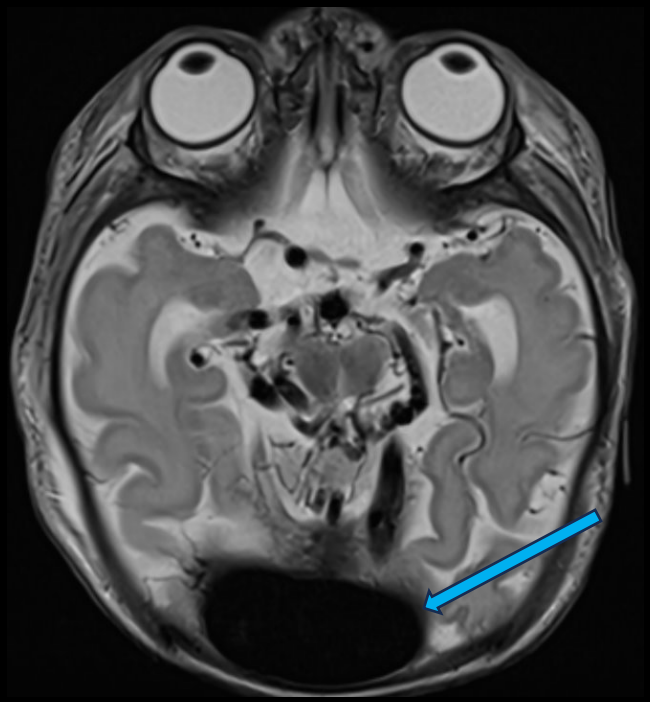
B&C) T2 MRI axial



A)



B)



C)

A) Ultrasound encephalogram with doppler

B&C) T2 MRI axial

Vein of Galen Malformation

Imaging Findings: Large high-flow Vein of Galen malformation observed (yellow arrows) with mild ventriculomegaly and mild prominence of the extra-axial space on ultrasound. Large midline flow void (blue arrows) corresponding to dilated malformation with mass effect on midline supratentorial structures on MRI.

Differential Diagnosis: arteriovenous malformation (AVM), vascular intracranial tumor.

Discussion: Vein of Galen Malformations are rare arteriovenous malformations resulting from 1 or more AV fistulas shunting blood towards the median prosencephalic vein of Markowski, an embryonic precursor to the vein of Galen, thus preventing its involution. It may be discovered on prenatal ultrasound, typically in the third trimester, or after birth. Complications can include high-output heart failure, pulmonary hypertension, hydrocephalus, neurodevelopmental delay, and seizures. Fetal circulation can have a protective effect due to low resistance placental circulation; however, shunt flow increases significantly after birth. Endovascular therapy is the treatment of choice. If hydrocephalus does not resolve after endovascular therapy, a ventriculoperitoneal shunt or endoscopic ventriculostomy may be indicated.

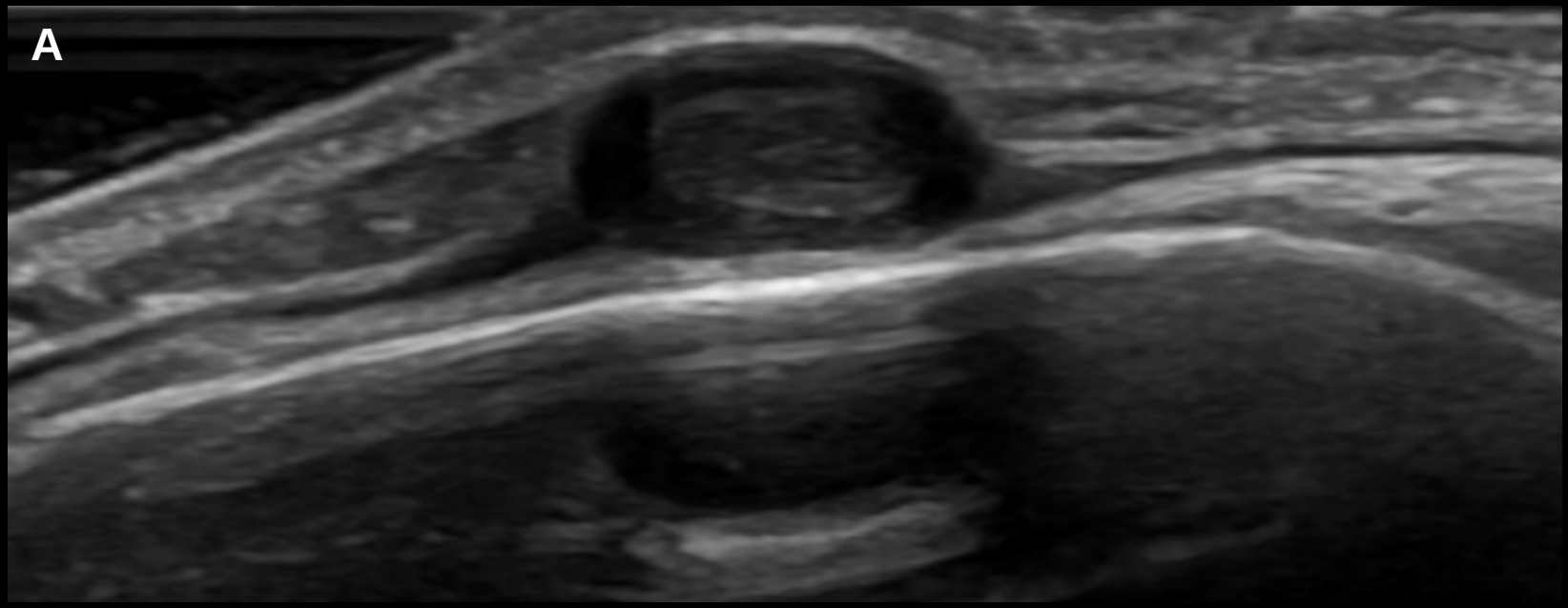
Case courtesy of Thomas Stack, OMS-IV; Susan Taylor, DO
Edward Via College of Osteopathic Medicine / Emory University

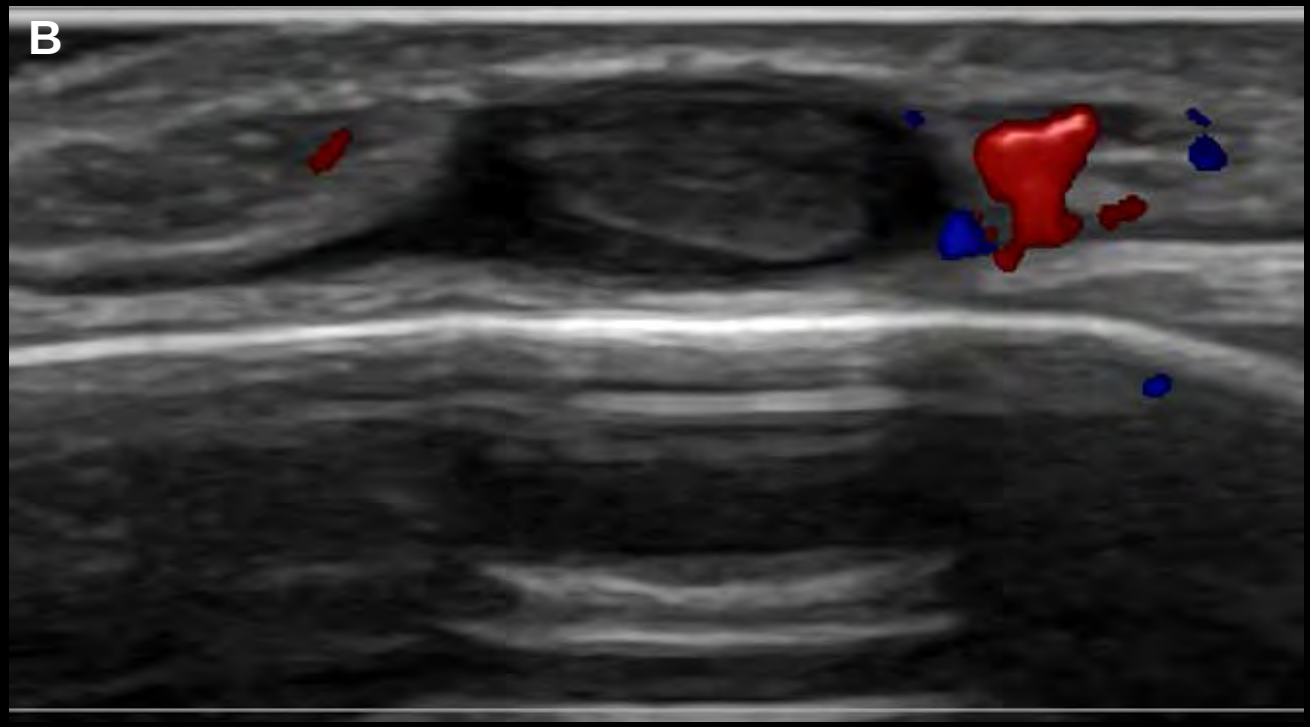
References

- Monteagudo, A. Vein of Galen Aneurysmal Malformations. *American Journal of Obstetrics & Gynecology* Volume 223, Issue 6, B27 – B29.
- Spazzapan P, Milosevic Z, Velnar T. Vein of Galen aneurismal malformations - clinical characteristics, treatment and presentation: Three cases report. *World Journal of Clinical Cases*. 2019;7(7):855-862. doi:10.12998/wjcc.v7.i7.855

Posted 1/9/2026

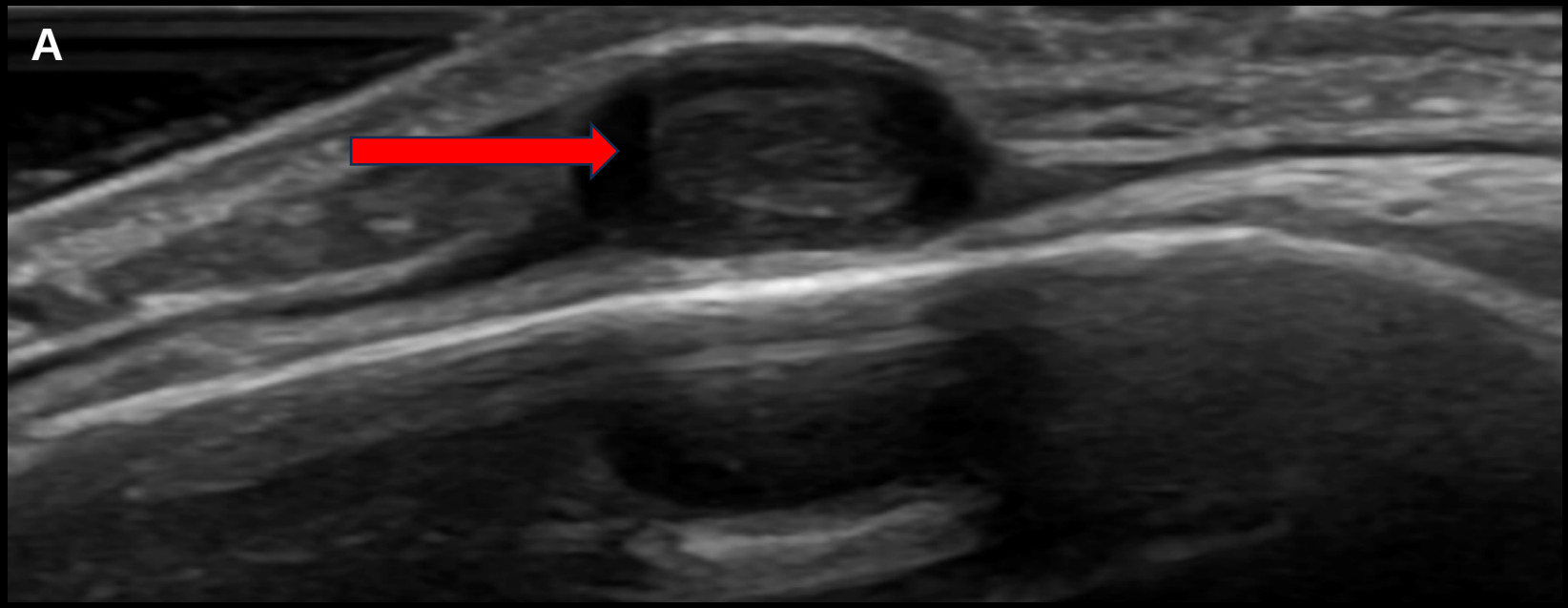
11 y/o f with no significant past medical history with a left forehead mass. The mass has been enlarging over the past few months.

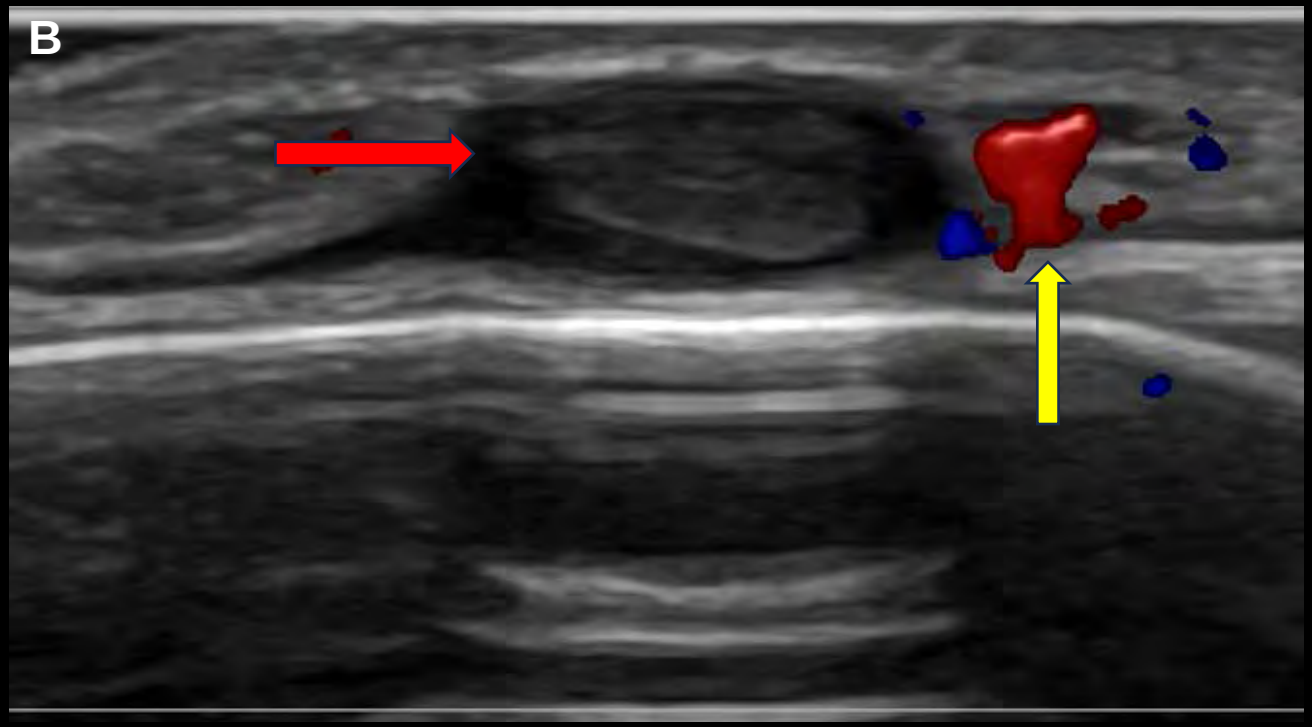




A - US transverse

B – US with color flow





A - US transverse

B – US with color flow

Pilomatrixoma

Imaging Findings: Ultrasound demonstrates well-circumscribed, ovoid mass. The mass appears targetoid on US and demonstrates a hyperechoic center suggesting complex or soft tissue. The mass is avascular.

Differential Diagnosis: Pilomatrixoma, epidermal inclusion cyst, dermoid cyst, giant cell tumor, chondroma

Discussion: Pilomatrixoma is a benign neoplasm hypothesized to arise from hair cortex cells. 50% of pilomatrixoma cases present in the head and neck region, 60% occur at the age of 20 and is more common in females. This is consistent with the presentation we observed with a solid mass on the forehead of an 11 y/o female. US confirms a well-circumscribed, avascular, targetoid mass which is further consistent with pilomatrixoma. Surgical resection is the curative treatment for pilomatrixoma.

@AOCRNews

@aocrnews

Case courtesy of Ryan Aturaliya, MS3, Felicia Yan, MS3, Robert Koenigsberg, DO FAOCR
St. Christopher's Hospital for Children
Drexel University College of Medicine, Lewis Katz School of Medicine

References

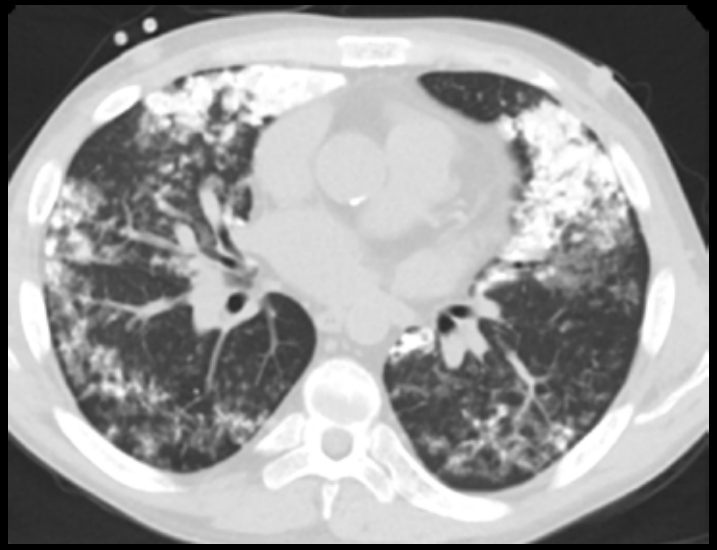
- **GARD.** *Pilomatrixoma*. Reference article, Genetic and Rare Diseases Information Center, NIH (Accessed on 31 Jul 2025) https://rarediseases.info.nih.gov/diseases/9452/pilomatrixoma

- Hughes J, Lam A, Rogers M. Use of ultrasonography in the diagnosis of childhood pilomatrixoma. Pediatr Dermatol. 1999 Sep-Oct;16(5):341-4. doi: 10.1046/j.1525-1470.1999.00090.x. PMID: 10571829.

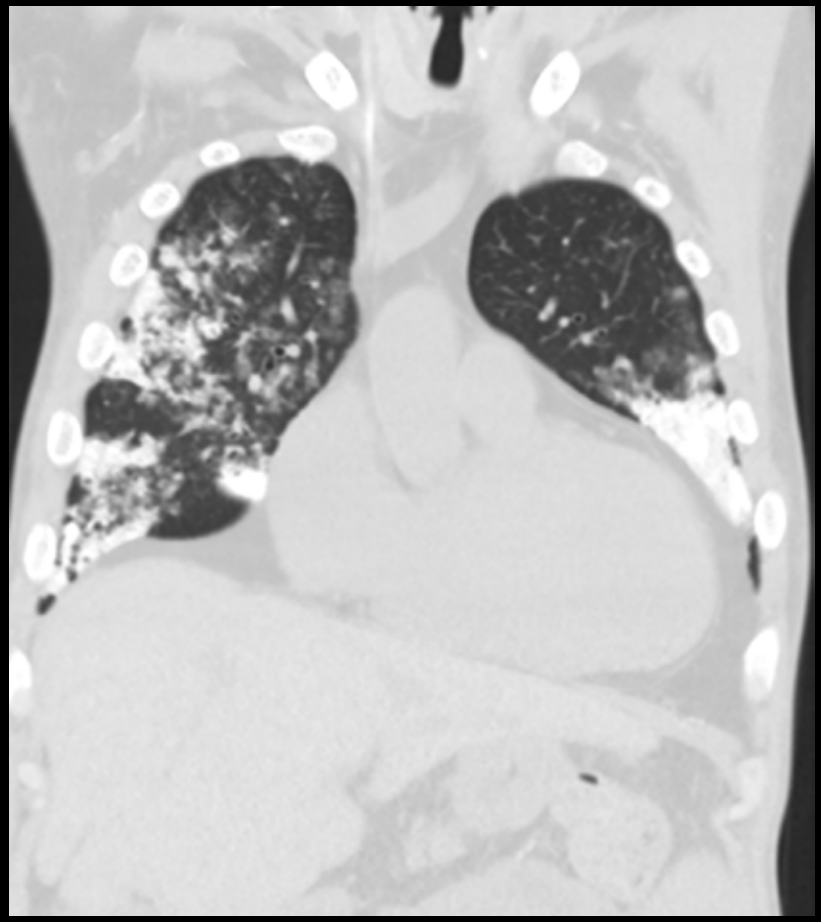
Posted 1/2/2026

29 y/o male with past hx of Alagille syndrome, cirrhosis, and ESRD presents for outpatient CT chest for liver transplant evaluation.

A



B



C

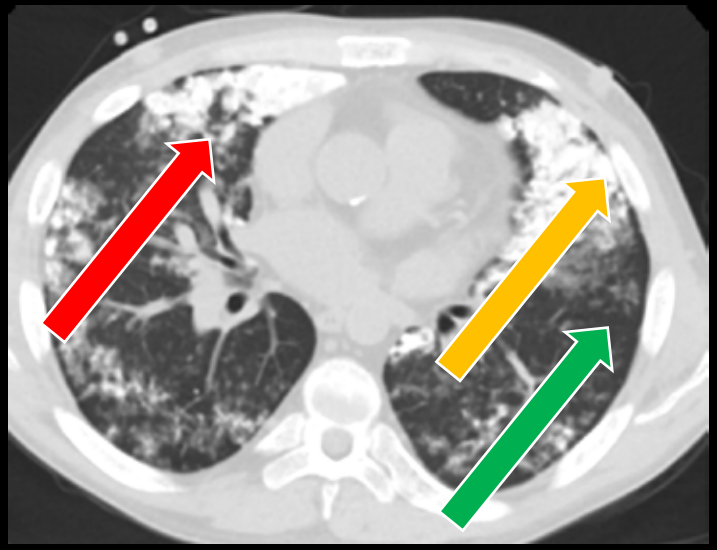


A – Axial CT Chest

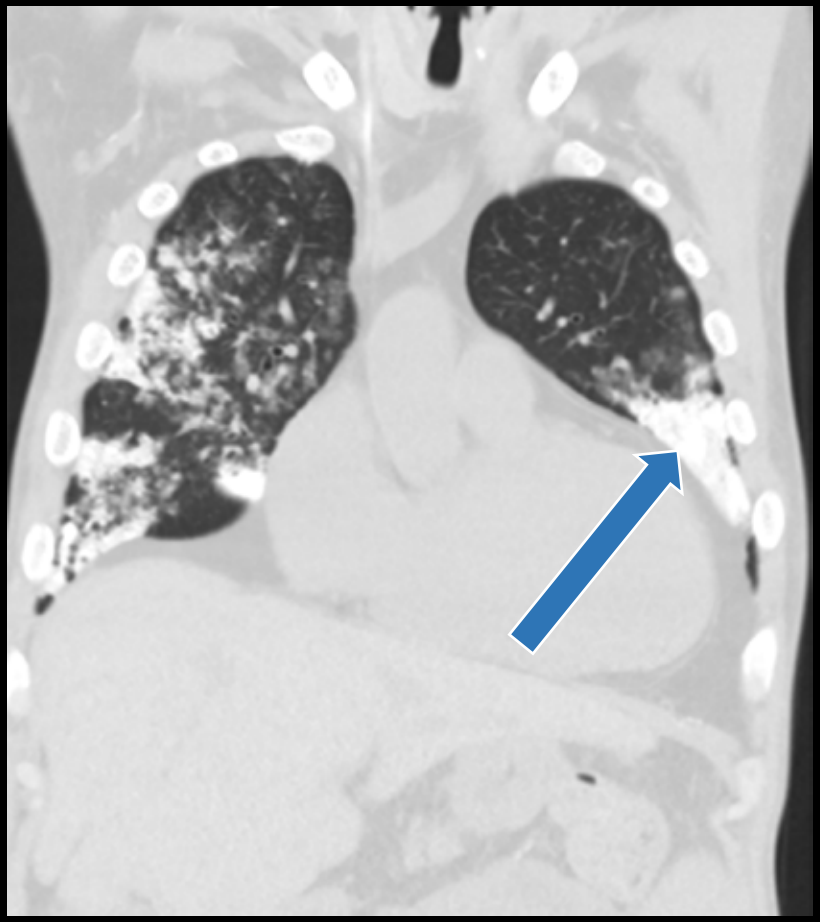
B – Coronal CT Chest

C – Chest x-ray

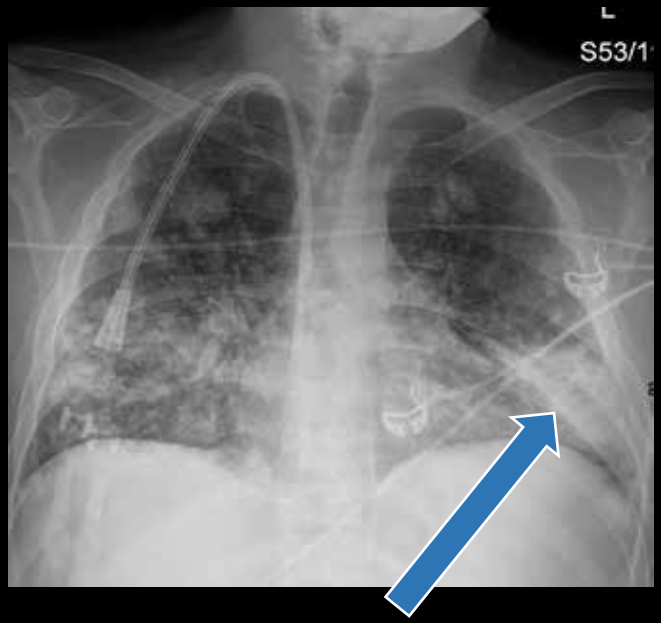
A



B



C



A – Axial CT Chest

B – Coronal CT Chest

C – Chest x-ray

Pulmonary Trichosporon

Imaging Findings: Extensive bilateral calcified consolidations are seen on both the chest x-ray and CT scan, with large dense consolidations abutting the pleura in the right middle lobe (red arrow, image A), and lingula (blue arrows, image B&C). In addition, there are diffuse centrilobular ground glass opacities (green arrow) as well as a black pleura sign (yellow arrow).

Differential Diagnosis: Alveolar microlithiasis, metastatic pulmonary calcification, pulmonary talcosis & silicosis.

Discussion: Pulmonary Trichosporon is an invasive pulmonary infection caused by the basidiomycetous, yeast-like fungi Trichosporon. Trichosporon spp. are primarily found in the soil and bodies of water in tropical areas and are known to commonly colonize the respiratory tract, skin, and gastrointestinal mucosa. This opportunistic pathogen contains several virulence factors that allow it to disseminate in immunocompromised hosts, particularly in those with cystic fibrosis or hematologic malignancies. Clinically, Trichosporon infections often begin superficially by affecting the hair shaft, a condition known as piedra. Deep-seated infections can subsequently occur, including pneumonia, pulmonary infiltrates, and fungemia. On CT imaging pulmonary Trichosporon typically presents as multiple mass-like or ground-glass opacities with consolidations. However, these imaging findings are non-specific and require correlation with cultures for accurate diagnosis. Our case was complicated by the patient having Alagille syndrome and ESRD. Initial differential diagnosis most concerning for metastatic pulmonary calcification vs alveolar microlithiasis given clinical history. Bronchioalveolar lavage grew Trichosporon, with decrease in calcified consolidations after antifungal therapy. This case highlights importance of broad differentials to include infectious process when nonspecific findings are present.

Case courtesy of Brandon Trevino, OMS4, Ryan Sanchez, DO, Vijay Aggarwal, MD | UTHSCSA, Sam Houston State COM

References

- Colombo AL, Padovan AC, Chaves GM. Current knowledge of Trichosporon spp. and Trichosporonosis. Clin Microbiol Rev. 2011 Oct;24(4):682-700. doi: 10.1128/CMR.00003-11
- Girmenia C, Pagano L, Martino B, D'Antonio D, Fanci R, Specchia G, Melillo L, Buelli M, Pizzarelli G, Venditti M, Martino P; GIMEMA Infection Program. Invasive infections caused by Trichosporon species and Geotrichum capitatum in patients with hematological malignancies: a retrospective multicenter study from Italy and review of literature. J Clin Microbiol. 2005 Apr;43(4):1818-28. doi: 10.1128/JCM.43.4.1818-1828.2005
- Hickey PW, Sutton DA, Fothergill AW, Rinaldi MG, Wickes BL, Schmidt HJ, Walsh TJ. Trichosporon mycotoxinivorans, a novel respiratory pathogen in patients with cystic fibrosis. J Clin Microbiol. 2009 Oct;47(10):3091-7. doi: 10.1128/JCM.00460-09